MECHANISM OF FLAKE DRYING AND ITS CORRELATION TO QUALITY

EDGAR DELA CRUZ DEOMANO

A dissertation submitted to the Faculty of
Virginia Polytechnic Institute and State University
in partial fulfillment of the requirements for the degree of

DOCTOR OF PHILOSOPHY
in
WOOD SCIENCE AND FOREST PRODUCTS

Dr. Audrey Zink-Sharp, Chair

Dr. Frederick A. Kamke

Dr. Fred M. Lamb

Dr. Robert L. Youngs

Dr. Klaus H. Hinkelmann

16 July 2001
Blacksburg, Virginia

Keywords: Small and thin wood, Drying kinetics

MECHANISM OF FLAKE DRYING AND ITS CORRELATION TO QUALITY

EDGAR DELA CRUZ DEOMANO

Audrey Zink-Sharp, Chair

ABSTRACT

This research focuses on experimental investigations of the drying and bending properties of wood flakes. Three species (southern yellow pine, sweetgum, and yellow-poplar) were tested. Experiments on flake drying and effect of flake properties (cutting direction and dimension) and an external factor (temperature) were used to evaluate the flake drying process. Drying experiments were conducted using a convection oven. Bending properties of dried flakes were also measured. Modulus of elasticity (MOE), modulus of rupture (MOR), and strength at proportional limit (SPL) of flakes were measured based on Methods of Testing Small Clear Specimens of Timber (ASTM D143-94) using a miniature material tester.

The drying curve was characterized by a second-order/quadratic equation. This equation was then differentiated to get the drying rate curve. Observation on drying and drying rate curves revealed that the rate of moisture loss consists of two falling rate periods; no constant rate drying period was observed. First falling rate drying period is controlled by convective heat transfer. Bound water diffusion controls the second falling rate drying period.

Species, cutting direction, dimension, and temperature were found to have significant effect on drying rate of wood flakes. Southern yellow pine has the fastest drying rate followed by sweetgum then yellow-poplar. Differences in drying rate between species were attributed to differences in specific gravity and other factors. Radially-cut specimens have a slower drying rate than tangentially-cut specimens. There were also significant differences in drying rate between the four different flake dimensions. Thickness was found to be the more sensitive parameter in terms of dimensions. As expected, drying temperature also had highly significant effect on drying rate. An increasing trend in drying rate was observed as drying temperature increased.

Simulation of flake drying using a numerical model yielded a different result. Simulated flake drying has two drying periods: a constant rate and falling rate. Moisture of the flake decreases constantly and surface temperature increases rapidly to boiling point and remains there in the constant rate drying period. During the falling rate period, rate of moisture transport is limited by the ability of water to diffuse through wood and flake temperature starts to rise.

Bending properties were found to vary between and within the three species. Southern yellow pine had the lowest bending stiffness and strength followed by sweetgum while yellow-poplar had the highest bending properties. Radially-cut specimens were found to have lower MOE, MOR, and SPL than tangentially-cut specimens. Drying temperature was also found to have a significant effect on bending stiffness and strength. A decreasing trend in bending properties was observed when drying temperature was increased.

Acknowledgements

I would like to express my sincere thanks and appreciation to the following:

Dr. Audrey Zink-Sharp, my advisor and committee chair for her words of encouragement and her guidance and suggestions in conducting my dissertation and preparation and improvement of this manuscript;

Drs. Fred Kamke, Fred Lamb, and Bob Youngs, members of my committee for their ideas and suggestions;

Dr. Klaus Hinkelmann, Seth Clark, and Xiao Yang for sharing their knowledge in statistics especially on experimental design and analyses;

Dr. Patrick Perre for providing the Front2D source code;

Faculty and staff members of the Department of Wood Science and Forest Products both at the Thomas M. Brooks Forest Products Center and Cheatham Hall. Thanks to Dr. Geza Ifju, former department head and Dr. Paul Winistorfer, current department head. Special thanks to Carlile, Kenny, Butch, Bob, Sharon, Debbie, and Angie;

Fellow graduate students at the Department of Wood Science and Forest Products. Special mention to Dr. Delton Alderman, Hongmei Gu, Jason Smart, and Scott Renneckar for being good company at the graduate loft;

This research was funded by the US Department of Energy. The financial support is greatly appreciated;

Georgia Pacific OSB Skippers Plant for providing some of the raw materials for this research;

Forest Products Research and Development Institute for their support and for allowing me to pursue graduate studies here in the United States;

Aileen, Alan, Camille and Ferdie, CB, Cesmac, Chinggay, Christine, Janet and Volker, John Paul, Jess, Kats, Mike and Rich, Ris, Roy, Dr. Ballweg and the Filipino families in Blacksburg for their camaraderie;

Cris and Deedee, Charity, Dewi and Jocel, Gino and Camilla, Homer and Shirley, and Matis for their regular phone calls and kind hospitality. Thanks to my friends who are in the Philippines: Baron, Jingle, Tavie, Teody, and William;

Tatay, Nanay, Kuya Edwin, Ate Lulu, Kuya Larry, Ching, Ara, Lisa, Leo, Joshua, Ellen, Paulo, and Emily who are in the Philippines to whom I owe appreciation and support;

Norilyn, my partner for life who has been very supportive and her encouragement helped my a lot. Aside from being a very good wife, she is also a dear friend and confidante. I love you very much;

Annika, my baby who has given me new meaning to life. She is now the best reason for all the things that I have done and will be pursuing next in my career. I also love you very much;

Finally, to the Almighty God for making all things possible.

Table of Contents

List of Figures

List of Tables

List of Appendices

CHAPTER 1. INTRODUCTION

One of the major advances in the forest products industry has been the introduction of Oriented Strand Boards (OSB). OSB is a weatherproof, adhesive-bonded, heat-cured structural panel made from compressed rectangular-shaped wood strands arranged in cross-oriented layers. OSB is a descendant of waferboard and oriented waferboard and is similar to plywood. All are reconstituted structural panels. This type of panel is widely used in residential and commercial construction. It is also gaining popularity in markets such as materials handling and upholstered furniture. According to APA-Engineered Wood Association (2001), US OSB production was about 11.9 billion sq. ft. - 3/8" basis in 2000 and projected to increase to 13.7 billion sq. ft. - 3/8" basis in 2005. There are currently 63 North American OSB plants in operation. Clearly there is a need to fully understand the processes involving quantities of wood at these magnitudes.

OSB is manufactured through a simple process. First, logs are debarked then crosscut into short bolts. These bolts are passed through flaking machines to reduce them into flakes and dried to desired moisture content. Resin is applied and the furnish is spread evenly forming a mat to be pressed to its final thickness. For the flake drying process, dryers (rotary or conveyor) that employ high temperature convective drying and short residence/dwell time are used to achieve drying of large volumes of flakes. These dryers use a significant amount of energy and so an optimized process is essential in order to save energy. Energy is usually in the form of natural gas or wood wastes. The industry currently relies on high temperature to drive the drying process. The challenge is to optimize residual heat of gas while maintaining acceptable drying rate and quality of dried materials. Spurred by the rising cost and shortage of energy, the industry needs innovative technology to conserve energy. To attain these goals, it is first necessary to gain the fundamental understanding of the drying kinetics of wood flakes.

Despite the increasing use of OSB, very few studies have been reported on the kinetics of flake drying. Drying of flakes is done in a different manner than conventional wood drying. Lumber drying must be done gradually to avoid defects and can take days or even weeks. In contrast, drying of flakes can take only seconds or minutes at high temperature. Recent research in flake drying has focused primarily on reduction of volatile organic compounds (VOC) and hazardous air pollutants (HAP) (Banerjee et al., 1995, 1998; Otwell et al., 2000; Su and Banerjee, 1999; Su et al., 1999). The lack of data on drying rate, bending properties and experimentally derived insight into the mechanism that control the drying of flakes were the motivating factors for this research.

Models that describe the drying process are vital for engineering design, and process understanding, control and optimization. These models allow a more scientific approach in the dryer design and control of drying conditions and capital costs subject to quality constraints. Models that can predict the drying behavior of wood particles in rotary (Kamke and Wilson, 1985, 1986a, 1986b; Kirk and Wilson, 1985; Plumb et al. 1978a, 1978b) and pneumatic-conveying (Fyhr and Rasmuson, 1997) dryers have been developed. One area in the modeling of dryers, which is often overlooked, is the transport mechanism occurring within the wood during the drying process. For accurate prediction of the performance of a certain dryer, both the conditions inside the dryer and the transport mechanism within a single piece of material to be dried must be well understood.

Good estimates of drying time and drying rate enhance optimization techniques. Numerical analyses of the complex drying process of solid wood, veneer, particles/chips, and wafers/flakes have been studied extensively in predicting wood drying behavior. These models derived through fundamental relations can predict the drying rates as well as the moisture content and temperature profiles. It involves complicated non-linear partial differential equations, which limits its practical application in design or optimization in which the drying rate is of the most important concern. Simplified representation of the drying rate will allow the easy use of this data in design and optimization leading to energy conservation.

The use of numerical models in dryer design and process optimization has been very limited. Most are still very much related to empirical knowledge. However, very few experimental investigations on the drying characteristics of wood particles/chips and wafers/flakes have been made. Intensive experiments on high temperature drying and effects of flake properties are minimal. Baseline experimental data on drying characteristics can be used to analyze drying trends in industrial flake drying. Drying data for wood flakes as a function of process and material variables is desired.

There are many variables that affect the drying and mechanical properties of wood flakes. These can be categorized as process and material variables. The process variable of primary interest from the standpoint of drying mechanism and quality is temperature. Material variables considered were wood species, cutting direction, and flake dimensions. These were variables considered of major importance to both categories although other variables could have been added.

Experiments were used to evaluate the drying of flakes. Species, cutting direction, flake dimensions, and drying temperature were incorporated to get a better understanding of the changes that occur during drying. This information was used for describing the flake drying process. Regression analyses were made descriptive of the drying process, so that meaningful predictions can be made. A regression model based on flake properties and temperature was developed. Moisture content, drying time and rate can be accurately predicted or estimated by this model.

Aside from drying time and rate, quality is another factor that is considered to be very important in the drying of flakes. Flake quality is quantified in terms of bending properties. Strength of OSB is a function of the mechanical properties of the flakes. Knowledge on bending properties of flakes can lead to improved strength and performance of OSB. Study of the effect of high temperature drying on bending stiffness and strength of wood flakes has been very limited. In this research, the effects of species, cutting direction and drying temperature on bending stiffness and strength were evaluated. Changes in bending properties were correlated to drying properties.

This dissertation reports on the drying and bending properties of wood flakes. Chapter 2 reviews the literature on drying of wood in general and concentrates on the drying of small and thin wood. Chapter 3 evaluates the drying properties of wood flakes. An experimental data set is compared to a numerical model in Chapter 4. Chapter 5 evaluates the bending properties of wood flakes. Last, Chapter 6 concludes the analyses of flake drying and bending.

Objectives

The goal of this research is to gain a comprehensive knowledge of the drying and bending properties of flakes. Specific objectives are the following:

1. To measure moisture content and surface temperature of drying flakes;
2. To represent the flake drying process with a regression model;
3. To determine the effects of species, cutting direction, flake dimensions, and drying temperature on drying rate;
4. To compare an experimental data set against a numerical drying model;
5. To measure the bending properties [modulus of elasticity (MOE), modulus of rupture (MOR), and strength at proportional limit (SPL)] of flakes;
6. To determine the effect of species, cutting direction, and temperature on bending properties; and
7. To correlate bending and drying properties.

CHAPTER 2. LITERATURE REVIEW

2.1. Introduction

Research on drying and bending properties of flakes has been very limited despite the extensive use of flakes in OSB manufacture. Literature on veneer, wafer and flake drying and wood particle and chip drying and pyrolysis were also reviewed since these wood materials were the closest to flakes in form. Both experimental and theoretical results of thin and small wood materials were reviewed to understand the drying and bending properties of flakes.

The literature review is presented in this chapter. Wood-moisture relations are discussed briefly in Section 2.2. Mathematical descriptions for drying wood were divided into three categories: diffusion models (Section 2.3), numerical models (Section 2.4), and empirical models (Section 2.5). Section 2.6 discusses the drying of thin and small wood. Last, literature on bending properties of flakes and OSB is presented in Section 2.7.

2.2. Wood-Moisture Relations

Moisture content of wood is defined as the weight of water in wood expressed as a fraction, usually a percentage, of the weight of ovendry wood. Moisture content varies widely between species and within species of wood (FPS, 1997 and 1999; Haygreen and Bowyer, 1996). It varies particularly between heartwood and sapwood. The amount of moisture in the cell wall may decrease as a result of extractive deposition when a tree undergoes change from sapwood to heartwood. In softwoods, sapwood usually has higher moisture content than heartwood. This is due to the active passageways for water transport in the living trees, which are abundant in the sapwood. In hardwoods, the difference in moisture content between heartwood and sapwood depends on the species. The butt logs of trees may contain more water than the top logs. Variability of moisture content exists even within individual boards cut from the same tree.

Green wood is often defined as freshly sawn wood in which the cell walls are completely saturated with water. Usually green wood contains additional water in the lumens. Moisture content at which both the cell lumens and cell walls are completely saturated with water is the maximum moisture content. Average green moisture content values taken from the Wood Handbook (FPS, 1999) and Dry Kiln Operator's Manual (FPS, 1997) of southern yellow pine (loblolly) is 33 and 110% for heartwood and sapwood, respectively. Sweetgum is 79 and 137% while yellow-poplar is 83 and 106% for heartwood and sapwood, respectively (FPS, 1997 and 1999).

2.2.1. Free and bound water

Water in wood is found in the cell cavities and cell walls. All void spaces in wood can be filled with liquid water called free water. Free water is held by adhesion and surface tension forces. Water in the cell walls is called bound water. Bound water is held by forces at the molecular level. Water molecules attach themselves to sites on the cellulose chain molecules. It is an intimate part of the cell wall but does not alter the chemical properties of wood. Hydrogen bonding is the predominant fixing mechanism.

If wood is allowed to dry, the first water to be removed is free water. No bound water is evaporated until all free water has been removed. During removal of water, molecular energy is expended. Energy requirement for vaporization of bound water is higher than free water. Moisture content at which only the cell walls are completely saturated (all bound water) but no free water exists in all lumens is called the fiber saturation point (fsp). Moisture content of individual cell walls at the fiber saturation point is usually about 30% but may be lower for other species. Fiber saturation point is important in drying because more energy is required to evaporate water from the cell wall than from the cell lumen.

2.2.2. Equilibrium moisture content

The moisture content approached by drying wood below the fiber saturation point is determined by the temperature and relative humidity of the drying air. Equilibrium moisture content (EMC) is defined as that moisture content at which the wood is neither gaining nor losing moisture. Species and previous moisture history have a slight effect on EMC. EMC is very important because of its direct relationship to drying problems. The relationship between temperature, relative humidity, and EMC can be found in the Wood Handbook (FPS, 1999) and Dry Kiln Operator's Manual (FPS, 1997).

2.2.3. Moisture removal

Water in wood normally moves from high to low zones of moisture content. The surface of the wood must be drier than the interior if moisture is to be removed. Drying can be divided into two phases: movement of water from the interior to the surface of the wood, and removal of water from the surface. Water moves through the interior of the wood as a liquid or water vapor through various air passageways in the cellular structure of wood and through the cell walls. Water moves by two main mechanisms: capillary action (liquid) and diffusion of bound water (vapor). Capillary action causes free water to flow through the cell cavities and pits. Diffusion of bound water moves moisture from zones of high concentration to zones of low concentration caused by differences in moisture content and relative humidity. When green wood starts to dry, evaporation of water from the surface cells exerts capillary forces that exert a pull on the free water and a flow results. The rate of diffusion depends largely on permeability of the cell walls and their thickness.

The process of water removal from wood also involves changing both free and bound water into free gaseous water molecules that diffuse to the external surface and then into the air. This moisture removal is caused by evaporation, capillary forces, and diffusion dependent upon the form and location of moisture in wood. Drying conditions in principle affect these mechanisms because they can alter the wood-moisture relations. In order to change the water into water vapor, energy must be added. Energy that is

applied is in the form of heat, which is transferred when the wood is contacted by the heated air. Water vapor evaporates until the air approaches saturation. The wood then becomes cooler as evaporation proceeds. As a result, heat flows from the drying air to the cooler wood flakes. This process occurs continuously as changes take place in moisture content, wood and air temperatures, and relative humidity of the drying air.

2.3. Diffusion Models

Fick's laws of diffusion have been applied to bound water diffusion in wood below fsp. The rate of bound water diffusion has been expressed as the product of diffusion coefficient and a driving force. Concentration gradient, moisture content gradient, temperature gradient, vapor pressure gradient, and chemical potential have been used as the driving force in analyzing the diffusion of moisture in wood (Siau, 1995).

Early investigators including Biggerstaff (1965), Comstock (1963), McNamara and Hart (1971), Skaar (1954), Stamm (1959, 1960), and Wengert (1977) used concentration gradient as the driving force in diffusion of bound water. This approach was successfully applied to many drying experiments. However, the diffusion coefficients derived were often strong functions of moisture content, temperature, or wood properties. Ashworth (1980) described the drying of wood by diffusion where the diffusion coefficient is a function of both moisture content and temperature.

Bui et al. (1980), Rosen (1976), Simpson (1993) and Soderstrom and Salin (1993) used moisture content gradient as the driving force in their wood drying model. Schultz and Kelly (1980) also used moisture content gradient for plywood drying while Atherton and Welty (1972) and Laity et al. (1974) used it for veneer drying. Fosberg (1970) also used the moisture gradient diffusion for wood particle drying. Langrish and Bohm (1997) investigated which best described the moisture movement in Australian hardwood timber, driving force based on gradient in moisture content or in partial pressure. The use of moisture content gradient diffusion model fitted the experimental data better than a model based on vapor pressure gradient. They noted that the use of a single moisture transport process through wood is at best only an approximation of the true behavior. The use of moisture content gradient gives questionable results since it is possible to have a moisture content gradient and yet have no appreciable flow (Wengert, 1977). With an imposed temperature gradient, net flow can be from low moisture content to high moisture content due to vapor pressure gradient (Erickson et al., 1981).

Erickson et al. (1981), Siau (1980) and Skaar and Siau (1981) explained that bound water in wood moves with temperature gradient in a non-isothermal condition. Skaar and Siau (1981) considered thermal diffusion of bound water through the cell wall of wood under a combined moisture and temperature gradients. Siau (1980) proposed that Soret potential (causing thermal diffusion) and chemical potential (resulting from gradients of water vapor pressure) are the two driving forces.

Bramhall (1976, 1979, 1995) contends that the gradient in water vapor pressure was the correct driving force for bound water diffusion. According to him, with vapor pressure-driven diffusion, the diffusion coefficient is a function of moisture content only and independent of temperature. Hunter (1993) agreed with this principle and derived a theoretical expression for the diffusion coefficient.

The chemical potential gradient was recognized by Kawai et al. (1978) as another measure of bound water diffusion driving force. Their calculated diffusion coefficients were exponentially related to moisture content. Siau (1983) also defined bound water flux in terms of chemical potential gradient. Chemical potential gradient alone accounts for the effects of both temperature and moisture content gradients. The use of chemical potential accentuates the influence of the thermal term at high wood moisture content and decreases at low moisture content. Stanish (1986) developed expressions for the net migration rate of water in bound and vapor phases through wood. Bound water diffusion is driven by chemical potential gradient while water vapor diffusion is driven by the gradient of mole fraction of water in the gas phase.

Above fsp, Spolek and Plumb (1981) proposed capillary pressure as the driving force for the movement of free water. They used capillary pressure as a function of moisture content to predict the transport of free water during the drying of softwood. The dependence of the capillary pressure on moisture content is predicted with a model and measured for isothermal movement in the tangential direction. Hunter (1995) considered the diffusion equation for the movement of water above fsp as also being driven by capillary pressure. The mass diffusivity is expressed in terms of capillarity diffusion coefficient (Hunter, 1996).

The use of integrated diffusion models has been overshadowed by the use of more sophisticated models based on thermodynamic principles. These drying models involve the series of complex interactions between liquid and vapor pressure driven flow, vapor and bound water diffusion, internal and external heat conduction, and external heat and mass transfer.

2.4. Numerical Drying Models

Drying of wood can be simulated by drying models by treating the drying phenomenon as a simultaneous process of heat and mass transfer through a multi-phase porous medium that occurs inside and outside the wood. In the past decades, many numerical models on wood drying have been developed to describe the wood drying process. Discussion of numerical drying models in this section will be limited to thin and small wood (i.e. veneer, wafers, flakes, particles, and chips). Key characteristics or components of drying models are the following: transfer mechanism of moisture movement, structural and thermodynamic assumptions, and methods of material properties, model solution, and model validation.

Latest models for drying of solid wood are given by Hukka (1996), Perre and Turner (1999a and 1999b), Tarasiewics et al. (1998). Perre and Turner (1999b) presented a three-dimensional drying model which is an improvement of a two-dimensional comprehensive drying model known as *TransPore* (Perre and Turner, 1999a). Tarasiewics et al. (1998) presented a model that describes the wood drying process as a whole system. Hukka's model (1996) analyzes the one-dimensional (along the thickness) drying of softwood above the boiling point of water. This model was revised using parameters derived from drying experiments (Hukka, 1997). The performance of 12 wood drying models developed between 1986 to 1994 was compared to a common set of drying data by Kamke and Vanek (1994). Variability among simulation was observed and most results were not in agreement with experimental data. Uncertain coefficients used by the models, degree of simplifications, and different ways of solving the heat and mass transfer equations were cited as explanations to the discrepancies. Earlier lumber drying models were developed by Plumb et al. (1985), Spolek and Plumb (1980), and Stanish et al. (1985, 1986). These are one-dimensional models that simulate the drying of wood also based on the fundamental heat and mass transfer.

2.4.1. Transfer mechanism and driving force

Modeling is complicated because more than one mechanism may contribute to the local flow and the contribution of different mechanisms may change as the drying process proceeds. The development of a generally applicable drying model requires the identification and inclusion of all contributing mechanisms. Evaporation rates are determined locally by the interaction of heat flows, moisture flows, and temperature changes. Driving forces may include heat and mass transfer, capillarity and diffusion due to gradients in chemical potential, concentration, pressure, moisture content, and temperature.

The drying process occurs due to external and internal evaporation, capillarity of free water, and the diffusion of bound water and water vapor. Migration of free water is by total pressure gradient (Di Blasi, 1998; Dorri, 1983; Fyhr and Rasmuson, 1996; Pang, 1996; Souza and Nebra, 2000). Kayihan and Stanish (1984) combined free and bound water and assumed they migrated due to a potential difference. Fyhr and Rasmuson (1996) disregarded the contribution of vapor to the total moisture content.

Pang (1996) and Souza and Nebra (2000) used the diffusion of bound water due to chemical potential gradient while Di Blasi (1998) used the gradient proportional to concentration. Transport of bound water was due to gradient in moisture content (Fyhr and Rasmuson, 1996) or temperature (Dorri, 1993). Dorri (1983), Di Blasi (1998), Kayihan and Stanish (1984), Pang (1996) and Souza and Nebra (2000) used diffusion of vapor due to partial pressure gradient in modeling the drying of veneer, flakes, and particles.

According to Alves and Figueiredo (1989), the drying of wood at high temperature (above the water boiling temperature) is controlled by heat supply and vapor-liquid equilibrium alone. Water vapor movement, bound water movement, and pressure gradients are negligible if the following conditions are fulfilled: a) drying temperature is greater than 150°C, b) the initial wood moisture content is below the free water continuity point (~0.45), and c) the sample dimension in the wood longitudinal direction is not much greater than the dimensions in the transverse directions.

Saastamoinen and Impola (1995) ignored mass transfer in steam and air high temperature drying since they claim the drying occurs at or close to the boiling point. For them, drying with high temperature, it is enough to solve the rate of heat transfer, which equals the required heat for heating and evaporation.

2.4.2. Model assumptions

Numerical solutions are difficult to obtain if simplifying assumptions are not made. Thus, several thermodynamic assumptions are made in modeling studies in wood drying. Gas, liquid and solid are considered separate phases. Local phase equilibrium and ideal gas behavior of vapor and air are also assumed. Three states of water in wood chips are considered: free water, bound water, and vapor. All three phases are assumed to be thermodynamic equilibrium at the local temperature (Alves and Figueiredo, 1989; Di Blasi, 1998; Dorri, 1983; Fyhr and Rasmuson, 1996; Kayihan and Stanish, 1984; Pang, 1996; Saastamoinen and Impola, 1995; Souza and Nebra, 2000).

In many cases, the solid material and water are assumed to comprise a homogeneous body at macroscopic level. Alves and Figueiredo (1989) and Fyhr and Rasmuson (1996) assumed that the initial solid is homogeneous. Kayihan and Stanish (1984) represented wood in terms of a rigid hygroscopic porous solid structure. Di Blasi (1998) modeled the drying medium as a solid matrix where the void is initially filled partly by an inert gas and partly by liquid water.

In general, wood is three-dimensional and can be of irregular shape. More easily defined geometry such as a slab, cylinder, or sphere is used to represent the solid, and moisture flux is assumed to occur on one direction only. One-dimensional models for wood particles were developed by Alves and Figueiredo (1989), Di Blasi (1998), Dorri (1983), Melaaen (1996), Saastamoinen and Impola (1995) and Souza and Nebra (2000). Heat and mass transfer are considered to occur preferentially in the transverse direction only except for Dorri's model, in which occurs in the longitudinal direction. Pang (1996) presented a one-dimensional model for veneer since width and length are two orders or more than thickness.

Two-dimensional wood particle drying models were developed by Dorri (1983), Fyhr and Rasmuson (1997), and Kayihan and Stanish (1984). Multidimensional model was used because of the strong anisotropicity of wood and magnitude of flow of liquid, gas, and heat are very dependent on the direction. Longitudinal and transverse directions were considered by Fyhr and Rasmuson (1996) and Dorri (1993). On the other hand, both transverse directions were modeled by Kayihan and Stanish (1984).

No material shrinkage was assumed by Alves and Figueiredo (1989), Fyhr and Rasmuson, (1996), Kayihan and Stanish (1984), and Souza and Nebra (2000) in their model. Solid volume is assumed to be constant throughout the drying process. Adsorbed water does not occupy any accessible volume. Free water and vapor share the available void space. The problem with this assumption is that no change in solid volume can lead to significant errors in drying of materials that really shrink, which actually happens in wood.

2.4.3. Wood properties required as inputs

Properties of wood required for the application of drying models include thermal properties, permeability, moisture sorption isotherm relationships, and mass transfer coefficients, among others. Most of these properties are taken from literature while the authors themselves experimentally derive some of them.

Thermal conductivity was taken from the Wood Handbook (USDA, 1974) while the specific heat was taken from Siau (1971) by Souza and Nebra (2000). Thermal conductivity of wood by Perre et al. (1993) was used by Fyhr and Rasmuson (1996). Thermal conductivity and specific heat values for the drying and pyrolysis model of Melaaen (1996) were taken from Kansa et al. (1977). Thermal conductivity, specific heat, gas permeability, and diffusion coefficient were taken from Siau (1971) by Dorri (1983). Kayihan and Stanish (1984) used Siau's (1971) suggestion for specific heat of moist wood and Wood Handbook (USDA, 1974) for correlation of thermal conductivity. Other properties were also taken from literature such as the simple correlation for water vapor diffusivity while correlating functions for vapor and liquid phases equilibrium and

heat of vaporization. Thermal conductivity of pine and convective heat transfer coefficient were experimentally determined by Alves and Figueredo (1989) while other parameters were taken from literature: specific heat and enthalpy of vaporization (Siau, 1984), and enthalpies of reaction (Beall, 1971).

EMC is related to temperature and relative humidity. The local vapor and bound water phases must be consistent with sorption isotherms at local temperature to satisfy the equilibrium requirement. Souza and Nebra (2000) and Pang (1996) used the thermodynamic relationship of moisture content-temperature-relative humidity given by Simpson and Rosen (1981). Fyhr and Rasmuson (1996) used the equilibrium between bound water and steam as investigated by Bjork and Rasmuson (1995). Alves and Figueiredo (1989) used the equilibrium moisture content as a function of temperature (above 100°C) given by Kent et al. (1981). Moisture sorption isotherms from Skaar (1972) were used by Kayihan and Stanish (1984) in their model. Desorption isotherm for Sitka spruce (Stamm, 1964) was used in the model by Dorri (1983).

Pang (1996) used external mass transfer coefficient over a flat surface that was converted from measured values and heat transfer coefficient is derived from Chilton-Coulborn analogy. Saastamoinen and Impola (1995) used the Ranz Marshall correlation for the heat and mass transfer coefficient of spherical particles. Experimental mass transfer coefficients were determined by Kayihan and Stanish (1984) using napthalene balls. Experimental Sherwood number was then correlated with Reynolds and Schmidt numbers. The functional form was assumed to follow spherical bodies and flat plate for sawdust-like and flake-like particles. Then by analogy, the heat transfer coefficients were calculated.

2.4.4. Model solution

Combination of flux equations with mass and energy balance equations gives rise, in general, to a system of non-linear partial differential equations which is difficult to solve. Numerical techniques such as finite difference approximations and finite element analysis are usually used to solve these systems of equations.

Implicit finite volumes method was used by Souza and Nebra (2000) to numerically solve the systems of equations system solved and converged by the TDMA line-by-line method. Each partial differential equation is transformed into algebraic equations by the discretization of time and thickness into control volumes. An algorithm solves the basic equations and equilibrium correlations separately at each time increment.

Di Blasi (1998) solved the equations through two stages according to the method of operator splitting. The first stage accounts for the evaporation process and the second stage accounts for the transport phenomena. Ordinary and partial differential equations of the first and second stages are solved through a semi-implicit procedure.

Non-linear coupled equations in Fyrh and Rasmuson's model (1996) are numerically solved using finite difference method. The control domain is discretised into smaller control volumes for which calculations are made. Calculations are made with a computer code called TOUGH (Transport of Unsaturated Groundwater and Heat) which is modified to simulate the drying of wood.

Simulation of wood particle drying is solved on a one-dimensional fixed Cartesian grid in space (Melaaen, 1996). Convective terms are discretized by first-order upwinding and whole central differencing is used for diffusive terms. Differential/Algebraic System Solver (DASSL) was employed for integrating the equation in time.

Equations of Saastamoinen and Impola (1995) are integrated numerically and iterative calculations are required in order to relate the evaporation rate to the evaporation temperature and to the location of the evaporation front. In the first stage, the evaporation rate at a time instant is solved. Then the new temperature of the evaporation front and saturation pressure is calculated. The moisture content is then calculated.

System of equations which constitutes model of Alves and Figueiredo (1989) was solved using the Crank-Nicholson method. This method is often used for solving partial differential equations in one spatial dimension. It provides an implicit scheme that is accurate in both space and time.

Three nonlinear equations plus equilibrium relations, physical property correlations and convective boundary conditions in the model of Kayihan and Stanish (1984) were solved simultaneously through a finite difference approach. Partial differential equations were transformed into ordinary differential equations using a discrete space compartment and continuous time approach.

Discretization of the system of nonlinear partial differential equation using an implicit finite difference technique was employed by Dorri (1983). The resultant systems of algebraic equations were solved using direct inversion together with an iterative method to account for nonlinearities.

2.4.5. Model validation

Numerical drying models that were developed must also be assessed for their validity. Comparison of simulated drying curves with experimental curves gives one measure of model validity. Comparison of actual and predicted moisture profiles gives a second measure of model validity. However, experimental measurement of moisture profiles in thin and small wood is difficult and has limited the ability to validate drying models. Most of the researchers did their own experiments to validate their model or just compared their simulations with reported literature.

Pang et al. (1997) performed industrial-scale drying tests on radiata pine (Pinus radiata) veneer sheets to verify their model. Close agreement between measured and predicted moisture content was achieved. Birch (Betula spp.) and pine (Pinus silvestris) were used in drying experiments that were carried out in a thermobalance by Saastamoinen and Impola (1995). There were also good agreement between calculations and measurements. Pine (Pinus pinaster) was also used by Alves and Figueiredo (1989) in thermogravimetric experiments using a vertical cylindrical refractory steel furnace.

Drying of wood at high temperature can be well simulated by their model but there was an effect of model simplification. There was a delay in simulating the beginning of drying since the model has to wait for the solid to reach 'boiling temperature' before drying starts.

An experimental device was developed by Fyhr and Rasmuson (1996) for simultaneous measurement of weight, center pressure and temperature during drying. Moisture content, temperature, and pressure curves of single spruce (Picea abies) chips were in fair agreement with simulations. Fyhr and Rasmuson (1997) performed the same drying simulations on experiments on pine and spruce to validate the same model and to determine the effect of permeability and different species. Effect of thickness and length of the wood chips were also studied. Comparisons between experiments again showed good agreement.

Experimental drying tests were performed by Kayihan and Stanish (1984) on sawdust and flake-like particles. Simulations on sawdust drying for different particle sizes, temperature and initial moisture contents were in agreement with experimental data. However, flake drying simulations were less effective in matching measured data.

Experimental results for Virginia pine (Pinus virginiana) by Kayihan (1982) were used by Souza and Nebra (2000) to validate their model. Results of the numerical simulations showed a good agreement with the experimental data. Model of Di Blasi (1999) reproduced well the thermal response of moist wood under similar conditions observed in experiments by Chan et al. (1988), Fredlund (1993), Kanury and Blackshear (1970), Lee and Diehl (1981), Sahota and Pagni (1979), Simms and Law (1966) and White and Schaffer (1981). The numerical model developed by Dorri (1983) was compared to the experimental results of Malte et al. (1976). The agreement between the numerical results and experimental data was also good.

Numerical models are very effective in explaining and predicting the drying behavior of thin and small wood. However, the large number of parameters and the differential equations are very complicated, thereby limiting its practical application.

2.5. Empirical Models

The evaluation of drying rate is very useful in understanding the mechanism of moisture movement within wood as well as the transport of moisture from the wood to the surrounding air. A drying rate curve is derived by drawing tangents from the drying curve (moisture content versus time) at various points along the length and plotting the slopes of the tangents against the corresponding moisture contents. Also, regression of the points in each interval of moisture contents gives an estimated slope of the drying curve and thus, the drying rate for the midpoint moisture content of the interval. Ideally, the drying curve is characterized by an equation that could then be differentiated to determine the drying rate curve.

Different forms of equations have been used to characterize the drying of wood. Logarithmic/exponential, linear and polynomial functions have been suggested for drying of wood. This section will dwell on these different functions to describe the drying process.

A very simple but useful empirical approach has been the assumption that the drying rate is proportional to the average moisture content during the falling rate period. This is expressed as:

$$\frac{dM}{dt} = -kM \qquad \text{(Eq. 2.1)}$$

where: M is moisture content

t is time

k is an empirical constant

This is a differential equation because it expresses a relationship between a function and its derivative. Putting the terms containing moisture content on the left hand side and those containing time on the right:

$$\int \frac{dM}{M} = -\int k dt \qquad \text{(Eq. 2.2)}$$

$$\ln \frac{M}{M_o} = -kt \qquad \text{(Eq. 2.3)}$$

$$\frac{M}{M_o} = \exp(-kt) \qquad \text{(Eq.2.4)}$$

Defining the left side as E, relative moisture content, the equation becomes:

$$E = \frac{M - M_e}{M_o - M_e} = \exp(-kt) \qquad \text{(Eq.2.5)}$$

where: M_e is equilibrium moisture content

M_o is initial moisture content

The equilibrium moisture content (M_e) is a function of drying medium temperature and relative humidity. The empirical constant, k, is experimentally determined by regression analysis as a function of wood species, material geometry, and external factors (i.e. temperature, relative humidity, air velocity).

This function was also used by Silitonga (1983) in determining the drying rate of aspen, balsam fir, and red pine wood chips. Relative moisture content versus time plot indicated a nonlinear relationship. A natural logarithmic transformation of the relative moisture content was performed to linearize the data. Using standard error of estimates of the slopes and coefficient of determination, the transformed data fit the data very well. The final model selected to describe the natural logarithm of the relative moisture content versus time for wood chip drying is given as:

$$E = \beta_o \exp(-\beta_1 t) \qquad \text{(Eq.2.6)}$$

where: β_o and β_1 are regression coefficients.

Tschernitz and Simpson (1979) used the same function to correlate the drying rate of northern red oak lumber but added board thickness and empirical thickness coefficient to the equation in order to establish the thickness effect of lumber:

$$E = \exp(\frac{-kt}{l^n}) \qquad \text{(Eq.2.7)}$$

where: l is board thickness

n is an empirical thickness coefficient

There was a deviation between the experimental and calculated values of E, due largely to the simplicity of the model. The model was also tested to predict the drying time of red oak lumber. Drying time was calculated and compared to actual drying time from previous experiments of Cuppert and Craft (1972), McMillen (1969), Rice (1971), and Wengert (1971). Actual drying times were greater than the calculated drying time. The author cited several reasons for the discrepancies including oversimplification of the model and that air velocity and length of air travel may be responsible for the difference.

Rosen (1978) presented a two-parameter model for jet drying of lumber. The equation relating E to time is:

$$E = 1 - E_o \int \exp(-at^{1/b})dt \qquad \text{(Eq.2.8)}$$

where: E_o is initial drying rate

$$E_o = \frac{ab}{b\Gamma(b)} \qquad \text{(Eq.2.9)}$$

a is rate factor

b is bend factor

Γ(b) is gamma function of b

The parameters a (rate factor) and b (bend factor) are related to the external drying conditions and wood properties, respectively. The drying rate then is:

$$E = \frac{-dE}{dt} = E_o \exp(-at^{1/b}) \qquad \text{(Eq.2.10)}$$

Approximations of the equation for short and long drying times were presented (Rosen, 1980a). The equation was fitted to literature data for jet-, kiln-, press-drying of wood and wood-based materials (Rosen, 1980b). The equation fit the drying curve of wood and wood-based materials based on the different drying techniques very well. DRIFIT, a computer program based on Rosen's model was developed by Chen (1980). The software was used to evaluate drying rates and drying times of press-dried boards.

Experimental convective drying data of Douglas-fir sawdust and flakes were fit in an empirical expression by Malte et al. (1984). An expression was obtained for nearly steady-state environmental conditions of temperature and relative velocity:

$$\frac{dM}{dt} = A[1-\exp(-bM)] \qquad \text{(Eq.2.11)}$$

It indicated that A was in agreement with engineering heat and mass transfer prediction and Ab was in agreement with mass diffusion rates for wood. A and b are empirical parameters which depend on particle size and shape and gas temperature, respectively.

Drying rate of wood has been described as a linear function of moisture content. Drying rate of veneer is a linear function of moisture content comprised of two falling rate periods described by Comstock (1971) as:

$$-\frac{dM}{dt} = A + BM \quad \text{for M>C} \qquad \text{(Eq.2.12)}$$

$$-\frac{dM}{dt} = \frac{A+BC}{C} * M \text{ for M<C} \qquad \text{(Eq.2.13)}$$

This allows specimens of different initial moisture content of the same density and thickness to be described by this equation. The intercept A is related to temperature and air velocity. Slope B is linearly related to velocity only. Point C is the break point where the two equations meet. These drying equations were employed by Resch and Scheurman (1977) in simulating the drying of veneer in jet dryers.

Pang et al. (1997) proposed that the three drying periods (constant rate, first falling rate, second falling rate) based on simulated drying of veneer be expressed by the following equations:

$$-\frac{dM}{dt} = j_o \quad \text{for M>M}_{cr1} \qquad \text{(Eq.2.14)}$$

$$-\frac{dM}{dt} = A + B*M \text{ for M}_{cr1}\text{>M>M}_{cr2} \qquad \text{(Eq.2.15)}$$

$$-\frac{dM}{dt} = \frac{A+B*M_{cr2}}{M_{cr2}-M_e} * (M - M_e) \quad \text{for M<M}_{cr2} \qquad \text{(Eq.2.16)}$$

where: j_o is constant drying rate

M_{cr1} is the first critical moisture content

M_{cr2} is the second critical moisture content

Similar to Comstock's model (1971), constants A and B also vary with veneer thickness, wood density, and drying conditions.

Polynomial equations have also been used to describe the drying the wood. Polynomials are used to describe curvilinear relationships. Drying curve of aspen wafers (Laytner, 1989) were fitted in a 5^{th} order polynomial equation in the form:

$$M = \beta_o + \beta_1 t + \beta_2 t^2 + \beta_3 t^3 + \beta_4 t^4 + \beta_5 t^5$$

where: β_o is the intercept

β_1, β_2, β_3, β_4, β_5 are regression coefficients

The drying rate curve was based on the differentiation of the polynomial equation.

These empirical functions were tested to describe the drying of flakes. The equation that gives the best fit to the experimental data is selected as the function that will characterize the flake drying process.

2.6. Drying of Thin and Small Wood Materials

Typically wood drying is divided into two distinct zones: a constant rate period and falling rate period. Under constant drying conditions most wood products show an initial constant rate period. In this period the external drying conditions (i.e. temperature, gas velocity, total pressure, and relative humidity) control the rate of drying. The controlling resistance may be associated with the transfer of energy to the solid, or the transfer of mass away from the solids. All energy transferred to the wood being dried is used in the evaporation of water. The water is replenished by the capillary flow of water from the interior of the material being dried. Mass transfer during the constant rate period involves diffusion of water vapor from the material surface through a boundary layer into the drying medium. The duration of this period depends on the rate of migration of water from the interior of the material. This rate is determined by porosity, specific gravity, and cell morphology. The surface of the material at this stage is covered with a film of water, so the rate of drying is equal to the rate of evaporation of liquid water heated by the drying air stream. The drying will remain constant until a decreasing rate period starts. The point at which the constant rate period ends and the falling rate period begin is called the critical point. The critical moisture content is the amount of water at that point.

The rate of moisture transport in the falling rate period is limited by the ability of the water to diffuse through the wood to its surface. The surface of the wood is not covered with a thin layer of water during this period. This period is characterized by decreased wetted surface area drying and internal diffusion of water. The capillary system becomes discontinuous as the wood dries out and air replaces the water wicked to the surface and thus unable to maintain a completely wetted surface. The drying rate is still proportional to the external driving force but the wetted surface area from which evaporation takes place is constantly decreasing. A drying front is formed below the surface once the flow of water to the surface has been completely interrupted by the intrusion of air in the capillary system. As free water recedes deeper, the drying front progresses toward the core until the material has reached an EMC with the external

drying conditions. Drying is controlled by the diffusion of water from the wet core to the surface during this period. The drying rate decreases with time and the rate of internal mass transfer to the wood surface typically controls the process. A falling drying rate may be observed when external mass transfer resistance is controlling factor and the surface vapor pressure of the solid is decreasing as moisture content drops.

Pang et al. (1997) divided the drying process of Radiata pine veneer sheet dried at 150 and 200^{o} C with an impinging air velocity of 12.3 m/sec also into three periods plus a short inducing period: a constant rate period followed by the first then a second falling rate period. In the constant rate period, liquid water vaporization occurs just beneath the surface layer. At the start of the first falling rate period, water deeper from the wood surface evaporates and temperature starts to rise. In the second falling rate period, bound water diffusion controls the drying rate, and the drying rate drops sharply. Constant rate drying period was not observed during the drying of Douglas-fir, loblolly pine, and yellow birch veneer using high temperatures and air velocity jets impinging at an angle of 90^{o} to the surface (Comstock, 1971). Rate of drying began to decrease immediately after the warm-up period ended. Results of the kinetic studies indicate that internal diffusion of moisture certainly does not control drying rate of veneer. External heat transfer is more important in controlling the drying rate. Thermal conduction through the wood to the zone of water vaporization is also important.

Fyhr and Rasmuson (1996) divided the steam drying of wood chips between 150 and 180°C into three stages: heatup period, constant rate period, and falling rate period. Condensation initially increases the moisture content during the heatup period. External heat transfer is the controlling mechanism in the constant rate period. Falling rate period is controlled by internal mass transfer.

Simulated drying rate of wood chip dried at 115°C (388.15°K) is close to constant when the liquid water is transported to the surface before evaporation (Melaaen, 1996). All evaporation appears at the surface and there is almost no movement of the gas mixture. Drying rate is reduced when bound water exists at the surface and the increase in convective gas mixture flux is extensive. Constant drying rate was observed by

Kayihan and Stanish (1984), Malte et al. (1983) and Souza and Nebra (2000) for sawdusts and flakes. Gas temperature for sawdusts ranged from 90-265°C (363-538°K) and 190-290°C (463-563°K) for flakes. Interpretation and analysis of the measurements indicated that heat transfer controlled drying occurred above critical moisture content. Below the critical moisture content, particle drying rate was controlled by internal moisture diffusion. Tangential diffusion occurred in thin flakes and longitudinal diffusion for large and medium sawdusts. Constant rate of drying was also observed by Silitonga (1983) on wood chips dried at 37.8°C (100°F). The decreasing rate begins long before the fiber saturation point has been reached. The decreasing rate for Balsam fir and red pine began when the moisture content was approximately 60% irrespective of the initial moisture content.

No constant rate of drying was observed by Alves and Figueiredo (1989), Di Blasi (1998), and Saastamoinen and Impola (1995) in the high temperature drying of wood particles. Gas temperature varied between 50-327°C (323-600°K). Absence of constant rate period for wood chips dried at 65.5°C and 93.3°C was related to the presence of moisture gradient in the chips or possibly to temperature gradient (Silitonga, 1983). The temperature of the wet surface of the chips was maintained at wet bulb temperature while the temperature of the dry areas increased above the wet bulb temperature.

Constant rate period was also not observed during drying of aspen wafers dried at 90, 120 and 150°C (Laytner, 1989). The gradual retreat of the air/water interface into the pores near the surface prevented a true constant rate period. There was no sharp inflection in the drying rate curve and were parabolic in shape. This indicated a gradual transition from one drying mechanism to the next at the same time overlapping of drying mechanisms due to uneven drying. The implication is that the dominant but not exclusive drying mechanism is unsaturated surface drying of capillary-driven free water high moisture contents coupled with contribution by free water moisture transport along the internal longitudinal pathways continues to prevail down to about 30% moisture content. Internal vapor transport of bound water controls the drying rate as the moisture content approaches zero.

2.6.1. Effect of external drying conditions

Influence of process variables on drying time and drying rate is of considerable interest and practical importance with dryer operation and design. External drying conditions relevant to the drying process of thin and small wood include temperature, airflow and velocity, humidity, and drying medium.

Temperature, by virtue of higher thermal energy and related mass transfer driving forces at higher temperature has an effect on drying time and rate. Temperature was found to have a significant influence on the total drying time of thin and small wood based on experiments and simulations (Anand et al., 1980, Atherton and Welty, 1972; Comstock, 1971; Di Blasi, 1998; Fyhr and Rasmuson, 1996; Johansson et al., 1997; Laity et al., 1974; Laytner, 1989; Malte et al., 1977a and 1977b; Saastamoinen and Impola, 1995; Silitonga, 1983; Tschernitz, 1985). An increase in temperature while keeping other variables constant decreases the drying time. Increase of drying temperature from 90 to 120°C produced a greater reduction in drying time of aspen wafers than an increase from 120 to 150°C (Laytner, 1989). Similar observation was made on wood chips wherein half drying time decreased very rapidly when temperature increased from 100 to 150°F but the decrease is less as the temperature increased to 200°F (Silitonga, 1983). Douglas-fir veneer dried in superheated steam at 400, 600, and 800°F resulted in drying times of 6, 3, and 1.5 minutes, respectively (Atherton and Welty, 1972).

Temperature has a non-linear effect on drying rate. The increase in drying rate of wafer is not the same for each 30°C increase in air temperature between 90 and 150°C (Laytner, 1989). Linear relationship between drying rate of veneer and temperature only holds true for temperature above 100°C (Comstock, 1971).

Increase of steam or air velocity reduces drying time of wood chips significantly (Fyhr and Rasmuson, 1996; Johansson et al., 1997; Malte et al., 1977). The effect of airflow is only important at lower velocity and additional airflow is less effective in increasing drying rate of wood chips (Silitonga, 1983). At lower velocity, the air created turbulence, thus breaking up the boundary film on the chip surface that may hinder heat and moisture transfer, hence retarding the drying rate. Anand et al. (1980), Comstock

(1971), Laity et al. (1974) also showed that airflow or velocity had an effect on the drying rate of veneer.

Humidity was shown to influence the drying rate of wood chips (Johansson et al., 1997) and veneer (Anand et al., 1980). The period of constant drying rate in wood chips becomes more significant with increasing humidity of the drying medium. Increased humidity also leads to lower drying rate during the initial falling rate period whereas the drying rate is independent of the humidity on the last stage of the falling rate period. Humidity above 100°C was found to be not significant on the drying rate of thin and small wood (Laytner, 1989). Water vapor diffusion is not a limiting factor since water vapor that evaporated at the drying front or from the cell walls is transported mainly by bulk flow. At temperatures above 100°C, the quantity of water vapor that could exist in air increases rapidly with increasing temperature thus, the humidity of the drying medium is no longer a significant process variable.

Air and steam was compared as a drying media for wood chips (Fyhr and Rasmuson, 1997) and veneer (Laity et al. 1974). Shorter period of constant rate drying, faster drying rate, and shorter drying time are obtained for wood chips dried in air than in steam. Likewise, Douglas-fir and Southern pine veneer dried faster in air than in steam. The difference can be assigned to the properties of the drying medium.

2.6.2. Effect of material properties

Properties of wood play a very important role in affecting drying rates. There are several properties that may affect drying properties: density, initial moisture content, and dimensions. Most of these properties may vary between species and within the same species. Fyhr and Rasmuson (1997) attributed the difference in drying properties between species (i.e. pine versus spruce) to their absolute permeability. Absolute permeability of the liquid phase is often higher for wood of lower density. However, due to its tendency to aspirate, the gas phase permeability is usually lower than for higher density wood. That is why total drying time is about 5% shorter for pine wood. Constant rate drying is longer for pine due to its higher permeability which allows the capillary forces to keep the surface above the fsp for a longer time. Drying in the falling rate

period is also faster for pine since the longitudinal permeability is greater than for spruce.

Initial moisture content, fractional void space, quantity of bound water per unit volume and other properties of wood are all related to its density. Wood density has a significant effect on the drying time. An increase in drying time or slower drying is expected as density increases due to more water present in wood for a given moisture content. As density increased, the effective thermal capacity of the medium also becomes larger and the drying process successively slower (Di Blasi, 1998). An almost linear variation of the drying time with density is observed.

It is expected to have an increase in drying time as initial moisture content increases because there is more water to be evaporated. According to Comstock (1971), for veneer of the same density and thickness, samples having different initial moisture content will follow the same drying rate curve. This curve is described as a linear function of moisture content.

The effect of thickness on drying rate of thin wood is predominantly on the quantity of water that must be removed per unit of surface area. General trends from Fyhr and Rasmuson (1997) draws that when thickness is doubled, the total drying time is approximately doubled. The opposite is also valid when the thickness is halved.

Total drying time is not as sensitive to wood chip length as to the thickness (Fyhr and Rasmuson (1997). Total time is affected only by a factor of 0.75 when the length is halved. This is due to the main input of heat, namely through the surface perpendicular to the transversal direction, increases or decreases in the same manner, even though the total volume of the chip changes. The effect of length on drying rate of aspen wafers is not linear (Laytner, 1989) especially at higher moisture content. Change in wafer length from 25 to 44 mm gave a significantly larger decrease in drying rate than the change from 44 to 63 mm. This is due to a developing boundary layer effect associated with external heat and mass transfer. Residual length effect is caused by the moisture transport along the internal longitudinal pathways that serve as additional moisture outlets. The longer the wafer, the greater the resistance thus, smaller contribution to the total drying rate.

2.6.3. Drying experiments on thin and small wood

There is no systematic experimental procedure to determine the effects of external conditions and wood properties on the drying characteristics of thin and small wood materials. The use of a thermobalance to a sophisticated drying apparatus has been used in determining the weight as well as temperature and pressure inside small wood particles. A thermobalance was used by Saastamoinen and Impola (1995) in experiments for wood particle drying. Thermogravimetric experiments were carried out inside a vertical cylindrical steel reactor by Alves and Figueiredo (1989), Malte et al. (1977) and Silitonga (1983). Industrial-scale experiments were done in a commercial veneer dryer by Pang et al. (1997).

Fyhr and Rasmuson (1996) used an experimental device that can simultaneously measure the weight, temperature, and center pressure during the drying of a single wood chip. The apparatus was built for pressures up to 10 bars and steam is produced by an electrically heated boiler. Temperature could be maintained between 100 and 200°C. Wood chip is mounted on a capillary tube. One end of the capillary tube is located at the center of the chip and the other is mounted on a load cell, which registers the weight loss during drying. A thermocouple is inserted through the capillary in order to measure the temperature in the center of the chip. The pressure in the center is transferred through oil in the space between the thermocouple and the capillary wall.

A drying apparatus was assembled by Laytner (1989) so that a wafer could be dried in an air stream having constant temperature, humidity, and direction of flow at the same time monitoring its weight loss. A convection oven was modified to provide unidirectional flow of air. A wafer to be dried is attached to one end of a wire that ran through the exhaust vent at the top and hooked to the bottom of an electronic balance. Temperature of circulating air is monitored by a thermocouple.

Drying apparatus used by Kayihan and Stanish (1984) can monitor the weight and temperature of the specimen. Wood specimen was hung vertically on a hangdown wire connected to an electronic balance. An infrared thermometer was used to measure the surface temperature as the specimen was dried.

Based on the information gathered from experiments as well as from simulations, drying mechanisms can be identified. Weight measurements are used to calculate moisture content. Measurement of specimen temperature during drying will help to identify whether a process is controlled by heat or mass transfer. A specimen temperature equal to the wet-bulb temperature of the surrounding medium is characteristic of heat transfer control. If the specimen reaches the dry bulb temperature of the drying medium, mass transfer is suggested.

2.7. Bending Properties

Temperature and moisture content have important effects on the mechanical properties of wood. In general, mechanical properties decrease when the wood is heated and increase when it is cooled. As long as temperatures do not exceed 100°C, there is little permanent strength loss. However, exposure to high temperatures for long periods can cause permanent strength loss (Haygreen and Bowyer, 1996). Almost all mechanical properties of wood increase as moisture decreases below the fsp.

At constant moisture content and below approximately 150°C, mechanical properties are approximately linearly related to temperature. Below 100°C, the change in properties that occurs when wood is quickly heated or cooled is essentially reversible, the property will return to the original value at the original temperature if the change in temperature is quick (FPS, 1999). At high temperature, there is an irreversible effect of strength loss. This permanent effect results in loss of weight and strength due to degradation of the wood substance. Loss may depend on moisture content, heating medium, temperature, and exposure period and may also include species and size involved.

Comprehensive reviews of the effect of temperature and moisture content on the mechanical properties of wood were made by Gerhards (1982) and Salamon (1969). Relevant studies reported in the literature on several mechanical properties of clear wood in relation to moisture content and temperature were summarized by Gerhards (1982). The following mechanical properties were included in the review: modulus of elasticity parallel to the grain, modulus of elasticity perpendicular to the grain, modulus of rigidity, modulus of rupture, tensile strength parallel to the grain, tensile strength perpendicular to the grain, maximum compressive strength parallel to the grain, shear parallel to the grain, and compressive strength at the proportional limit perpendicular to the grain. Moisture content has an effect on almost all mechanical properties. Temperature generally tends to have a greater effect at higher moisture contents.

Salamon (1969) reviewed the quality of softwood and hardwood thin boards and dimension lumber dried at constant high temperatures and under a varied level of low-high temperatures and humidity. It was reported that lumber dried at high temperature showed excessive degrade while moderate temperature produced comparable losses to conventional-dried materials. Softwood boards were dried successfully with acceptable quality while hardwood boards needed air-drying to prevent quality degradation due to high temperature. Some species do not lose strength when dried at high temperature but others lost 7 to 20% compared to conventional-dried samples.

Current research relating mechanical properties have focused not on flakes but on wood composite panels. Wu (1999) studied the effect of flake orientation, density gradient across panel thickness, and resin content on linear expansion and bending properties of single-layer OSB. MOE and MOR varied with flake orientation, and density. Effect of resin content on MOE and MOR was relatively small.

Tabarsa and Chui (1997) studied the effect of transverse compression and press temperature on springback, compression set, density, EMC, MOE, and MOR of wood composites. They indicated that no further improvement in mechanical properties of wood composite panels can be achieved if these are hot-pressed beyond 150^{o}C.

Xu and Suchsland (1998) developed an analytical model to predict the MOE of wood composites panels. Simulation showed that the MOE of particleboard decrease as average orientation angle of particles increase. In OSB, MOE increased as orientation angle increased.

The predictive equations expressing the bending properties and thickness swelling as a function of moisture content and MOE/MOR loss as a function of thickness swelling were established for various products (Wu and Suchsland, 1997; Wu, 1998). MOE and MOR decrease with increase in board moisture content.

Only research on properties of flakes was done by Plagemann (1982). He assessed the effect of high temperature drying on the chemical (acid and base buffering capacities and soluble, bound, and total acid contents) and mechanical (MOE and MOR) properties of flakes. Changes in these properties were correlated with board properties such as MOE, MOR, wet MOR, and internal bond. Red oak, white oak, and sweetgum flakes dried at 20, 150, and 350°C were tested. Bending tests indicated that the strength and stiffness of the flakes were adversely affected by high temperature drying. However, the effect did not manifest itself on the panels.

2.8. References

ALVES, S.S. and J.L. FIGUEIREDO. 1989. A model for pyrolysis of wet wood. Chem. Engg. Sci. 44(12): 2861-2869.

ANAND, V., G.D. SURENDER and V.J. VICTOR. 1980. Investigation of the kinetics of jet drying of veneer. Drying '80 Vol. I. Developments in Drying. pp. 443-450.

ASHWORTH, J.C. 1980. Design of drying schedules for kiln-drying of softwood timber. Drying '80 Vol. I. Developments in Drying. pp. 431-442.

ATHERTON, G.A. and J.R. WELTY. 1972. Drying rates of Douglas-fir veneer in superheated steam at temperatures to 800°F. Wood Sci. 4(4): 209-218.

BANERJEE, S., W. SU, M.P. WILD, L.P. OTWELL, M.E. HITTMEIER and K.M. NICHOLS. 1998. Wet line extension reduces VOCs from softwood drying. Envi. Sci. Tech. 32(9): 1303-1307.

BANERJEE, S., M. HUTTEN, W. SU, L. OTWELL and L. NEWTON. Release of water and volatile organics from wood drying. Envi. Sci. Tech. 29(4): 1135-1136.

BEALL, F.C. 1971. Differential calorimetric analysis of wood and wood components. Wood Sci. Tech. 5(3): 159-175.

BIGGERSTAFF, T. 1965. Drying diffusion coefficients in wood as affected by temperature. For. Prod. J. 15(3): 127-133.

BJORK, H. and A. RASMUSON. 1995. Moisture equilibrium of wood and bark chips in superheated steam. Fuel 74: 1887.

BRAMHALL, G. 1995. Diffusion and drying of wood. Wood Sci. Tech. 29(3): 209-215.

BRAMHALL, G. 1979. Sorption diffusion in wood. Wood Sci. 12(1): 3-13.

BRAMHALL, G. 1976. Fick's laws and bound water diffusion. Wood Sci. 8(3): 153-161.

BUI, X., E.T. CHOONG, and W.G. RUDD. 1980. Numerical methods for solving the equation for diffusion through wood during drying. Wood Sci. 13(2): 117-121.

CHAN, W.R., M. KELBON and B.B. KRIEGER-BROCKETT. Single-particle biomass pyrolysis: Correlation of reaction products with process conditions. Ind. Engng. Chem. Res. 27:2261.

CHEN, P.Y.S. 1980. Press conditions affect drying rate and shrinkage of hardwood boards. For. Prod. J. 30(7): 43-47.

COMSTOCK, G.L. 1971. The kinetics of veneer jet drying. For. Prod. J. 21(9): 104-111.

COMSTOCK, G.L. 1963. Moisture coefficients in wood as calculated from adsorption, desorption, and steady state data. For. Prod. J. 13(3): 97-103.

CUPPERT, D.G. and E.P. CRAFT. 1972. Kiln drying of presurfaced 4/4 Appalachian oak. For. Prod. J. 22(6): 36-41.

Di BLASI, C. 1998. Multi-phase moisture transfer in the high-temperature drying of wood particles. Chem. Engg. Sci. 53(2): 353-366.

DORRI, B., A.F. EMERY and P.C. MALTE. 1985. Drying rates of wood particles with longitudinal mass transfer. J. Heat Transfer. 107(1): 12-18.

DORRI, B. 1983. Simultaneous Heat and Mass Transfer Modeling for Small Wood Particle Drying. Ph. D dissertation. University of Washington.

ERICKSON, R.W., R.T. SEAVY and S.L. QUARLES. 1981. Moisture adsorption and transport by wood due to thermal gradient caused by air to air thermal difference. Wood and Fiber 13(4): 237-245.

FREDLUND, B. 1993. Modelling of heat and mass transfer in wood structures during fire. Fire Safety J. 20: 39.

FHYR, C. and A. RASMUSON. 1997. Some aspects of the modeling of wood chips drying in superheated steam. Int'l J. Heat and Mass Transfer 40(12): 2825-2842.

FHYR, C. and A. RASMUSON. 1996. Mathematical model of steam drying on wood chips and other hygroscopic porous media. AIChE J. 42(9): 2491-2502.

FOREST PRODUCTS SOCIETY (FPS). 1999. Wood Handbook: Wood as an Engineering Material. Reprinted from USDA Forest Service Forest Products Laboratory General Technical Report FPL-GTR 113.

FOREST PRODUCTS SOCIETY (FPS). 1997. Dry Kiln Operator's Manual. Reprinted from USDA Agricultural Handbook No. 188.

FOSBERG, M.A. 1970. Drying rates of heartwood below fiber saturation. Forest Sci. 16(1): 57-63.

GERHARDS, C.C. 1982. Effect of moisture content and temperature on the mechanical properties of wood: An analysis of immediate effects. Wood and Fiber 14(1): 4-36.

HAYGREEN, J.G. and J.L. BOWYER. 1996. Forest Products and Wood Science: An Introduction. Iowa State University Press, Ames, Iowa.

HUKKA, A. 1997. Evaluation of parameter values for a high-temperature drying simulation model using direct drying experiments. Drying Tech. 15(3&4): 1213-1229.

HUKKA, A. 1996. A mathematical model for simulation of softwood drying in temperatures above the boiling point of water with special attention to the boundary conditions. Drying Tech. 14(7&8): 1719-1732.

HUNTER, A.J. 1996. Wood drying and Fick's second law. Wood Sci. and Tech. 30: 355-359.

HUNTER, A.J. 1995. Equilibrium moisture content and the movement of water through wood above fiber saturation. Wood Sci. Tech. 29(2): 129-135.

HUNTER, A.J. 1993. On movement of water through wood-The diffusion coefficient. Wood Sci. Tech. 27:401-408.

JOHANSSON A., C. FYHR and A. RASMUSON. 1997. High temperature convective drying of wood chips with air and superheated steam. International Journal of Heat and Mass Transfer 40(12): 2843-2858.

KAMKE, F.A. and M. VANEK. 1994. Comparison of wood drying models. Proc. Fourth IUFRO Conference on Wood Drying. pp. 1-21.

KAMKE, F.A. and J.B. WILSON. 1986a. Computer simulation of a rotary dryer Part I: Retention time. AIChE J. 32(2): 263-268.

KAMKE, F.A. and J.B. WILSON. 1986b. Computer simulation of a rotary dryer Part II: Heat and Mass Transfer. AIChE J. 32(2): 269-275.

KAMKE, F.A. and J.B. WILSON. 1985. Analysis of a rotary dryer: Drying of wood particles. For. Prod. J. 35(9): 32-40.

KANSA, K.E., H.E. PERLEE and R.F. CHAIKEN. Mathematical model of wood pyrolysis including internal forced convection. Combustion Flame 29: 311-324.

KANURY, A.M. and P.L. BLACKSHEAR. 1970. Some considerations pertaining to the problem of wood-burning. Combustion Sci. Tech. 97: 469.

KAWAI, S., K. NAKATO, and T. SAHOH. 1978. Moisture movement in wood below the fiber saturation point. Mokuzai Gakkaishi 24(5): 273-280.

KAYIHAN, F. and M.A. STANISH. 1984**.** Wood particle drying: A mathematical model with experimental evaluation. In Drying '84. pp. 330-347.

KAYIHAN, F. 1982. Simultaneous heat and mass transfer with local three-phase equilibrium in wood drying. In Proc. Third International Drying Symposium. Birmingham, England.

KENT, A.C., H.N. ROSEN and B.M. HARI. 1981. Determination of equilibrium moisture content of yellow-poplar sapwood above 100°C with the aid of an experimental psychrometer. Wood. Sci. Tech. 15: 93-103.

KIRK, R.W. and J.B. WILSON. 1986. Rotary drying of wood waste fuels with boiler exhaust gases: Simulation, field studies, economics. For. Prod. J. 36(7&8): 57-62.

LAITY, W.W., G.H. ATHERTON and J.R. WELTY. 1974. Comparisons of air and steam as veneer drying media. For. Prod. J. 24(6): 21-29.

LANGRISH, T.A.G. and N. BOHM. 1997. An experimental assessment of driving forces for drying in hardwoods. Wood Sci. Tech. 31: 415-422.

LAYTNER, F., N. EIPSTEIN, J.R. GRACE and L. PINDER. 1992. Kinetics of wood wafer drying. Drying '92. pp. 1135-1144.

LAYTNER, F. 1989. Fundamentals and technology of wafer drying. Ph.D dissertation. University of British Columbia, Vancouver, Canada.

LEE, C.K., and J.R. DIEHL. 1981. Combustion of irradiated dry and wet oak. Combust. Flame 42: 123.

MALTE, P.C., B. DORRI, A.F. EMERY, R.W. COX and R.J. ROBERTUS. 1984**.** The drying of small wood particles. Drying Technology 1(1): 83-115.

MALTE, P.C., R.W. COX, R.J. ROBERTUS, G.R. MESSINGER and M.D. STRICKLER. 1977. Wood particle drying rates. Proc. 11th WSU International Particleboard/Composite Materials Symposium, Pullman, WA. pp. 231-257.

MALTE, P.C., R.W. COX, W.J. KENNISH, S.C. SCHMIDT, R.J. ROBERTUS, G.R. MESSINGER and M.D. STRICKLER. 1976**.** Experiments on the kinetics and mechanisms of drying small wood particles. Research Report TEL-76-8. Thermal Energy Laboratory, College of Engineering, Washington State University, Pullman, WA.

McMILLEN, J. 1969. Accelerated kiln drying of presurfaced 1-inch northern red oak. USDA Forest Service Res. Paper FPL 122. FPL, Madison, WI.

McNAMARA, W.S. and C.A. HART. 1971. An analysis of interval and average diffusion coefficients for unsteady-state movement of moisture in wood. Wood Sci. 4(1): 37-45.

MELAAEN, M.C. 1996. Numerical analysis of heat and mass transfer in drying and pyrolysis of porous media. Numerical Heat Transfer, Part A 29(4): 331-355.

PANG, S., S.G. RILEY and A.N. HASLETT. 1997. Simulation of Pinus radiata veneer drying: Moisture content and temperature profiles. For. Prod. J. 47(8): 51-58.

PANG, S. 1996. Moisture content gradient in a softwood board during drying: Simulation from a 2-D model and measurement. Wood. Sci. Tech. 30:165-178.

PEASE, D. A. 1994. Panels: Products, Applications and Production Trends. Miller Freeman Inc., San Francisco, CA.

PERRE, P., and I.W. TURNER. 1999a. Transpore: A generic heat and mass transfer computational model for understanding and visualising the drying of porous media. Drying Tech. 17(7&8): 1273-1289.

PERRE, P., and I.W. TURNER . 1999b. A 3-D version of TransPore: A comprehensive heat and mass transfer computational model for simulation the drying of porous media. Intl. J. Heat Mass Transfer 42: 4501-4521.

PERRE, P. , M. MOSER and M. MARTIN. 1993. Advances in transport phenomena during convective drying with superheated steam and moist air. Intl. J. Heat Mass Transfer 36(11): 2725.

PLAGEMANN, W.L., E.W. PRICE and W.E. JOHNS. 1984. The response of hardwood flakes and flakeboard to high temperature drying. J. Adhesion 16:311-338.

PLAGEMANN, W.L. 1982. The response of hardwood flakes and flakeboard to high temperature drying. Master's thesis. Washington State University, Pullman, WA.

PLUMB, O.A., G.A. SPOLEK and B.A. OLMSTEAD. 1985. Heat and mass transfer in wood during drying. Intl. J. Heat Mass Transfer. 28(9): 1669-1678.

PLUMB, O.A., P.C. MALTE and R.W. COX. 1978a. A numerical study of optimum operating conditions for convective wood particle dryers. In Proc. 12th Washington State University International Particleboard/Composite Materials Symposium. Pullman, WA. pp. 151-173.

PLUMB, O.A., P.C. MALTE, R.W. COX and R.J. ROBERTUS. 1978b. Convective drying of small wood particles. Proc. First International Symposium on Drying. pp. 110-116.

RICE, W.W. 1971. Field test of a schedule for accelerated kiln drying of presurfaced 1-inch northern red oak. University of Massachussettes Agric. Expt. Station. Res. Bull. 95. Amherst, MA.

ROSEN, H.N. 1980a. Wood behavior during impingement drying. Drying '80 pp. 413-421.

ROSEN, H.N. 1980b. Empirical model for characterizing wood drying curves. Wood Sci. 12 (4): 201-206.

ROSEN, H.N. 1978. Evaluation of drying time, drying rates, and evaporative fluxes when drying with impinging jets. Proc. First International Symposium on Drying. McGill University, Science Press, Princeton, NJ. pp. 192-200.

ROSEN, H.N. 1976. Exponential dependency of moisture diffusion coefficient on moisture content. Wood Sci. 8(3): 174-179.

SAASTAMOINEN, J.J. and R.K. IMPOLA. 1995. Drying of solid fuel particles in hot gases. Drying Tech. 13(5-7): 1305-1315.

SAHOTA, M.S. and P.J. PAGNI. 1979. Heat and mass transfer in porous media subject to fires. Intl. J. Heat Mass Transfer. 22: 1069.

SALAMON, M. 1969. High-temperature drying and its effect on wood properties. For. Prod. J. 19(3): 27-34.

SCHULTZ, T.P. and M.W. KELLY. 1980. Steady state diffusion of moisture through plywood. Wood Sci. 13(1): 14-17.

SIAU, J.F. 1995. Wood: Influence of Moisture on Physical Properties. Department of Wood Science and Forest Products, Virginia Polytechnic Institute and State University, Blacksburg, VA.

SIAU, J.F. 1984. Transport Processes in Wood. Springer, Berlin.

SIAU, J.F. 1983. Chemical potential as a driving force for nonisothermal moisture movement in wood. Wood. Sci. Tech. 17(2): 101-105.

SIAU, J.F. 1980. Nonisothermal moisture movement in wood. Wood Sci. 13(1): 11-13.

SIAU, J.F. 1971. Flow in Wood. Syracuse University Press, New York.

SILITONGA, T.M. 1983. Moisture transport rate and energy consumption for convective drying of fuelwood chips. PhD dissertation. University of Minnesota.

SIMMS, D.L. and M. LAW. 1967. The ignition of wet and dry wood by irradiation. Combust. Flame 11: 377.

SIMPSON, W.T. 1993. Determination and use of moisture diffusion coefficient to characterize drying of northern red oak (Quercus rubra). Wood Sci. Tech. 27(6): 409-420.

SIMPSON, W.T. and H.N. ROSEN. 1981. Equilibrium moisture content of wood at high temperatures. Wood and Fiber 13(3): 150-158.

SKAAR, C. and J.F. SIAU. 1981. Thermal diffusion of bound water in wood. Wood Sci. Tech. 15(2):105-112.

SKAAR, C. 1972. Water in Wood. Syracuse University Press, New York.

SKAAR, C. 1954. Analysis of methods for determining the coefficient of moisture diffusion in wood. For. Prod. J. 4(6): 403-410.

SODERSTROM, O. and J. SALIN. 1993. On determination of surface emission factors in wood drying. Holzforschung 47: 391-397.

SOUZA, M.E.P. and S.A. NEBRA. 2000. Heat and mass transfer model in wood chip drying. Wood and Fiber Sci. 32(2): 156-163.

SPOLEK, G.A. and O.A. PLUMB. 1981. Capillary pressure in softwoods. Wood Sci. Tech. 15: 189-199.

SPOLEK, G.A. and O.A. PLUMB. 1980. A numerical model of heat and mass transfer in wood during drying. Drying '80 pp. 84-92.

STAMM, A.J. 1960. Bound-water diffusion into wood in across-the-fiber directions. For. Prod. J. 10(10): 524-528.

STAMM, A.J. 1959. Bound-water diffusion into wood in the fiber direction. For. Prod. J. 9(1): 27-32.

STANISH, M.A. 1986. The roles of bound water chemical potential and gas phase diffusion in moisture transport through wood. Wood Sci. Tech. 19:53-70.

STANISH, M.A., G.S. SCHAJER and F. KAYIHAN. 1986. A mathematical model of drying for hygroscopic porous media. AIChE J. 32(8): 1301-1311.

STANISH, M.A., G.S. SCHAJER and F. KAYIHAN. 1985. Mathematical modeling of wood drying from heat and mass transfer fundamentals. Drying '85 pp. 360-367.

STANISH, M.A. and F. KAYIHAN. 1984. Moisture transport in wood particles during drying. AIChE Symposium Series. S-239(80); 9-20.

SU, W., J.R. BOERNER, U. HOODA, H. YAN, S. BANERJEE, R. SHMULSKY, L.L. INGRAM and T.E. CONNERS. 1999. VOC extraction from softwood through low-headspace heating. Holzforschung 53(6): 641-647.

SU, W., H. YAN and S. BANERJEE. 1999. Field-proven strategies for reducing volatile organic carbons from hardwood drying. Envi. Sci. Tech. 33(7): 1056-1059.

TABARSA, T. and Y.H. CHUI. Effects of hot pressing on properties of white spruce. For. Prod. J. 47(5): 71-76.

TARASIEWICZ, S. and F. LEGER. 1998. Modeling simulation and control of the wood drying process. Part 1. A set of PDE's as an internal model. Drying Tech. 16(6): 1075-1084.

TSCHERNITZ, J.L. and W.T. SIMPSON. 1979. Drying rate of northern red oak lumber as an analytical function of temperature, relative humidity, and thickness. Wood Sci. 11(4): 202-208.

TSCHERNITZ, J.L. 1985. Empirical correlations for estimating drying times of thick rotary-cut veneer in press and jet dryers. USDA Forest Service Forest Products Laboratory Research Paper FPL 453.

UNITED STATES DEPARTMENT OF AGRICULTURE (USDA). 1974. Wood Handbook: Wood as an Engineering Material. USDA Forest Service Forest Products Laboratory General Technical Report FPL-GTR 113.

WEN, C.Y. and W.E. LOOS. 1969. Rate of veneer drying in a fluidized bed. Wood Sci. 2(2): 87-90.

WENGERT, E.M. 1977. Some considerations in modeling and measuring moisture flow in wood. Wood Sci. 10(1): 49-52.

WENGERT, E.M. 1971. Accelerating oak drying by presurfacing, accelerated schedules, and kiln automation. USDA Forest Service Research Note FPL-0214. FPL, Madison, WI.

WHITE, R.H. AND E.L. SCHAFFER. 1981. Transient moisture gradient in fire-exposed wood slab. Wood Fiber 13: 17.

WU, Q.L. 1999. In-plane dimensional stability of oriented strand panel: Effect of processing variables. Wood and Fiber Sci. 31(1): 28-40.

WU, Q.L. 1998. Effect of moisture on bending and breaking resistance of commercial oriented strandboards. Wood and Fiber Sci. 30(2): 205-209.

WU, Q.L. and O. SUCHSLAND. 1997. Effect of moisture on the flexural properties of commercial oriented strandboards. Wood and Fiber Sci. 29(1): 47-57.

XU, W. and O. SUCHSLAND. Modulus of elasticity of wood composite panels with a uniform verticle density profile: A model. Wood and Fiber Sci. 30(3): 293-300.

CHAPTER 3. FLAKE DRYING TEST

3.1. Introduction

Convective drying of wood flakes is a continuous process with changes in moisture content and temperature of the material. These changes occur simultaneously and vary for different conditions and methods. A series of experiments was undertaken to achieve the following objectives: 1) to determine the moisture content and surface temperature of flakes during drying; 2) to develop a regression model that fits the flake drying curve; and 3) to determine the effect of several parameters on drying rate. This information will be the basis for understanding the flake drying process and to supplement the knowledge obtained from the literature.

A drying curve is a plot of moisture content versus time. By drawing tangents along the various points of the drying curve, the drying rate curve can be derived. The slopes of the tangents are plotted against the corresponding moisture content. The drying curve can also be characterized by an equation that is differentiated to obtain the drying rate curve.

Various equations have been used to characterize the drying of wood. A simple analytical approach has been the assumption that the drying rate is proportional to the average moisture content. This can expressed as:

$$E=\exp(-kt) \qquad \text{(Eq. 3.1)}$$

where: E is relative moisture content

k is an empirical constant

t is time

Tschernitz and Simpson (1979) used this equation in determining the drying rate of northern red oak lumber but they added an empirical thickness coefficient to account for the effect of thickness. Rosen (1978, 1980a) presented a two-parameter model based on the exponential relationship of relative moisture content and time. The model fits the drying of wood and wood-based materials very well (Rosen , 1980b)

Silitonga (1983) used linearized transformation of the analytical equation (Eq. 3.1) in describing the drying curve of wood chips. His equation was in the form:

$$\ln E = -kt \qquad \text{(Eq. 3.2)}$$

Polynomials are also used in describing curvilinear relationships. These types of models are useful in situations where curvilinear effects are present in the response function. They are also useful in approximating functions to unknown and possibly very complex nonlinear relationships. Laytner (1989) used a 5^{th} order polynomial equation to describe the drying of wafers:

$$M = \beta_o + \beta_1 t + \beta_2 t^2 + \beta_3 t^3 + \beta_4 t^4 + \beta_5 t^5 \qquad \text{(Eq.3.3)}$$

where: M is moisture content

β_o, β_1, β_2, β_3, β_4, β_5 are regression coefficients

Another form of describing the drying of wood is piecewise linear regression. Comstock (1971) described the drying of veneer as a linear function of moisture content comprised of two falling rate periods. The same approach was done by Pang et al. (1997) to express the three drying periods (constant rate followed by two falling rate periods) of veneer based on simulations.

This study incorporates several parameters that may have an effect on flake drying at high temperature. Species, cutting direction, flake dimension, and drying temperature were selected as parameters because of their affects on drying behavior. Southern yellow pine, sweetgum, and yellow poplar were used in the experiments based on their wide use in the OSB industry. Flakes were cut along two directions (radial and tangential). Four flake sizes were cut: 15x117, 15x152, 25x117, and 25x152 mm. Drying temperatures were above the boiling point of water (150, 200, and 250°C).

3.2. Experimental

3.2.1. Materials

Fresh, green bolts, 1.5 m and around 30 cm in diameter of southern yellow pine (Pinus spp.) and sweetgum (Liquidambar styraciflua) were obtained from Georgia Pacific OSB plant in Skippers, VA. The logs were transported to Blacksburg, VA and cut into 50-mm boards using a portable sawmill. Freshly-cut yellow-poplar (Liriodendron tulipifera) boards 50 mm in thickness were obtained from Turman Lumber in Radford, VA. Sound boards from each species were segregated according to type of cut: flatsawn or quartersawn. Radially-cut specimens were taken from the flatsawn boards while tangentially-cut specimens were taken from quartersawn boards (Figure 1). Four block dimension (15x117, 15x152, 25x117, and 25x152 mm) were then randomly selected from the boards. Each block was properly labeled for easy identification. The blocks were placed in plastic bags segregated according to species and cutting direction and stored in a refrigerated room maintained at 2°C.

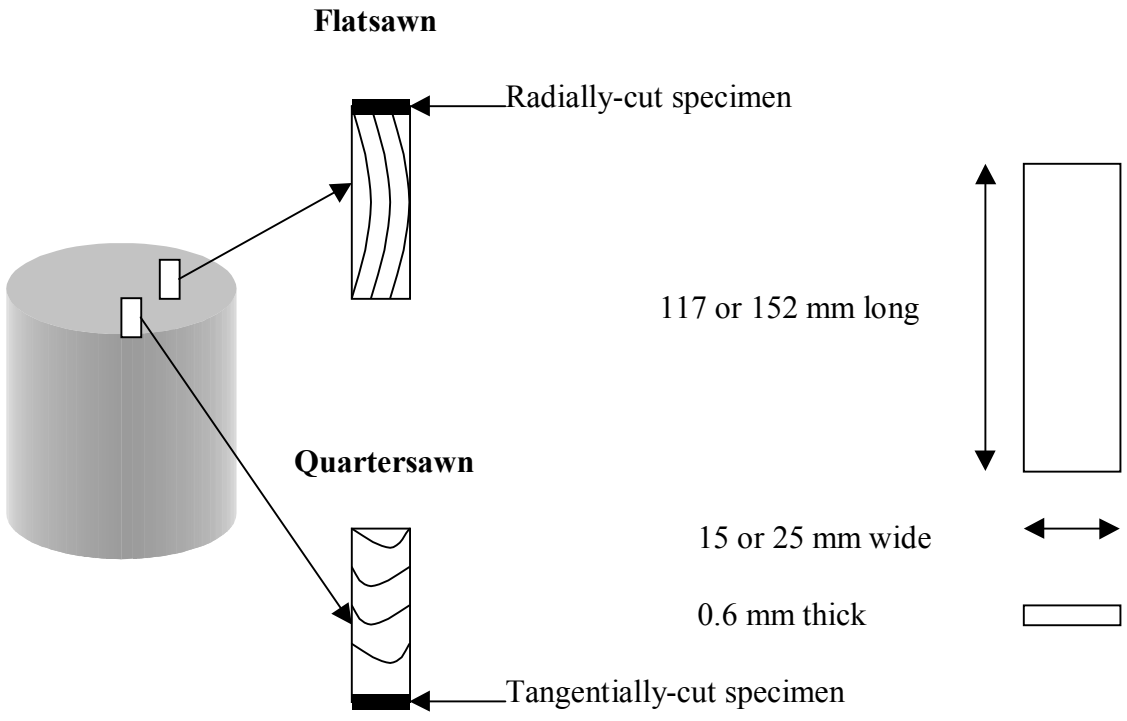

Figure 1. Cutting Diagram of Flake Drying Specimens.

A block was randomly selected for cutting of wafers and subsequent drying of the flakes. Seven flakes with a target thickness of 0.6 mm were cut from each block using a CAE flaker. There were variations in the thickness of the flakes as shown in Table 1. Two flakes were used for drying at every drying temperature level (150, 200, and 250°C). Five replicates were done for every flake dimension. Total number of flakes dried in this experiment was 720.

Table 1. Average Thickness Based on the Different Parameters.

	THICKNESS (MM)			
PARAMETER	**ALL**	**SYP**	**SWEETGUM**	**YELLOW-POPLAR**
Cutting Direction				
Radial	0.70	0.73	0.64	0.73
Tangential	0.69	0.73	0.68	0.68
Dimension (mm)				
15x117	0.75	0.80	0.69	0.76
15x152	0.68	0.72	0.63	0.69
25x117	0.69	0.70	0.66	0.71
25x152	0.67	0.70	0.65	0.66
Width (mm)				
15	0.72	0.76	0.66	0.73
25	0.68	0.70	0.66	0.69
Length (mm)				
117	0.72	0.75	0.68	0.74
152	0.68	0.71	0.64	0.68
Temperature (^{o}C)				
150	0.70	0.72	0.66	0.72
200	0.70	0.73	0.65	0.71
250	0.70	0.74	0.66	0.69

The extra flake was used for determination of moisture content and specific gravity. Moisture content and specific gravity were determined by ovendry (ASTM D 4442-92, 1994) and immersion (ASTM D 2395-93, 1994) methods , respectively. Initial weight of the flake was determined right after flaking. Green volume of the flake was determined by clipping one end of the flake using an alligator clip connected to a stand and immersing the flake inside a tube containing distilled water. The weight of the tube with water was determined before and after immersing the flake. The difference in weight is converted into volume of the flake. Ovendry weight of the flake was determined by placing the flake inside an oven at 102±3°C overnight. The moisture content for each flake was calculated using the ovendry and initial weights. Ovendry weight and green volume was used to calculate specific gravity. Table 2 shows the average initial moisture content and specific gravity of the flakes.

Table 2. Average Initial Moisture Content and Specific Gravity of the Flakes.

SPECIES	MOISTURE CONTENT (%)	SPECIFIC GRAVITY
SYP	138.6	0.46
Sweetgum	96.6	0.55
Yellow-poplar	78.3	0.49

3.2.2. Drying apparatus for single wafer drying

An experimental drying apparatus was assembled so that a single flake could be dried at constant temperature and airflow while monitoring weight loss and surface temperature. It consisted of the following sub-assemblies as shown in Figure 2:

- A drying chamber with temperature control and uniform unidirectional flow;
- Balance for measuring weight loss;
- Infrared (IR) thermometer and thermocouple for measuring flake and air temperatures, respectively; and

Automated data acquisition systems for monitoring of flake weight and temperature, and air temperature during drying. The system is very similar to what Laytner (1989) used in his drying experiments for wood wafers. Initial test runs showed good results and the setup was accurate and precise for the drying experiments.

Figure 2. Flake Drying Apparatus.

The drying chamber was a mechanical convection oven (Lindberg/Blue MO 1440SA) with modifications particularly on the door. The door was installed with a double-walled glass panel for the IR thermometer. A zinc crystal was fitted at the center of the inner glass panel. The oven was properly insulated for ease in controlling and maintaining a constant temperature inside the chamber. A uniform unidirectional airflow was provided by a factory-installed fan inside the oven that passed through the flake suspended inside the chamber.

A balance (Mettler PR1203) was placed on top center of the oven to measure the weight loss of the flake during drying. A wire that passes through the ceiling of the oven through a small hole was connected to the bottom weighing hook of the balance. An alligator clip was connected at the other end of the wire (inside the oven) where a single flake was suspended. The balance was connected to an automated data acquisition system to facilitate continuous recording of weight loss.

Flake temperature was measured using the IR thermometer (Omega OS552-MA-1). The IR thermometer was mounted right in front of the oven door. Distance between the sensor and flake was 60 cm for a spot diameter of 9 mm (Omega, 2000).

Temperature of the circulating air inside the oven was monitored using a Type K fiberglass insulated thermocouple probe connected to a thermocouple thermometer (Cole-Parmer Digi-Sense 91100-50). The thermocouple was positioned right beside the flake. Air temperature was controlled and maintained at desired level by adjusting the temperature controller of the oven. Both flake and air temperatures were monitored using separate automated data acquisition systems.

3.2.3. Flake drying experiments

Prior to drying, a block was randomly selected. Six out of seven flakes cut from the block were used for drying experiments and the other one for moisture content and specific gravity determination (refer to Section 3.2.1). The first and second flakes were dried at 150^{o}C, one at a time. The third and fourth flakes were dried at 200^{o}C and the last two flakes were dried at 250^{o}C. All flakes dried at the end of the day were placed inside the oven overnight at 102$\pm$3°C for determination of ovendry weight. Ovendry weight was used for calculating the moisture content of the flake.

The drying oven was turned on and allowed to reach the desired drying temperature. Balance, IR thermometer, thermocouple thermometer, and data acquisition systems were also switched on prior to any drying experiment. Balance was tared and the IR thermometer was aimed correctly at the wire rod. Once the temperature reading inside the oven had stabilized, balance and both thermometers started to acquire data. The oven door was opened and the wafer attached to the alligator clip quickly and the door closed immediately. The flake weight and temperature, and air temperature inside the oven were collected by the data acquisition systems every five seconds. Data logging was terminated when no significant weight loss was observed. The wafer was then taken out of the oven and then measured for thickness and labeled properly.

3.2.4. Statistical analyses

The experimental data were analyzed. Experimental values of moisture content were plotted against time. This resulted in the drying curve of each flake. Each curve was fitted into an equation (i.e. Eq. 3.1, 3.2). The equation that best fit the experimental data was selected to describe the flake drying curve. General Linear Model (GLM) and Nonlinear (NLIN) procedures of SAS were used in the regression analyses of the drying curve. Several criteria were used in testing validity of the regression model. Test for significance of the regression model was performed. Mean square error (MSE) and mean square regression (MSR) were checked. Tests on the parameter coefficients were also performed. Coefficient of determination (R^2) was also checked. Plots of observed versus fitted values and residuals were observed.

The drying rate was obtained by differentiating the drying curve model. Drying rates at specified moisture content levels were calculated. Multiple comparisons of drying rates between the several parameters were done using analyses of variance (ANOVA) and Tukey's test. Drying rate at specified moisture content levels was compared between species, flake dimension, cutting direction, and drying temperature using the split-plot design (Snedecor and Cochran, 1980; Steele and Torrie, 1980). Species represented the whole plots. Cutting direction, flake dimension, and temperature represented the sub-plots. The linear model considered for the analysis of drying rate is shown next and in Table 3:

$$y_{ijklm} = \mu + S_i + C_j + SC_{ij} + D_k + SD_{ik} + CD_{jk} + SCD_{ijk} + \varepsilon^{(A)}_{ijkl} + T_m + ST_{im} + CT_{jm} + SCT_{ijm} + DT_{km} + SDT_{ikm} + CDT_{jkm} + SCDT_{ijkm} + \varepsilon^{(B)}_{ijklm} + \varepsilon_{ijklmp} \quad \text{(Eq. 3.4)}$$

where: y_{ijklm} is calculated drying rate

μ is mean

S_i is species effect

C_j is effect of cutting direction

SC_{ij} is interaction effect of species and cutting direction

D_k is effect of flake dimension

SD_{ik} is interaction effect of species and flake dimension

CD_{jk} is interaction effect of cutting direction and flake dimension

SCD_{ijk} is interaction effect of species, cutting direction, and flake dimension

$\varepsilon^{(A)}_{ijkl}$ is whole-plot error

T_m is temperature effect

ST_{im} is interaction effect of species and temperature

CT_{jm} is interaction effect of cutting direction and temperature

SCT_{ijm} is interaction effect of species, cutting direction, and temperature

DT_{km} is interaction effect of flake dimension and temperature

SDT_{ikm} is interaction effect of species, flake dimension, and temperature

CDT_{jkm} is interaction effect of cutting direction, flake dimension, and temperature

$SCDT_{ijkm}$ is interaction effect of species, cutting direction, flake dimension, and temperature

$\varepsilon^{(B)}_{ijklm}$ is split-plot error

ε_{ijklmp} is sampling error

Table 3. ANOVA Table For Comparing Drying Rates Between Species.

SOURCE	DF	SS	MS	F
Species (S)	(s-1)	SSS	MSS	MSS/MSEa
Cutting Direction (C)	(c-1)	SSC	MSC	MSc/MSEa
S x C	(s-1)(c-1)	SSSC	MSSC	MSSC/MSEa
Dimension (D)	(d-1)	SSD	MSD	MSD/MSEa
S x D	(s-1)(d-1)	SSSD	MSSD	MSSD/MSEa
C x D	(c-1)(d-1)	SSCD	MSCD	MSCD/MSEa
S x C x D	(s-1)(c-1)(d-1)	SSSCD	MSSCD	MSSCD/MSEa
Error (a)	(r-1)scd	SSEa	MSEa	
Temperature (T)	(t-1)	SST	MST	MST/MSEb
S x T	(s-1)(t-1)	SSST	MSST	MSST/MSEb
C x T	(c-1)(t-1)	SSCT	MSCT	MSCT/MSEb
S x C x T	(s-1)(c-1)(t-1)	SSSCT	MSSCT	MSSCT/MSEb
D x T	(d-1)(t-1)	SSDT	MSDT	MSDT/MSEb
S x D x T	(s-1)(d-1)(t-1)	SSSDT	MSSDT	MSSDT/MSEb
C x D x T	(c-1)(d-1)(t-1)	SSCDT	MSCDT	MSCDT/MSEb
S x C x D x T	(s-1)(c-1)(d-1)(t-1)	SSSCDT	MSSCDT	MSSCDT/MSEb
Error (b)	(r-1)(t-1)scd	SSEb	MSEb	
Error	scdtr(n-1)	SSE	MSE	

SV is Source of Variation
DF is degrees of Freedom
SS is Sum of Squares
MS is Mean Square
F is the F-value
P is Probability

Comparison of drying rates between cutting direction, dimension, and temperature by species was analyzed using ANOVA. The split-plot linear model shown below and in Table 4 was used in analyzing these variables on drying rate:

$$y_{ijkl} = \mu + C_i + D_j + CD_{ij} + \varepsilon^{(A)}_{ijk} + T_l + CT_{il} + DT_{jl} + CDT_{ijl} + \varepsilon^{(B)}_{ijkl} + \varepsilon_{ijklp} \quad \text{(Eq. 3.5)}$$

where: y_{ijkl} is calculated drying rate

μ is mean

Ci is effect of cutting direction

Dj is effect of flake dimension

CD_{ij} is interaction effect of cutting direction and flake dimension

$\varepsilon^{(A)}_{ijk}$ is whole-plot error

T_l is temperature effect

CT_{il} is interaction effect of cutting direction and temperature

DT_{jl} is interaction effect of flake dimension and temperature

CDT_{ijl} is interaction effect of cutting direction, flake dimension, and temperature

$\varepsilon^{(B)}_{ijkl}$ is split-plot error

ε_{ijklp} is sampling error

Treatment levels were compared using the means and Tukey's test. GLM procedure of the SAS software was used in the analyses.

Table 4. ANOVA Table For Comparing Drying Rates By Species.

SOURCE	DF	SS	MS	F
Cutting Direction (C)	(c-1)	SSC	MSC	MSC/MSEa
Dimension (D)	(d-1)	SSD	MSD	MSD/MSEa
C x D	(c-1)(d-1)	SSCD	MSCD	MSCD/MSEa
Error (a)	(r-1)scd	SSEa	MSEa	
Temperature (T)	(t-1)	SST	MST	MST/MSEb
C x T	(c-1)(t-1)	SSCT	MSCT	MSCT/MSEb
D x T	(d-1)(t-1)	SSDT	MSDT	MSDT/MSEb
C x D x T	(c-1)(d-1)(t-1)	SSCDT	MSCDT	MSCDT/MSEb
Error (b)	(r-1)(t-1)scd	SSEb	MSEb	
Error	cdtr(n-1)	SSE	MSE	

3.3. Results and Discussion

Depending on flake properties and drying temperature, each drying test produced a data file of 10 to 50 records that included flake weight and surface temperature, and air temperature. Experimental data from 720 test specimens were obtained for the analyses of drying curve and drying rate. Moisture content versus time plot (drying curve) of every flake was observed.

3.3.1. Drying Curve

A typical flake drying curve (Figure 3) indicates a non-linear relationship throughout the entire drying period. A continuous falling rate period was observed right from the start of every drying test. A linear trend reflecting a constant rate period typical of wood drying was not observed in all cases. Just like any other curve, the drying curve can be characterized by an equation. The mathematical relation between moisture content versus time of wood flakes is not well documented. This relation will be the discussion of this subsection.

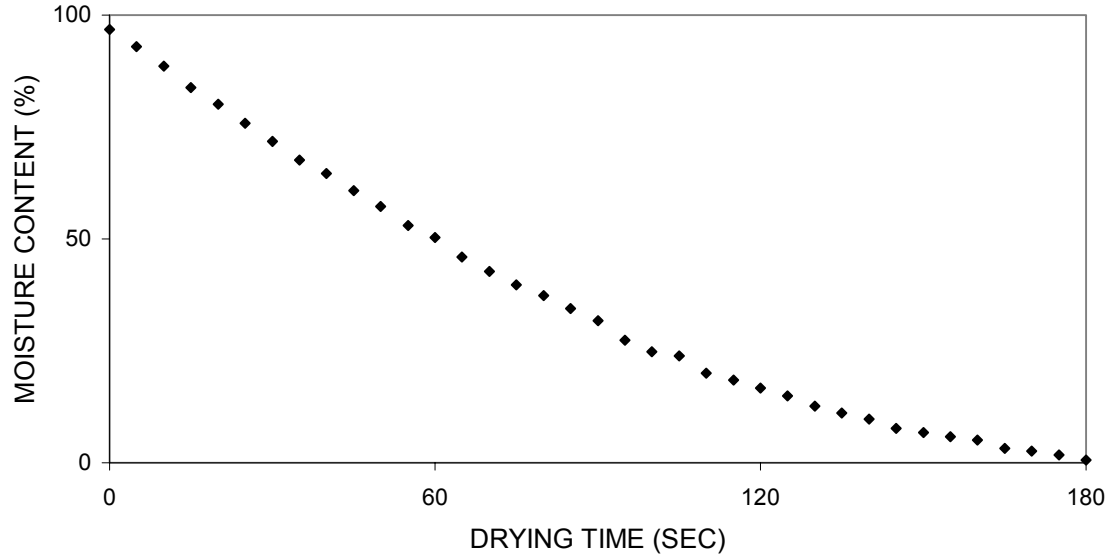

Figure 3. Typical Flake Drying Curve.

Transformation of the data to get a linear fit was first tested. Logarithmic transformation of the relative moisture content (Eq. 3.2) still resulted in a curvilinear trend (Figure 4). Silitonga (1983) used the same logarithmic transformation in describing the drying of wood chips. However, his data transformation resulted in a near perfect linear fit. Various statistical tests suggested that his transformation was appropriate.

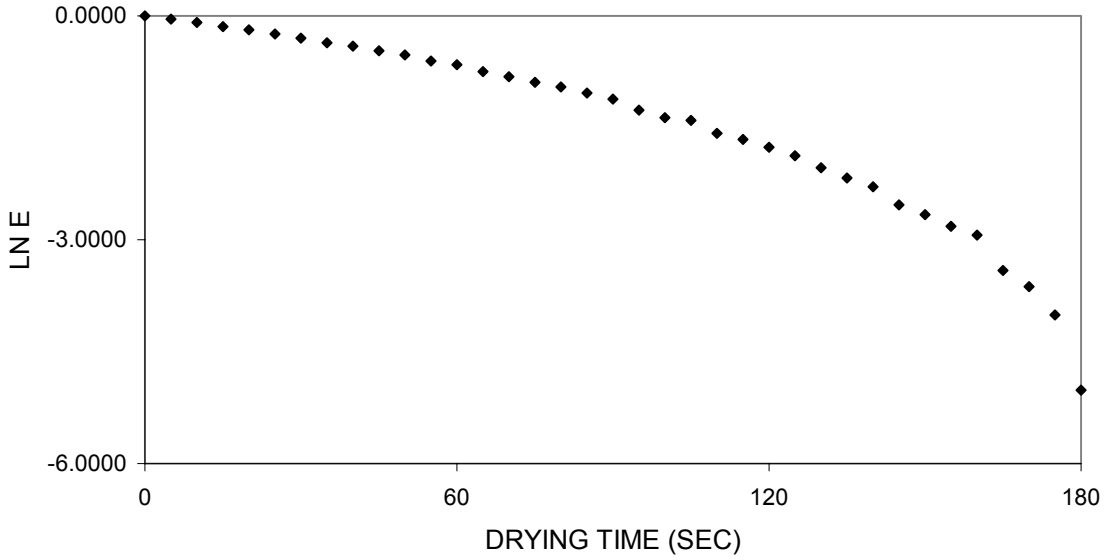

Figure 4. Plot of Experimental Data and Fitted Exponential Model.

Since the logarithmic transformation was not appropriate to describe the drying of flakes, the data were fitted using the analytical relation (Eq. 3.1) between moisture content and drying time. Figure 5 shows the observed data and the fitted model. The fit was not perfect with the exponential curve overestimating the early part of drying. Even with the addition of another parameter [i.e. bend factor (Rosen, 1978)], the exponential model was still not a good fit.

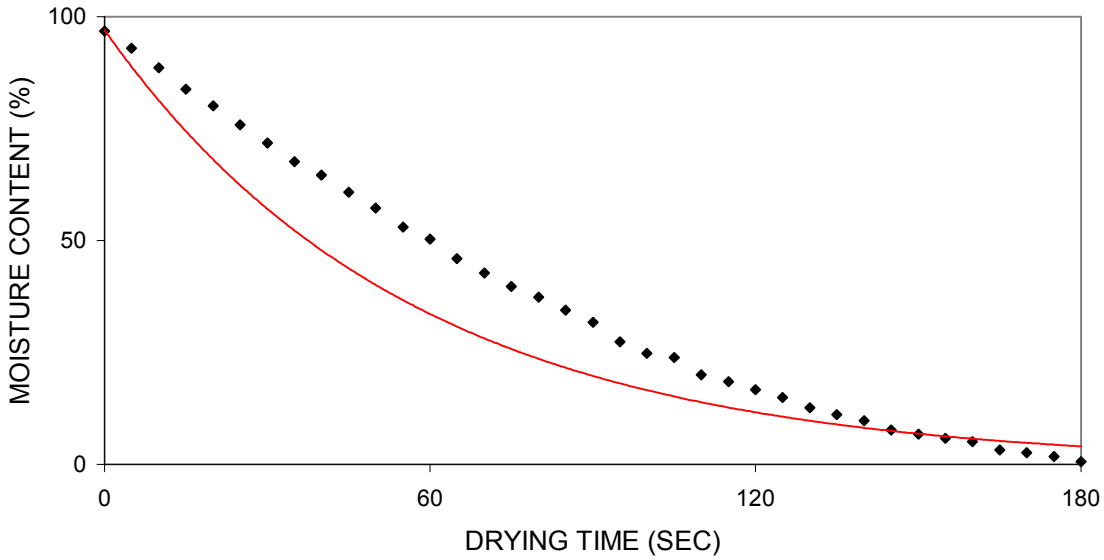

Figure 5. Plot of Experimental Data and Fitted Exponential Model.

Since the logarithmic and exponential relationship of relative moisture content versus time was not good enough in describing the drying of flakes, the use of a polynomial equation was tested. Polynomial models are useful where a curvilinear effect is present in the true response function and for approximating functions to unknown and possibly very complex nonlinear relationships (Montgomery and Peck, 1992).

A near perfect fit was obtained for a second-order/quadratic model (Figure 6). The order of the model was kept as low as possible. The use of higher-order polynomials should be avoided unless they are justified (Montgomery and Peck, 1992). A low-order model is always preferable to a high-order model. According to them, arbitrary fitting of high-order polynomials is a serious abuse of regression analysis. The drying curve of aspen was fitted in a fifth-order equation by Laytner (1989) and also resulted in near perfect fit.

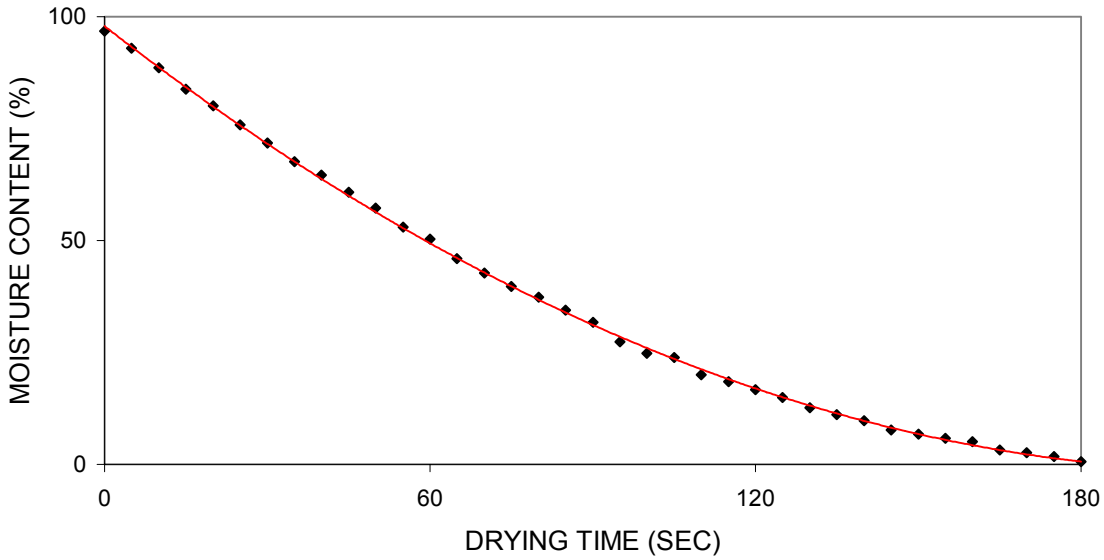

Figure 6. Plot of Experimental Data and Fitted Quadratic Model.

The quadratic model was highly significant based on its ANOVA. MSE for every case was very small compared to the MSR. All three parameter coefficients (β_o, β_1, and β_2) in every case were significant. Standard error of the coefficients was very small. R^2 was at least 0.9900 for all cases (see Appendix A to X). Observed values were very close to fitted values. As observed values of moisture content increased, the predicted value also increased. Residual plots showed random distribution of residuals above and below the zero reference line. No distinct distribution pattern of residuals was observed indicating no obvious model defect.

The drying curve of flakes can now be modeled as:

$$E(y) = \beta o + \beta_1 x + \beta_2 x^2 \qquad \text{(Esq. 3.4.)}$$

where: E(y) is estimated moisture content

β_o is the intercept

β_1 is the linear effect coefficient

β_2 is the quadratic effect coefficient

x is time.

β_o is related to initial moisture content. β_1 and β_2 are both related to the properties of the flakes and drying conditions.

The quadratic model is adequate to describe the convective drying of wood flakes. This model can also be used to estimate the drying time needed to reach a given moisture content. Parameter coefficients for each flake are presented in Appendix A to X.

Initial moisture contents of the flakes were different. Therefore, the actual drying times were inappropriate for comparing the influence of flake properties and drying conditions on drying time. The drying rates at certain moisture content levels were calculated and used as a variable to measure the drying property of the flakes.

3.3.2. Drying Rate

One way to compute the drying rate at a certain moisture content level is to perform linear regression of data points included in each interval of moisture content to give an estimate of the slope of the drying curve thus, the drying rate for this moisture content interval. The disadvantage of this approach is it would entail a lot of regression analyses and with the data on hand, it would be very difficult to get an accurate value for the drying rate.

The way the drying rate of each flake at prescribed moisture content was determined was by differentiating the quadratic model that described the drying curve accurately. This approach gave the advantage of analyzing the data with the use of a single equation. Since the quadratic equation fitted the data very well, the resulting drying curve should also be accurate. The drying rate curve is smooth having the same basic shape of the drying curve. Figure 7 shows the drying rate curve of the moisture content versus time plot shown in Figure 3. The curve is based on the drying data of a sweetgum flake measuring 15x117 mm cut radially and dried at 150^{o}C.

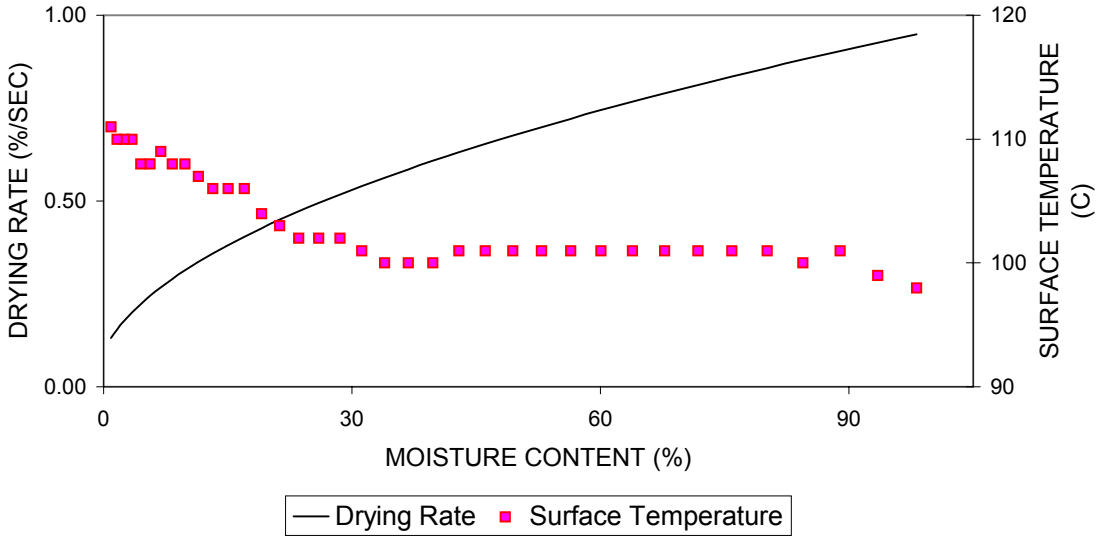

Figure 7. Typical Drying Rate Curve.

Observations on drying rate curves revealed two drying regimes: first falling rate period followed by a second falling rate period. None of the specimens produced a constant rate drying period in the range of moisture contents under investigation, which is typical in the drying of wood. Similar observations were made on drying of wafers (Laytner, 1989), veneer (Comstock, 1971), and wood particles (Alves and Figueiredo, 1989; Di Blasi, 1998; Saastamoinen and Impola, 1995; Silitonga, 1983). This means that decreasing rate can occur in the presence of free water in the flakes.

All the drying rate curves have similar parabolic decrease in drying rate with decreasing moisture content. The decreasing rate begins right at the very start of the drying process. The severeness of the drying conditions caused the decreasing rate to occur immediately in the drying period. At more severe drying conditions, the flake surface was probably not completely wetted. Some areas drop below the fsp before others. The free evaporation of liquid water occurs over a decreasing wetted surface area thus, a falling rate rather than a constant rate drying period. The presence of moisture gradient in small and thin wood have been observed based on experiments and simulations by several authors (Di Blasi, 1998; Laytner, 1989; Melaaen, 1996; Pang et al. 1997; Silitonga, 1983; Souza and Nebra, 2000). The extent of the gradient has significant

bearing on the drying rate curve. At this stage of drying, convective heat transfer is the controlling mechanism. Same controlling mechanism was postulated for wafer (Laytner, 1989), veneer (Comstock, 1971; Pang et al. 1997), and wood particles (Alves and Figueiredo, 1989; Di Blasi, 1998; Melaaen, 1995; Saastamoinen and Impola, 1995; Silitonga, 1983; Souza and Nebra, 2000).

Laytner (1989) explained the absence of the constant rate period in wafers. Water is evaporated from the cell lumens and vessels open to the wafer surface during saturated state. As drying progresses, water is wicked from the surrounding vessels to replenish the surface water. But the tortuosity of the capillary system causes the air-water interface to recede into the pores at the surface resulting in a gradual reduction in drying rate thus, no constant rate drying period.

At about 30% moisture content, the rate of moisture loss indicates another decreasing rate. The drying rate curves have no abrupt deflection at this moisture content indicative of gradual switch from one drying mechanism to another. Temperature of the flake starts to increase. Surface moisture content reaches its maximum sorptive value. No free water exists. The moisture flow is produced by bound water only. The rate of moisture transport is limited by the ability of bound water to diffuse through the wood to its surface (Comstock, 1971; Fyhr and Rasmuson, 1996; Kayihan and Stanish, 1984; Laytner, 1989; Malte et al. 1976; Pang et al. 1997; Silitonga, 1983).

Drying rates at every 5% (below fsp) or 10% (above fsp) change in moisture content of each flake was determined. The succeeding subsections discuss the effect of several parameters on the drying rate of wood flakes. These parameters include species, cutting direction, dimensions, and drying temperature. ANOVA (see Appendix Y and Z) indicate that there were variations in drying rates between the main parameters. The analyses showed that there were highly significant differences in drying rates between species, cutting direction, dimensions, and drying temperature.

Effect of species

Analyses of the whole data set were limited to the 50 to 5% moisture content range. This was constrained by the data of yellow-poplar that had a low range of initial moisture content (50-101%). Analyses from 80 to 60% were between southern yellow pine and sweetgum only. Statistical analyses indicates that there were highly significant differences in drying rates from 80 to 60% between southern yellow pine and sweetgum and from 50 to 5% moisture content between the three species (see Appendix Y and Z). This is expected since wood has been established to have variations in drying properties between species (FPS, 1997 and 1999).

Drying rates are presented in Table 5 and Figure 8 shows the drying rate curves of the three species. Among the three species, southern yellow pine had the fastest drying rate. This was followed by sweetgum, and yellow-poplar had the slowest drying rate except at 50%. From 80 to 60% moisture content, drying rates of southern yellow pine and sweetgum were statistically different. Drying rate of southern yellow pine remained significantly different from sweetgum and yellow-poplar from 50 to 5% moisture content. Higher drying rate of southern yellow pine can be attributed primarily to its specific gravity. Southern yellow pine had the lowest average (0.46) compared to the two other species (sweetgum had 0.55 and yellow-poplar had 0.49). Faster drying is expected as specific gravity decreases due to less water present in wood for a given moisture content. Also, drying rate increases with decreasing specific gravity because of a larger proportion of voids that promotes bulk flow and vapor diffusion. These are faster mechanisms than bound water diffusion that affect the drying rate.

Table 5. Average Drying Rate of the Three Species.

	DRYING RATE (%/SEC)		
MC (%)	**SYP**	**SWEETGUM**	**YELLOW-POPLAR**
120	1.498		
110	1.438		
100	1.378		
90	1.312		
80	1.244	1.193	
	a	B	
70	1.172	1.121	
	a	B	
60	1.095	1.044	
	a	B	
50	1.012	0.960	0.981
	a	B	b
40	0.922	0.885	0.869
	a	B	b
30	0.823	0.771	0.767
	a	B	b
25	0.768	0.710	0.707
	a	B	b
20	0.709	0.648	0.636
	a	B	b
15	0.644	0.580	0.557
	a	B	c
10	0.571	0.502	0.464
	a	B	c
5	0.488	0.408	0.345
	a	B	c

Means with the same letter are not significantly different at p=0.05

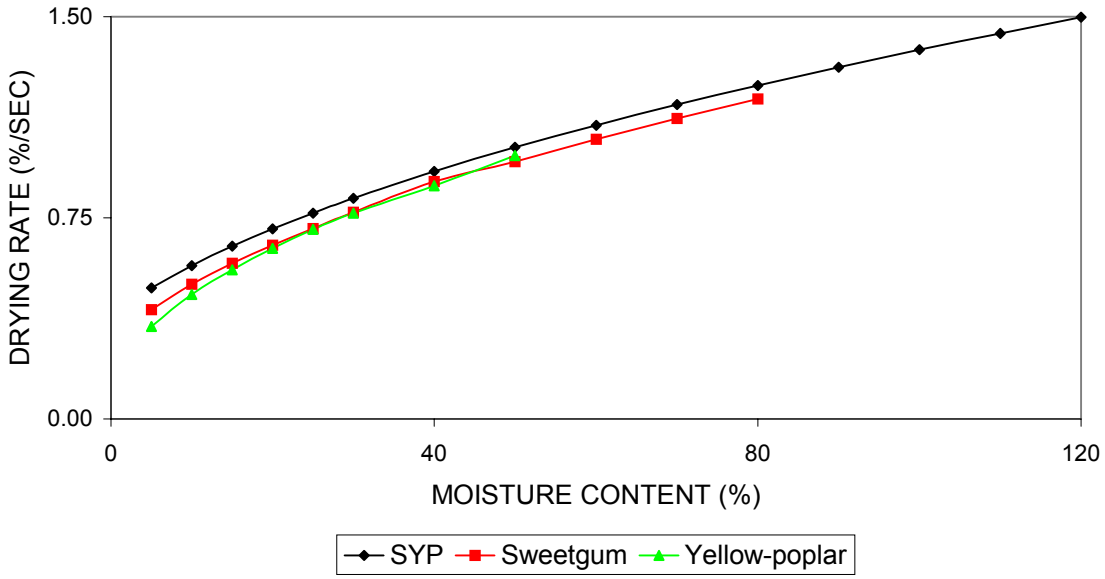

Figure 8. Drying Rate Curves of the Three Species.

Differences in drying rates of sweetgum and yellow-poplar were not significantly different at 50 to 20% but were significant at 15, 10, and 5%. According to Comstock (1971), veneer of the same density and thickness will follow the same drying curve. In this experiment, sweetgum and yellow-poplar have different average specific gravity and almost equal thickness but followed the same drying rate curve within a certain moisture content range. This may be explained by other factors such as permeability, porosity, and cell morphology, among others.

Effect of cutting direction

Cutting direction was found to have an effect on the drying rates of flakes at all moisture content levels (Appendix Y and Z). Drying rates between the two cutting directions are presented in Table 6 and the drying rate curves in Figure 9. Radially-cut specimens consistently have slower drying rates than tangentially-cut specimens at all moisture content levels. This may be explained by the exposure of wood rays on the wide surface of tangentially-cut specimens that provide passageways for water coming out of the flakes. Thus, faster drying rates for tangentially-cut specimens.

Drying rates of radially-cut southern yellow pine specimens were slower than the drying rates of tangentially-cut specimens (Table 6 and Figure 10). There were no significant differences in drying rates between the two cutting directions from 120 to 60%. However, from 50 to 5% the effect of cutting direction on drying rate was already significant. Apparently, the effect of cutting direction on the drying rate of southern yellow pine flakes is only below 60%.

Table 6 and Figure 11show the drying rate and drying rates of sweetgum. Cutting direction had a significant effect on drying rates of sweetgum except at 5% moisture content. Again, radially-cut specimens have slower drying rates than tangentially-cut specimens.

There were differences in drying rates between the two cutting directions of yellow-poplar as shown in Table 6 and Figure 12. Similar to the results of southern yellow pine and sweetgum, radially-cut specimens always have slower drying rates than tangentially-cut specimens. However, it is only in yellow-poplar where the effect of cutting direction is throughout the entire moisture content ranges.

Table 6. Average Drying Rates of the Two Cutting Directions.

	DRYING RATE (%/SEC)							
			SYP		SG		YP	
MC (%)	R	T	R	T	R	T	R	T
120			1.467 a	1.528 a				
110			1.409 a	1.468 a				
100			1.348 a	1.405 a				
90			1.284 a	1.340 a				
80	1.186 a	1.251 b	1.217 a	1.271 a	1.154 a	1.232 b		
70	1.115 a	1.177 b	1.146 a	1.198 a	1.084 a	1.157 b		
60	1.040 a	1.099 b	1.070 a	1.120 a	1.010 a	1.077 b		
50	0.945 a	1.024 b	0.989 a	1.036 b	0.929 a	0.991 b	0.917 a	1.046 b
40	0.855 a	0.929 b	0.900 a	0.945 b	0.841 a	0.896 b	0.823 a	0.947 b
30	0.753 a	0.820 b	0.801 a	0.844 b	0.743 a	0.790 b	0.716 a	0.825 b
25	0.697 a	0.759 b	0.747 a	0.788 b	0.688 a	0.732 b	0.656 a	0.757 b
20	0.636 a	0.693 b	0.688 a	0.729 b	0.629 a	0.668 b	0.590 a	0.683 b
15	0.567 a	0.619 b	0.624 a	0.664 b	0.563 a	0.596 b	0.515 a	0.598 b
10	0.489 a	0.535 b	0.552 a	0.591 b	0.488 a	0.515 b	0.428 a	0.500 b
5	0.394 a	0.433 b	0.468 a	0.508 b	0.398 a	0.417 a	0.316 a	0.375 b

R - Radially-cut specimen
T - Tangentially-cut specimen
Means with the same letter are not significantly different at p=0.05

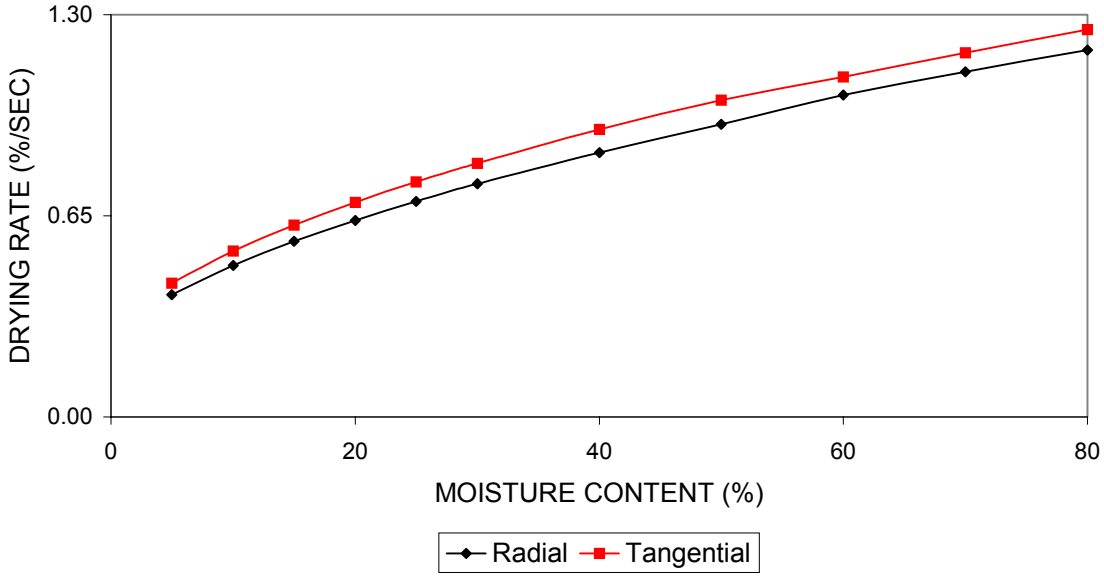

Figure 9. Drying Rate Curves of the Two Cutting Directions.

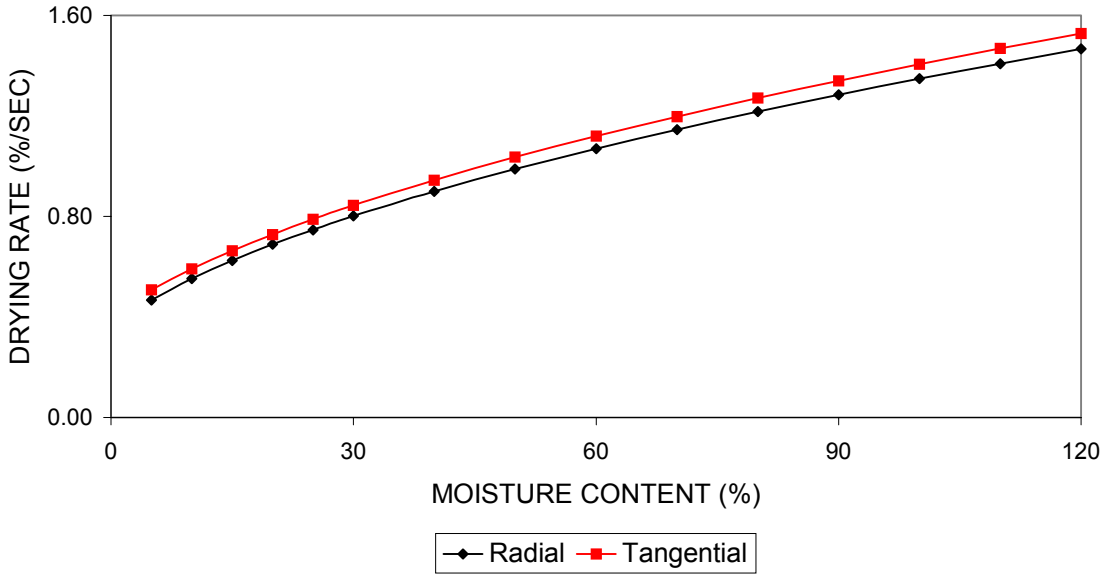

Figure 10. Drying Rate Curves of Southern Yellow Pine According to Cutting Direction.

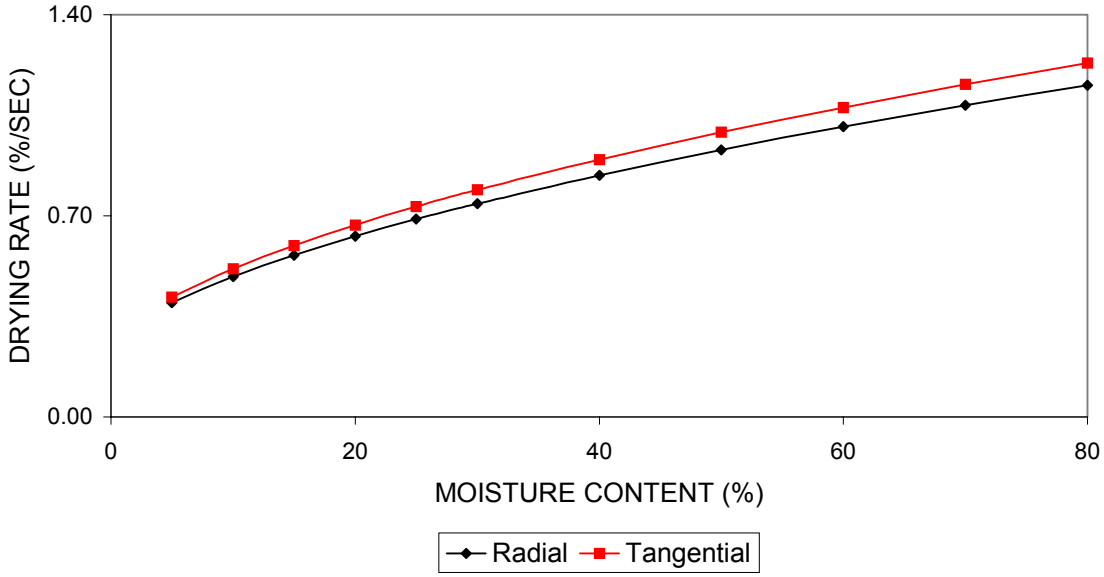

Figure 11. Drying Rate Curves of Sweetgum According to Cutting Direction..

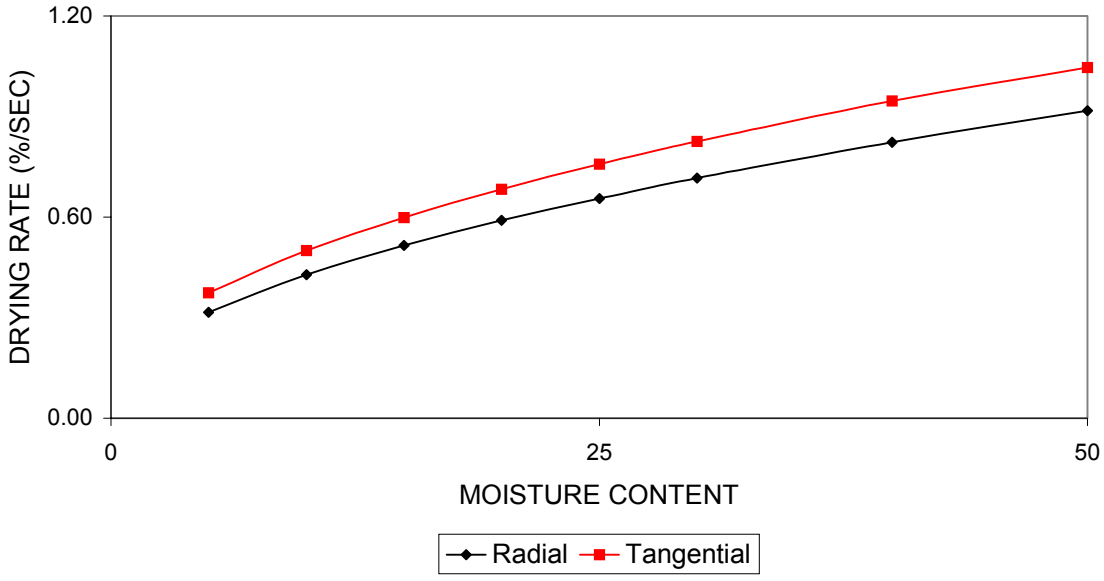

Figure 12. Drying Rate Curves of Yellow-poplar According to Cutting Direction.

Effect of dimension

Differences in drying rate between the four flake dimensions were found to be significant at all moisture content levels (Appendix Y and Z). Drying rates of the four dimensions are shown in Table 7. Drying rate curves of the four dimensions are presented in Figure 13. Narrow flakes (15x117 and 15x152 mm) have faster drying rates than the wide flakes (25x117 and 25x152 mm). Width effect is caused by moisture transport along the transverse pathways (perpendicular to the wide surface) that serve as additional moisture passageways. Shorter width translates to lesser resistance thus, faster drying rate.

However, long flakes (15x152 and 25x152 mm) have faster drying rates than short flakes (15x117 and 25x117 mm). This can be explained by the lower average thickness of long flakes (0.68 mm) than the short flakes (0.72 mm). Drying rate of wood is generally more sensitive to thickness. Using the argument for the width effect, the short flakes should have faster drying rate than long flakes. This was consistent with the findings of Laytner (1989) on length effect on the drying of wafers.

Similar trend was observed with the effect of flake dimensions on the drying rates of southern yellow pine (Table 7 and Figure 14). However, there were significant differences in drying rates between the four dimensions only at 5, 10, 15, and 20% and were no longer significant above 20%. The narrow flakes (15x117 and 15x152 mm) usually have faster drying rates than the wide flakes (25x117 and 25x152 mm) throughout all moisture content levels.

Table 7. Average Drying Rates of the Four Dimensions.

MC (%)	DRYING RATE (%/SEC)							
					SYP			
	15x117	15x152	25x117	25x152	15x117	15x152	25x117	25x152
120					1.538 a	1.554 a	1.464 a	1.435 a
110					1.476 a	1.493 a	1.406 a	1.379 a
100					1.412 a	1.430 a	1.345 a	1.320 a
90					1.344 a	1.363 a	1.281 a	1.259 a
80	1.231 ab	1.301 a	1.174 b	1.167 b	1.274 a	1.294 a	1.214 a	1.194 a
70	1.157 ab	1.225 a	1.105 b	1.100 b	1.198 a	1.220 a	1.143 a	1.126 a
60	1.077 ab	1.143 a	1.030 b	1.027 b	1.118 a	1.141 a	1.067 a	1.053 a
50	0.977 a	1.041 b	0.953 a	0.965 a	1.032 a	1.057 a	0.986 a	0.975 a
40	0.881 a	0.944 b	0.865 a	0.878 a	0.937 a	0.965 a	0.897 a	0.890 a
30	0.774 a	0.833 b	0.764 a	0.776 a	0.832 a	0.864 a	0.798 a	0.796 a
25	0.715 a	0.772 b	0.706 a	0.720 a	0.774 a	0.808 a	0.744 a	0.744 a
20	0.650 a	0.705 b	0.644 a	0.659 a	0.712 ab	0.749 a	0.685 b	0.689 ab
15	0.577 a	0.630 b	0.575 a	0.591 a	0.643 ab	0.683 a	0.621 b	0.628 ab
10	0.493 a	0.545 b	0.497 a	0.514 a	0.561 ab	0.612 a	0.549 b	0.565 ab
5	0.390 a	0.442 c	0.401 ab	0.421 bc	0.473 ab	0.529 a	0.465 b	0.484 ab

Dimensions in mm

Means with the same letter are not significantly different at p=0.05

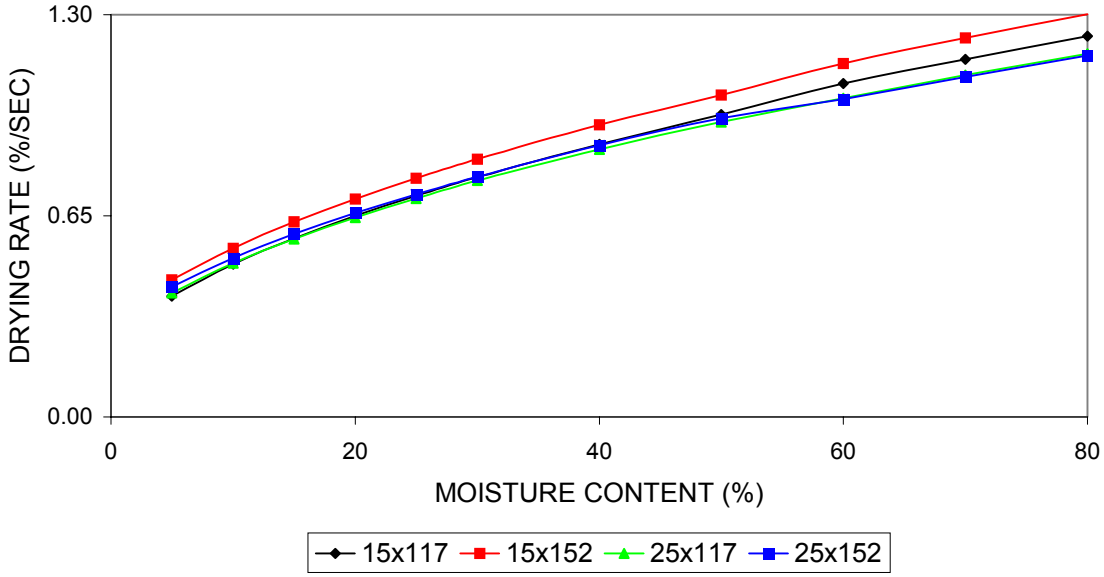

Figure 13. Drying Curves of the Four Dimensions.

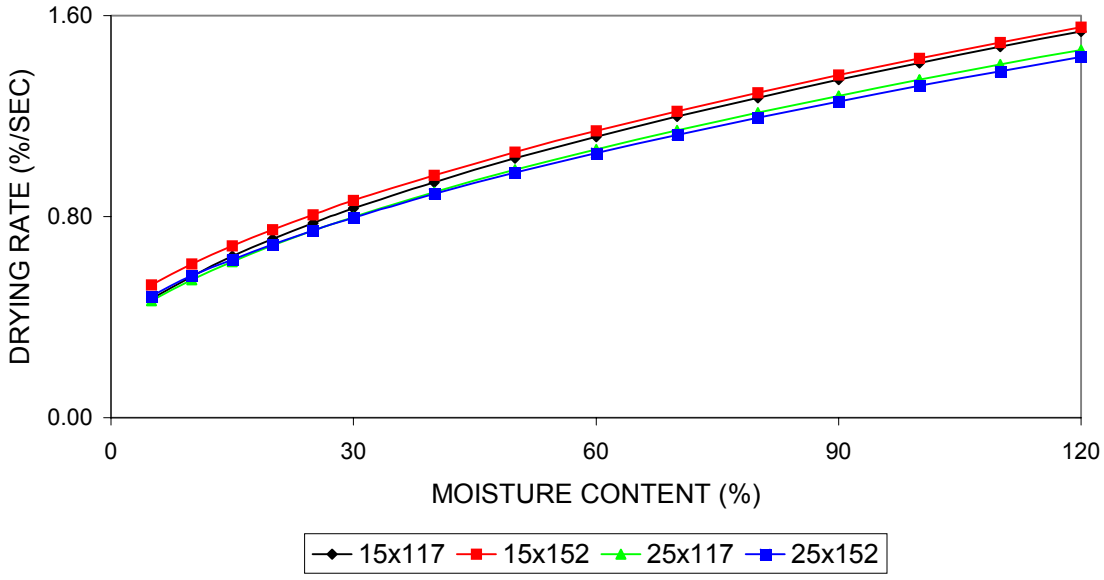

Figure 14. Drying Curves of Southern Yellow Pine According to Dimension.

There were significant differences in the effect of flake dimensions on the drying rates of sweetgum (Table 8 and Figure 15). Above 15%, 15x152 mm flakes have the fastest drying rates compared to the other three flake dimensions. Among the four flake dimensions, it had the lowest mean thickness (0.63 mm). At 15, 10 and 5%, long flakes have faster drying rates than short flakes. Again, this is due to the difference in average thickness between long (0.64 mm) and short (0.68 mm) flakes. Flake drying is more sensitive along the thickness since this is the shortest path thus, less resistance for moisture transport.

Significant differences in drying rates were also observed in yellow-poplar as shown in Table 8 and Figure 16. Narrow flakes have higher drying rates than wide flakes. As explained earlier, shorter width means lower resistance for moisture transport thus, higher drying rate. The difference was observed at all moisture content levels.

Table 8. Average Drying Rates of the Four Dimensions.

MC (%)	DRYING RATE (%/SEC)							
	SWEETGUM				YELLOW-POPLAR			
	15x117	15x152	25x117	25x152	15x117	15x152	25x117	25x152
80	1.188 a	1.309 b	1.134 a	1.140 a				
70	1.115 b	1.229 a	1.066 b	1.073 b				
60	1.036 a	1.144 b	0.993 a	1.001 a				
50	0.951 a	1.052 b	0.915 a	0.923 a	0.947 a	1.021 b	0.960 ab	0.998 b
40	0.858 a	0.950 b	0.829 a	0.839 a	0.849 a	0.917 b	0.869 ab	0.904 b
30	0.753 a	0.837 b	0.733 a	0.744 a	0.738 a	0.799 b	0.757 ab	0.788 b
25	0.694 a	0.774 b	0.679 a	0.692 a	0.676 a	0.733 b	0.695 ab	0.723 b
20	0.630 a	0.705 b	0.621 a	0.636 a	0.607 a	0.661 b	0.626 ab	0.651 b
15	0.557 a	0.629 b	0.559 a	0.574 ab	0.530 a	0.579 b	0.548 ab	0.571 b
10	0.476 a	0.541 b	0.485 a	0.504 ab	0.439 a	0.484 b	0.457 ab	0.476 b
5	0.375 a	0.435 b	0.398 ab	0.422 b	0.321 a	0.363 b	0.341 ab	0.357 ab

Dimensions in mm
Means with the same letter are not significantly different at p=0.05

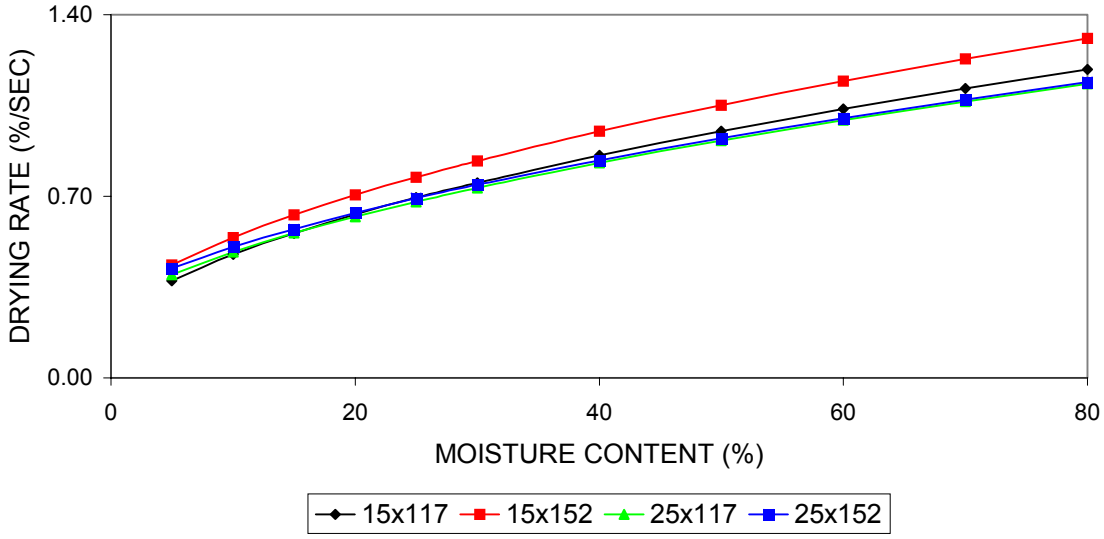

Figure 15. Drying Curves of Sweetgum According to Dimension.

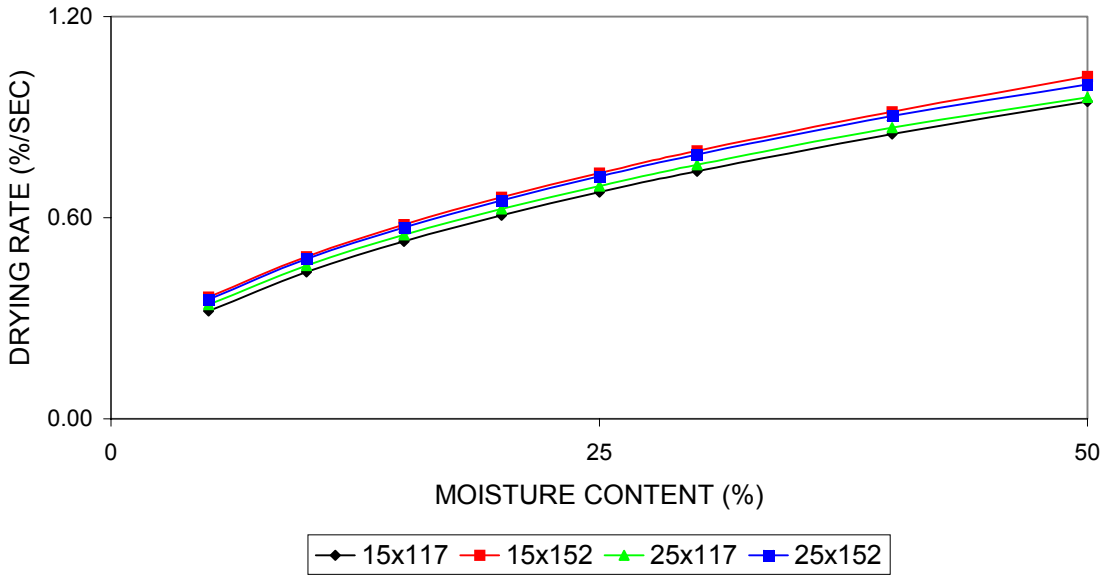

Figure 16. Drying Curves of Yellow-poplar According to Dimension.

Effect of Temperature

Effect of temperature was found to be significant at all moisture content levels (Appendix Y and Z). Influence of temperature on the drying rates is shown in Table 9 and Figure 17. Higher temperature has an effect on drying rate by virtue of higher thermal energy and mass transfer. An increase in temperature resulted in a roughly linear increase in drying rate of flakes. According to Comstock (1971), linear relationship between veneer drying rate and temperature holds true for temperatures above 100^{o}C. The linear increase in drying rate with increase in temperature is caused by the dependence of diffusivity, partial pressure and vapor pressure on temperature.

Temperature effect on the drying rate of southern yellow pine is also significant at all moisture content levels (Table 9 and Figure 18). The same trend was observed on sweetgum (Table 9 and Figure 19) and yellow-poplar (Table 9 and Figure 20) flakes. Increase in temperature resulted in increase in drying rates for all species.

Table 9. Average Drying Rates of the Three Temperatures.

MC (%)	DRYING RATE (%/SEC)											
				SYP			SG			YP		
	150	200	250	150	200	250	150	200	250	150	200	250
120				1.047 a	1.479 b	1.967 c						
110				1.005 a	1.420 b	1.890 c						
100				0.962 a	1.359 b	1.809 c						
90				0.916 a	1.295 b	1.724 c						
80	0.850 a	1.208 b	1.597 c	0.868 a	1.229 b	1.635 c	0.832 a	1.188 b	1.559 c			
70	0.799 a	1.137 b	1.503 c	0.817 a	1.157 b	1.541 c	0.781 a	1.116 b	1.466 c			
60	0.744 a	1.060 b	1.403 c	0.763 a	1.081 b	1.441 c	0.726 a	1.039 b	1.366 c			
50	0.682 a	0.973 b	1.301 c	0.705 a	1.000 a	1.333 a	0.666 a	0.955 b	1.259 c	0.675 a	0.965 b	1.311 c
40	0.616 a	0.880 b	1.180 c	0.641 a	0.911 b	1.215 c	0.601 a	0.864 b	1.142 c	0.605 a	0.867 b	1.183 c
30	0.541 a	0.776 b	1.042 c	0.570 a	0.812 b	1.085 c	0.528 a	0.761 b	1.010 c	0.525 a	0.755 b	1.032 c
25	0.499 a	0.719 b	0.966 c	0.531 a	0.758 b	1.013 c	0.487 a	0.704 b	0.938 c	0.480 a	0.693 b	0.947 c
20	0.454 a	0.656 b	0.883 c	0.489 a	0.700 b	0.936 c	0.442 a	0.646 b	0.859 c	0.430 a	0.624 b	0.854 c
15	0.403 a	0.586 b	0.791 c	0.443 a	0.636 b	0.852 c	0.393 a	0.574 b	0.772 c	0.374 a	0.547 b	0.750 c
10	0.345 a	0.506 b	0.687 c	0.391 a	0.565 b	0.758 c	0.335 a	0.496 b	0.673 c	0.307 a	0.456 b	0.628 c
5	0.272 a	0.409 b	0.560 c	0.331 a	0.483 b	0.649 c	0.265 a	0.402 b	0.555 c	0.220 a	0.341 b	0.475 c

Temperature in ^{o}C

Means with the same letter are not significantly different at p=0.05

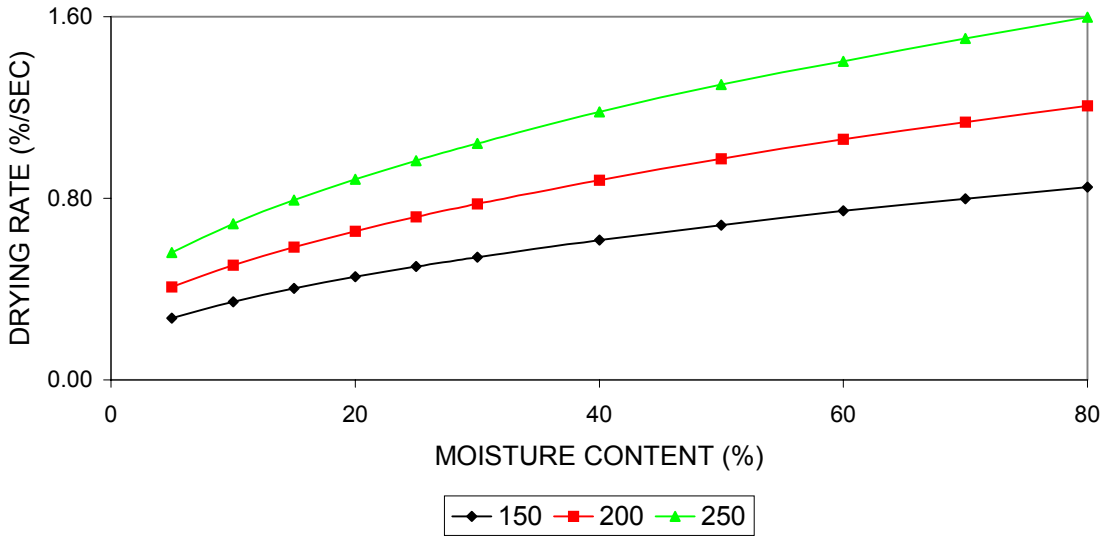

Figure 17. Drying Rate Curves of the Three Temperatures.

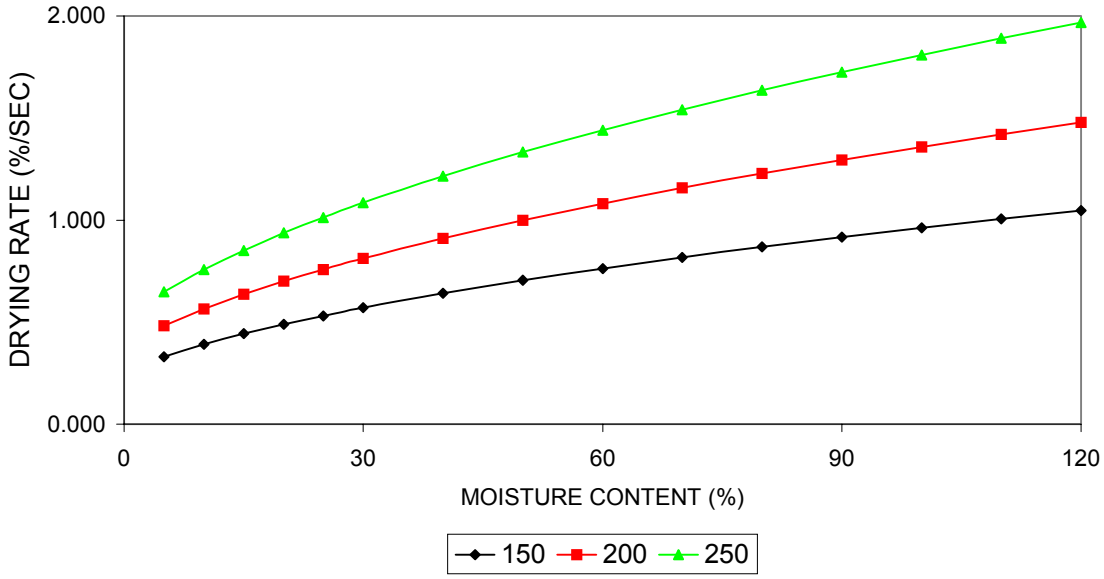

Figure 18. Drying Rate Curves of Southern Yellow Pine According to Temperature.

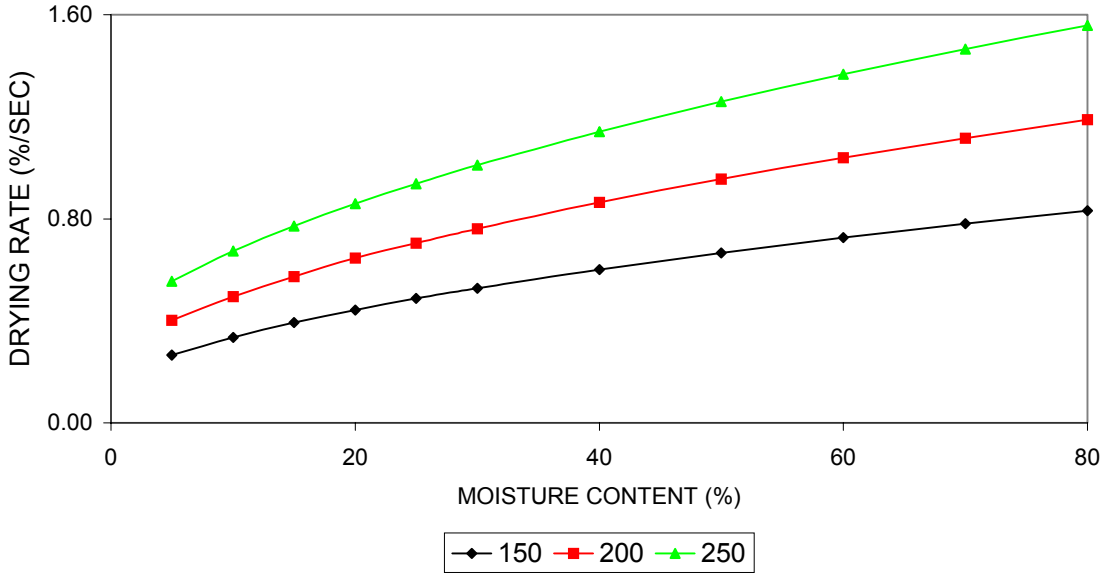

Figure 19. Drying Rate Curves of Sweetgum According to Temperature.

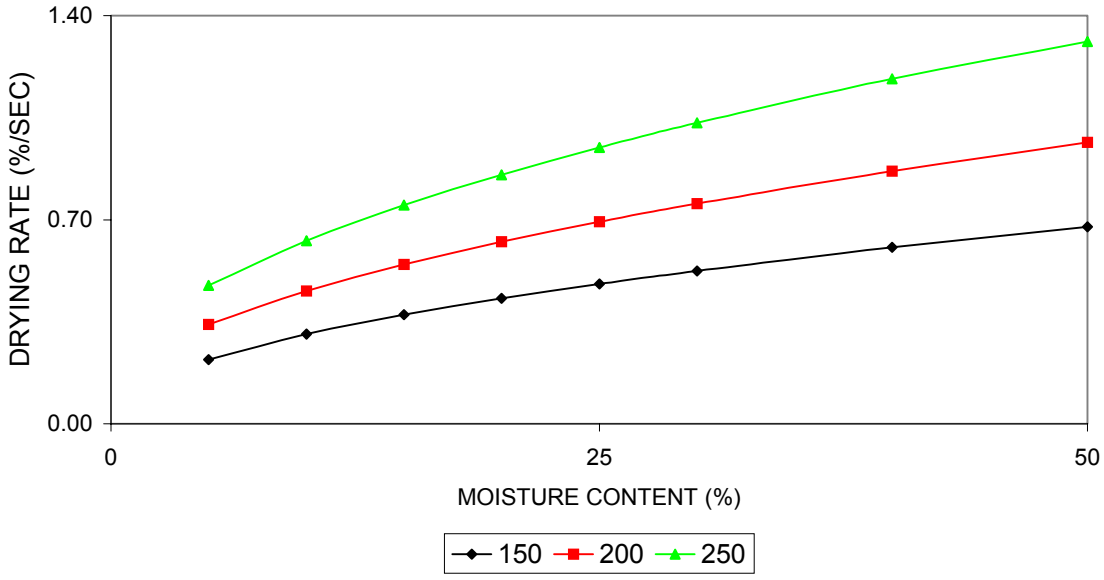

Figure 20. Drying Rate Curves of Yellow-poplar According to Temperature.

3.4. Conclusions

The drying curve of flakes can be accurately described by a second-order/quadratic model. The validity of the model was tested using several criteria (i.e. test of significance of the model and parameter coefficients, MSE, MSR, R^2, and plots of observed values versus fitted values and residuals).

Drying rate of the flakes was calculated by differentiating the quadratic model. Observation of drying rate curves revealed two falling rate drying periods. No constant rate drying was observed. The first falling rate period at the start of drying is attributed to the decreasing wetted surface area caused by severe drying conditions. Free evaporation of liquid occurs over a decreasing wetted surface area thus, no constant rate drying period. This period is predominantly controlled by convective heat transfer. At about 30% moisture content, the drying rate indicates a second falling rate. Temperature of the flake starts to rise. This period is controlled by internal bound water diffusion. The drying rate curve has no deflection indicative of a gradual switch from one mechanism to another.

Drying rates were found to vary between species. Southern yellow pine had the fastest drying rate at all moisture content levels followed by sweetgum. Yellow-poplar had the slowest drying rate. Difference in drying rates between species is attributed to specific gravity. Other factors such as permeability, porosity, and cell morphology may also play a role in affecting drying rates of flakes.

Cutting direction was found to have an effect on drying rates. Radially-cut specimens have slower drying rates than tangentially-cut specimens. This is due to the exposure of wood rays on the wide surface of tangentially-cut specimens that provide passageways for moisture coming out of the flakes. Effect of cutting direction was dependent on the moisture content level of the species. Cutting direction was not significant on southern yellow pine above 60%. From 50 to 5%, the effect of cutting direction became significant. The effect of cutting direction on sweetgum was significant above 5% but no longer significant at 5%. For yellow-poplar, the effect of cutting direction was significant at all moisture content levels.

Dimension of the flakes also had an effect on the drying rate. Narrow flakes have faster drying rates than wider flakes. Width effect is caused by moisture transport along the transverse direction that serves as additional passageways. Shorter distance means less resistance thus, higher drying rate. Following the same argument, short flakes should have higher drying rate than long flakes. However, long thinner flakes were found to have faster drying rates than the short thicker flakes. This brings the effect of thickness which is more sensitive to drying properties of flakes. Dimension only had an effect on the drying rate of southern yellow pine from 20 to 5%. There was significant effect of dimension on the drying rates of sweetgum and yellow-poplar at all moisture content levels.

Temperature was found to have a highly significant effect on drying rate. An increase in temperature resulted in an approximately linear increase in drying rate at all moisture content levels. Same trend holds true for all three species. This is caused by the temperature dependence of moisture transport parameters. Influence of temperature on the drying rates of southern yellow pine, sweetgum, and yellow-poplar were highly significant at all moisture content levels tested.

It is apparent that flake properties and drying condition have significant effects on drying rates. Therefore, these properties and conditions can be altered to optimize the drying rate of flakes. Flake properties were found to have an affect on drying rate. Thin, narrow, short, and tangentially-cut flakes are ideal to increase the drying rate. However, both cutting directions and flake dimensions can be very difficult to control in the actual flaking process in OSB manufacture. Given also the variability of properties (i.e. specific gravity, initial moisture content) that is usual in wood-based materials, flake properties may not be the variable to be controlled.

Drying condition (i.e. temperature) may be the better alternative since this parameter can be easily controlled and monitored to increase the drying rate. Since the early part of drying is controlled by heat transfer, temperature plays an important role in the flake drying process.

3.5. References

ALVES, S.S. and J.L. FIGUEIREDO. 1989. A model for pyrolysis of wet wood. Chem. Engg. Sci. 44(12): 2861-2869.

AMERICAN SOCIETY OF TESTING MATERIALS (ASTM). 1994. Standard test methods for specific gravity of wood and wood-base materials D 2395-93. 1994 Annual Book of ASTM Standards Vol. 04.10. Philadelphia, PA.

AMERICAN SOCIETY OF TESTING MATERIALS (ASTM). 1994. Standard test methods for direct moisture content measurement of wood and wood-base materials D 4442-92. 1994 Annual Book of ASTM Standards Vol. 04.10. Philadelphia, PA.

COMSTOCK, G.L. 1971. The kinetics of veneer jet drying. For. Prod. J. 21(9): 104-111.

Di BLASI, C. 1998. Multi-phase moisture transfer in the high-temperature drying of wood particles. Chem. Engg. Sci. 53(2): 353-366.

FHYR, C. and A. RASMUSON. 1996. Mathematical model of steam drying on wood chips and other hygroscopic porous media. AIChE J. 42(9): 2491-2502.

FOREST PRODUCTS SOCIETY (FPS). 1999. Wood Handbook: Wood as an Engineering Material. Reprinted from USDA Forest Service Forest Products Laboratory General Technical Report FPL-GTR 113.

FOREST PRODUCTS SOCIETY (FPS). 1997. Dry Kiln Operator's Manual. Reprinted from USDA Agricultural Handbook No. 188.

KAYIHAN, F. and M.A. STANISH. 1984**.** Wood particle drying: A mathematical model with experimental evaluation. In Drying '84. pp. 330-347.

LAYTNER, F., N. EIPSTEIN, J.R. GRACE and K.L. PINDER. 1991. Kinetics of wood wafer drying. Drying '92. pp. 1135-1144.

LAYTNER, F. 1989. Fundamentals and Technology of Wafer Drying. Ph. D dissertation. University of British Columbia.

MALTE, P.C., R.W. COX, W.J. KENNISH, S.C. SCHMIDT, R.J. ROBERTUS, G.R. MESSINGER and M.D. STRICKLER. 1976**.** Experiments on the kinetics and mechanisms of drying small wood particles. Research Report TEL-76-8. Thermal Energy Laboratory, College of Engineering, Washington State University, Pullman, WA.

MELAAEN, M.C. 1996. Numerical analysis of heat and mass transfer in drying and pyrolysis of porous media. Numerical Heat Transfer, Part A 29(4): 331-355.

MONTGOMERY, D.C. and E.A. PECK. 1992. Introduction to Linear Regression Analysis. 2nd ed. Wiley-Interscience.

OMEGA. 2000. OS550/OS550-BB Series Industrial Infrared Thermometer/Transmitter User's Guide.

PANG, S., S.G. RILEY and A.N. HASLETT. 1997. Simulation of Pinus radiata veneer drying: Moisture content and temperature profiles. For. Prod. J. 47(8): 51-58.

ROSEN, H.N. 1980a. Wood behavior during impingement drying. Dying '80 pp. 413-421.

ROSEN, H.N. 1980b. Empirical model for characterizing wood drying curves. Wood Sci. 12 (4): 201-206.

ROSEN, H.N. 1978. Evaluation of drying time, drying rates, and evaporative fluxes when drying with impinging jets. Proc. First International Symposium on Drying. McGill Univ, Science Press, Princeton, NJ. pp. 192-200.

SAASTAMOINEN, J.J. and R.K. IMPOLA. 1995. Drying of solid fuel particles in hot gases. Drying Tech. 13(5-7): 1305-1315.

SILITONGA, T.M. 1983. Moisture transport rate and energy consumption for convective drying of fuelwood chips. PhD dissertation. University of Minnesota.

SNEDECOR, G.W. and W.G. COCHRAN. 1980. Statistical Methods. 7th ed. Iowa State University Press, Ames, Iowa.

SOUZA, M.E.P. and S.A. NEBRA. 2000. Heat and mass transfer model in wood chip drying. Wood and Fiber Sci. 32(2): 156-163.

STEELE, R.G.D. and J.H. TORRIE. 1980. Principles and Procedures of Statistics: A Biometrical Approach. 2nd ed. McGraw Hill, New York.

TSCHERNITZ, J.L. and W.T. SIMPSON. 1979. Drying rate of northern red oak lumber as an analytical function of temperature, relative humidity, and thickness. Wood Sci. 11(4): 202-208.

CHAPTER 4. COMPARISON OF EXPERIMENTAL DATA WITH A NUMERICAL DRYING MODEL

4.1. Introduction

As seen in the previous chapter, the drying of flakes depends on many parameters such as species, initial moisture content, specific gravity, cutting direction, dimensions, and temperature. Due to many parameters involved, it is very difficult to develop a correlation for drying based on empirical correlations. Thus, others prefer a theoretical model. The theoretical model is more advantageous since it is based on fundamental physics and the physical mechanism that occurs during the drying process can be easily explained whereas experimental correlation can not represent the drying process functionally.

Drying of wood is a complex physical phenomenon that can be modeled. It involves heat and mass transfer and can be represented by equations that are strongly coupled and highly non-linear. Numerical models have been employed to solve these sets of equations. Because of its complexity and the fact that these models need a lot of parameters that are often a function of other variables, the use of these models in industrial applications has been very limited.

Current research efforts on the drying of wood products have focused primarily on numerical modeling. This has become prominent in light of better computing power of personal computers. Although this is desirable considering the advantages of numerical modeling, it has tended to cause more research into modeling rather than experiments. Most research has been done on drying of lumber and wood particles. Drying research on wood particles has focused on numerical modeling of drying for particleboard and biomass/biofuel. Drying research on flakes for oriented strand board (OSB) production has been very limited considering the wide use of these composite panels.

Front2D (Perre et al. 1999) is a numerical wood drying model based on physical formulation. It is a bridge between a simple modeling approach and a more comprehensive and rigorous modeling strategy. This model provides an efficient and realistic simulation that represents the drying process of anisotropic materials such as wood.

In this chapter, an experimental data set is compared to a numerical model. Internal and external parameters taken from literature and geometrical parameters based on the experimental drying set were used in the numerical model. The drying mechanism of flakes based on the simulation is presented. The effects of various drying parameters tested on the experiments were likewise tested on the numerical model.

4.2. Theory

Front2D (Perre et al. 1999) is a drying simulation of a porous medium exposed to convective and/or radiative heating based on a set of physical assumptions. Physical parameters (liquid migration coefficient, permeability, and thermal conductivity) are used in the simulation. Geometrical parameters (length and thickness) are also included in the model. The philosophy of the model is to use enough physical assumptions to enable the drying equations to be resolved by a semi-analytical method. The following discussions focus on the model assumptions, pressure-field calculations, heat and mass transfer formulation, and numerical solution.

4.2.1. Pressure field

The analytical model is based on a set of simplifying assumptions. The following assumptions allow the two-dimensional (longitudinal and transverse directions) pressure field to be resolved:

1. use of a drying front (Figure 21);
2. zone between the drying front and exchange surface consist of water vapor only;
3. water vapor is assumed to migrate according to Darcy's law;
4. porous medium is divided into vapor and liquid zones; and

5. pressure field is assumed to have attained steady state.

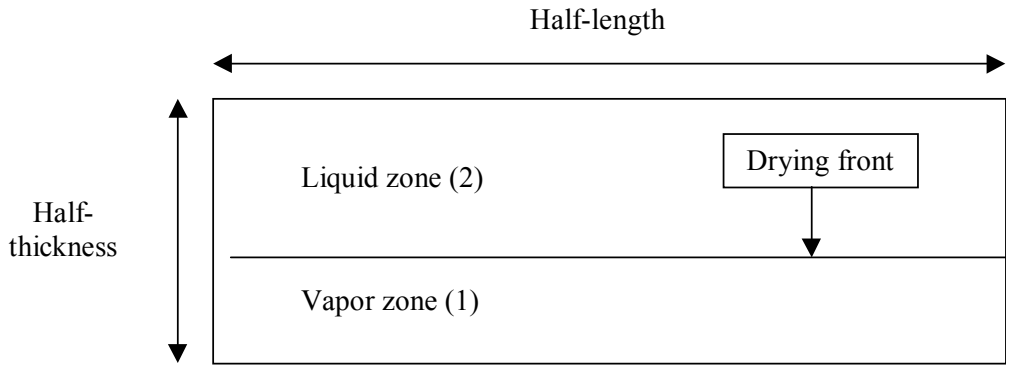

Figure 21. Drying Front Configuration.

This will determine the global vapor flux:

$$\langle q_m \rangle = -\rho_v \frac{K_{1y}}{\mu_v}\left(\frac{e}{\beta}\right)\frac{\Delta P}{e} \qquad \text{(Eq.4.1)}$$

where: q_m is the global vapor flux

ρ_v is the vapor density

K is the relative permeability

μ_v is the vapor dynamic viscosity

e is the front thickness

ΔP is pressure difference between front and surface

4.2.2. Heat transfer

To define the drying model, the relationship between mass and heat flux must be established. Two more assumptions are made to allow the temperature field within the medium to be governed by a linear one-dimensional equation:

6. heat transfer is assumed to occur along the thickness only; and
7. sensible heat (heat to raise the temperature of wood) is negligible.

The internal thermal flux is used entirely to change liquid into vapor at the front position. The heat flux reads:

$$q_c = -\lambda_y \frac{\partial T}{\partial y} \qquad \text{(Eq.4.2)}$$

where: q_c is the heat transfer flux

λ thermal conductivity

T is temperature

y is thickness

The energy balance in the vapor and liquid zones are governed by the equations:

$$\lambda_{1y} \frac{\partial T_1}{\partial y_1} = -\langle q_m \rangle L_v \qquad \text{(Eq.4.3)}$$

$$\lambda_{2y} \frac{\partial T_1}{\partial y_2} = 0 \qquad \text{(Eq.4.4)}$$

where: L_v is latent heat of vaporization

Convection heat transfer is considered for the boundary condition:

$$q_{cext} = h\{T_{ext} - T_1(y_1 = o)\} \qquad \text{(Eq.4.5)}$$

where: h is the convection heat transfer coefficient.

4.2.3. Mass transfer

Two other assumptions are made to describe the way the liquid migrates within the medium:

8. liquid propagates along the thickness only; and
9. the one-dimensional moisture content profile has a quadratic shape.

The moisture content gradient is related to the liquid flux through the migration coefficient:

$$q_l = -a_{ml} \nabla(X) = -\rho_l \frac{K_{y2}}{\mu_l} \frac{\partial P_c}{\partial X} \nabla(X) \qquad \text{(Eq.4.6)}$$

where: q_l is the liquid flux

a_{ml} is coefficient of liquid migration

X is moisture content

4.2.4. Numerical solution

A computer code was developed by Perre et al. (1999) using the set of equations presented in the previous subsections. The code written in Fortran 90 was supplied Dr. Patrick Perre of ENGREF/INRA. The algorithm is presented in the Appendix. The calculations were made using Compaq Visual Fortran.

4.3. Drying Case

The initial conditions for the simulation were set to be similar to an experiment plot. These conditions were based on the drying of southern yellow pine flakes measuring 0.83 mm x 15 mm x 117 mm (thickness, width, and length) dried at 150^{o}C. The initial moisture content was 142% with density of 450 kg/m^3.

Internal transfer parameters used in the model included thermal conductivity, transverse permeability, permeability ratio, and liquid migration coefficient. Thermal conductivity for the green flakes was computed using MacLean equation (Siau, 1995):

$$K_t = G(0.200 + 0.0052M) + 0.024 \quad \text{(Eq.4.7)}$$

where: K_t is tranverse thermal conductivity

G is specific gravity

M is moisture content

Transverse permeability value of 10^{-15} m^2 was used (Perre et al. 1999). Permeability ratio between longitudinal and transverse directions was set at 1000, which is common for softwood species (Siau, 1995). Liquid migration coefficient value of 5 x 10^{-6} kg/m*s was used (Perre et al. 1999).

Heat transfer parameter that was calculated was the convection heat transfer coefficient (h). This coefficient was determined based on the drying condition (150^{o}C and 0.8 m/s). For flakes, the functional form for a flat plate was adopted. The following correlations were used (Incropera and DeWitt, 1996):

$$Nu = 0.664\, Re^{0.5}\, Pr^{0.33} \quad \text{(Eq.4.8)}$$

$$Re_L = \rho VL/\mu \quad \text{(Eq.4.9)}$$

$$Pr = C_p\mu/k \quad \text{(Eq.4.10)}$$

where: Nu is the Nusselt number

Re is the Reynolds number

Pr is the Prandtl number

ρ is the air density

V is the air velocity

L is the boundary length

μ is the air viscocity

C_p is the specific heat of air

k is the thermal conductivity of air

Results of the simulations are presented next. The effect of drying parameters such as species, cutting direction, width, length, and temperature were also tested on the model.

4.4. Results and Discussion

A direct comparison between the experimental and simulated drying behavior of southern yellow pine is shown in Figure 22. It should be noted that all the transport parameters used in the simulations were taken from the literature and no information was taken from the experiments to obtain a good fit to the experimental data.

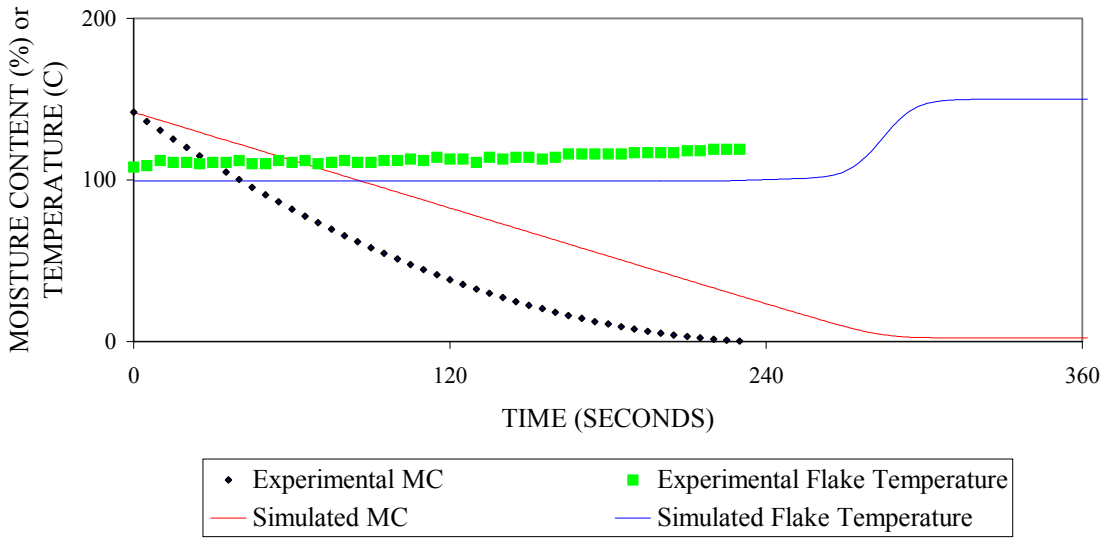

Figure 22. Experimental and Simulated Drying Curves and Surface Temperature.

Based on the figure, it can be seen that the simulation and experiments have little in common. The simulation shows a constant rate drying period followed by a falling rate drying period. Two drying periods were also observed on drying simulation of flakes (Kayihan, 1982; Kayihan and Stanish, 1986; Stanish and Kayihan; 1984), veneer (Pang et al. 1997), wood chips (Fyhr and Rasmuson, 1996; Melaaen, 1996; Souza and Nebra, 2000) and sawdusts and wood blocks (Kayihan and Stanish, 1986; Stanish and Kayihan; 1984). The constant rate period in the simulation extends all the way down to about 30% moisture content. Below 30%, the drying rate decreases (i.e. falling rate drying period). Compared to the experiment, there was no constant rate period at all. Falling rate period was observed right at the start of drying. Simulated drying of wood particles by Alves

and Figueiredo (1989) and Di Blasi (1989) only has a falling rate drying period and no constant rate drying period.

It is expected that the drying curves will not match exactly because the maximum drying rates are different due to the different sizes of the exchange surface. This discrepancy can be avoided by introducing the second and even third dimension to the simulations. However, this will lead to more equations and very long computing times. One alternative would be to increase the convection heat transfer coefficient in order to compensate for the difference in total surface area (Fyhr and Rasmuson, 1996). This would provide the correct drying rate in the constant rate period but would cause deviations in the falling rate period.

The temperature curves exhibit more variety. The difference indicates that the thermal conductivity in the simulations is not close to the rates for wood, both in magnitude and temperature dependence. Discrepancy between the curves in the last stage of drying may be attributed to differences in heat transfer to the surface, differences in distribution of the moisture or in moisture dependence of the heat transfer coefficient, or a combination of these factors (Fyhr and Rasmuson, 1996).

The physical parameters (i.e. thermal conductivity, permeability, and liquid migration) that were used in the simulation were assumed to be constant in both vapor and liquid zones. However, these parameters are functions of other parameters such as temperature and moisture content. Thus, these parameters will have an effect on the results of the simulation since the moisture content and temperature change as drying progresses. The use of constant physical parameters was done in order to simplify the simulation and so that the drying equations can be solved by a semi-analytical approach.

4.4.1. Simulated drying mechanism

The moisture content of the flake decreases constantly and the surface temperature increases rapidly to the boiling point and remains there during the constant rate drying period. All energy transferred to the flake is used in the evaporation of water. Water is replenished by the capillary flow of water from the interior to the surface. During this period, internal moisture resistance to liquid migration is very low coupled with high external flux due to the drying condition and thickness of the flakes. Hence, heat transfer predominantly controls drying of flakes during the constant rate drying period (Fyhr and Rasmuson, 1996; Kayihan, 1982; Kayihan and Stanish, 1986; Melaaen, 1996; Pang et al. 1997; Stanish and Kayihan; 1984; Souza and Nebra, 2000). The duration of the constant rate drying period is directly connected to the liquid migration, whose gradient depends on both the drying flux and on the liquid migration coefficient (Perre et al. 1999). Total drying time of wood is not determined by heat transfer rate alone in the constant rate drying period (Fyhr and Rasmuson, 1996). A certain increase in maximum heat transfer rate does not necessarily lead to an equivalent shortening of the total drying time. The internal overpressure also enhances the drying rate.

When the surface enters the hygroscopic range, a considerable moisture content gradient develops (Di Blasi, 1998; Fyhr and Rasmuson, 1996; Melaaen, 1996; Pang et al. 1997; Perre et al. 1999; Souza and Nebra, 2000) and the drying rate starts to decrease. This is known as the falling rate drying period. The temperature also starts to rise above the boiling point. Decrease in drying rate and increase in temperature is reflected in Figure 4.2. Liquid migration to the surface is no longer sufficient to consume the heat transferred by evaporation thus, the temperature rises. The rate of moisture transport in this period is limited by the ability of water to diffuse through the wood to its surface. This period is characterized by decreased wetted surface area drying and internal diffusion of bound water. As it is, mass transfer inside the material controls drying (Di Blasi, 1998; Fyhr and Rasmuson, 1996; Kayihan, 1982; Kayihan and Stanish, 1986; Melaaen, 1996; Pang et al. 1997; Perre et al. 1999; Stanish and Kayihan, 1984; Souza and Nebra, 2000).

4.4.2. Effect of drying parameters

Physical properties of wood depend on the species (i.e. hardwood and softwood). For the same type of wood, variability in properties along and across the grain are also observed (FPS, 1997 and 1999). Parametric studies on the effects of species, cutting direction, dimensions, and temperature were performed using the numerical model. As these properties were changed, the drying mechanism remained unchanged or the same qualitatively. However, some parameters caused significant quantitative differences in drying behavior.

Effect of species

The influence of species on the simulated drying of flakes is tested. Parameters in the numerical model that were changed to reflect the differences between southern yellow pine, sweetgum, and yellow-poplar were density, initial moisture content, transverse permeability, and anisotropic ratio (Table 10). Density and initial moisture content values were based from experimental data sets (15 mm x117 mm flakes cut radially). Transverse permeability (10^{-4}) and anistropic ratio (10,000) for both hardwoods were taken from Siau (1995). All other parameters (i.e. temperature at 150^{o}C, convection heat coefficient, dimensions) were kept the same.

Table 10. Parameters of the Three Species.

	SYP	SWEETGUM	YELLOW-POPLAR
Initial MC (%)	142	105	82
Density (kg/m^3)	450	430	330
Transverse permeability (m^2)	10^{-3}	10^{-4}	10^{-4}
Anisotropic ratio	1000	10000	10000

Effect of species on flake drying simulation is shown in Figure 23. The initial moisture content had a significant effect on drying time of flakes. As expected, as initial moisture content increases, the drying time also increases because there is more water to be evaporated. Many properties of wood including initial moisture content are all related to density. Density also has a significant effect on drying time. Generally, an increase in drying time or slower drying is expected as density increases due to more water in wood at a given moisture content.

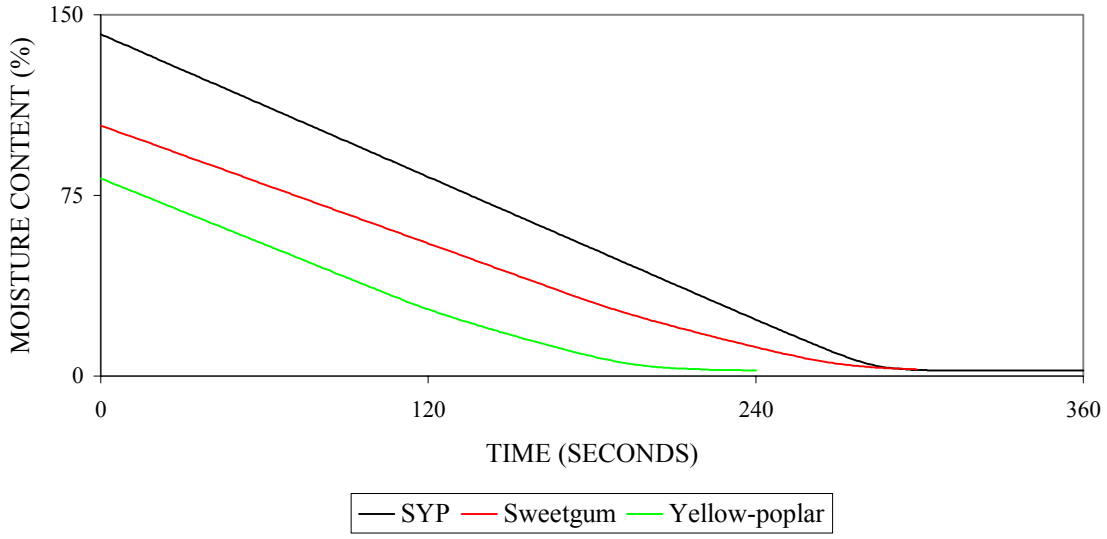

Figure 23. Simulated Drying Curves of the Three Species.

Analyzing the simulated drying curves of the three species, the general trend does not apply. Southern yellow pine and sweetgum have almost similar density but the drying rates of the two species are qualitatively different. On the other hand, sweetgum and yellow-poplar have differences in density but their drying curves are almost similar. Thus, others factors must affect flake drying behavior.

Another factor that may affect the drying behavior of wood and was manipulated in the numerical model is transverse permeability. Constant rate of drying in southern yellow pine is longer and this can be due to its higher permeability which allows the capillary forces to keep the surface wet for a longer period. Falling rate is also faster for southern yellow pine probably because its longitudinal permeability is higher compared to the two hardwood species.

Effect of cutting direction

Effect of cutting direction was tested by adjusting only one parameter: the transverse permeability. Radial and tangential permeability values of 1.13×10^{-2} and 3.0×10^{-4}, respectively for southern pine were taken from Comstock (1970). The two curves for both cutting directions exactly follow the same curve (Figure 24). Thus, the value of transverse permeability is not really critical in the drying simulation of southern yellow pine flakes. But that does not mean that permeability has no effect on drying rate as discussed in the previous paragraph.

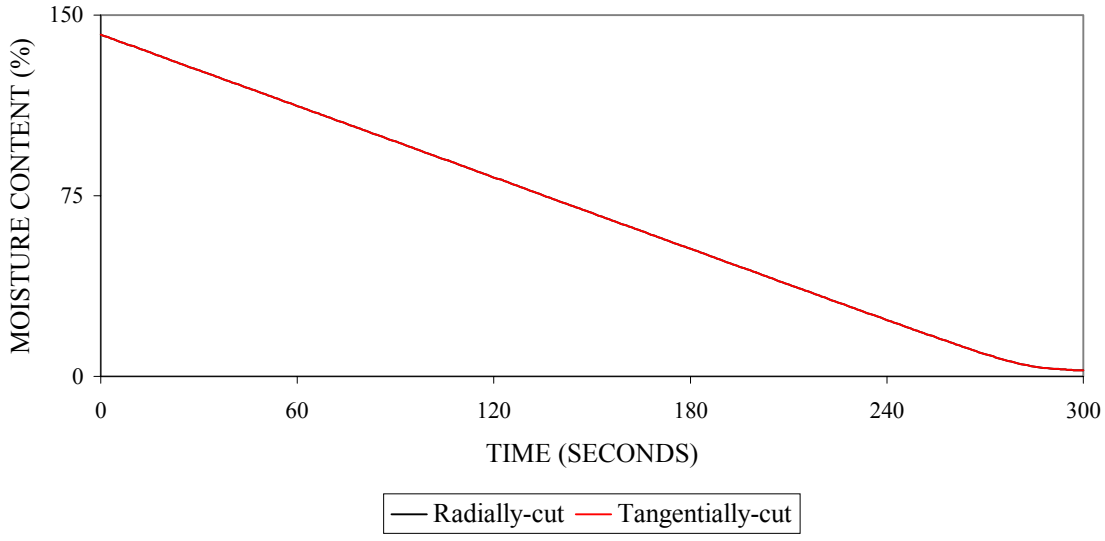

Figure 24. Simulated Drying Curves of the Two Cutting Directions.

Effect of dimensions

Influence of dimensions in simulation of flake drying was done by subdividing the effect of thickness, width, and length. In determining the effects of thickness and length on drying simulations, only these geometric parameters have to be changed. It is assumed that the boundary conditions are directed across the width of the flake. For width effect, the other parameter that was affected was the convection heat transfer coefficient since it is dependent on the boundary dimension. This coefficient is also a function of the Reynolds number (Eq. 4.9), which also takes into account the width since the boundary conditions is assumed to be across the width.

Only two thickness were compared, 0.6 and 0.8 mm. Figure 25 shows the effect of thickness on the drying simulation of flakes. Thinner flakes translate faster drying rate thus, shorter drying time. Since the model is based on the assumption that liquid migration is through the thickness only, it is logical that thinner flakes have shorter drying time since there is a shorter pathway for liquid migration. General trends for wood particles show that when thickness is doubled, the total drying time is approximately doubled and the opposite when the thickness is halved (Fyhr and Rasmuson, 1997).

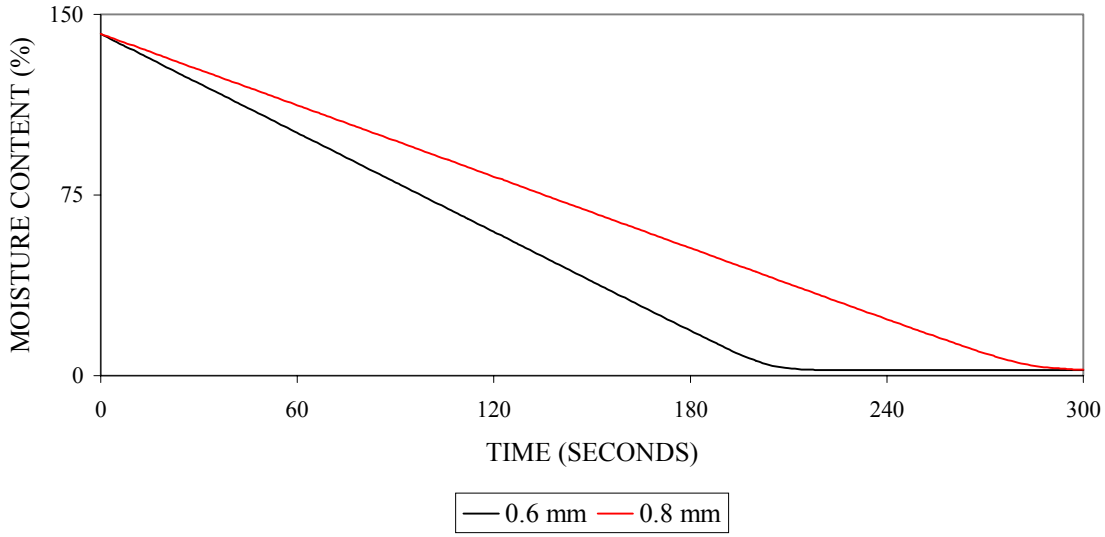

Figure 25. Simulated Drying Curves of the Thicknesses.

The effect of the flake lengths (117 and 152 mm) was also tested. There was no difference between the two drying curves (Figure 26). The difference between the two lengths has not caused any considerable change in the pressure field to alter the drying behavior. It should be noted that the length was only considered in the pressure field calculation and not on the heat and mass transfer. Similar to cutting directions, the model parameter related to this drying parameter is not critical on the drying behavior of flakes.

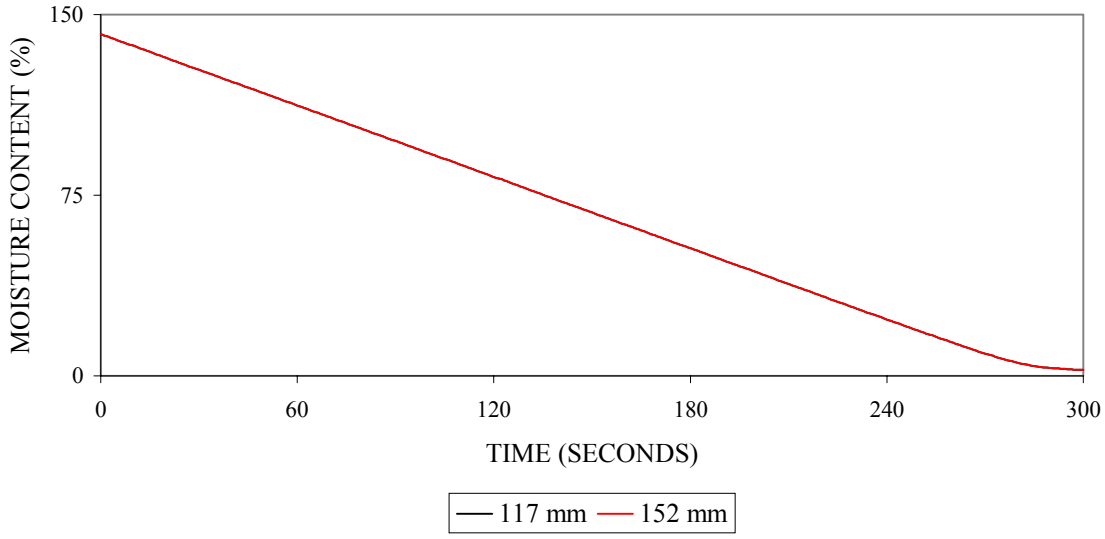

Figure 26. Simulated Drying Curves of the Lengths.

The effect of width is shown in Figure 27. Wider flakes translate to slower drying rate and longer drying time. This is caused by the lower convection heat transfer coefficient for wider flakes. Lower convection heat transfer causes less thermal energy that has a major effect on drying time and rate.

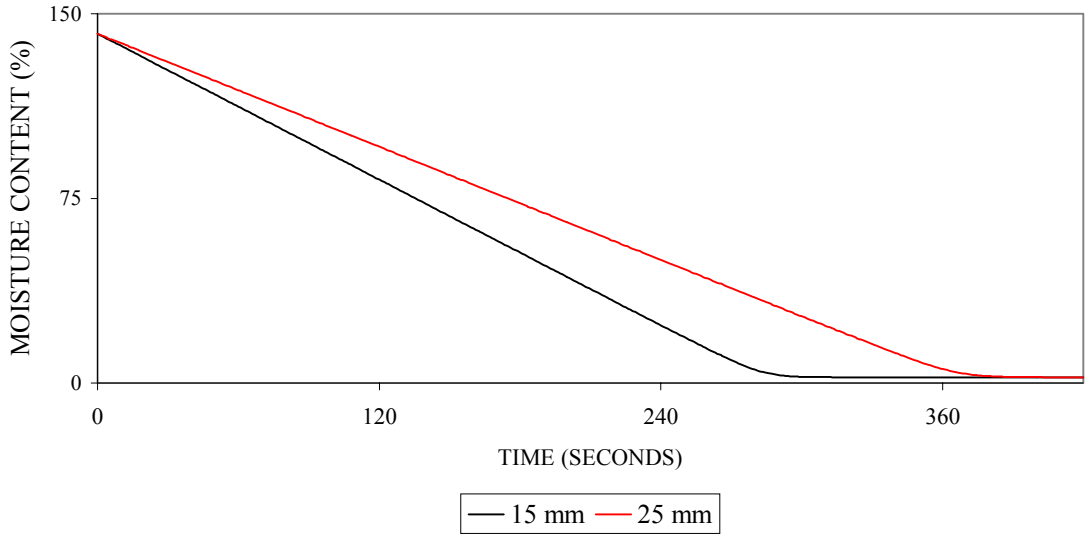

Figure 27. Simulated Drying Curves of the Two Widths.

Effect of temperature

With temperature effect, many parameters had to be changed. Not only is the external parameter affected (temperature and convection heat transfer coefficient), but also the thermo-physical data (latent heat of vaporization and viscosity). These parameters are listed in Table 11. Figure 28 shows the influence of temperature on simulated drying. As temperature increases, the drying rate increases and drying time decreases. This is by virtue of the higher thermal energy and related mass transfer associated with higher temperature. There is a roughly linear change in the drying rate as the temperature is changed.

Table 11. External Parameters and Thermo-physical Data.

PARAMETER	TEMPERATURE (^{o}C) 150	200	250
Re	207	171	144
Pr	0.6883	0.6840	0.6831
Nu	8.4	7.7	7.0
Hconv (W/m^2*K)	40	40	39
Hfg (kJ/kg)	2188	2083	1979
Viscosity (N*s/m^2)	2.40E-05	2.60E-05	2.79E-05

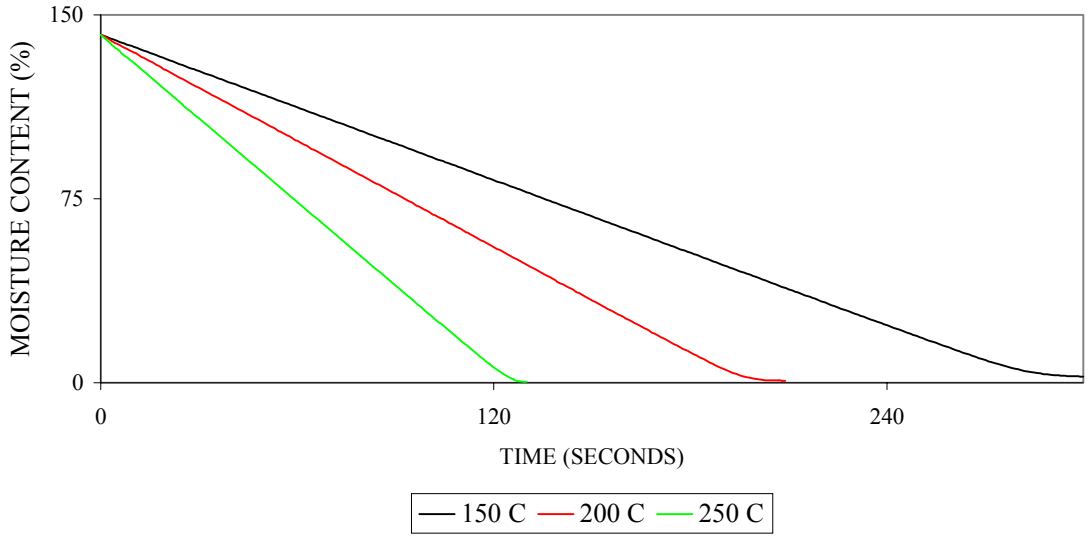

Figure 28. Simulated Drying Curves of the Three Temperatures.

4.5 Conclusions

Simulated drying behavior of flakes using Front2D has little in common with experimental data. Simulated drying is divided into two periods: constant rate and falling rate. External heat transfer controls the constant rate drying period. The moisture content of the flake decreases constantly and the surface temperature increases rapidly to the boiling point and remains there during this period. All energy transferred to the flake is used in the evaporation of water. Water is replenished by the capillary flow of water from the interior to the surface.

Internal mass transfer controls the falling rate period. The rate of moisture transport in this period is limited by the ability of water to diffuse through the wood to its surface. Liquid migration to the surface is no longer sufficient to consume the heat transferred by evaporation. This causes the temperature to rise above the boiling point.

Parametric studies on the effects of several drying parameters (species, cutting direction, dimensions, and temperature) that were considered in the experiments were tested on the numerical model. Effect of species was tested by changing several physical properties based on the experimental data (density and initial moisture content) and others taken from literature (transverse permeability and anisotropic ratio). Density and initial moisture content were found to have effects on simulated drying behavior. Influence of cutting direction was tested by changing the transverse (radial and tangential) permeabilities. This parameter had no effect on simulated drying.

Among the dimensions, length had no effect on simulated drying of flakes. Thickness and width both have influences on drying time and rate. Thicker flakes have slower drying rate thus, longer drying time since the pathway for liquid migration is longer. The influence of width on simulated drying is attributed to differences in convection heat transfer coefficients between the two widths. Wider flakes have slower drying rate and longer drying time due to lower convection heat transfer coefficient.

The effect of temperature is by virtue of higher thermal energy at higher temperature. As temperature increases, the drying rate also increases thus, shorter drying time.

Front2D is a drying model that is easy to use. This kind of numerical model is a valuable tool in understanding and analyzing the drying mechanism of any porous medium. As long as the correct parameters are used, a fairly accurate simulation of the drying process of any material can be obtained.

The model can be calibrated by using experimental results. Physical parameters such as the thermal conductivity, permeability, anisotrpy ratio, liquid migration coefficient, and heat transfer coefficient can be adjusted to get a good fit. This can be done by using regression analyses (i.e. ordinary least squares estimation).

4.6. References

ALVES, S.S. and J.L. FIGUEIREDO. 1989. A model for pyrolysis of wet wood. Chem. Engg. Sci. 44(12): 2861-2869.

COMSTOCK, G.L. 1970. Directional permeability of softwoods. Wood and Fiber 1(4): 283-289.

DI BLASI, C. 1998. Multi-phase moisture transfer in the high-temperature drying of wood particles. Chem. Engg. Sci. 53(2): 353-366.

FOREST PRODUCTS SOCIETY (FPS). 1999. Wood Handbook: Wood as an Engineering Material. Reprinted from USDA Forest Service Forest Products Laboratory General Technical Report FPL-GTR 113.

FOREST PRODUCTS SOCIETY (FPS). 1997. Dry Kiln Operator's Manual. Reprinted from USDA Agricultural Handbook No. 188.

FYHR, C AND A. RASMUSON. 1996. Mathematical Model of Steam Drying of Wood Chips and Other Hygroscopic Porous Media. AIChE J. 42(9): 2491-2502.

INCROPERA, F.P. and D.P. DeWITT. Fundamentals of Heat and Mass Transfer. 4th ed. John Wiley & Sons, Inc.

KAYIHAN, F. 1982. Simultaneous heat and mass transfer with local three-phase equilibrium in wood drying. In Proc. Third International Drying Symposium. Birmingham, England.

KAYIHAN, F. and M.A. STANISH. 1984**.** Wood particle drying: A mathematical model with experimental evaluation. In Drying '84. pp. 330-347.

MELAAEN, M.C. 1996. Numerical analysis of heat and mass transfer in drying and pyrolysis of porous media. Numerical Heat Transfer, Part A 29(4): 331-355.

PANG, S., S.G. RILEY and A.N. HASLETT. 1997. Simulation of Pinus radiata veneer drying: Moisture content and temperature profiles. For. Prod. J. 47(8): 51-58.

PERRE, P., I.W. TURNER AND J. PASSARD. 1999. 2-D solution for drying with internal vaporization of anisotropic media. AIChE J. 45(1): 13-26.

SIAU, J.F. 1995. Wood: Influence of Moisture on Physical Properties. Department of Wood Science and Forest Products, Virginia Polytechnic Institute and State University, Blacksburg, VA

STANISH, M.A. and F. KAYIHAN. 1984. Moisture transport in wood particles during drying. AIChE Symposium Series. S-239 (80): 9-20.

SOUZA, M.E.P. and S.A. NEBRA. 2000. Heat and mass transfer model in wood chip drying. Wood and Fiber Sci. 32(2): 156-163.

CHAPTER 5. FLAKE BENDING TEST

5.1. Introduction

Quality of any wood composite material depends upon the quality of the raw materials used. Strength of OSB is a function of the mechanical properties of the flakes. Knowledge of mechanical properties of flakes can lead to better strength and performance of OSB. Flakes used in manufacture of OSB are generally dried to very low moisture content using high temperature. When wood is dried below the fiber saturation point, its physical, chemical, and mechanical properties are affected. Also, temperature may have an effect on the mechanical properties of wood. Generally, wood strength decreases when the wood is heated and increases when it is cooled. There is minimal permanent strength loss when temperature does not exceed 100°C, but exposure to high temperature for long periods can cause permanent strength loss (Haygreen and Bowyer, 1996).

General discussions on temperature effect on mechanical properties of wood have been presented in the Wood Handbook (FPS, 1999) and by Haygreen and Bowyer (1996). Research on the effect of temperature on various mechanical properties of wood specimens has been performed through the years. Gerhards (1982) summarizes the relevant studies on the immediate effects of moisture content and temperature on mechanical properties of clear wood. A detailed account is given by Salaman (1969) of changes in mechanical properties from thin boards to dimension lumber of softwoods and hardwoods dried at high temperature.

Current research relating to mechanical properties has focused on composite panels and not on flakes. Wu (1999) studied the effect of flake orientation, density gradient across panel thickness, and resin content on the linear expansion, and bending properties on single-layer OSB. Modulus of elasticity (MOE) and modulus of rupture (MOR) varied significantly with flake orientation and density. Effect of resin content on MOE and MOR was relatively small. The simultaneous effect of transverse compression and press temperature on springback, compression set, density, EMC, MOE, and MOR of wood composite was studied by Tabarsa and Chui (1997). Results show that specimens

that were subjected to low compression and press temperature exhibited virtually no change in MOE and MOR despite an increase in density. Differences in mechanical properties were small between specimens pressed at 150 and 200^{o}C.

The only research done on the effect of temperature on wood flakes was performed by Plagemann (1982). Red oak, white oak, and sweetgum flakes were dried at 20, 150, and 350°C and conditioned at 21.1°C (70°F) and 65% relative humidity. Small beams measuring 0.5 x 3.8 x 14.2 mm (0.02 x 0.15 x .56 in.) were tested for MOE and MOR . Results of flake bending tests are presented in Table 12. Bending tests indicated a general trend of decreased flake strength and stiffness with increased drying temperature. However, the trend toward decreasing flake bending properties associated with high temperature drying did not manifest in board properties (i.e. MOR and MOE).

Table 12. Average Flake Bending Properties at Various Dryer Temperature for Three Southern Hardwood Species (Plagemann, 1982).

SPECIES	DRYER TEMPERATURE (^{o}C)	MOE (PSI)	MOE (N/mm^2)	MOR (PSI)	MOR (N/mm^2)
Red oak	20	696000	4799	14776	102
	150	750000	5171	15237	105
	350	513000	3537	12757	88
White oak	20	590000	4068	13233	91
	150	502000	3461	12023	83
	350	534000	3682	13171	91
Sweetgum	20	766000	5281	14641	101
	150	691000	4764	13401	92
	350	650000	4482	12610	87

The objective of this study is to determine the bending properties of flakes. Bending properties of southern yellow pine, sweetgum, and yellow-poplar flakes that were measured are MOE, MOR, and stress at proportional limit (SPL). The effect of species, cutting direction, and drying temperature on bending stiffness and strength were analyzed.

5.2. Experimental

5.2.1. Material

The raw materials used for drying experiments were also used for testing of bending properties of flakes. Fresh, green bolts, 1.5 m and around 30 cm in diameter of southern yellow pine (Pinus spp.) and sweetgum (Liquidambar styraciflua) were obtained from Georgia Pacific OSB plant in Skippers, VA and freshly-cut yellow-poplar (Liriodendron tulipifera) boards 50 mm in thickness were obtained from Turman Lumber in Radford, VA. The logs and boards were transported to Blacksburg, VA. The logs were cut into 50-mm boards using a portable sawmill. Sound boards from the three species were segregated according to type of cut: flatsawn or quartersawn. Radially- and tangentially-cut specimens were taken from the flatsawn and quartersawn boards, respectively (Figure 29). Randomly selected blocks measuring 25x152 mm were prepared from the flatsawn and quartersawn boards. Each block was properly labeled for easy identification. The blocks were placed in plastic bags segregated according to species and cutting direction and stored in a refrigerated room maintained at 2°C.

A block was randomly selected for cutting of wafers and subsequently drying of the flakes. Three flakes 0.6 mm in thickness were cut from each block using a CAE flaker. One flake was dried at every drying temperature level (150, 200, and 250°C). Ten replicates were used. Total number of flakes dried in this experiment was 180. After drying, flakes were conditioned based on ASTM D 4933-91 (ASTM, 1994). Flakes were tested for bending properties when they reached EMC (temperature and relative humidity set at 20°C and 65%, respectively).

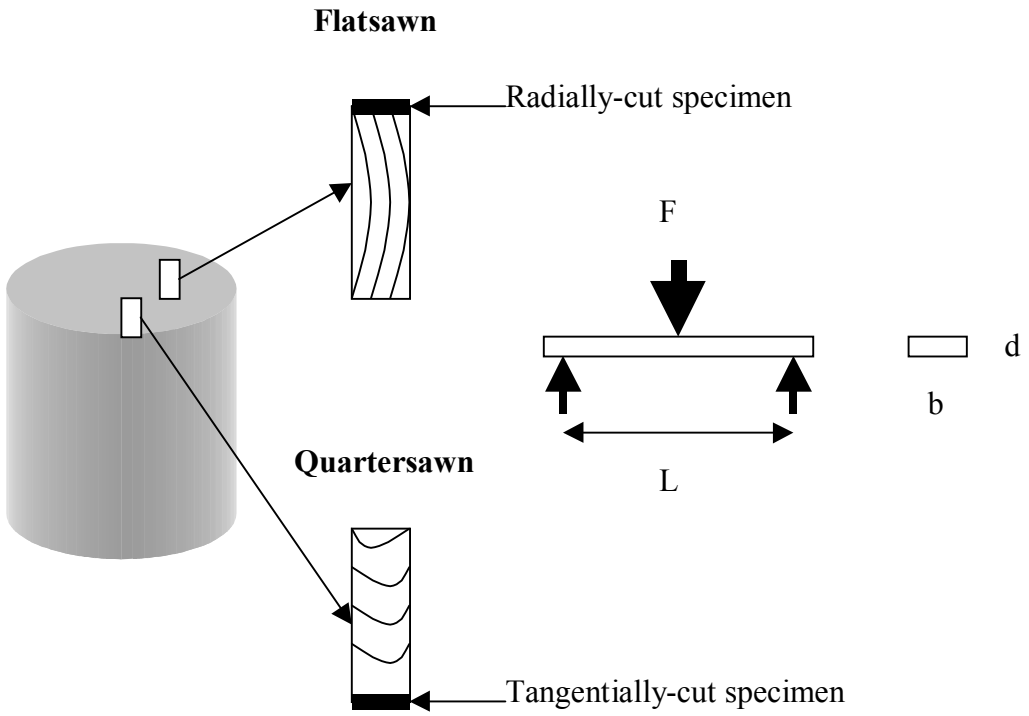

Figure 29. Cutting Diagram of Flake Bending Specimens.

5.2.2. Methods

Bending test based on Methods of Testing Small Clear Specimens of Timber ASTM D 143-94 (ASTM, 1994) was adopted. The following bending properties were measured: MOE, MOR and SPL. Static bending tests on small specimens cut from the each flake were performed. A small specimen measuring 5.0 mm (width) x 25.0 mm (length) was cut using a mounted razor blade. Bending tests were performed using a miniature material tester (Rheometric Scientific MiniMat 2000) at a cross-head speed of 2.54 mm/min. MOE, MOR, and SPL were calculated using the following equations (Bodig and Jayne, 1982; Haygreen and Bowyer, 1996):

$$MOE = P_{pl}L^3/4\Delta_{pl}bd^3 \quad \text{(Eq. 5.1)}$$

$$MOR = 1.5\ P_{ult}L/bd^2 \quad \text{(Eq. 5.2)}$$

$$SPL = 1.5\ P_{pl}L/bd^2 \quad \text{(Eq. 5.3)}$$

where: P_{pl} is load at proportional limit (N)

L is span of the bending specimen (mm)

Δ_{pl} is the deflection of the bending specimen (mm)

b is the width of the bending specimen (mm)

d is the thickness of the bending specimen (mm)

P_{ult} is the ultimate load (N)

Excess material from the flake where the specimen was cut was used for moisture content and specific gravity determinations using the ovendry (ASTM D 2395-93, 1994) and water displacement (ASTM D 4442-92, 1994) methods, respectively. Initial weight of the flake was measured. Volume of the flake was determined by clipping one end of the flake using an alligator clip connected to a stand and immersing the flake inside a tube containing distilled water. The weight of the tube with water was determined before and after immersing the flake. The difference in weight is converted into volume of the flake. Ovendry weight of the flake was determined by placing the flake inside an oven at 102$\pm$3°C overnight. The moisture content for each flake was calculated using the ovendry and initial weights. Ovendry weight and green volume was used to calculate specific gravity. Table 13 shows the average moisture content and specific gravity of the flakes.

Table 13. Average Moisture Content and Specific Gravity of the Flakes.

SPECIES	MOISTURE CONTENT (%)	SPECIFIC GRAVITY
SYP	10.3	0.58
Sweetgum	12.0	0.64
Yellow-poplar	9.5	0.58

5.2.3. Statistical Analyses

Multiple comparisons of bending properties between species, cutting direction, and drying temperature were done using ANOVA and Tukey's test. MOE, MOR, and SPL were compared between species, cutting direction, and drying temperature using the split-plot design (Snedecor and Cochran, 1980; Steel and Torrie, 1980). Species represented the whole plots. Cutting direction and temperature represented the sub-plots. Linear model considered for the analysis of bending properties is shown below and in Table 14:

$$y_{ijkl} = \mu + S_i + C_j + SC_{ij} + \varepsilon^{(A)}_{ijk} + T_l + ST_{il} + CT_{jl} + SCT_{ijl} + \varepsilon^{(B)}_{ijkl} \qquad \text{(Eq. 5.1)}$$

where: y_{ijklm} is bending property (MOE, MOR, or SPL)

μ is mean

S_i is species effect

C_j is effect of cutting direction

SC_{ij} is interaction effect of species and cutting direction

$\varepsilon^{(A)}_{ijk}$ is error

T_l is temperature effect

ST_{il} is interaction effect of species and temperature

CT_{jl} is interaction effect of cutting direction and temperature

SCT_{ijl} is interaction effect of species, cutting direction, and temperature

$\varepsilon^{(B)}_{ijkl}$ is error

Means and Tukey's test were used in comparing the main parameters. Analyses were done using GLM procedure of the SAS software package

Table 14. ANOVA Table.

SV	DF	SS	MS	F
Species (S)	(s-1)	SSS	MSS=SSS/(s-1)	MSS/MSEa
Cutting Direction (C)	(c-1)	SSC	MSC=SSC/(c-1)	MSC/MSEa
S x C	(s-1)(c-1)	SSSC	MSSC=SSSC/(s-1)(c-1)	MSSC/MSEa
Error(A)	Sc(r-1)	SSEa	MSEa=SSEa/sc(r-1)	
Drying Temperature (T)	(t-1)	SST	MST=SST/(t-1)	MST/MSE
S x T	(s-1)(t-1)	SSST	MSST=SSST/(s-1)(t-1)	MSST/MSE
C x T	(c-1)(t-1)	SSCT	MSCT=SSCT/(c-1)(t-1)	MSCT/MSE
S x C x T	(s-1)(c-1)(t-1)	SSSCT	MSSCT=SSSCT/(s-1)(c-1)(t-1)	MSSCT/MSE
Error(B)	sc(t-1)(r-1)	SSE	MSEb=SSE/sc(t-1)(r-1)	

Comparison of bending properties between cutting directions and drying temperature by species was analyzed using an analysis of covariance (ANACOVA) (Ott, 1992) with specific gravity as covariate. The linear model of the split-plot design shown below and in Table 15 was used in the analysis of the bending properties:

$$y_{ijk} = \mu + C_i + \varepsilon^{(A)}_{ij} + T_k + CT_{ik} + \beta G_{ijk} + \varepsilon^{(B)}_{ijk} \quad \text{(Eq. 5.2)}$$

where: y_{ijk} is bending property (MOE, MOR, or SPL)

μ is mean

C_i is effect of cutting direction

$\varepsilon^{(A)}_{ij}$ is error

T_k is temperature effect

CT_{ik} is interaction effect of cutting direction and temperature

β is regression coefficient

G_{ijk} is covariate (specific gravity)

$\varepsilon^{(B)}_{ijk}$ is error

Treatment levels were compared using the least squares means and Tukey's test. GLM procedure of the SAS software was also used in the analyses.

Table 15. ANACOVA Table.

SV	DF	SS	MS	F
Cutting Direction (C)	(c-1)	SSC	MSC=SSC/(c-1)	MSC/MSEa
Error(a)	c(r-1)	SSEa	MSEa=SSEa/c(r-1)	
Drying Temperature (T)	(t-1)	SST	MST=SST/(t-1)	MST/MSE
C x T	(c-1)(t-1)	SSCT	MSCT=SSCT/(c-1)(t-1)	MSCT/MSE
Specific Gravity (G)	1	SSG	MSG=SSG/1	MSG/MSE
Error (b)	c(t-1)(r-1)-1	SSE	MSEb=SSE/sc(t-1)(r-1)	

5.3. Results and Discussion

The purpose of this experiment was to measure the bending properties of flakes. The effect of species, cutting direction and dryer temperature on bending stiffness and strength were also analyzed. The data set was analyzed as a whole and then by species.

Bending properties of the three species, between radial and tangential cutting directions, and the effect of drying temperature and their interaction are discussed. ANOVA indicates variation of bending stiffness and strength between species, cutting direction, and drying temperature (Table 16). The analyses showed that there were highly significant differences in flake MOE, MOR, and SPL between species. There was also a highly significant difference between radial and tangential cutting directions in terms of bending properties. It is well established that there are variations between and within species in mechanical properties of wood (FPS, 1999). Interaction of species and cutting direction was not significant for all bending stiffness and strength. This means that the effect of cutting direction on flake MOE, MOR, and SPL was the same for the three species.

Table 16. ANOVA of Bending Properties Between Species, Cutting Direction, and Temperature.

		MOE			MOR			SPL		
SV	**DF**	**SS**	**F**	**P**	**SS**	**F**	**P**	**SS**	**F**	**P**
S	2	102224878	20.8	<.01	15976	15.4	<.01	9682	14.5	<.01
C	1	40487197	16.5	<.01	13989	27.0	<.01	13236	39.7	<.01
S x C	2	3807129	0.8	0.47	1348	1.3	0.28	1192	1.8	0.18
T	2	38953089	13.0	<.01	11326	14.1	<.01	6838	13.5	<.01
S x T	4	14031884	2.4	0.06	1639	1.0	0.40	1548	1.5	0.20
C x T	2	590742	0.2	0.82	509	0.6	0.53	546	1.1	0.35
S x C x T	4	1251021	0.2	0.93	1177	0.7	0.57	837	0.8	0.51

There were highly significant differences in flake bending properties between drying temperature. However, interaction of temperature with species and with cutting direction were not significant at p=0.05. This implies that the difference in bending properties caused by temperature did not depend on the species or on cutting direction. Three-way interaction among species, cutting direction, and drying temperature was also not significant.

The results of flake bending tests are presented in Table 17 and Figure 30, Figure 31, and Figure 32. Among the three species, southern yellow pine had the lowest average bending properties (Table 17 and Figure 30). Average MOE, MOR, and SPL of southern yellow pine were 4086.9, 66.0, and 48.1 N/mm^2, respectively. Sweetgum had higher bending strength and stiffness than southern yellow pine except for MOE which was not significantly different. Mean MOE, MOR, and SPL of sweetgum were 4430.6, 78.6 and 56.5 N/mm^2, respectively. Yellow-poplar had the highest MOR, MOE, and SPL with average values of 5829.4 N/mm^2, 89.0, and 66.0 N/mm^2, respectively.

Table 17. Average Flake Bending Properties of the Three Species, Two Cutting Directions, and Three Temperatures.

PARAMETER	MOE (N/mm^2)	MOR (N/mm^2)	SPL (N/mm^2)
Species			
SYP	4086.9 a	66.0 a	48.1 a
Sweetgum	4430.6 a	78.6 b	56.5 b
Yellow-poplar	5829.4 b	89.0 c	66.0 c
Cutting Direction			
Radial	4308.0 a	69.1 a	48.3 a
Tangential	5256.6 b	86.7 b	65.5 b
Temperature (°C)			
150	5401.6 a	87.7 a	64.3 a
200	4665.4 b	77.6 b	56.5 b
250	4280.3 c	68.3 c	49.6 c

Means with the same letter are not significantly different at p=0.05

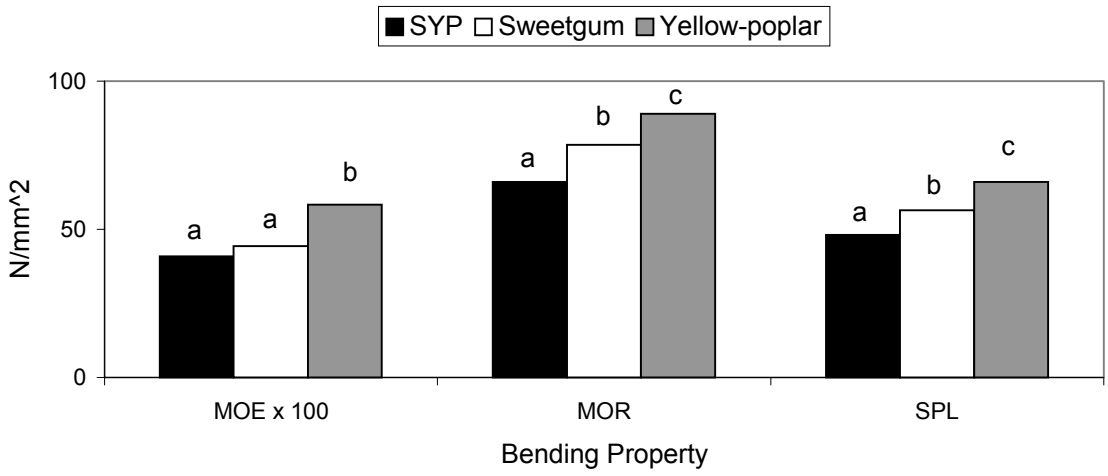

Note: Means with the same letter are not significantly different at p=0.05

Figure 30. Average Bending Stiffness and Strength of the Three Species.

Radially-cut specimens have lower bending properties than tangentially-cut specimens (Table 17 and Figure 31). Radially-cut specimens have average values 4308.0, 69.1, and 86.7 N/mm^2 for MOE, MOR, and SPL, respectively. On the other hand, tangentially-cut specimens have average values of 5256.6, 86.7, and 65.5 N/mm^2 for MOE, MOR, and SPL, respectively.

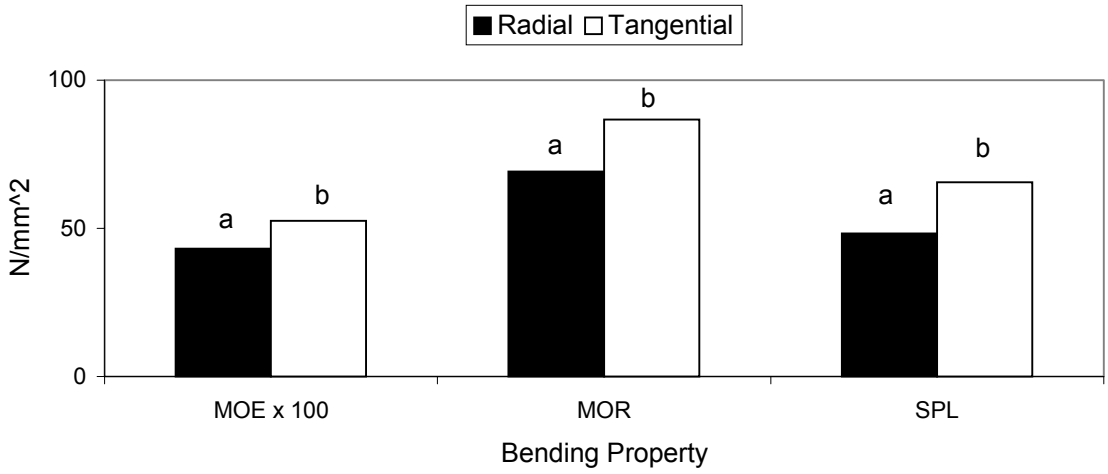

Note: Means of the same letter are not significantly different at p=0.05

Figure 31. Average Bending Stiffness and Strength of the Two Cutting Directions.

The effect of temperature on bending properties is shown in Table 17 and Figure 32. A decreasing trend in flake bending strength and stiffness with increased temperature was observed. The same trend was observed by Plagemann (1982), however, statistical analysis indicated that only MOE of flakes was significantly affected by temperature in his tests. In this experiment, the effect of temperature on MOE, MOR, and SPL were all highly significant. Specimens dried at 150°C have higher mean bending properties (MOE=5401.6 N/mm^2, MOR=87.7 N/mm^2, and SPL=64.3 N/mm^2) than specimens dried at 200°C (MOE=4665.4 N/mm^2, MOR=77.6 N/mm^2, and SPL=56.5 N/mm^2). Specimens dried at 250°C have the lowest mean bending stiffness and strength (MOE=4280.3 N/mm^2, MOR=68.3 N/mm^2, and SPL=49.6 N/mm^2).

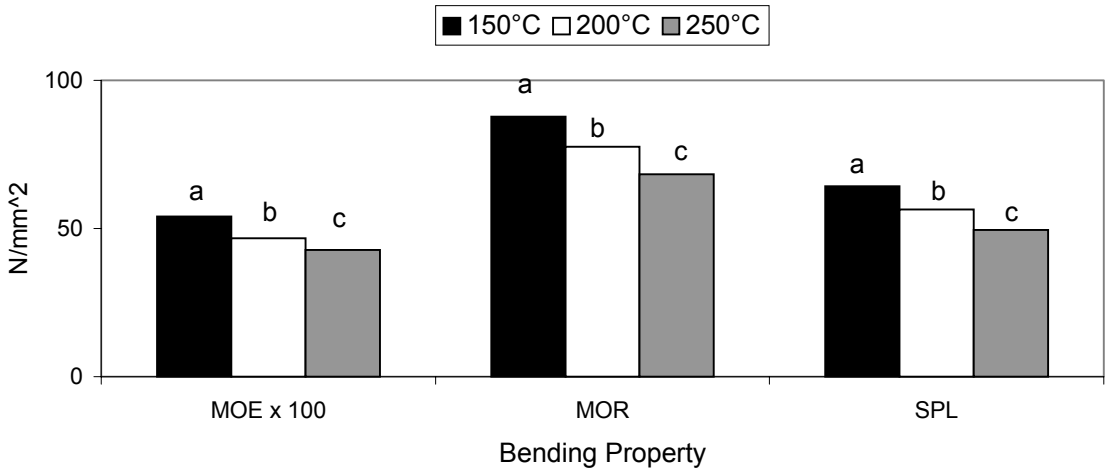

Note: Means with the same letter are not significantly different at p=0.05

Figure 32. Average Bending Stiffness and Strength of the Three Temperatures.

The previous discussion dealt with the ANOVA of measured bending properties of the three species combined. The succeeding discussions focus on the ANACOVA of adjusted bending strength and stiffness. Specific gravity was used as covariate to compute for the adjusted means for MOE, MOR, and SPL. Analyses were made by species. Southern yellow pine was analyzed first followed by sweetgum then finally yellow-poplar.

5.3.1. Southern Yellow Pine

Bending properties of southern yellow pine are discussed. Shown in Table 18 is the ANACOVA of adjusted MOE, MOR, and SPL means of southern yellow pine using specific gravity as covariate and as influenced by cutting direction and drying temperature and their interaction. Cutting direction had a highly significant influence on all three bending properties of southern yellow pine. Effect of drying temperature was significant (at p=0.05) only on the MOE . Interaction of cutting direction and drying temperature was not significant. Thus, influence of drying temperature on bending properties of southern yellow pine flakes was not affected by cutting direction.

Table 18. ANACOVA of Bending Stiffness and Strength of Southern Yellow Pine.

		MOE			MOR			SPL		
SV	**DF**	**SS**	**F**	**P**	**SS**	**F**	**P**	**SS**	**F**	**P**
C	1	36216115	9.4	0.01	11233	8.7	0.01	10074	12.9	<0.01
T	2	22949100	4.3	0.02	3927	2.4	0.10	1419	1.5	0.24
C x T	2	1179979	0.2	0.80	1187	0.7	0.49	934	1.0	0.39

Bending test results of southern yellow pine are presented in Table 19, Figure 33, and Figure 34. Cutting direction had a significant effect on MOE, MOR, and SPL. Radially-cut specimens have lower bending properties than tangentially-cut specimens (Table 19 and Figure 33). Adjusted means of MOE, MOR, and SPL of radially-cut specimens were only 3030.2, 47.4, and 30.5 N/mm^2, respectively. Tangentially-cut specimens have higher adjusted means of MOE, MOR, and SPL calculated at 5143.6, 84.6, and 65.7 N/mm^2, respectively.

Table 19. Adjusted Means of Bending Stiffness and Strength of Southern Yellow Pine.

PARAMETER	SPECIFIC GRAVITY	MOE (N/mm^2) MEAN	MOE (N/mm^2) ADJ	MOR (N/mm^2) MEAN	MOR (N/mm^2) ADJ	SPL (N/mm^2) MEAN	SPL (N/mm^2) ADJ
Cutting Direction							
Radial	0.61	3469.9	3030.2 a	55.2	47.4 a	36.7	30.5 a
Tangential	0.54	4710.8	5143.6 b	76.9	84.6 b	59.5	65.7 b
Temperature (°C)							
150	0.60	5206.9	4940.1 a	79.3	74.5 a	55.3	51.4 a
200	0.56	3772.6	3959.6 ab	65.4	68.7 a	49.0	51.6 a
250	0.57	3281.1	3360.9 b	53.4	54.8 a	40.0	41.2 a

Means with the same letter are not significantly different at p=0.05

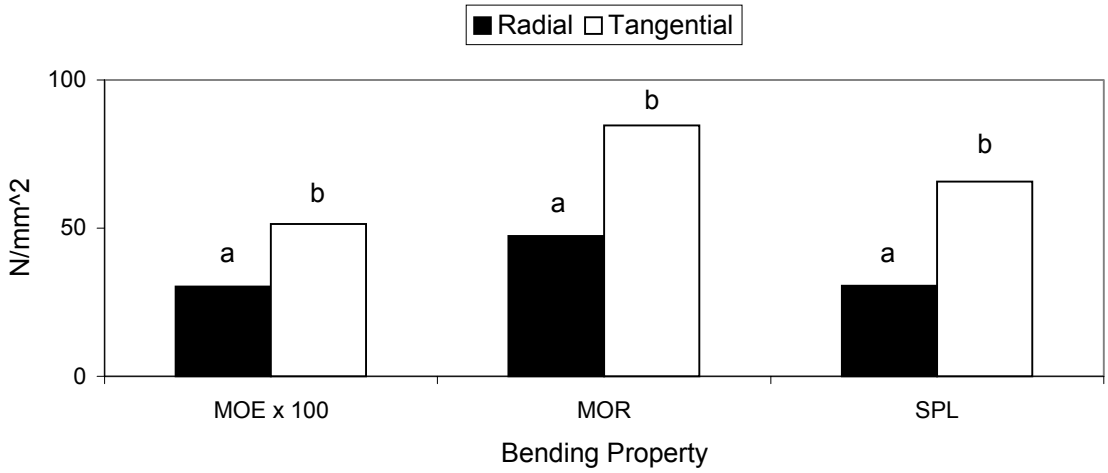

Note: Means with the same letter are not significantly different at p=0.05

Figure 33. Adjusted Means of Bending Stiffness and Strength of Southern Yellow Pine According to Cutting Direction.

A decreasing trend in bending properties was observed when drying temperature increased (Table 19 and Figure 34). However, statistical analyses showed that drying temperature only had a significant effect on MOE of southern yellow pine. Specimens dried at 150 (4940.1 N/mm^2) and 200°C (3959.6 N/mm^2) was significantly different from specimens dried at 250°C (3360.9 N/mm^2). Also, specimens dried at 200 and 250°C have lower MOE than specimens dried at 150°C. Drying temperature was found to have no significant effect on MOR and SPL. Adjusted MOR means were 74.5, 68.7, and 54.8 N/mm^2 for specimens dried 150, 200, and 250°C, respectively. Adjusted means of SPL were 51.4, 51.6, and 41.2 N/mm^2 for specimens dried at 150, 200, and 250°C, respectively.

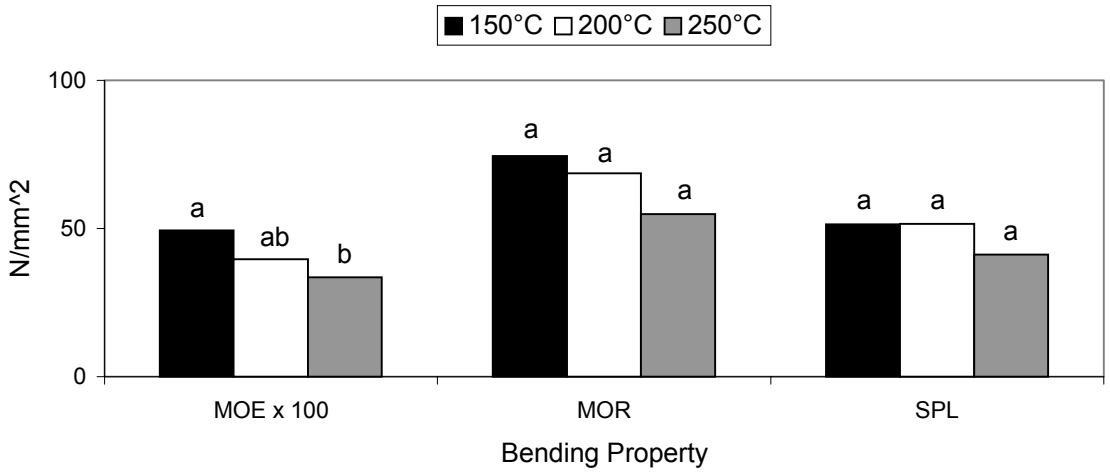

Note: Means of the same letter are not significantly different at p=0.05

Figure 34. Adjusted Means of Bending Stiffness and Strength of Southern Yellow Pine According to Temperature.

5.3.2. Sweetgum

ANACOVA (Table 20) of bending stiffness and strength of sweetgum is discussed. Effect of cutting direction was highly significant for all bending properties. Effect of temperature was also highly significant on MOE, MOR, and SPL. Interaction of cutting direction and drying temperature was not significant, similar to southern yellow pine. Thus, influence of temperature on bending properties of sweetgum was not affected by cutting direction.

Table 20. ANACOVA of Bending Stiffness and Strength of Sweetgum.

		MOE			MOR			SPL		
SV	**DF**	**SS**	**F**	**P**	**SS**	**F**	**P**	**SS**	**F**	**P**
C	1	5012570	12.9	<.01	6943	91.1	<.01	4888	106.6	<.01
T	2	6078022	6.5	<.01	4075	15.6	<.01	3578	21.8	<.01
C x T	2	402970	0.4	0.65	249	1.0	0.40	115	0.7	0.50

Table 21, Figure 35 and Figure 36 show the bending test results of sweetgum. Cutting direction had a significant effect on adjusted means of MOR, MOE, and SPL. Similar to southern yellow pine, radially-cut specimens consistently have lower bending strength and stiffness than tangentially-cut specimens (Table 21 and Figure 35). Adjusted MOE, MOR, and SPL of 4135.2, 67.6, and 47.3 N/mm^2, respectively were calculated for specimens cut radially. On the other hand, specimens that were cut tangentially have adjusted MOR, MOE, and SPL means of 4726.1, 89.6, and 65.8 N/mm^2, respectively.

Table 21. Adjusted Means of Bending Stiffness and Strength of Sweetgum.

PARAMETER	SPECIFIC GRAVITY	MOE (N/mm^2) MEAN	MOE (N/mm^2) ADJ	MOR (N/mm^2) MEAN	MOR (N/mm^2) ADJ	SPL (N/mm^2) MEAN	SPL (N/mm^2) ADJ
Cutting Direction							
Radial	0.64	4153.4	4135.2 a	67.9	67.6 a	47.4	47.3 a
Tangential	0.63	4707.9	4726.1 b	89.2	89.6 b	65.6	65.8 b
Temperature (°C)							
150	0.61	4912.2	5012.2 a	90.7	92.6 a	69.4	70.1 a
200	0.66	4205.0	4144.6 b	75.9	74.7 b	52.2	51.8 b
250	0.65	4174.7	4135.1 b	69.2	68.4 b	48.0	47.7 b

Means with the same letter are not significantly different at p=0.05

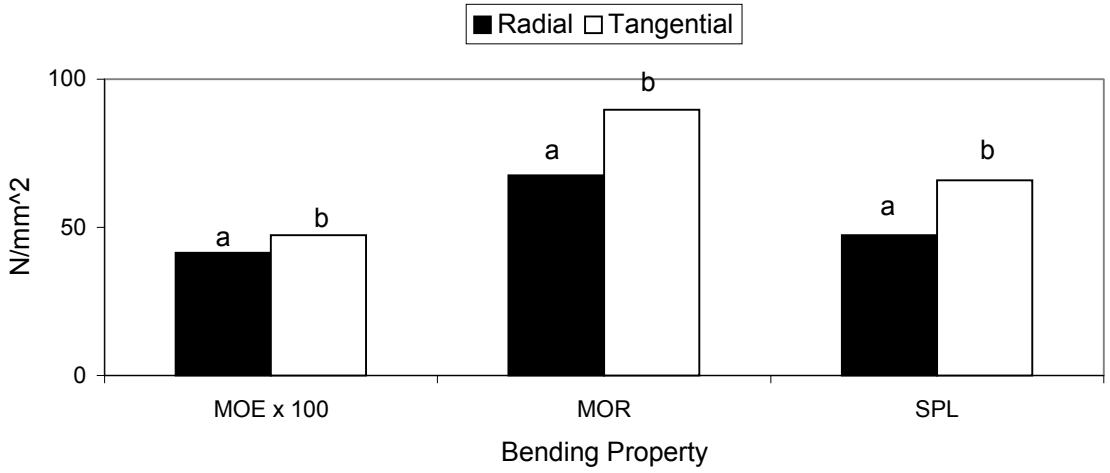

Note: Means of the same letter are not significantly different at p=0.05

Figure 35. Adjusted Means of Bending Stiffness and Strength of Sweetgum According to Cutting Direction.

Similar to southern yellow pine, a decreasing trend in bending properties when drying temperature increased was also observed in sweetgum (Table 21 and Figure 36). Drying temperature had a significant effect on all bending properties of sweetgum, unlike in southern yellow pine wherein only MOE was affected. Specimens dried at 150°C were significantly different from specimens dried at 200 and 250°C. Bending properties of specimens dried at 200 and 250°C were no longer statistically significant. Adjusted MOR values of 5012.2, 4144.6, and 4135.1 N/mm^2 were calculated for specimens dried at 150, 200, and 250°C, respectively. Adjusted means of MOE for specimens dried at 150, 200, and 250°C were 92.6, 74.7 and 68.4 N/mm^2, respectively. Adjusted SPL values for specimens dried at 150, 200, and 250°C were 70.1, 51.8, and 47.7 N/mm^2, respectively.

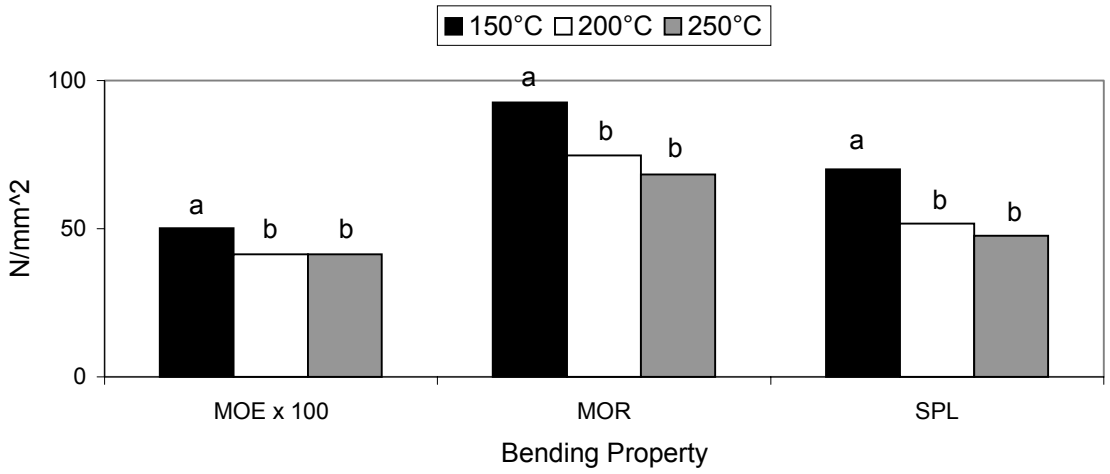

Note: Means of the same letter are not significantly different at p=0.05

Figure 36. Adjusted Means of Bending Stiffness and Strength of Sweetgum According to Temperature.

5.3.3. Yellow-poplar

ANACOVA of the bending properties of yellow-poplar is shown in Table 22. Effect of cutting direction on bending properties of yellow-poplar was not significant. Among the three species, only yellow-poplar had an insignificant effect of cutting direction on bending stiffness and strength. Temperature effect was significant on MOR but not significant on MOE and SPL at p=0.05. Cutting direction and drying temperature interaction was again insignificant, similar to southern yellow pine and sweetgum. Therefore, influence of temperature on bending properties of yellow-poplar was not affected by cutting direction.

Table 22. ANACOVA of Bending Stiffness and Strength of Yellow-poplar.

		MOE			MOR			SPL		
SV	**DF**	**SS**	**F**	**P**	**SS**	**F**	**P**	**SS**	**F**	**P**
C	1	6914231	2.0	0.17	460	1.6	0.22	647	3.1	0.10
T	2	6193902	2.9	0.07	1434	4.3	0.02	915	3.1	0.06
C x T	2	138936	0.1	0.94	12	0.0	0.96	30	0.1	0.90

Presented in Table 23, Figure 37, and Figure 38 are the bending test results of yellow-poplar. Radially-cut specimens consistently have lower bending properties than tangentially-cut specimens (Table 23 and Figure 37.), similar with southern yellow pine and sweetgum. However, the effect of cutting direction on bending properties of yellow-poplar was shown to be statistically insignificant. Adjusted means of MOE, MOR, and SPL were 5365.3, 85.3, and 61.6 N/mm^2, respectively for radially-cut specimens. MOE, MOR, and SPL adjusted values were 6293.5, 92.8, and 70.5 N/mm^2, respectively for tangentially-cut specimens.

Table 23. Adjusted Means of Bending Stiffness and Strength of Yellow-poplar.

PARAMETER	SPECIFIC GRAVITY	MOE (N/mm^2) MEAN	MOE (N/mm^2) ADJ	MOR (N/mm^2) MEAN	MOR (N/mm^2) ADJ	SPL (N/mm^2) MEAN	SPL (N/mm^2) ADJ
Cutting Direction							
Radial	0.60	5307.8	5365.3 a	84.1	85.3 a	60.8	61.6 a
Tangential	0.55	6351.0	6293.5 a	94.0	92.8 a	71.2	70.5 a
Temperature (°C)							
150	0.58	6085.6	6080.0 a	93.2	93.1 a	69.2	69.2 a
200	0.58	6017.6	6043.1 a	91.6	92.1 a	68.3	68.6 a
250	0.59	5385.1	5364.4 a	82.4	82.0 b	60.6	60.4 a

Means with the same letter are not significantly different at p=0.05

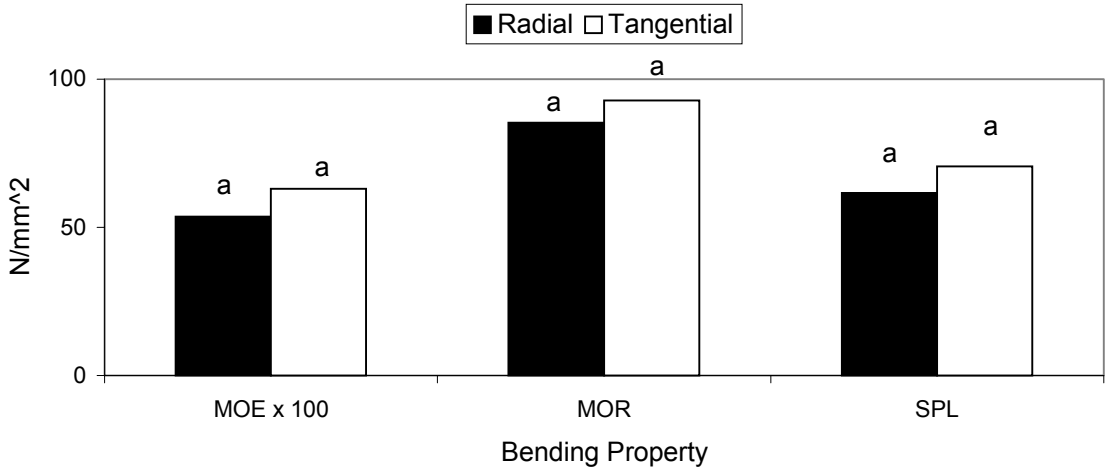

Note: Means of the same letter are not significantly different at p=0.05

Figure 37. Adjusted Means of Bending Stiffness and Strength of Yellow-poplar According to Cutting Direction.

Table 23 and Figure 38 show the influence of drying temperature on bending properties of yellow-poplar. Drying temperature only had a significant effect on MOR wherein specimens dried at 150 (93.1 N/mm^2) and 200°C (92.1 N/mm^2) have higher bending strength than specimens dried at 250°C (82.0 N/mm^2). Decreasing MOE and SPL at higher temperature was observed but found to be statistically not significant. Adjusted MOE of 6080.0, 6043.1, and 5364.4 N/mm^2 for specimens dried 150, 200, and 250°C, respectively were calculated. SPL adjusted values of 69.2, 68.6, and 60.4 N/mm^2, respectively were calculated for specimens dried 150, 200, and 250°C.

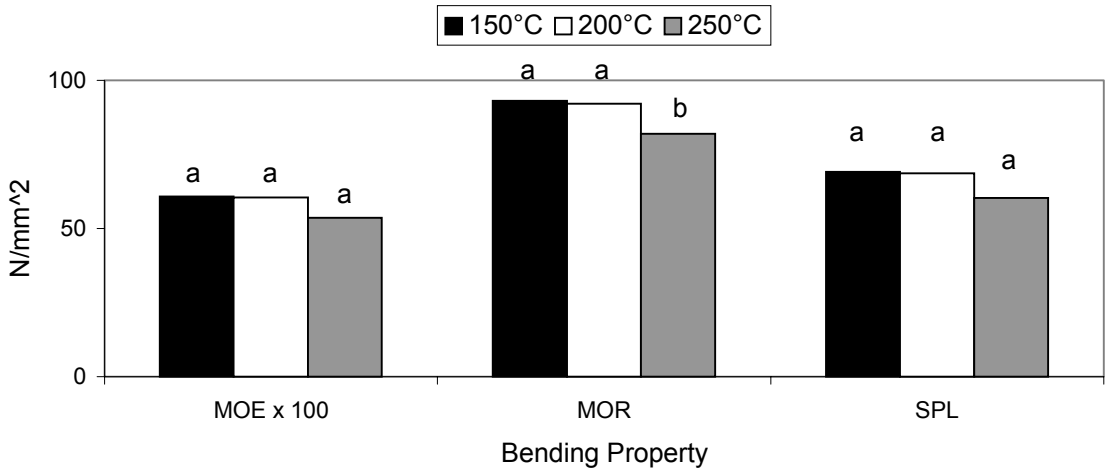

Note: Means of the same letter are not significantly different at p=0.05

Figure 38. Adjusted Means of Bending Stiffness and Strength of Yellow-poplar According to Temperature.

Results of flake bending properties of the three species were compared with MOE and MOR of clear wood specimens taken from the Wood Handbook (FPS, 1999). Adjusted means of the bending properties of flakes were compared to bending properties of clear wood specimens dried at 12%. Variations between species and differences between flakes and clear wood specimens on bending stiffness and strength were observed. Table 24 clearly shows that flakes dried at high temperature have lower bending stiffness and strength compared to clear wood specimens dried conventionally. The reduction in bending properties was affected by high temperature. Exposure to high temperature for long periods causes permanent strength loss (Haygreen and Bowyer, 1996). This strength loss is a permanent effect due to degradation of wood substance (FPS, 1999).

Table 24. Comparison of Bending Properties Between Flake and Clear Wood Specimens.

	FLAKE			CLEAR WOOD		
SPECIES	SPECIFIC GRAVITY	MOE (N/mm^2)	MOR	SPECIFIC GRAVITY	MOE (N/mm^2)	MOR
Southern yellow pine	0.58	4067	66	0.51	12300	88
Sweetgum	0.64	4431	79	0.52	11300	86
Yellow-poplar	0.58	5829	89	0.42	10900	70

Southern yellow pine had the greatest loss on MOE followed by sweetgum then yellow-poplar. Southern yellow pine remained to have the highest MOR loss followed by sweetgum. Clear wood specimens of southern yellow pine have the highest bending properties but southern yellow pine flakes have the lowest bending properties. On the other hand, clear wood specimens of yellow-poplar have the least MOE and MOR but yellow-poplar flakes have the highest MOE and MOR. Apparently high temperature drying has a greater effect on the bending properties of southern yellow pine than on yellow-poplar.

Differences in bending properties observed between species can be related to differences in specific gravity. Approximate relationship between various mechanical properties and specific gravity for clear straight-grained wood of hardwoods and softwoods are given as power functions (FPS, 1999). In the case of flakes, the coefficients must be changed so that the equations can be applied to bending properties of flakes dried at high temperature.

Even with equal average values of specific gravity, southern yellow pine had lower MOE and MOR than yellow-poplar. Yellow-poplar had a lower average specific gravity than sweetgum but yellow-poplar had better bending properties than sweetgum. Other than specific gravity, many factors may also be considered like anatomical differences, moisture content, and relative size of the test specimens, among others to account for the differences in bending properties between species.

Cutting direction had a significant effect on bending properties. Analyses by species revealed that effect of cutting direction was only significant on southern yellow pine and sweetgum but not on yellow-poplar. Radially-cut specimens consistently had lower MOE, MOR, and SPL than tangentially-cut specimens. This was expected since force applied on radially-cut specimens was directed along the tangential axis of the flake specimens while force applied on tangentially-cut specimens is directed along the radial axis. Elastic behavior of wood along the tangential axis is always lower than elastic behavior along the radial axis. This is due to the fact that wood is an orthotropic material: i.e. it has unique and independent mechanical properties along the three mutually independent axes: longitudinal, radial, and tangential. Elastic ratios vary within species. This ratio also varies with specific gravity and moisture content.

Comparisons of the E_R/E_T ratio of the flakes and of clear wood specimens (FPS, 1999) show big differences (Table 25). Difference in elastic ratio between flake and clear wood can be attributed to the effect of high temperature on the bending properties of flakes. It is either the radial elasticity is greatly reduced in the case of sweetgum and yellow-poplar or the tangential elasticity is affected in the case of southern yellow pine.

Table 25. Comparison of Radial/Tangential Elasticity (E_R/E_T) of Flakes and Clear Wood Specimens.

SPECIES	FLAKE	CLEAR WOOD
Southern yellow pine	1.7	1.4
Sweetgum	1.1	2.3
Yellow-poplar	1.2	2.1

A general trend of decreasing bending properties for increasing drying temperature was observed. Although significant differences were only detected on the MOE of SYP, on MOE, MOR, and SPL of sweetgum, and on MOR of yellow-poplar, the trend was consistently observed on all bending properties of the three species. Plagemann (1982) observed the same trend in his flake bending tests (Table 12), however, only MOE was found to be affected by dryer temperature while MOR was not affected. The decrease in bending properties as influenced by dryer temperature can be easily attributed to thermal degradation of the wood components when exposed at high temperature. Haygreen and Bowyer (1996) stated that wood subjected to high temperature lead to permanent strength loss. The strength loss is a permanent effect due to degradation of the wood.

5.4. Conclusions

Bending properties of flakes differed between and within the three species. Yellow-poplar had the highest bending properties followed by sweetgum and southern yellow pine had the lowest bending stiffness and strength. The effect of cutting direction was similar on the three species. Radially-cut specimens were found to have lower MOE, MOR, and SPL than tangentially-cut specimens. Drying temperature was also found to have a significant effect on the bending properties of flakes. Effect of temperature was similar for the three species and did not depend on the cutting direction. A decreasing trend was observed for flakes dried at higher temperature.

Correlation between bending properties and specific gravity was analyzed by species. Measured bending properties were adjusted using specific gravity as covariate. This lead to a slight change in least square means of the MOE, MOR, and SPL of all three species. Bending properties were determined to be significantly different between radial and tangential cutting directions on southern yellow pine and sweetgum but not on yellow-poplar. Significant difference caused by drying temperature was only detected on MOE of southern yellow pine; MOE, MOR, and SPL of sweetgum; and only MOR of yellow-poplar.

Drying of flakes at high temperature resulted in a dramatic decrease in bending properties when compared to clear wood specimens dried conventionally. MOE and MOR decreased by as much as 67% as in the case of southern yellow pine. The reduction of flake bending stiffness and strength was attributed to the thermal degradation. Wood subjected to high temperature lead to permanent strength loss and this loss is a permanent effect due to degradation of the wood substance.

Relative to OSB production, it would be ideal to use yellow-poplar or more of it in combination with other species and dried at lower temperature due to better bending properties as gleaned from the results of the flake bending experiments. Since southern yellow pine is the species predominantly used in OSB production, it may be an advantage to cut more flakes in the tangential direction to have flakes with higher bending properties but this is not yet practical. This idea may lead to better panels due to better

bending properties of raw materials. Variability in properties between and within species causes variabilities in raw material properties but this is unavoidable. The only way to reduce the effect of variability is to spread out the materials within the panel.

Taking a closer look at the variables that affect bending properties, drying temperature is the most important parameter that radically affects the bending stiffness and strength of flakes. This is also the only parameter that can be easily controlled and monitored. Lower drying temperature definitely assures higher MOE, MOR, and SPL for dried flakes.

5.5. References

AMERICAN SOCIETY OF TESTING MATERIALS (ASTM). 1994. Methods of testing small clear specimens of timber D 143-94. 1994 Annual Book of ASTM Standards Vol. 04.10. Philadelphia, PA.

AMERICAN SOCIETY OF TESTING MATERIALS (ASTM). 1994. Standard test methods for specific gravity of wood and wood-base materials D 2395-93. 1994 Annual Book of ASTM Standards Vol. 04.10. Philadelphia, PA.

AMERICAN SOCIETY OF TESTING MATERIALS (ASTM). 1994. Standard test methods for direct moisture content measurement of wood and wood-base materials D 4442-92. 1994 Annual Book of ASTM Standards Vol. 04.10. Philadelphia, PA.

AMERICAN SOCIETY OF TESTING MATERIALS (ASTM). 1994. Standard guide for moisture conditioning of wood and wood-base materials D 4933-91. 1994 Annual Book of ASTM Standards Vol. 04.10. Philadelphia, PA.

BODIG, J. and B.A. JAYNE. 1982. Mechanics of Wood and Wood Composites. Van Nostrand Reinhold Co.

FOREST PRODUCTS SOCIETY (FPS). 1999. Wood Handbook: Wood as an Engineering Material. Reprinted from USDA Forest Service Forest Products Laboratory General Technical Report FPL-GTR 113.

GERHARDS, C.C. 1982. Effect of moisture content and temperature on the mechanical properties of wood: An analysis of immediate effects. Wood and Fiber 14(1): 4-36.

HAYGREEN, J.G. and J.L. BOWYER. 1996. Forest Products and Wood Science: An Introduction. 3rd ed. Iowa State University Press, Ames, Iowa.

OTT, R.L. 1992. An Introduction to Statistical Methods and Data Analysis. 4th ed. Wadsworth Publishing Co., Belmont, CA.

PLAGEMANN, W.L., E.W. PRICE and W.E. JOHNS. 1984. The response of hardwood flakes and flakeboard to high temperature drying. J. Adhesion 16:311-338.

PLAGEMANN, W.L. 1982. . The response of hardwood flakes and flakeboard to high temperature drying. Master's thesis. Washington State University, Pullman, WA.

SALAMAN, M. 1969. High-temperature drying and its effect on wood properties. For. Prod. J. 19(3): 27-34.

SNEDECOR, G.W. and W.G. COCHRAN. 1980. Statistical Methods. 7th ed. Iowa State University Press, Ames, Iowa.

STEELE, R.G.D. and J.H. TORRIE. 1980. Principles and Procedures of Statistics: A Biometrical Approach. 2nd ed. McGraw Hill, New York.

CHAPTER 6. CONCLUSIONS AND RECOMMENDATIONS

6.1. Conclusions

Based on regression analysis, flake drying curve is accurately represented by a second-order/quadratic model. By differentiating this equation, the drying rate can be calculated. This gives the advantage of analyzing the data with the use of a single equation rather than performing linear regression analysis of data at different moisture content intervals to get the slope thus, the drying rate.

Observations on the drying and drying rate curves revealed two falling rate drying periods on all cases, no constant rate drying period typical of wood drying was observed. The first falling rate drying period is caused by severe drying conditions and is controlled by convective heat transfer. The second falling rate period is controlled by internal bound water diffusion. The curves have no abrupt deflection indicative of gradual switch from one mechanism to another.

The effects of species, cutting direction, flake dimension, and temperature on drying rates of flakes were analyzed. Drying rates were found to vary between and within species. Southern yellow pine has the highest drying rate followed by sweetgum and lastly, yellow-poplar. The difference is attributed to specific gravity. Woods with lower specific gravity normally have higher drying rate due less water present in a given moisture content. Other factors such as permeability, porosity, and cell morphology also affect the drying rate.

Cutting direction was found to have an effect on drying rates of flakes. Tangentially-cut flakes have higher drying rates than radially-cut flakes due to the wood rays that are exposed on the wide surface of tangentially-cut specimens. These wood rays provide passageways for moisture. Effect of cutting direction depends on the moisture content of the species. Cutting direction was only significant below 50% for southern yellow pine. For sweetgum, it was significant above 5%. It was significant at all moisture content levels for yellow-poplar.

Flake dimension had a significant influence on drying rate. Similar to cutting direction, effect of dimension depends on the moisture content of the species. Effect of dimension on drying rate of southern yellow pine was only at low moisture content (5 to 20%) while the effect of dimension for sweetgum and yellow-poplar was at all moisture contents. Narrow flakes have faster drying rate due to shorter distance for moisture transport. Long flakes were found to have higher faster drying rate than short flakes. This brings the effect of thickness. Thickness effect is the most sensitive parameter in terms of dimensions. Based on the geometry of flakes, moisture transport along the thickness provides the best avenue for moisture loss since it is the shortest distance covering the widest surface.

Increase in drying rate was affected by the increase in drying temperature. An approximate linear increase in drying rate was observed as temperature increases. Influence of temperature on drying rates of southern yellow pine, sweetgum, and yellow-poplar here highly significant at all moisture content levels. Of all the parameters that were analyzed, temperature has more influence on drying rate of flakes.

Simulated flake drying behavior using Front2D developed by Perre et al. (1999) had a difference to experimental data. Simulated drying was divided into a constant rate and falling rate drying periods. External heat transfer controls the constant rate drying period. The falling rate period is controlled by mass transfer. Parametric studies on the effect of drying parameters were tested on the model. Density, initial moisture content, thickness, width, and temperature were found to affect the simulations. Transverse permeabilities and length have little or no effect at all.

Flake MOR, MOE, and SPL were measured. The influence of species, cutting direction, and temperature on bending stiffness and strength were analyzed. Results of bending tests show that bending properties vary between and within species. Yellow-poplar had the highest bending properties followed by sweetgum and southern yellow pine had the lowest bending stiffness and strength. Radially-cut flakes were found to have lower MOE, MOR, and SPL than tangentially-cut flakes. Drying temperature was

also found to have an influence on flake bending properties. When increasing temperature, a decreasing trend in MOE, MOR, and SPL were observed.

The drying and bending properties values observed within species might have been related to variability. There were significant cutting direction, dimension, and temperature effects within each species. However, drying temperature had a greater influence on drying and bending properties. Thus, the contribution of cutting direction and dimension play a secondary role in flake drying and bending properties within the framework of this study.

There were highly significant species effect present in drying and bending properties of flakes and this is not surprising. It was interesting however, to note the ranking when comparisons were made between species. When drying rates of the flakes were analyzed, the following was observed: southern yellow pine > sweetgum > yellow-poplar. However, this trend was reversed when the results of bending properties were considered: yellow-poplar > sweetgum > southern yellow pine. It is apparent that increase in drying rate does not compensate for great bending property losses resulting from increase in drying temperature. Arguably, there is an optimum drying condition that will maximize the drying rate and minimize the stiffness and strength losses of flakes.

6.2. Recommendations

The main objective of this study was to investigate the drying and bending properties of flakes. Experiments have been conducted which allow the understanding of the flake drying process and bending behavior of flakes. Valuable information has been gathered through the determination of physical, drying, and bending properties of southern yellow pine, sweetgum, and yellow-poplar, species commonly used in OSB manufacture.

Experiments used in this dissertation can be employed in the future as a basis to assess the drying and bending properties of other wood and wood-based materials for composite applications. Study of other wood species that is currently used or potentially-viable for OSB manufacture is recommended. This may lead to better drying of flakes and improve the quality of flakes for better OSB boards. This may also expand the utilization of other wood species for composite materials.

Study on the effect of drying conditions on the mechanical properties on OSB boards is critical. Quality of wood composites relies on the quality of raw materials used. Relation of anatomical, physical, chemical, and mechanical properties of raw materials to board properties should be investigated.

The development of a numerical flake drying model is also desired. The study showed that flakes have different drying mechanism compared to lumber and other wood materials. It has also been shown how a numerical model is more advantageous than an empirical correlation. This numerical model should be developed based on the drying mechanism that was observed so that reliable predictions of moisture content can be made and subject to quality constraints. A simple yet accurate model of the flake drying process is definitely preferred.

The flake drying model can be incorporated to a flake drying process model (i.e. rotary or conveyor dryer) . This will allow better design of flake dryers as well as process control and optimization that will lead to the ultimate goal of flake drying: to attain target moisture content and retain quality of flakes. This may also lead to lower energy consumption and less environmental hazards.

APPENDICES

Appendix A. Coefficient of Determination, Parameter Estimates, and Drying Rates of Radially-cut 15x117 mm Southern Yellow Pine Flakes.

TEMP						DRYING RATE (%/SEC)																		
(C)	REP	R^2	β_0	β_1	β_2	5	10	15	20	25	30	40	50	60	70	80	90	100	110	120	130	140	150	160	170
150	1	0.9990	133.1	-1.262	0.00290	0.329	0.407	0.473	0.531	0.583	0.631	0.717	0.793	0.863	0.928	0.989	1.046	1.100	1.151	1.200	1.248	.	.	.	.
150	1	0.9991	133.3	-1.240	0.00273	0.367	0.435	0.494	0.547	0.595	0.639	0.719	0.792	0.858	0.920	0.977	1.032	1.083	1.133	1.180	1.225	.	.	.	.
150	2	0.9995	128.3	-1.046	0.00211	0.234	0.312	0.373	0.426	0.473	0.515	0.592	0.659	0.720	0.776	0.829	0.878	0.925	0.969	1.012	.	.	.	.	.
150	2	0.9986	129.4	-1.086	0.00223	0.264	0.338	0.399	0.451	0.498	0.541	0.618	0.687	0.749	0.806	0.860	0.910	0.958	1.003	1.047	.	.	.	.	.
150	3	0.9990	148.4	-1.059	0.00179	0.308	0.362	0.408	0.450	0.488	0.523	0.588	0.646	0.699	0.748	0.795	0.839	0.880	0.920	0.958	0.995	1.030	.	.	.
150	3	0.9992	142.0	-1.049	0.00183	0.308	0.363	0.410	0.453	0.492	0.528	0.593	0.652	0.706	0.756	0.803	0.848	0.890	0.930	0.969	1.006	1.042	.	.	.
150	4	0.9988	165.1	-1.166	0.00197	0.310	0.368	0.418	0.463	0.504	0.542	0.610	0.672	0.728	0.780	0.829	0.875	0.919	0.961	1.001	1.040	1.077	1.113	1.148	.
150	4	0.9993	145.1	-1.074	0.00197	0.229	0.303	0.362	0.413	0.458	0.499	0.572	0.637	0.696	0.751	0.801	0.849	0.894	0.937	0.978	1.017	1.055	.	.	.
150	5	0.9990	145.3	-1.076	0.00191	0.296	0.355	0.405	0.450	0.490	0.528	0.596	0.657	0.712	0.764	0.812	0.858	0.901	0.943	0.982	1.020	1.057	.	.	.
150	5	0.9990	144.6	-1.097	0.00189	0.381	0.428	0.470	0.509	0.545	0.579	0.641	0.697	0.750	0.799	0.845	0.888	0.930	0.970	1.008	1.045	1.081	.	.	.
200	1	0.9990	137.9	-1.773	0.00564	0.385	0.511	0.611	0.697	0.774	0.844	0.968	1.078	1.178	1.270	1.356	1.437	1.513	1.586	1.655	1.722	.	.	.	.
200	1	0.9979	140.1	-1.794	0.00539	0.551	0.642	0.721	0.792	0.857	0.918	1.029	1.129	1.221	1.306	1.386	1.462	1.534	1.603	1.669	1.732	1.793	.	.	.
200	2	0.9990	134.3	-1.560	0.00456	0.276	0.409	0.508	0.591	0.664	0.729	0.845	0.947	1.038	1.123	1.201	1.275	1.344	1.411	1.474	1.534	.	.	.	.
200	2	0.9986	129.4	-1.539	0.00447	0.382	0.485	0.570	0.644	0.710	0.770	0.878	0.975	1.062	1.143	1.219	1.290	1.358	1.422	1.483	1.542	.	.	.	.
200	3	0.9987	138.6	-1.558	0.00394	0.569	0.635	0.694	0.748	0.799	0.847	0.935	1.016	1.091	1.161	1.227	1.289	1.349	1.406	1.461	1.514	.	.	.	.
200	3	0.9992	135.6	-1.592	0.00438	0.497	0.578	0.649	0.714	0.773	0.827	0.927	1.017	1.100	1.177	1.249	1.317	1.382	1.444	1.503	1.561	.	.	.	.
200	4	0.9985	144.0	-1.457	0.00353	0.402	0.482	0.550	0.611	0.666	0.717	0.810	0.892	0.968	1.039	1.104	1.166	1.225	1.282	1.336	1.387	1.437	.	.	.
200	4	0.9984	140.6	-1.487	0.00366	0.473	0.545	0.609	0.666	0.719	0.768	0.858	0.940	1.015	1.084	1.150	1.212	1.271	1.327	1.381	1.433	1.484	.	.	.
200	5	0.9986	155.4	-1.672	0.00411	0.567	0.636	0.697	0.754	0.807	0.856	0.947	1.031	1.108	1.179	1.247	1.312	1.373	1.431	1.488	1.542	1.595	1.645	.	.
200	5	0.9984	148.3	-1.581	0.00385	0.538	0.605	0.666	0.722	0.773	0.822	0.911	0.992	1.067	1.136	1.202	1.265	1.324	1.381	1.436	1.489	1.540	.	.	.
250	1	0.9989	137.6	-2.398	0.00987	0.718	0.844	0.954	1.053	1.142	1.226	1.377	1.514	1.639	1.755	1.864	1.967	2.065	2.159	2.248	2.334	.	.	.	.
250	1	0.9973	135.2	-2.255	0.00848	0.817	0.915	1.003	1.085	1.160	1.231	1.362	1.481	1.592	1.695	1.792	1.885	1.973	2.057	2.138	2.216	.	.	.	.
250	2	0.9970	146.7	-2.253	0.00856	0.473	0.629	0.753	0.859	0.953	1.039	1.193	1.328	1.452	1.565	1.671	1.770	1.865	1.954	2.040	2.122	2.201	.	.	.
250	2	0.9988	139.7	-2.226	0.00886	0.428	0.600	0.733	0.845	0.944	1.034	1.193	1.333	1.460	1.577	1.685	1.788	1.884	1.976	2.064	2.148	2.229	.	.	.
250	3	0.9955	149.5	-2.121	0.00664	0.812	0.890	0.962	1.028	1.091	1.150	1.260	1.362	1.456	1.545	1.628	1.708	1.784	1.857	1.927	1.995	2.060	2.124	.	.
250	3	0.9986	135.2	-2.263	0.00916	0.594	0.732	0.848	0.950	1.042	1.126	1.278	1.414	1.538	1.653	1.760	1.862	1.957	2.049	2.136	2.220	.	.	.	.
250	4	0.9983	157.7	-2.148	0.00693	0.614	0.718	0.809	0.890	0.965	1.034	1.161	1.275	1.379	1.476	1.567	1.653	1.735	1.813	1.888	1.960	2.030	2.097	.	.
250	4	0.9979	170.1	-2.229	0.00652	0.815	0.891	0.962	1.027	1.089	1.147	1.256	1.355	1.448	1.536	1.619	1.697	1.772	1.844	1.914	1.981	2.046	2.108	2.169	2.229
250	5	0.9988	146.4	-2.208	0.00803	0.581	0.706	0.811	0.905	0.990	1.068	1.209	1.335	1.450	1.557	1.657	1.751	1.841	1.926	2.007	2.086	2.161	.	.	.
250	5	0.9988	129.6	-2.065	0.00778	0.621	0.736	0.835	0.923	1.004	1.079	1.214	1.336	1.448	1.552	1.649	1.741	1.828	1.911	1.991	2.068	.	.	.	.

Appendix B. Coefficient of Determination, Parameter Estimates, and Drying Rates of Radially-cut 15x152 mm Southern Yellow Pine Flakes.

TEMP						DRYING RATE (%/SEC)																	
(C)	REP	R^2	β_0	β_1	β_2	5	10	15	20	25	30	40	50	60	70	80	90	100	110	120	130	140	150	160
150	1	0.9995	135.0	-1.090	0.00209	0.322	0.381	0.432	0.478	0.520	0.559	0.629	0.692	0.750	0.804	0.854	0.901	0.947	0.990	1.031	1.071	.	.	.
150	1	0.9993	134.0	-1.155	0.00242	0.293	0.367	0.427	0.481	0.529	0.573	0.652	0.722	0.786	0.846	0.901	0.953	1.003	1.050	1.095	1.138	.	.	.
150	2	0.9989	157.7	-1.299	0.00254	0.370	0.433	0.488	0.537	0.583	0.625	0.701	0.770	0.834	0.892	0.948	1.000	1.049	1.097	1.142	1.186	1.228	1.268	.
150	2	0.9987	161.3	-1.312	0.00250	0.401	0.459	0.511	0.558	0.601	0.641	0.714	0.781	0.843	0.900	0.954	1.005	1.053	1.100	1.144	1.187	1.228	1.268	1.307
150	3	0.9990	149.6	-1.154	0.00206	0.373	0.425	0.471	0.513	0.551	0.588	0.654	0.714	0.770	0.822	0.870	0.917	0.961	1.003	1.043	1.082	1.119	1.155	.
150	3	0.9990	152.0	-1.230	0.00236	0.350	0.412	0.466	0.514	0.558	0.599	0.673	0.740	0.801	0.858	0.912	0.962	1.010	1.056	1.100	1.142	1.183	1.222	.
150	4	0.9992	146.2	-1.297	0.00273	0.376	0.442	0.500	0.552	0.600	0.644	0.723	0.795	0.861	0.922	0.980	1.034	1.086	1.135	1.182	1.227	1.271	.	.
150	4	0.9988	150.6	-1.185	0.00217	0.376	0.430	0.478	0.521	0.561	0.599	0.667	0.729	0.786	0.840	0.890	0.937	0.982	1.026	1.067	1.107	1.145	1.183	.
150	5	0.9989	138.7	-1.191	0.00252	0.261	0.344	0.411	0.469	0.520	0.566	0.649	0.723	0.790	0.851	0.908	0.962	1.014	1.062	1.109	1.153	.	.	.
150	5	0.9995	132.5	-1.134	0.00233	0.308	0.376	0.434	0.485	0.531	0.573	0.649	0.718	0.780	0.838	0.892	0.943	0.991	1.037	1.081	1.123	.	.	.
200	1	0.9992	155.5	-1.689	0.00434	0.488	0.570	0.641	0.706	0.765	0.820	0.920	1.010	1.092	1.169	1.241	1.309	1.374	1.436	1.495	1.552	1.607	1.660	.
200	1	0.9994	153.3	-1.701	0.00453	0.450	0.542	0.620	0.689	0.752	0.810	0.915	1.010	1.096	1.176	1.250	1.321	1.388	1.452	1.513	1.572	1.628	1.683	.
200	2	0.9991	167.9	-1.827	0.00463	0.567	0.644	0.712	0.774	0.832	0.886	0.985	1.075	1.158	1.235	1.308	1.377	1.442	1.505	1.566	1.624	1.680	1.734	.
200	2	0.9903	148.3	-1.742	0.00478	0.542	0.624	0.696	0.762	0.822	0.878	0.981	1.074	1.160	1.240	1.315	1.386	1.453	1.517	1.579	1.639	1.696	.	.
200	3	0.9988	147.3	-1.659	0.00442	0.484	0.568	0.641	0.707	0.767	0.822	0.924	1.015	1.099	1.176	1.249	1.318	1.384	1.446	1.506	1.564	1.619	.	.
200	3	0.9984	143.5	-1.614	0.00425	0.500	0.579	0.648	0.710	0.768	0.821	0.919	1.007	1.088	1.164	1.235	1.302	1.365	1.426	1.484	1.541	1.595	.	.
200	4	0.9989	159.1	-1.653	0.00394	0.554	0.621	0.682	0.737	0.789	0.837	0.926	1.008	1.083	1.153	1.220	1.283	1.343	1.400	1.455	1.508	1.559	1.609	.
200	4	0.9988	147.5	-1.493	0.00349	0.489	0.556	0.615	0.670	0.720	0.767	0.853	0.931	1.003	1.071	1.134	1.194	1.251	1.306	1.358	1.408	1.457	.	.
200	5	0.9986	145.1	-1.661	0.00453	0.470	0.558	0.634	0.702	0.763	0.821	0.924	1.018	1.103	1.182	1.256	1.327	1.393	1.457	1.518	1.576	1.633	.	.
200	5	0.9992	138.3	-1.594	0.00454	0.345	0.458	0.549	0.626	0.695	0.757	0.869	0.968	1.058	1.140	1.218	1.290	1.359	1.424	1.486	1.546	.	.	.
250	1	0.9977	160.5	-2.175	0.00682	0.698	0.790	0.872	0.947	1.017	1.082	1.201	1.310	1.410	1.504	1.592	1.675	1.755	1.831	1.904	1.974	2.042	2.108	2.172
250	1	0.9992	148.5	-2.206	0.00768	0.676	0.781	0.874	0.958	1.035	1.107	1.238	1.356	1.465	1.567	1.662	1.752	1.837	1.919	1.998	2.073	2.146	.	.
250	2	0.9983	147.8	-2.233	0.00790	0.686	0.793	0.887	0.972	1.050	1.123	1.256	1.376	1.486	1.589	1.686	1.777	1.864	1.947	2.026	2.103	2.177	.	.
250	2	0.9986	142.8	-2.325	0.00907	0.638	0.767	0.877	0.975	1.064	1.146	1.295	1.428	1.550	1.663	1.769	1.868	1.963	2.053	2.140	2.223	2.303	.	.
250	3	0.9985	155.1	-2.139	0.00695	0.635	0.736	0.825	0.905	0.979	1.048	1.173	1.286	1.390	1.487	1.578	1.663	1.745	1.823	1.898	1.970	2.039	2.106	.
250	3	0.9976	153.5	-2.115	0.00693	0.599	0.705	0.797	0.880	0.955	1.025	1.153	1.267	1.372	1.470	1.561	1.648	1.730	1.808	1.883	1.955	2.025	2.092	.
250	4	0.9989	164.7	-2.071	0.00590	0.722	0.800	0.870	0.936	0.997	1.054	1.161	1.258	1.349	1.433	1.513	1.589	1.662	1.731	1.798	1.863	1.925	1.985	2.044
250	4	0.9982	151.1	-2.123	0.00718	0.556	0.673	0.773	0.861	0.940	1.014	1.147	1.266	1.375	1.475	1.570	1.659	1.743	1.824	1.901	1.975	2.046	2.115	.
250	5	0.9992	137.2	-2.158	0.00802	0.643	0.757	0.857	0.946	1.027	1.103	1.240	1.363	1.476	1.581	1.679	1.772	1.861	1.945	2.026	2.104	.	.	.
250	5	0.9978	142.9	-2.233	0.00852	0.535	0.676	0.792	0.893	0.984	1.067	1.216	1.349	1.470	1.582	1.686	1.784	1.877	1.966	2.051	2.132	2.211	.	.

Appendix C. Coefficient of Determination, Parameter Estimates, and Drying Rates of Radially-cut 25x117 mm Southern Yellow Pine Flakes.

TEMP						DRYING RATE (%/SEC)																		
(C)	REP	R^2	β_0	β_1	β_2	5	10	15	20	25	30	40	50	60	70	80	90	100	110	120	130	140	150	160
150	1	0.9994	134.1	-0.944	0.00146	0.369	0.406	0.441	0.473	0.503	0.531	0.584	0.632	0.677	0.719	0.758	0.796	0.832	0.866	0.900	0.932	.	.	.
150	1	0.9994	132.1	-0.962	0.00165	0.297	0.348	0.392	0.432	0.469	0.503	0.564	0.620	0.671	0.719	0.763	0.805	0.845	0.883	0.920	0.955	.	.	.
150	2	0.9993	134.1	-1.126	0.00223	0.346	0.405	0.457	0.503	0.546	0.585	0.657	0.721	0.781	0.836	0.887	0.936	0.983	1.027	1.069	1.110	.	.	.
150	2	0.9995	138.5	-1.085	0.00195	0.372	0.421	0.465	0.505	0.542	0.577	0.641	0.699	0.753	0.803	0.850	0.894	0.937	0.978	1.017	1.054	.	.	.
150	3	0.9996	138.2	-0.933	0.00147	0.299	0.345	0.385	0.421	0.455	0.486	0.543	0.594	0.642	0.686	0.727	0.767	0.804	0.840	0.874	0.907	.	.	.
150	3	0.9996	136.7	-0.915	0.00142	0.294	0.339	0.378	0.414	0.447	0.478	0.534	0.585	0.632	0.676	0.717	0.755	0.792	0.827	0.861	0.893	.	.	.
150	4	0.9993	136.5	-0.934	0.00153	0.260	0.314	0.359	0.399	0.436	0.470	0.531	0.586	0.636	0.682	0.726	0.767	0.805	0.843	0.878	0.912	.	.	.
150	4	0.9993	140.2	-0.975	0.00156	0.327	0.371	0.411	0.448	0.481	0.513	0.570	0.622	0.671	0.716	0.758	0.798	0.836	0.873	0.908	0.942	0.974	.	.
150	5	0.9993	134.5	-1.023	0.00179	0.346	0.394	0.437	0.476	0.512	0.546	0.608	0.664	0.716	0.765	0.810	0.853	0.894	0.933	0.971	1.007	.	.	.
150	5	0.9995	132.0	-0.994	0.00176	0.312	0.364	0.409	0.450	0.487	0.522	0.586	0.643	0.695	0.744	0.790	0.833	0.874	0.914	0.951	0.987	.	.	.
200	1	0.9984	142.5	-1.394	0.00322	0.412	0.484	0.547	0.603	0.654	0.702	0.788	0.866	0.938	1.004	1.066	1.125	1.181	1.234	1.286	1.335	1.382	.	.
200	1	0.9991	133.2	-1.419	0.00368	0.354	0.446	0.522	0.588	0.648	0.702	0.800	0.888	0.967	1.040	1.109	1.173	1.234	1.293	1.348	1.402	.	.	.
200	2	0.9989	137.8	-1.574	0.00410	0.548	0.618	0.681	0.739	0.793	0.843	0.935	1.019	1.096	1.169	1.237	1.301	1.363	1.422	1.478	1.533	.	.	.
200	2	0.9987	140.2	-1.773	0.00520	0.575	0.660	0.734	0.802	0.864	0.923	1.029	1.126	1.215	1.297	1.375	1.449	1.519	1.586	1.650	1.712	1.772	.	.
200	3	0.9988	162.4	-1.416	0.00277	0.508	0.560	0.607	0.651	0.693	0.731	0.804	0.870	0.932	0.989	1.044	1.096	1.145	1.193	1.238	1.282	1.325	1.366	1.406
200	3	0.9991	133.7	-1.293	0.00294	0.401	0.469	0.528	0.581	0.629	0.674	0.756	0.830	0.898	0.961	1.021	1.077	1.130	1.181	1.229	1.276	.	.	.
200	4	0.9990	155.8	-1.595	0.00387	0.459	0.536	0.604	0.665	0.721	0.773	0.867	0.952	1.030	1.103	1.171	1.235	1.296	1.355	1.410	1.464	1.516	1.566	.
200	4	0.9990	166.6	-1.447	0.00288	0.479	0.535	0.587	0.634	0.678	0.719	0.796	0.865	0.929	0.989	1.046	1.100	1.151	1.200	1.247	1.293	1.337	1.379	1.420
200	5	0.9986	157.8	-1.436	0.00302	0.462	0.523	0.578	0.628	0.675	0.718	0.798	0.870	0.937	1.000	1.058	1.114	1.167	1.218	1.267	1.313	1.359	1.403	.
200	5	0.9990	151.6	-1.468	0.00325	0.496	0.557	0.613	0.664	0.711	0.756	0.837	0.912	0.981	1.045	1.105	1.163	1.217	1.270	1.320	1.368	1.415	1.460	.
250	1	0.9985	135.1	-1.839	0.00614	0.434	0.558	0.658	0.746	0.824	0.895	1.023	1.137	1.240	1.336	1.424	1.508	1.587	1.663	1.735	1.805	.	.	.
250	1	0.9991	126.3	-1.872	0.00688	0.405	0.550	0.663	0.760	0.846	0.923	1.062	1.185	1.296	1.398	1.493	1.583	1.667	1.748	1.825	.	.	.	.
250	2	0.9991	143.1	-2.470	0.00993	0.786	0.904	1.007	1.102	1.188	1.269	1.417	1.551	1.674	1.789	1.896	1.998	2.095	2.188	2.277	2.363	2.445	.	.
250	2	0.9988	144.6	-2.471	0.01007	0.696	0.828	0.942	1.043	1.136	1.221	1.376	1.516	1.643	1.761	1.872	1.977	2.076	2.171	2.262	2.350	2.434	.	.
250	3	0.9988	141.8	-1.899	0.00611	0.512	0.620	0.712	0.793	0.867	0.935	1.057	1.167	1.268	1.361	1.448	1.530	1.608	1.682	1.753	1.822	1.888	.	.
250	3	0.9997	139.5	-1.836	0.00583	0.481	0.590	0.682	0.763	0.836	0.903	1.024	1.132	1.231	1.322	1.408	1.488	1.565	1.638	1.707	1.774	1.839	.	.
250	4	0.9995	153.2	-1.984	0.00611	0.562	0.662	0.748	0.826	0.897	0.963	1.082	1.190	1.288	1.380	1.466	1.547	1.624	1.698	1.768	1.836	1.901	1.964	.
250	4	0.9991	159.3	-2.024	0.00600	0.630	0.719	0.798	0.870	0.936	0.998	1.112	1.215	1.310	1.398	1.482	1.560	1.636	1.707	1.776	1.842	1.906	1.968	2.028
250	5	0.9990	140.7	-2.047	0.00720	0.533	0.654	0.756	0.846	0.927	1.002	1.137	1.257	1.367	1.468	1.563	1.653	1.738	1.819	1.896	1.971	2.043	.	.
250	5	0.9999	155.5	-2.042	0.00648	0.518	0.631	0.726	0.811	0.887	0.957	1.084	1.198	1.302	1.398	1.488	1.572	1.653	1.729	1.803	1.873	1.941	2.007	.

Appendix D. Coefficient of Determination, Parameter Estimates, and Drying Rates of Radially-cut 25x152 mm Southern Yellow Pine Flakes.

TEMP						DRYING RATE (%/SEC)																			
(C)	REP	R^2	β_0	β_1	β_2	5	10	15	20	25	30	40	50	60	70	80	90	100	110	120	130	140	150	160	170
150	1	0.9990	134.7	-1.295	0.00302	0.326	0.408	0.477	0.537	0.590	0.639	0.728	0.807	0.879	0.945	1.007	1.065	1.121	1.173	1.224	1.272	.	.	.	.
150	1	0.9990	131.8	-1.226	0.00274	0.341	0.414	0.475	0.530	0.579	0.624	0.707	0.780	0.847	0.910	0.968	1.023	1.075	1.125	1.172	1.218	.	.	.	.
150	2	0.9992	161.6	-1.049	0.00161	0.301	0.350	0.394	0.433	0.468	0.502	0.562	0.617	0.667	0.714	0.758	0.799	0.839	0.876	0.913	0.947	0.981	1.013	1.045	.
150	2	0.9989	151.6	-0.910	0.00126	0.300	0.339	0.374	0.407	0.436	0.464	0.516	0.562	0.605	0.646	0.684	0.719	0.754	0.786	0.818	0.848	0.877	0.905	.	.
150	3	0.9988	138.9	-1.068	0.00199	0.270	0.336	0.391	0.439	0.482	0.522	0.594	0.657	0.716	0.769	0.820	0.867	0.912	0.954	0.995	1.035	.	.	.	.
150	3	0.9998	149.6	-1.321	0.00288	0.281	0.370	0.441	0.502	0.556	0.606	0.695	0.773	0.844	0.910	0.971	1.029	1.083	1.135	1.185	1.233	1.279	1.323	.	.
150	4	0.9988	138.8	-1.040	0.00187	0.287	0.346	0.396	0.441	0.481	0.519	0.586	0.647	0.702	0.754	0.802	0.847	0.890	0.931	0.970	1.008	.	.	.	.
150	4	0.9992	144.0	-1.194	0.00224	0.426	0.476	0.521	0.562	0.600	0.637	0.703	0.764	0.821	0.874	0.923	0.971	1.016	1.059	1.100	1.140	1.179	.	.	.
150	5	0.9992	138.8	-1.083	0.00189	0.398	0.443	0.484	0.521	0.556	0.590	0.651	0.706	0.758	0.807	0.852	0.896	0.937	0.977	1.015	1.051	.	.	.	.
150	5	0.9986	135.6	-1.001	0.00170	0.338	0.385	0.427	0.465	0.500	0.533	0.594	0.648	0.699	0.746	0.790	0.832	0.872	0.910	0.947	0.982	.	.	.	.
200	1	0.9988	126.2	-1.665	0.00514	0.529	0.619	0.697	0.767	0.832	0.891	1.000	1.098	1.188	1.271	1.350	1.424	1.494	1.562	1.626	.	.	.	.	.
200	1	0.9991	122.2	-1.652	0.00535	0.471	0.573	0.660	0.737	0.806	0.870	0.985	1.088	1.183	1.270	1.351	1.428	1.501	1.571	1.638	.	.	.	.	.
200	2	0.9985	148.2	-1.329	0.00277	0.422	0.484	0.538	0.587	0.632	0.675	0.753	0.823	0.888	0.948	1.005	1.058	1.110	1.158	1.205	1.250	1.294	.	.	.
200	2	0.9991	156.6	-1.442	0.00306	0.476	0.537	0.591	0.641	0.687	0.730	0.809	0.882	0.949	1.011	1.070	1.125	1.179	1.229	1.278	1.325	1.370	1.414	.	.
200	3	0.9985	146.0	-1.613	0.00424	0.459	0.544	0.617	0.682	0.742	0.797	0.897	0.987	1.069	1.146	1.218	1.286	1.350	1.411	1.470	1.527	1.581	.	.	.
200	3	0.9995	150.3	-1.608	0.00427	0.319	0.433	0.522	0.598	0.666	0.727	0.837	0.933	1.021	1.101	1.176	1.247	1.313	1.377	1.438	1.496	1.552	1.606	.	.
200	4	0.9990	144.3	-1.589	0.00408	0.500	0.576	0.643	0.703	0.759	0.811	0.906	0.992	1.071	1.145	1.214	1.280	1.342	1.402	1.459	1.514	1.567	.	.	.
200	4	0.9993	145.6	-1.584	0.00411	0.448	0.532	0.604	0.669	0.728	0.782	0.881	0.970	1.051	1.126	1.197	1.264	1.327	1.388	1.446	1.501	1.555	.	.	.
200	5	0.9988	140.0	-1.456	0.00367	0.375	0.463	0.536	0.601	0.659	0.712	0.809	0.895	0.973	1.046	1.114	1.178	1.239	1.297	1.352	1.405	1.456	.	.	.
200	5	0.9986	140.2	-1.413	0.00325	0.490	0.552	0.608	0.659	0.707	0.751	0.833	0.908	0.977	1.041	1.102	1.159	1.214	1.266	1.316	1.365	1.412	.	.	.
250	1	0.9992	125.9	-2.172	0.00903	0.592	0.728	0.843	0.944	1.036	1.119	1.270	1.405	1.529	1.642	1.749	1.849	1.945	2.035	2.122	.	.	.	.	.
250	1	0.9973	130.8	-2.099	0.00771	0.724	0.824	0.912	0.993	1.068	1.138	1.266	1.383	1.490	1.590	1.685	1.774	1.859	1.940	2.018	2.093	.	.	.	.
250	2	0.9982	159.6	-1.964	0.00548	0.684	0.759	0.828	0.892	0.952	1.008	1.111	1.206	1.293	1.375	1.453	1.526	1.597	1.664	1.728	1.791	1.851	1.909	1.966	.
250	2	0.9989	169.6	-2.047	0.00568	0.668	0.748	0.820	0.887	0.949	1.007	1.114	1.212	1.302	1.387	1.467	1.542	1.614	1.683	1.749	1.813	1.875	1.935	1.992	2.049
250	3	0.9995	155.1	-2.008	0.00621	0.553	0.656	0.744	0.824	0.896	0.963	1.084	1.193	1.293	1.386	1.473	1.555	1.633	1.707	1.778	1.847	1.913	1.977	.	.
250	3	0.9980	152.6	-2.196	0.00736	0.693	0.792	0.880	0.960	1.034	1.103	1.229	1.343	1.449	1.547	1.639	1.727	1.810	1.889	1.966	2.039	2.110	2.179	.	.
250	4	0.9989	143.7	-1.876	0.00580	0.548	0.645	0.729	0.805	0.874	0.938	1.055	1.159	1.255	1.345	1.428	1.507	1.583	1.654	1.723	1.789	1.853	.	.	.
250	4	0.9990	137.9	-1.960	0.00662	0.565	0.672	0.764	0.847	0.921	0.991	1.116	1.229	1.333	1.429	1.518	1.603	1.684	1.761	1.834	1.905	.	.	.	.
250	5	0.9990	133.1	-2.023	0.00743	0.534	0.659	0.763	0.855	0.938	1.014	1.151	1.274	1.386	1.489	1.586	1.677	1.763	1.846	1.924	2.000	.	.	.	.
250	5	0.9988	135.7	-1.972	0.00699	0.480	0.609	0.714	0.806	0.889	0.964	1.100	1.220	1.330	1.431	1.526	1.615	1.699	1.780	1.857	1.931	.	.	.	.

Appendix E. Coefficient of Determination, Parameter Estimates, and Drying Rates of Tangentially-cut 15x117 mm Southern Yellow Pine Flakes.

TEMP						DRYING RATE (%/SEC)																
(C)	REP	R^2	β_0	β_1	β_2	5	10	15	20	25	30	40	50	60	70	80	90	100	110	120	130	140	150
150	1	0.9989	139.5	-1.120	0.00219	0.281	0.351	0.408	0.459	0.504	0.546	0.621	0.687	0.748	0.805	0.857	0.907	0.954	0.999	1.041	1.083	1.122	.
150	1	0.9994	137.1	-1.132	0.00218	0.363	0.419	0.468	0.512	0.553	0.591	0.661	0.724	0.781	0.835	0.886	0.934	0.979	1.023	1.064	1.105	.	.
150	2	0.9990	137.7	-1.251	0.00271	0.353	0.423	0.483	0.536	0.584	0.629	0.710	0.783	0.849	0.911	0.969	1.023	1.075	1.124	1.171	1.217	.	.
150	2	0.9988	137.2	-1.269	0.00277	0.385	0.451	0.509	0.561	0.608	0.652	0.732	0.804	0.870	0.931	0.989	1.043	1.095	1.145	1.192	1.238	.	.
150	3	0.9990	128.9	-1.142	0.00239	0.347	0.410	0.464	0.513	0.558	0.599	0.674	0.742	0.804	0.861	0.915	0.966	1.014	1.060	1.104	.	.	.
150	3	0.9986	127.6	-1.101	0.00224	0.336	0.397	0.450	0.498	0.541	0.581	0.653	0.719	0.779	0.834	0.887	0.936	0.983	1.027	1.070	.	.	.
150	4	0.9985	143.4	-1.108	0.00202	0.327	0.384	0.433	0.478	0.518	0.556	0.625	0.686	0.743	0.796	0.845	0.892	0.936	0.978	1.019	1.058	1.095	.
150	4	0.9986	151.5	-1.157	0.00216	0.271	0.341	0.400	0.451	0.496	0.538	0.613	0.680	0.741	0.797	0.850	0.899	0.946	0.991	1.033	1.074	1.114	1.152
150	5	0.9986	150.6	-1.187	0.00230	0.270	0.345	0.406	0.459	0.507	0.550	0.628	0.697	0.760	0.819	0.873	0.924	0.972	1.019	1.063	1.105	1.146	1.185
150	5	0.9989	142.7	-1.113	0.00206	0.324	0.383	0.433	0.478	0.519	0.558	0.627	0.690	0.747	0.800	0.850	0.897	0.942	0.985	1.025	1.065	1.103	.
200	1	0.9989	135.9	-1.623	0.00446	0.545	0.622	0.690	0.752	0.809	0.862	0.960	1.049	1.131	1.207	1.279	1.347	1.412	1.474	1.533	1.590	.	.
200	1	0.9991	128.0	-1.543	0.00431	0.514	0.592	0.660	0.723	0.780	0.833	0.931	1.019	1.101	1.176	1.247	1.314	1.378	1.440	1.498	.	.	.
200	2	0.9984	141.6	-1.799	0.00547	0.500	0.600	0.685	0.760	0.829	0.893	1.008	1.111	1.205	1.293	1.375	1.452	1.526	1.596	1.663	1.727	1.789	.
200	2	0.9983	137.1	-1.784	0.00561	0.469	0.576	0.666	0.746	0.818	0.883	1.002	1.109	1.205	1.295	1.379	1.458	1.533	1.604	1.673	1.739	.	.
200	3	0.9984	130.4	-1.679	0.00520	0.455	0.558	0.645	0.721	0.790	0.853	0.967	1.070	1.163	1.249	1.330	1.406	1.478	1.547	1.613	1.676	.	.
200	3	0.9988	128.8	-1.657	0.00514	0.447	0.550	0.637	0.713	0.782	0.845	0.959	1.061	1.154	1.240	1.320	1.396	1.468	1.536	1.602	.	.	.
200	4	0.9991	153.4	-1.704	0.00461	0.412	0.512	0.595	0.668	0.733	0.794	0.902	0.999	1.088	1.169	1.246	1.317	1.386	1.451	1.513	1.572	1.630	1.686
200	4	0.9987	150.8	-1.640	0.00428	0.440	0.529	0.604	0.671	0.732	0.789	0.891	0.982	1.066	1.143	1.216	1.284	1.349	1.411	1.471	1.528	1.583	1.636
200	5	0.9985	138.2	-1.558	0.00417	0.451	0.536	0.609	0.674	0.733	0.788	0.888	0.977	1.059	1.135	1.206	1.274	1.338	1.399	1.457	1.513	.	.
200	5	0.9991	139.1	-1.597	0.00437	0.456	0.543	0.618	0.685	0.746	0.803	0.905	0.997	1.081	1.159	1.232	1.301	1.367	1.429	1.489	1.547	.	.
250	1	0.9988	145.0	-2.278	0.00861	0.609	0.737	0.846	0.942	1.029	1.110	1.255	1.386	1.505	1.615	1.719	1.816	1.908	1.997	2.081	2.162	2.240	.
250	1	0.9988	135.0	-2.084	0.00769	0.590	0.708	0.810	0.900	0.981	1.057	1.193	1.316	1.428	1.532	1.629	1.721	1.808	1.891	1.971	2.047	.	.
250	2	0.9989	134.8	-2.421	0.01064	0.578	0.740	0.872	0.986	1.089	1.183	1.351	1.500	1.636	1.761	1.878	1.988	2.093	2.192	2.287	2.378	.	.
250	2	0.9982	124.7	-2.299	0.01027	0.608	0.758	0.883	0.993	1.091	1.182	1.344	1.489	1.621	1.743	1.857	1.965	2.067	2.164	2.257	.	.	.
250	3	0.9989	134.1	-2.124	0.00801	0.612	0.732	0.834	0.925	1.008	1.084	1.223	1.348	1.462	1.568	1.667	1.760	1.849	1.934	2.015	2.093	.	.
250	3	0.9989	133.5	-2.258	0.00879	0.763	0.871	0.967	1.054	1.134	1.209	1.346	1.471	1.586	1.693	1.794	1.889	1.980	2.067	2.150	2.231	.	.
250	4	0.9984	146.7	-2.041	0.00649	0.695	0.783	0.862	0.934	1.001	1.064	1.180	1.285	1.383	1.474	1.559	1.640	1.718	1.792	1.863	1.931	1.997	.
250	4	0.9984	145.4	-2.120	0.00734	0.609	0.719	0.815	0.901	0.979	1.051	1.183	1.301	1.409	1.510	1.604	1.693	1.778	1.859	1.936	2.011	2.082	.
250	5	0.9975	132.2	-2.009	0.00715	0.629	0.734	0.826	0.908	0.984	1.054	1.182	1.297	1.403	1.502	1.594	1.681	1.765	1.844	1.920	1.993	.	.
250	5	0.9973	131.0	-1.992	0.00708	0.630	0.734	0.825	0.907	0.982	1.051	1.178	1.293	1.398	1.496	1.588	1.675	1.757	1.836	1.912	1.984	.	.

Appendix F. Coefficient of Determination, Parameter Estimates, and Drying Rates of Tangentially-cut 15x152 mm Southern Yellow Pine Flakes.

TEMP						DRYING RATE (%/SEC)																
(C)	REP	R^2	β_0	β_1	β_2	5	10	15	20	25	30	40	50	60	70	80	90	100	110	120	130	140	150
150	1	0.9990	142.3	-1.148	0.00219	0.335	0.395	0.447	0.494	0.536	0.576	0.648	0.712	0.771	0.826	0.878	0.926	0.973	1.017	1.059	1.100	1.139	.
150	1	0.9989	141.3	-1.123	0.00210	0.340	0.397	0.447	0.492	0.533	0.571	0.640	0.703	0.760	0.813	0.863	0.911	0.956	0.999	1.040	1.080	1.118	.
150	2	0.9987	145.6	-1.244	0.00245	0.414	0.469	0.519	0.564	0.606	0.645	0.717	0.782	0.842	0.899	0.952	1.002	1.049	1.095	1.139	1.181	1.222	.
150	2	0.9988	143.5	-1.246	0.00249	0.416	0.472	0.522	0.568	0.610	0.649	0.722	0.788	0.849	0.906	0.959	1.010	1.058	1.104	1.148	1.191	1.232	.
150	3	0.9984	141.1	-1.330	0.00298	0.381	0.452	0.514	0.569	0.619	0.666	0.750	0.826	0.895	0.959	1.020	1.077	1.131	1.182	1.232	1.279	1.325	.
150	3	0.9982	139.8	-1.320	0.00294	0.396	0.464	0.524	0.577	0.626	0.671	0.754	0.828	0.896	0.960	1.019	1.075	1.129	1.180	1.229	1.276	1.321	.
150	4	0.9975	136.4	-1.276	0.00288	0.341	0.417	0.481	0.538	0.589	0.636	0.721	0.796	0.866	0.930	0.990	1.046	1.100	1.151	1.200	1.247	.	.
150	4	0.9985	135.2	-1.237	0.00258	0.432	0.488	0.539	0.585	0.627	0.667	0.740	0.807	0.869	0.926	0.980	1.031	1.080	1.127	1.172	1.215	.	.
150	5	0.9984	146.5	-1.100	0.00197	0.307	0.366	0.416	0.461	0.502	0.540	0.608	0.670	0.727	0.779	0.828	0.874	0.918	0.960	1.000	1.039	1.076	.
150	5	0.9981	145.5	-1.141	0.00213	0.327	0.387	0.438	0.485	0.527	0.566	0.636	0.700	0.758	0.812	0.863	0.911	0.957	1.000	1.042	1.082	1.120	.
200	1	0.9990	144.3	-1.607	0.00402	0.588	0.653	0.711	0.766	0.817	0.864	0.953	1.034	1.109	1.179	1.245	1.308	1.368	1.426	1.481	1.534	1.586	.
200	1	0.9979	149.6	-1.615	0.00393	0.577	0.642	0.700	0.755	0.805	0.852	0.940	1.020	1.095	1.164	1.230	1.292	1.352	1.409	1.463	1.516	1.567	1.616
200	2	0.9975	153.1	-1.841	0.00519	0.560	0.646	0.722	0.791	0.854	0.913	1.020	1.117	1.207	1.290	1.368	1.442	1.512	1.579	1.644	1.706	1.766	1.823
200	2	0.9981	146.8	-1.849	0.00551	0.545	0.638	0.719	0.792	0.859	0.921	1.034	1.135	1.228	1.315	1.396	1.473	1.546	1.615	1.682	1.746	1.808	.
200	3	0.9988	139.3	-1.850	0.00575	0.575	0.668	0.749	0.822	0.889	0.952	1.066	1.169	1.264	1.352	1.434	1.512	1.587	1.658	1.726	1.791	1.854	.
200	3	0.9976	144.5	-1.814	0.00535	0.553	0.642	0.721	0.792	0.856	0.917	1.027	1.126	1.217	1.302	1.382	1.457	1.529	1.597	1.663	1.726	1.787	.
200	4	0.9984	137.6	-1.775	0.00523	0.613	0.693	0.765	0.831	0.891	0.948	1.053	1.148	1.236	1.318	1.395	1.468	1.538	1.604	1.668	1.730	.	.
200	4	0.9991	131.5	-1.716	0.00524	0.543	0.632	0.710	0.780	0.845	0.905	1.014	1.112	1.203	1.287	1.366	1.441	1.512	1.579	1.644	1.707	.	.
200	5	0.9984	131.4	-1.461	0.00362	0.551	0.613	0.670	0.722	0.770	0.816	0.900	0.977	1.049	1.116	1.179	1.239	1.296	1.351	1.403	1.454	.	.
200	5	0.9987	131.6	-1.487	0.00381	0.531	0.598	0.659	0.714	0.766	0.814	0.903	0.983	1.058	1.128	1.193	1.256	1.315	1.372	1.426	1.478	.	.
250	1	0.9978	151.8	-2.083	0.00624	0.823	0.896	0.963	1.026	1.085	1.141	1.245	1.342	1.432	1.516	1.597	1.673	1.746	1.816	1.883	1.948	2.011	2.073
250	1	0.9986	145.7	-2.116	0.00670	0.842	0.918	0.988	1.054	1.115	1.174	1.283	1.384	1.477	1.565	1.649	1.728	1.804	1.877	1.947	2.014	2.080	.
250	2	0.9990	143.5	-2.433	0.00953	0.801	0.912	1.011	1.101	1.185	1.263	1.405	1.535	1.655	1.766	1.871	1.970	2.064	2.155	2.241	2.325	2.405	.
250	2	0.9987	141.0	-2.280	0.00850	0.759	0.864	0.957	1.042	1.121	1.194	1.329	1.451	1.564	1.669	1.768	1.861	1.950	2.036	2.118	2.196	2.272	.
250	3	0.9984	138.1	-2.274	0.00870	0.738	0.847	0.945	1.032	1.114	1.189	1.327	1.452	1.568	1.675	1.776	1.871	1.962	2.049	2.132	2.212	.	.
250	3	0.9972	140.2	-2.230	0.00772	0.892	0.975	1.051	1.122	1.189	1.253	1.370	1.479	1.580	1.675	1.765	1.850	1.932	2.010	2.086	2.158	2.229	.
250	4	0.9956	150.8	-2.497	0.00999	0.640	0.781	0.900	1.005	1.100	1.187	1.345	1.486	1.615	1.734	1.846	1.951	2.051	2.146	2.237	2.325	2.409	2.491
250	4	0.9967	140.3	-2.335	0.00872	0.859	0.955	1.042	1.123	1.198	1.269	1.399	1.519	1.629	1.733	1.831	1.924	2.012	2.097	2.179	2.257	2.333	.
250	5	0.9987	132.3	-1.948	0.00662	0.652	0.747	0.831	0.907	0.977	1.043	1.163	1.271	1.371	1.465	1.553	1.636	1.715	1.790	1.863	1.932	.	.
250	5	0.9987	137.9	-2.040	0.00696	0.681	0.777	0.862	0.939	1.010	1.077	1.199	1.310	1.412	1.507	1.597	1.682	1.763	1.840	1.914	1.985	.	.

Appendix G. Coefficient of Determination, Parameter Estimates, and Drying Rates of Tangentially-cut 25x117 mm Southern Yellow Pine Flakes.

TEMP						DRYING RATE (%/SEC)															
(C)	REP	R^2	β_0	β_1	β_2	5	10	15	20	25	30	40	50	60	70	80	90	100	110	120	130	140
150	1	0.9991	134.8	-0.975	0.00155	0.379	0.418	0.453	0.486	0.517	0.547	0.601	0.650	0.696	0.740	0.781	0.819	0.857	0.892	0.926	0.959	.
150	1	0.9991	134.2	-0.987	0.00166	0.345	0.390	0.430	0.467	0.502	0.534	0.592	0.646	0.695	0.741	0.785	0.826	0.865	0.903	0.939	0.973	.
150	2	0.9990	133.6	-1.154	0.00241	0.302	0.373	0.433	0.485	0.533	0.576	0.655	0.725	0.788	0.847	0.902	0.954	1.004	1.051	1.095	1.139	.
150	2	0.9984	134.5	-1.138	0.00231	0.313	0.380	0.437	0.487	0.532	0.574	0.650	0.717	0.779	0.836	0.890	0.940	0.988	1.034	1.078	1.120	.
150	3	0.9988	136.8	-1.134	0.00222	0.342	0.402	0.454	0.500	0.543	0.582	0.654	0.719	0.778	0.833	0.885	0.934	0.980	1.024	1.067	1.107	.
150	3	0.9988	136.6	-1.180	0.00245	0.321	0.390	0.448	0.500	0.547	0.590	0.668	0.738	0.801	0.860	0.916	0.968	1.017	1.064	1.109	1.153	.
150	4	0.9990	129.8	-1.119	0.00229	0.329	0.392	0.447	0.496	0.540	0.581	0.655	0.721	0.782	0.839	0.892	0.942	0.989	1.034	1.078	1.119	.
150	4	0.9991	128.3	-1.152	0.00246	0.340	0.406	0.462	0.513	0.559	0.601	0.678	0.747	0.810	0.868	0.923	0.975	1.024	1.071	1.116	.	.
150	5	0.9988	131.4	-1.192	0.00263	0.301	0.378	0.442	0.498	0.549	0.595	0.677	0.751	0.818	0.880	0.938	0.992	1.044	1.093	1.140	1.186	.
150	5	0.9988	131.0	-1.227	0.00281	0.300	0.382	0.450	0.508	0.561	0.609	0.695	0.772	0.841	0.906	0.966	1.022	1.076	1.127	1.176	1.223	.
200	1	0.9991	134.0	-1.436	0.00356	0.475	0.544	0.606	0.662	0.714	0.762	0.850	0.930	1.004	1.072	1.137	1.198	1.256	1.311	1.364	1.416	.
200	1	0.9982	133.7	-1.401	0.00345	0.434	0.507	0.571	0.629	0.681	0.730	0.819	0.900	0.973	1.042	1.106	1.167	1.224	1.279	1.332	1.383	.
200	2	0.9987	136.0	-1.673	0.00491	0.472	0.566	0.647	0.719	0.785	0.845	0.954	1.052	1.142	1.225	1.303	1.376	1.446	1.512	1.576	1.637	.
200	2	0.9982	134.2	-1.693	0.00523	0.407	0.520	0.612	0.692	0.764	0.830	0.947	1.052	1.147	1.235	1.317	1.394	1.467	1.537	1.603	1.667	.
200	3	0.9976	146.3	-1.722	0.00491	0.438	0.538	0.623	0.697	0.764	0.826	0.938	1.037	1.128	1.212	1.290	1.364	1.434	1.501	1.565	1.627	1.686
200	3	0.9986	135.1	-1.676	0.00503	0.438	0.540	0.627	0.702	0.770	0.833	0.946	1.047	1.139	1.224	1.304	1.379	1.450	1.518	1.582	1.645	.
200	4	0.9992	137.6	-1.621	0.00448	0.501	0.584	0.656	0.721	0.781	0.836	0.937	1.028	1.112	1.190	1.263	1.332	1.397	1.460	1.520	1.578	.
200	4	0.9987	129.1	-1.629	0.00497	0.436	0.538	0.624	0.699	0.767	0.829	0.941	1.041	1.133	1.217	1.296	1.371	1.441	1.509	1.573	.	.
200	5	0.9969	136.0	-1.690	0.00492	0.529	0.615	0.690	0.758	0.821	0.879	0.984	1.079	1.167	1.248	1.325	1.397	1.466	1.532	1.594	1.655	.
200	5	0.9977	135.2	-1.708	0.00511	0.506	0.599	0.679	0.750	0.816	0.876	0.986	1.085	1.175	1.259	1.338	1.412	1.483	1.550	1.615	1.677	.
250	1	0.9971	136.1	-1.866	0.00592	0.616	0.705	0.785	0.857	0.923	0.985	1.099	1.202	1.296	1.385	1.468	1.546	1.621	1.692	1.761	1.827	.
250	1	0.9988	124.1	-1.782	0.00581	0.637	0.723	0.799	0.869	0.933	0.994	1.105	1.205	1.298	1.385	1.466	1.543	1.617	1.687	1.755	.	.
250	2	0.9970	137.3	-2.078	0.00709	0.752	0.841	0.921	0.995	1.064	1.129	1.248	1.357	1.458	1.552	1.641	1.725	1.805	1.882	1.956	2.027	.
250	2	0.9989	127.0	-2.200	0.00920	0.591	0.731	0.847	0.950	1.042	1.127	1.280	1.416	1.541	1.656	1.764	1.865	1.961	2.053	2.141	.	.
250	3	0.9976	137.7	-2.064	0.00723	0.653	0.755	0.846	0.927	1.002	1.072	1.199	1.314	1.420	1.518	1.611	1.698	1.781	1.860	1.937	2.010	.
250	3	0.9989	131.5	-2.127	0.00836	0.540	0.677	0.791	0.890	0.980	1.062	1.209	1.340	1.460	1.570	1.673	1.770	1.862	1.950	2.034	2.115	.
250	4	0.9988	135.8	-2.256	0.00903	0.605	0.739	0.853	0.953	1.043	1.126	1.277	1.411	1.534	1.647	1.753	1.854	1.949	2.039	2.126	2.209	.
250	4	0.9966	140.2	-2.090	0.00698	0.772	0.857	0.935	1.007	1.074	1.137	1.254	1.361	1.460	1.552	1.640	1.723	1.802	1.878	1.951	2.021	2.089
250	5	0.9989	130.9	-2.388	0.01049	0.647	0.793	0.916	1.024	1.121	1.211	1.374	1.519	1.651	1.773	1.888	1.996	2.098	2.196	2.290	2.379	.
250	5	0.9970	137.3	-2.352	0.00955	0.689	0.816	0.925	1.023	1.113	1.196	1.346	1.481	1.605	1.720	1.827	1.929	2.026	2.118	2.206	2.291	.

Appendix H. Coefficient of Determination, Parameter Estimates, and Drying Rates of Tangentially-cut 25x152 mm Southern Yellow Pine Flakes.

TEMP						DRYING RATE (%/SEC)																
(C)	REP	R^2	β_0	β_1	β_2	5	10	15	20	25	30	40	50	60	70	80	90	100	110	120	130	140
150	1	0.9990	136.0	-0.985	0.00161	0.358	0.401	0.439	0.474	0.507	0.538	0.595	0.646	0.694	0.739	0.782	0.822	0.860	0.897	0.932	0.966	.
150	1	0.9987	131.8	-0.972	0.00163	0.343	0.388	0.428	0.464	0.498	0.530	0.588	0.641	0.690	0.736	0.779	0.820	0.859	0.896	0.932	0.966	.
150	2	0.9983	143.8	-1.072	0.00192	0.290	0.350	0.401	0.446	0.487	0.525	0.594	0.655	0.711	0.763	0.812	0.858	0.901	0.943	0.983	1.021	1.058
150	2	0.9979	139.2	-1.118	0.00213	0.323	0.384	0.436	0.482	0.525	0.564	0.635	0.699	0.758	0.812	0.863	0.911	0.957	1.000	1.042	1.082	.
150	3	0.9975	144.1	-1.171	0.00224	0.351	0.410	0.462	0.508	0.550	0.590	0.661	0.726	0.785	0.841	0.892	0.941	0.988	1.032	1.075	1.116	1.155
150	3	0.9983	137.0	-1.143	0.00224	0.353	0.412	0.463	0.509	0.551	0.590	0.662	0.726	0.785	0.840	0.892	0.941	0.987	1.032	1.074	1.115	.
150	4	0.9983	138.9	-1.159	0.00222	0.392	0.445	0.493	0.536	0.576	0.613	0.682	0.744	0.802	0.855	0.906	0.954	0.999	1.043	1.085	1.125	.
150	4	0.9985	138.0	-1.185	0.00235	0.394	0.450	0.499	0.544	0.586	0.625	0.696	0.760	0.820	0.875	0.927	0.976	1.023	1.068	1.111	1.153	.
150	5	0.9987	134.2	-0.904	0.00143	0.279	0.326	0.367	0.404	0.438	0.470	0.527	0.579	0.626	0.671	0.712	0.751	0.788	0.824	0.858	0.890	.
150	5	0.9988	134.1	-0.929	0.00157	0.231	0.291	0.341	0.384	0.423	0.458	0.522	0.579	0.631	0.679	0.724	0.766	0.805	0.843	0.880	0.915	.
200	1	0.9989	132.5	-1.388	0.00329	0.499	0.561	0.617	0.668	0.716	0.760	0.842	0.917	0.986	1.051	1.112	1.169	1.224	1.277	1.328	1.376	.
200	1	0.9994	139.3	-1.437	0.00342	0.478	0.545	0.605	0.659	0.709	0.755	0.841	0.919	0.990	1.057	1.120	1.179	1.236	1.290	1.342	1.392	1.440
200	2	0.9984	137.9	-1.515	0.00385	0.500	0.572	0.636	0.694	0.747	0.797	0.888	0.971	1.047	1.118	1.185	1.248	1.309	1.366	1.421	1.475	.
200	2	0.9989	138.5	-1.535	0.00393	0.510	0.582	0.646	0.704	0.758	0.808	0.900	0.983	1.060	1.132	1.199	1.263	1.324	1.382	1.438	1.491	.
200	3	0.9985	137.6	-1.630	0.00450	0.520	0.600	0.671	0.735	0.794	0.849	0.949	1.040	1.123	1.200	1.273	1.342	1.407	1.470	1.530	1.588	.
200	3	0.9978	137.9	-1.643	0.00456	0.525	0.605	0.677	0.741	0.800	0.855	0.956	1.047	1.131	1.209	1.282	1.351	1.417	1.480	1.540	1.599	.
200	4	0.9985	139.5	-1.630	0.00427	0.601	0.668	0.729	0.786	0.838	0.888	0.979	1.063	1.140	1.213	1.281	1.346	1.408	1.467	1.525	1.580	1.633
200	4	0.9982	140.2	-1.694	0.00471	0.566	0.644	0.714	0.777	0.835	0.890	0.990	1.081	1.165	1.244	1.317	1.387	1.453	1.517	1.578	1.636	1.693
200	5	0.9987	136.7	-1.298	0.00298	0.338	0.417	0.483	0.541	0.594	0.642	0.729	0.807	0.878	0.943	1.004	1.062	1.117	1.169	1.219	1.267	.
200	5	0.9984	138.8	-1.282	0.00278	0.396	0.461	0.518	0.569	0.616	0.659	0.739	0.810	0.876	0.938	0.995	1.049	1.101	1.150	1.198	1.243	.
250	1	0.9986	132.1	-1.811	0.00560	0.658	0.738	0.811	0.877	0.939	0.997	1.103	1.200	1.290	1.374	1.454	1.529	1.600	1.669	1.735	1.798	.
250	1	0.9985	140.9	-1.965	0.00600	0.774	0.848	0.916	0.979	1.039	1.095	1.200	1.296	1.385	1.469	1.549	1.625	1.697	1.766	1.833	1.897	1.959
250	2	0.9989	137.1	-2.086	0.00730	0.705	0.802	0.888	0.967	1.039	1.107	1.232	1.345	1.450	1.547	1.639	1.725	1.808	1.887	1.963	2.036	.
250	2	0.9987	138.9	-2.116	0.00707	0.833	0.914	0.988	1.057	1.122	1.183	1.297	1.402	1.500	1.591	1.678	1.760	1.839	1.914	1.986	2.056	.
250	3	0.9987	135.2	-2.119	0.00771	0.687	0.792	0.884	0.967	1.044	1.115	1.246	1.364	1.473	1.574	1.669	1.759	1.845	1.927	2.005	2.081	.
250	3	0.9965	141.1	-2.029	0.00652	0.756	0.838	0.912	0.981	1.045	1.106	1.218	1.321	1.416	1.505	1.589	1.669	1.746	1.819	1.889	1.957	2.022
250	4	0.9986	133.1	-2.098	0.00749	0.751	0.845	0.929	1.007	1.078	1.146	1.270	1.383	1.487	1.584	1.676	1.763	1.846	1.926	2.002	2.075	.
250	4	0.9982	133.9	-2.226	0.00870	0.686	0.803	0.905	0.996	1.080	1.158	1.299	1.427	1.544	1.653	1.755	1.851	1.943	2.031	2.114	2.195	.
250	5	0.9990	136.2	-1.734	0.00518	0.536	0.625	0.703	0.774	0.838	0.898	1.006	1.105	1.195	1.278	1.357	1.431	1.502	1.570	1.634	1.696	.
250	5	0.9986	138.4	-1.707	0.00480	0.595	0.671	0.739	0.801	0.859	0.913	1.013	1.104	1.187	1.266	1.339	1.409	1.476	1.539	1.601	1.659	.

Appendix I. Coefficient of Determination, Parameter Estimates, and Drying Rates of Radially-cut 15x117 mm Sweetgum Flakes.

TEMP						DRYING RATE (%/SEC)														
(C)	REP	R^2	β_0	β_1	β_2	5	10	15	20	25	30	40	50	60	70	80	90	100	110	120
150	1	0.9996	98.2	-0.949	0.00227	0.233	0.316	0.381	0.437	0.486	0.530	0.610	0.680	0.744	0.803	0.858	0.909	.	.	.
150	1	0.9994	95.9	-0.907	0.00218	0.175	0.272	0.343	0.401	0.452	0.498	0.579	0.650	0.714	0.772	0.827	0.878	.	.	.
150	2	0.9993	99.6	-0.877	0.00190	0.226	0.298	0.356	0.406	0.450	0.491	0.563	0.626	0.684	0.738	0.787	0.834	0.878	.	.
150	2	0.9993	95.1	-0.839	0.00178	0.248	0.312	0.364	0.410	0.452	0.490	0.558	0.618	0.673	0.724	0.772	0.817	.	.	.
150	3	0.9998	103.0	-0.897	0.00193	0.223	0.297	0.356	0.407	0.452	0.492	0.565	0.630	0.688	0.742	0.792	0.839	0.884	.	.
150	3	0.9996	99.0	-0.887	0.00195	0.236	0.307	0.365	0.415	0.459	0.500	0.573	0.637	0.695	0.749	0.799	0.847	.	.	.
150	4	0.9997	116.3	-0.961	0.00196	0.221	0.297	0.357	0.408	0.454	0.495	0.569	0.634	0.693	0.748	0.799	0.847	0.892	0.935	.
150	4	0.9994	116.6	-0.924	0.00179	0.229	0.297	0.353	0.400	0.443	0.482	0.551	0.613	0.669	0.721	0.769	0.814	0.857	0.898	.
150	5	0.9996	108.1	-0.767	0.00135	0.179	0.243	0.293	0.336	0.374	0.409	0.470	0.524	0.573	0.619	0.661	0.701	0.738	.	.
150	5	0.9995	110.8	-0.778	0.00135	0.189	0.250	0.299	0.341	0.378	0.412	0.473	0.527	0.576	0.621	0.663	0.702	0.740	0.775	.
200	1	0.9991	95.1	-1.276	0.00421	0.331	0.441	0.528	0.602	0.668	0.729	0.836	0.932	1.018	1.098	1.172	1.242	.	.	.
200	1	0.9995	100.0	-1.264	0.00393	0.324	0.428	0.512	0.584	0.647	0.706	0.809	0.901	0.985	1.061	1.133	1.200	1.264	.	.
200	2	0.9995	100.7	-1.227	0.00369	0.308	0.410	0.492	0.562	0.624	0.681	0.782	0.871	0.952	1.026	1.096	1.161	1.223	.	.
200	2	0.9986	103.8	-1.226	0.00342	0.392	0.471	0.539	0.599	0.653	0.704	0.795	0.877	0.952	1.021	1.086	1.147	1.205	.	.
200	3	0.9997	103.4	-1.268	0.00380	0.336	0.434	0.514	0.584	0.645	0.702	0.803	0.893	0.974	1.049	1.119	1.185	1.248	.	.
200	3	0.9996	103.0	-1.307	0.00395	0.401	0.490	0.565	0.631	0.691	0.746	0.845	0.934	1.015	1.090	1.160	1.227	1.289	.	.
200	4	0.9995	123.0	-1.430	0.00409	0.340	0.444	0.528	0.601	0.665	0.724	0.829	0.923	1.007	1.086	1.158	1.227	1.292	1.354	1.413
200	4	0.9991	118.1	-1.389	0.00401	0.343	0.445	0.527	0.598	0.662	0.720	0.824	0.916	0.999	1.077	1.149	1.216	1.281	1.342	.
200	5	0.9991	110.4	-1.138	0.00281	0.330	0.406	0.470	0.527	0.578	0.624	0.709	0.784	0.853	0.917	0.976	1.032	1.085	1.136	.
200	5	0.9992	111.0	-1.111	0.00257	0.380	0.442	0.497	0.546	0.592	0.634	0.710	0.779	0.843	0.902	0.957	1.010	1.059	1.107	.
250	1	0.9961	104.8	-1.572	0.00528	0.602	0.684	0.757	0.824	0.886	0.944	1.049	1.146	1.234	1.317	1.395	1.469	1.539	.	.
250	1	0.9996	104.3	-1.643	0.00596	0.578	0.673	0.756	0.831	0.900	0.964	1.081	1.186	1.282	1.372	1.456	1.536	1.612	.	.
250	2	0.9985	100.1	-1.594	0.00601	0.505	0.613	0.704	0.785	0.858	0.925	1.047	1.156	1.256	1.348	1.434	1.516	1.593	.	.
250	2	0.9996	94.6	-1.503	0.00561	0.499	0.601	0.688	0.765	0.835	0.900	1.017	1.122	1.217	1.306	1.390	1.468	.	.	.
250	3	0.9984	107.4	-1.684	0.00624	0.529	0.636	0.727	0.809	0.882	0.950	1.074	1.184	1.285	1.379	1.467	1.549	1.628	.	.
250	3	0.9973	105.3	-1.690	0.00621	0.603	0.699	0.783	0.858	0.928	0.993	1.111	1.217	1.316	1.407	1.493	1.574	1.651	.	.
250	4	0.9996	115.8	-1.730	0.00633	0.435	0.562	0.665	0.754	0.834	0.906	1.037	1.152	1.257	1.354	1.445	1.530	1.610	1.687	.
250	4	0.9994	116.1	-1.752	0.00630	0.521	0.630	0.723	0.805	0.880	0.949	1.073	1.185	1.287	1.381	1.470	1.553	1.632	1.707	.
250	5	0.9983	112.1	-1.448	0.00433	0.489	0.571	0.643	0.707	0.766	0.820	0.920	1.010	1.092	1.169	1.241	1.309	1.373	1.435	.
250	5	0.9990	108.0	-1.429	0.00437	0.492	0.574	0.645	0.710	0.769	0.824	0.924	1.014	1.097	1.174	1.246	1.315	1.380	.	.

Appendix J. Coefficient of Determination, Parameter Estimates, and Drying Rates of Radially-cut 15x152 mm Sweetgum Flakes.

TEMP						DRYING RATE (%/SEC)														
(C)	REP	R^2	β_0	β_1	β_2	5	10	15	20	25	30	40	50	60	70	80	90	100	110	120
150	1	0.9995	107.5	-0.967	0.00217	0.212	0.298	0.363	0.419	0.468	0.512	0.591	0.660	0.723	0.781	0.835	0.885	0.933	.	.
150	1	0.9993	104.9	-0.914	0.00185	0.307	0.363	0.411	0.454	0.493	0.529	0.595	0.654	0.709	0.759	0.806	0.851	0.894	.	.
150	2	0.9991	111.0	-1.049	0.00242	0.273	0.351	0.414	0.469	0.518	0.563	0.643	0.714	0.779	0.839	0.895	0.947	0.997	1.044	.
150	2	0.9994	107.8	-1.021	0.00225	0.339	0.400	0.453	0.500	0.544	0.584	0.656	0.722	0.782	0.838	0.890	0.939	0.986	.	.
150	3	0.9982	110.9	-1.040	0.00237	0.277	0.352	0.414	0.468	0.516	0.560	0.639	0.710	0.774	0.833	0.888	0.940	0.989	1.036	.
150	3	0.9989	109.5	-1.025	0.00229	0.308	0.375	0.432	0.482	0.527	0.569	0.644	0.712	0.773	0.830	0.884	0.934	0.982	1.027	.
150	4	0.9993	110.4	-1.054	0.00246	0.267	0.347	0.412	0.468	0.518	0.564	0.645	0.718	0.783	0.844	0.900	0.954	1.004	1.052	.
150	4	0.9994	107.9	-1.029	0.00242	0.254	0.336	0.402	0.458	0.508	0.554	0.635	0.707	0.772	0.832	0.889	0.941	0.991	.	.
150	5	0.9996	112.3	-0.907	0.00180	0.222	0.292	0.348	0.397	0.440	0.479	0.549	0.611	0.667	0.719	0.768	0.813	0.857	0.898	.
150	5	0.9994	112.8	-0.892	0.00165	0.293	0.345	0.390	0.430	0.467	0.501	0.563	0.619	0.670	0.717	0.762	0.804	0.844	0.882	.
200	1	0.9991	110.4	-1.372	0.00407	0.409	0.498	0.574	0.641	0.702	0.758	0.858	0.948	1.031	1.107	1.178	1.245	1.309	1.370	.
200	1	0.9993	108.6	-1.356	0.00406	0.394	0.486	0.564	0.632	0.693	0.749	0.851	0.942	1.024	1.101	1.172	1.240	1.304	.	.
200	2	0.9986	113.0	-1.506	0.00478	0.450	0.546	0.628	0.700	0.765	0.825	0.934	1.031	1.120	1.202	1.279	1.352	1.421	1.487	.
200	2	0.9992	106.4	-1.456	0.00474	0.447	0.543	0.624	0.696	0.761	0.821	0.929	1.026	1.114	1.196	1.273	1.345	1.414	.	.
200	3	0.9985	116.2	-1.485	0.00449	0.455	0.545	0.622	0.690	0.753	0.810	0.914	1.008	1.093	1.173	1.247	1.317	1.384	1.447	.
200	3	0.9982	113.5	-1.471	0.00453	0.447	0.538	0.617	0.686	0.749	0.808	0.913	1.007	1.093	1.173	1.248	1.319	1.386	1.449	.
200	4	0.9993	108.6	-1.530	0.00517	0.445	0.549	0.637	0.713	0.782	0.846	0.960	1.062	1.156	1.242	1.323	1.399	1.471	.	.
200	4	0.9988	108.0	-1.517	0.00509	0.453	0.554	0.639	0.714	0.782	0.845	0.958	1.059	1.151	1.236	1.316	1.391	1.463	.	.
200	5	0.9993	111.5	-1.251	0.00321	0.446	0.513	0.572	0.625	0.675	0.721	0.805	0.881	0.951	1.016	1.078	1.136	1.191	1.243	.
200	5	0.9993	111.6	-1.265	0.00345	0.358	0.444	0.516	0.579	0.636	0.688	0.782	0.866	0.942	1.013	1.079	1.141	1.200	1.256	.
250	1	0.9991	110.6	-1.844	0.00733	0.553	0.672	0.774	0.863	0.944	1.019	1.154	1.274	1.385	1.487	1.582	1.672	1.758	1.839	.
250	1	0.9991	107.7	-1.872	0.00792	0.500	0.639	0.752	0.851	0.940	1.020	1.165	1.294	1.411	1.519	1.620	1.715	1.805	.	.
250	2	0.9982	115.5	-1.894	0.00699	0.704	0.797	0.881	0.957	1.027	1.093	1.214	1.324	1.426	1.521	1.610	1.695	1.776	1.853	.
250	2	0.9962	110.4	-1.825	0.00644	0.786	0.864	0.935	1.002	1.064	1.123	1.232	1.333	1.426	1.514	1.597	1.675	1.750	1.823	.
250	3	0.9975	119.1	-1.960	0.00772	0.564	0.687	0.792	0.884	0.967	1.044	1.183	1.307	1.420	1.525	1.623	1.716	1.803	1.887	1.967
250	3	0.9971	111.6	-1.920	0.00788	0.572	0.696	0.801	0.894	0.978	1.056	1.196	1.321	1.435	1.541	1.640	1.734	1.822	1.907	.
250	4	0.9982	115.5	-1.929	0.00733	0.696	0.795	0.882	0.961	1.035	1.103	1.229	1.343	1.448	1.546	1.638	1.725	1.808	1.887	.
250	4	0.9981	113.5	-1.919	0.00743	0.675	0.777	0.867	0.949	1.025	1.095	1.223	1.339	1.446	1.545	1.638	1.727	1.811	1.891	.
250	5	0.9981	110.8	-1.564	0.00471	0.672	0.739	0.800	0.857	0.911	0.961	1.055	1.140	1.220	1.295	1.366	1.434	1.498	1.560	.
250	5	0.9994	108.7	-1.658	0.00585	0.567	0.662	0.745	0.820	0.888	0.952	1.068	1.172	1.268	1.357	1.441	1.520	1.595	.	.

Appendix K. Coefficient of Determination, Parameter Estimates, and Drying Rates of Radially-cut 25x117 mm Sweetgum Flakes.

TEMP						DRYING RATE (%/SEC)												
(C)	REP	R^2	β_0	β_1	β_2	5	10	15	20	25	30	40	50	60	70	80	90	100
150	1	0.9995	83.5	-0.870	0.00215	0.286	0.353	0.410	0.459	0.504	0.545	0.618	0.684	0.744	0.800	0.852	.	.
150	1	0.9989	86.6	-0.857	0.00203	0.265	0.333	0.389	0.439	0.483	0.523	0.596	0.661	0.720	0.774	0.825	.	.
150	2	0.9993	89.4	-0.871	0.00210	0.220	0.301	0.364	0.418	0.465	0.509	0.586	0.654	0.715	0.772	0.824	.	.
150	2	0.9990	91.1	-0.882	0.00207	0.254	0.326	0.384	0.435	0.480	0.521	0.595	0.661	0.721	0.776	0.828	0.877	.
150	3	0.9993	94.0	-0.905	0.00218	0.206	0.294	0.360	0.416	0.466	0.511	0.590	0.660	0.723	0.781	0.835	0.885	.
150	3	0.9991	93.2	-0.901	0.00215	0.233	0.312	0.374	0.428	0.475	0.519	0.596	0.664	0.726	0.783	0.836	0.886	.
150	4	0.9995	95.8	-0.787	0.00154	0.246	0.302	0.349	0.391	0.428	0.463	0.525	0.581	0.631	0.678	0.722	0.764	.
150	4	0.9996	95.7	-0.812	0.00168	0.225	0.290	0.343	0.389	0.430	0.467	0.534	0.594	0.648	0.697	0.744	0.788	.
150	5	0.9988	95.0	-0.794	0.00158	0.249	0.306	0.354	0.396	0.434	0.469	0.532	0.589	0.640	0.688	0.732	0.774	.
150	5	0.9994	97.9	-0.805	0.00162	0.218	0.283	0.335	0.380	0.420	0.457	0.523	0.582	0.635	0.684	0.730	0.773	.
200	1	0.9994	86.9	-1.297	0.00461	0.413	0.513	0.596	0.669	0.735	0.795	0.904	1.001	1.089	1.170	1.247	.	.
200	1	0.9989	90.1	-1.293	0.00448	0.379	0.483	0.568	0.643	0.709	0.770	0.878	0.975	1.063	1.144	1.220	1.292	.
200	2	0.9987	98.1	-1.303	0.00431	0.302	0.421	0.513	0.591	0.660	0.723	0.833	0.931	1.019	1.101	1.176	1.247	.
200	2	0.9979	100.4	-1.340	0.00443	0.319	0.437	0.529	0.607	0.676	0.739	0.850	0.949	1.038	1.120	1.197	1.269	1.337
200	3	0.9983	95.1	-1.311	0.00444	0.345	0.456	0.545	0.621	0.688	0.750	0.860	0.958	1.046	1.128	1.204	1.276	.
200	3	0.9983	95.5	-1.283	0.00419	0.360	0.462	0.545	0.617	0.682	0.741	0.846	0.940	1.026	1.104	1.178	1.247	.
200	4	0.9988	101.9	-1.154	0.00307	0.379	0.453	0.516	0.573	0.624	0.671	0.757	0.834	0.905	0.970	1.031	1.089	1.144
200	4	0.9990	101.0	-1.178	0.00327	0.361	0.442	0.511	0.572	0.626	0.676	0.767	0.848	0.922	0.990	1.054	1.115	1.172
200	5	0.9988	97.2	-1.127	0.00317	0.319	0.407	0.478	0.540	0.596	0.647	0.739	0.820	0.894	0.962	1.026	1.086	.
200	5	0.9991	95.7	-1.124	0.00318	0.331	0.416	0.486	0.548	0.603	0.654	0.745	0.826	0.899	0.967	1.031	1.091	.
250	1	0.9991	86.8	-1.684	0.00778	0.537	0.667	0.774	0.869	0.954	1.033	1.174	1.300	1.414	1.520	1.619	.	.
250	1	0.9990	87.7	-1.729	0.00817	0.537	0.672	0.784	0.882	0.971	1.051	1.197	1.326	1.444	1.553	1.655	.	.
250	2	0.9968	96.2	-1.651	0.00680	0.495	0.618	0.719	0.808	0.889	0.962	1.095	1.212	1.320	1.419	1.512	1.600	.
250	2	0.9972	93.8	-1.681	0.00734	0.466	0.603	0.715	0.811	0.897	0.975	1.116	1.241	1.354	1.458	1.556	1.647	.
250	3	0.9980	96.2	-1.689	0.00724	0.462	0.599	0.709	0.805	0.890	0.968	1.108	1.232	1.344	1.448	1.545	1.636	.
250	3	0.9975	93.0	-1.627	0.00670	0.535	0.648	0.745	0.830	0.907	0.978	1.107	1.222	1.327	1.424	1.515	1.601	.
250	4	0.9992	102.4	-1.513	0.00526	0.491	0.589	0.672	0.746	0.814	0.876	0.989	1.090	1.182	1.268	1.349	1.424	.
250	4	0.9990	98.4	-1.479	0.00510	0.532	0.620	0.698	0.767	0.831	0.891	0.999	1.096	1.185	1.269	1.347	1.420	.
250	5	0.9972	100.2	-1.427	0.00458	0.540	0.619	0.689	0.753	0.811	0.866	0.966	1.056	1.140	1.217	1.290	1.359	.
250	5	0.9988	93.6	-1.462	0.00518	0.550	0.637	0.714	0.783	0.847	0.906	1.013	1.111	1.200	1.284	1.362	1.436	.

Appendix L. Coefficient of Determination, Parameter Estimates, and Drying Rates of Radially-cut 25x152 mm Sweetgum Flakes.

TEMP						DRYING RATE (%/SEC)												
(C)	REP	R^2	β_0	β_1	β_2	5	10	15	20	25	30	40	50	60	70	80	90	100
150	1	0.9990	90.6	-0.955	0.00250	0.240	0.328	0.397	0.455	0.507	0.554	0.638	0.712	0.779	0.841	0.898	0.952	.
150	1	0.9993	87.5	-0.909	0.00227	0.277	0.349	0.409	0.461	0.508	0.551	0.628	0.697	0.759	0.817	0.871	.	.
150	2	0.9994	88.9	-0.816	0.00185	0.215	0.289	0.347	0.396	0.441	0.481	0.552	0.615	0.673	0.726	0.775	.	.
150	2	0.9991	86.9	-0.805	0.00182	0.230	0.299	0.354	0.402	0.445	0.484	0.554	0.617	0.673	0.725	0.773	.	.
150	3	0.9986	94.0	-0.887	0.00195	0.301	0.360	0.411	0.456	0.497	0.535	0.604	0.665	0.722	0.774	0.823	0.869	.
150	3	0.9990	92.8	-0.914	0.00216	0.274	0.344	0.402	0.453	0.498	0.540	0.615	0.682	0.743	0.799	0.851	0.901	.
150	4	0.9988	91.5	-0.912	0.00215	0.299	0.364	0.418	0.467	0.511	0.551	0.624	0.690	0.749	0.805	0.856	0.905	.
150	4	0.9987	93.3	-0.927	0.00218	0.300	0.365	0.421	0.470	0.514	0.555	0.629	0.695	0.755	0.810	0.863	0.912	.
150	5	0.9989	97.4	-0.794	0.00158	0.213	0.278	0.330	0.374	0.415	0.451	0.516	0.574	0.627	0.675	0.721	0.763	.
150	5	0.9989	98.3	-0.789	0.00155	0.215	0.278	0.329	0.373	0.412	0.448	0.513	0.570	0.622	0.669	0.714	0.756	.
200	1	0.9995	89.5	-1.309	0.00448	0.450	0.540	0.617	0.686	0.748	0.806	0.910	1.004	1.089	1.169	1.243	1.313	.
200	1	0.9992	92.1	-1.362	0.00493	0.372	0.487	0.579	0.659	0.730	0.795	0.910	1.013	1.106	1.192	1.272	1.347	.
200	2	0.9994	88.1	-1.151	0.00365	0.333	0.429	0.507	0.574	0.635	0.690	0.788	0.876	0.956	1.029	1.098	.	.
200	2	0.9990	88.0	-1.181	0.00378	0.377	0.466	0.541	0.607	0.666	0.721	0.819	0.906	0.986	1.060	1.129	.	.
200	3	0.9982	89.6	-1.337	0.00478	0.412	0.515	0.601	0.676	0.743	0.805	0.916	1.015	1.106	1.189	1.267	1.340	.
200	3	0.9983	94.0	-1.310	0.00421	0.463	0.546	0.619	0.683	0.743	0.797	0.897	0.986	1.068	1.145	1.216	1.283	.
200	4	0.9976	98.8	-1.321	0.00407	0.470	0.550	0.619	0.682	0.739	0.792	0.889	0.976	1.056	1.130	1.200	1.266	.
200	4	0.9982	95.5	-1.328	0.00424	0.479	0.561	0.632	0.696	0.754	0.808	0.907	0.996	1.078	1.154	1.225	1.292	.
200	5	0.9982	102.8	-1.113	0.00285	0.350	0.424	0.486	0.542	0.592	0.638	0.722	0.797	0.866	0.930	0.989	1.045	1.098
200	5	0.9982	100.5	-1.132	0.00303	0.353	0.430	0.496	0.553	0.606	0.654	0.740	0.818	0.889	0.955	1.016	1.074	1.134
250	1	0.9973	93.1	-1.714	0.00711	0.660	0.760	0.848	0.928	1.002	1.070	1.196	1.309	1.414	1.511	1.602	1.689	.
250	1	0.9974	91.9	-1.693	0.00710	0.631	0.735	0.826	0.908	0.983	1.053	1.180	1.295	1.400	1.498	1.590	1.677	.
250	2	0.9993	89.9	-1.547	0.00630	0.503	0.616	0.711	0.794	0.870	0.940	1.065	1.178	1.280	1.375	1.464	1.548	.
250	2	0.9994	89.3	-1.529	0.00596	0.575	0.670	0.754	0.829	0.898	0.962	1.079	1.184	1.281	1.371	1.455	1.535	.
250	3	0.9987	88.7	-1.747	0.00782	0.659	0.769	0.865	0.951	1.030	1.103	1.237	1.358	1.468	1.571	1.668	.	.
250	3	0.9977	91.3	-1.755	0.00786	0.604	0.723	0.824	0.915	0.997	1.073	1.211	1.334	1.447	1.552	1.650	1.743	.
250	4	0.9980	94.6	-1.771	0.00763	0.634	0.745	0.841	0.927	1.006	1.079	1.213	1.332	1.442	1.544	1.640	1.731	.
250	4	0.9992	88.7	-1.825	0.00897	0.571	0.711	0.827	0.930	1.022	1.106	1.258	1.393	1.517	1.631	1.737	.	.
250	5	0.9979	98.5	-1.417	0.00462	0.531	0.612	0.683	0.748	0.807	0.862	0.963	1.055	1.139	1.217	1.291	1.361	.
250	5	0.9981	98.3	-1.414	0.00461	0.529	0.610	0.681	0.746	0.805	0.861	0.962	1.053	1.137	1.216	1.289	1.359	.

Appendix M. Coefficient of Determination, Parameter Estimates, and Drying Rates of Tangentially-cut 15x117 mm Sweetgum Flakes.

TEMP						DRYING RATE (%/SEC)												
(C)	REP	R^2	β_0	β_1	β_2	5	10	15	20	25	30	40	50	60	70	80	90	100
150	1	0.9985	109.5	-1.000	0.00209	0.356	0.410	0.459	0.502	0.542	0.579	0.647	0.709	0.766	0.818	0.868	0.915	0.959
150	1	0.9989	105.5	-1.003	0.00220	0.345	0.404	0.455	0.501	0.544	0.583	0.654	0.718	0.777	0.832	0.884	0.932	0.978
150	2	0.9996	99.6	-1.019	0.00249	0.310	0.382	0.442	0.496	0.544	0.588	0.667	0.738	0.803	0.862	0.918	0.971	1.021
150	2	0.9995	97.6	-0.973	0.00217	0.376	0.430	0.478	0.521	0.562	0.599	0.668	0.730	0.787	0.841	0.891	0.938	.
150	3	0.9985	89.6	-0.907	0.00223	0.262	0.337	0.397	0.450	0.497	0.540	0.617	0.685	0.747	0.805	0.858	0.909	.
150	3	0.9994	88.7	-0.976	0.00271	0.215	0.316	0.393	0.456	0.512	0.563	0.652	0.730	0.801	0.866	0.926	.	.
150	4	0.9992	84.0	-0.986	0.00286	0.260	0.353	0.427	0.489	0.544	0.595	0.684	0.763	0.835	0.900	0.962	.	.
150	4	0.9994	87.4	-0.982	0.00268	0.286	0.368	0.435	0.493	0.544	0.591	0.676	0.751	0.819	0.882	0.941	.	.
150	5	0.9993	93.6	-0.938	0.00241	0.158	0.271	0.349	0.412	0.467	0.516	0.602	0.678	0.745	0.808	0.865	0.919	.
150	5	0.9990	92.3	-0.863	0.00203	0.189	0.276	0.342	0.397	0.445	0.489	0.566	0.633	0.694	0.751	0.803	0.852	.
200	1	0.9982	109.0	-1.538	0.00519	0.455	0.557	0.644	0.720	0.789	0.852	0.966	1.068	1.161	1.248	1.328	1.404	1.476
200	1	0.9988	92.8	-1.356	0.00478	0.400	0.506	0.593	0.669	0.737	0.799	0.911	1.010	1.101	1.184	1.262	1.336	.
200	2	0.9996	98.8	-1.357	0.00432	0.470	0.554	0.627	0.693	0.753	0.808	0.909	0.999	1.083	1.160	1.232	1.300	.
200	2	0.9994	104.3	-1.333	0.00407	0.402	0.493	0.569	0.637	0.698	0.754	0.855	0.945	1.028	1.104	1.175	1.242	1.306
200	3	0.9988	93.8	-1.455	0.00565	0.331	0.472	0.580	0.670	0.750	0.822	0.949	1.062	1.163	1.257	1.344	1.425	.
200	3	0.9984	100.4	-1.571	0.00611	0.375	0.512	0.620	0.712	0.793	0.867	0.998	1.113	1.218	1.315	1.404	1.489	1.569
200	4	0.9995	95.9	-1.476	0.00564	0.361	0.493	0.596	0.684	0.762	0.833	0.959	1.070	1.170	1.263	1.349	1.430	.
200	4	0.9973	96.3	-1.434	0.00515	0.422	0.530	0.619	0.698	0.768	0.832	0.948	1.051	1.145	1.231	1.312	1.388	.
200	5	0.9993	90.8	-1.226	0.00400	0.364	0.461	0.540	0.610	0.672	0.729	0.832	0.923	1.006	1.082	1.154	1.221	.
200	5	0.9993	91.8	-1.268	0.00427	0.353	0.459	0.544	0.617	0.683	0.743	0.850	0.945	1.032	1.111	1.186	1.256	.
250	1	0.9993	89.1	-1.892	0.01002	0.458	0.640	0.781	0.900	1.006	1.101	1.270	1.419	1.554	1.678	1.793	1.902	.
250	1	0.9971	93.1	-1.823	0.00884	0.456	0.620	0.749	0.859	0.957	1.045	1.202	1.341	1.467	1.583	1.691	1.793	.
250	2	0.9992	100.4	-1.661	0.00654	0.513	0.628	0.725	0.810	0.887	0.958	1.086	1.200	1.305	1.401	1.492	1.577	1.658
250	2	0.9981	106.6	-1.797	0.00719	0.556	0.673	0.772	0.860	0.940	1.014	1.147	1.266	1.375	1.476	1.570	1.659	1.744
250	3	0.9994	98.5	-1.941	0.00950	0.467	0.639	0.773	0.887	0.989	1.081	1.244	1.388	1.519	1.639	1.751	1.857	.
250	3	0.9977	101.1	-1.854	0.00850	0.411	0.582	0.713	0.824	0.921	1.010	1.166	1.304	1.428	1.543	1.649	1.749	1.844
250	4	0.9982	100.6	-2.075	0.01057	0.515	0.690	0.830	0.948	1.054	1.150	1.321	1.472	1.610	1.736	1.854	1.964	2.069
250	4	0.9990	93.0	-2.000	0.01063	0.506	0.685	0.825	0.945	1.052	1.149	1.321	1.473	1.611	1.738	1.856	1.967	.
250	5	0.9995	93.5	-1.750	0.00788	0.522	0.656	0.767	0.863	0.950	1.030	1.173	1.300	1.416	1.523	1.624	1.718	.
250	5	0.9992	88.7	-1.645	0.00732	0.506	0.634	0.741	0.834	0.917	0.994	1.132	1.254	1.366	1.469	1.566	.	.

Appendix N. Coefficient of Determination, Parameter Estimates, and Drying Rates of Tangentially-cut 15x152 mm Sweetgum Flakes.

TEMP						DRYING RATE (%/SEC)													
(C)	REP	R^2	β_0	β_1	β_2	5	10	15	20	25	30	40	50	60	70	80	90	100	110
150	1	0.9981	91.4	-1.035	0.00281	0.316	0.395	0.461	0.518	0.570	0.617	0.702	0.778	0.847	0.911	0.971	1.027	.	.
150	1	0.9991	86.4	-1.089	0.00338	0.296	0.394	0.472	0.539	0.598	0.652	0.749	0.834	0.911	0.983	1.049	.	.	.
150	2	0.9987	80.6	-1.117	0.00389	0.267	0.386	0.477	0.552	0.619	0.679	0.785	0.878	0.963	1.040	1.113	.	.	.
150	2	0.9983	90.2	-1.126	0.00341	0.326	0.418	0.493	0.557	0.616	0.669	0.764	0.848	0.925	0.996	1.062	1.125	.	.
150	3	0.9991	83.2	-1.199	0.00417	0.365	0.465	0.548	0.619	0.683	0.742	0.847	0.940	1.025	1.103	1.177	.	.	.
150	3	0.9982	94.4	-1.187	0.00347	0.409	0.486	0.553	0.613	0.667	0.717	0.808	0.890	0.965	1.034	1.100	1.161	.	.
150	4	0.9991	107.1	-0.959	0.00205	0.286	0.350	0.405	0.453	0.496	0.536	0.608	0.672	0.730	0.784	0.835	0.883	0.928	.
150	4	0.9981	119.1	-0.982	0.00195	0.271	0.335	0.389	0.436	0.479	0.518	0.589	0.652	0.709	0.762	0.812	0.859	0.903	0.945
150	5	0.9992	86.1	-0.911	0.00230	0.293	0.363	0.422	0.473	0.519	0.562	0.638	0.707	0.769	0.826	0.880	.	.	.
150	5	0.9986	116.3	-0.941	0.00181	0.284	0.342	0.391	0.435	0.475	0.511	0.578	0.637	0.692	0.742	0.789	0.834	0.876	0.916
200	1	0.9983	84.3	-1.464	0.00600	0.490	0.600	0.693	0.775	0.849	0.917	1.039	1.149	1.249	1.342	1.428	.	.	.
200	1	0.9983	82.7	-1.482	0.00638	0.460	0.583	0.684	0.771	0.850	0.922	1.052	1.167	1.271	1.368	1.459	.	.	.
200	2	0.9988	82.1	-1.567	0.00725	0.469	0.604	0.714	0.809	0.894	0.972	1.111	1.235	1.347	1.451	1.547	.	.	.
200	2	0.9974	85.9	-1.475	0.00592	0.511	0.616	0.706	0.785	0.857	0.924	1.044	1.152	1.250	1.342	1.427	.	.	.
200	3	0.9969	104.7	-1.819	0.00775	0.468	0.611	0.727	0.827	0.916	0.997	1.142	1.270	1.387	1.495	1.595	1.689	1.779	.
200	3	0.9983	99.5	-1.713	0.00707	0.510	0.634	0.737	0.827	0.909	0.983	1.118	1.238	1.347	1.449	1.543	1.632	1.717	.
200	4	0.9988	111.1	-1.418	0.00451	0.307	0.430	0.524	0.604	0.675	0.739	0.852	0.952	1.043	1.126	1.203	1.276	1.345	1.411
200	4	0.9989	107.9	-1.382	0.00419	0.429	0.517	0.593	0.660	0.720	0.776	0.878	0.969	1.052	1.129	1.201	1.268	1.333	.
200	5	0.9992	104.6	-1.405	0.00460	0.378	0.485	0.572	0.647	0.715	0.776	0.887	0.985	1.074	1.157	1.234	1.306	1.375	.
200	5	0.9990	95.3	-1.295	0.00412	0.436	0.522	0.596	0.661	0.721	0.776	0.876	0.965	1.047	1.123	1.194	1.261	.	.
250	1	0.9990	79.6	-1.982	0.01234	0.500	0.705	0.862	0.995	1.112	1.218	1.406	1.572	1.722	1.860	1.988	.	.	.
250	1	0.9985	79.9	-1.984	0.01227	0.511	0.712	0.867	0.999	1.115	1.220	1.407	1.571	1.720	1.858	1.985	.	.	.
250	2	0.9987	82.5	-2.039	0.01251	0.526	0.726	0.881	1.014	1.130	1.236	1.424	1.590	1.741	1.879	2.008	.	.	.
250	2	0.9949	86.5	-2.009	0.01154	0.525	0.711	0.858	0.984	1.095	1.195	1.375	1.534	1.677	1.810	1.933	.	.	.
250	3	0.9990	107.4	-2.227	0.01129	0.580	0.750	0.888	1.007	1.113	1.211	1.385	1.539	1.679	1.809	1.930	2.043	2.151	.
250	3	0.9949	116.3	-2.415	0.01243	0.545	0.739	0.891	1.021	1.136	1.241	1.427	1.592	1.741	1.879	2.007	2.127	2.241	2.349
250	4	0.9976	110.2	-1.823	0.00711	0.575	0.688	0.784	0.870	0.948	1.021	1.152	1.269	1.377	1.476	1.570	1.658	1.741	1.821
250	4	0.9987	98.8	-1.790	0.00783	0.518	0.652	0.762	0.859	0.946	1.025	1.168	1.295	1.411	1.518	1.618	1.712	.	.
250	5	0.9995	94.0	-1.818	0.00861	0.486	0.639	0.762	0.868	0.962	1.047	1.201	1.336	1.460	1.573	1.679	1.779	.	.
250	5	0.9993	99.1	-1.926	0.00932	0.446	0.621	0.756	0.871	0.972	1.063	1.226	1.370	1.500	1.619	1.730	1.835	1.934	.

Appendix O. Coefficient of Determination, Parameter Estimates, and Drying Rates of Tangentially-cut 25x117 mm Sweetgum Flakes.

TEMP						DRYING RATE (%/SEC)												
(C)	REP	R^2	β_0	β_1	β_2	5	10	15	20	25	30	40	50	60	70	80	90	100
150	1	0.9992	87.1	-0.803	0.00163	0.332	0.378	0.418	0.456	0.490	0.522	0.581	0.635	0.684	0.730	0.774	.	.
150	1	0.9994	87.5	-0.794	0.00167	0.283	0.336	0.383	0.424	0.462	0.497	0.560	0.617	0.669	0.717	0.762	.	.
150	2	0.9984	100.8	-0.906	0.00195	0.269	0.334	0.388	0.435	0.478	0.517	0.588	0.651	0.708	0.761	0.811	0.858	0.902
150	2	0.9986	95.5	-0.883	0.00189	0.307	0.364	0.413	0.456	0.496	0.533	0.599	0.660	0.715	0.766	0.814	0.859	.
150	3	0.9985	102.2	-0.885	0.00179	0.296	0.351	0.399	0.442	0.480	0.516	0.582	0.640	0.694	0.744	0.790	0.834	0.876
150	3	0.9989	96.5	-0.876	0.00178	0.340	0.389	0.432	0.472	0.508	0.542	0.604	0.661	0.713	0.761	0.806	0.849	.
150	4	0.9990	102.2	-0.910	0.00201	0.216	0.295	0.357	0.409	0.456	0.498	0.573	0.639	0.699	0.755	0.806	0.855	0.900
150	4	0.9989	97.3	-0.893	0.00197	0.261	0.328	0.384	0.432	0.476	0.516	0.587	0.651	0.709	0.763	0.813	0.860	.
150	5	0.9990	93.3	-0.804	0.00170	0.217	0.285	0.339	0.386	0.428	0.466	0.534	0.594	0.649	0.699	0.746	0.790	.
150	5	0.9983	94.6	-0.801	0.00164	0.232	0.294	0.346	0.390	0.430	0.467	0.532	0.591	0.644	0.693	0.739	0.782	.
200	1	0.9988	94.1	-1.199	0.00370	0.349	0.443	0.519	0.586	0.646	0.701	0.800	0.887	0.967	1.041	1.109	1.174	.
200	1	0.9990	97.4	-1.212	0.00345	0.442	0.514	0.577	0.634	0.687	0.735	0.824	0.903	0.977	1.045	1.109	1.170	.
200	2	0.9977	102.2	-1.293	0.00375	0.463	0.538	0.603	0.663	0.717	0.768	0.860	0.943	1.019	1.091	1.157	1.220	1.280
200	2	0.9984	105.4	-1.248	0.00332	0.475	0.540	0.599	0.652	0.701	0.747	0.831	0.907	0.978	1.043	1.105	1.163	1.219
200	3	0.9994	96.6	-1.239	0.00361	0.461	0.534	0.598	0.655	0.708	0.758	0.848	0.929	1.004	1.073	1.139	1.200	.
200	3	0.9989	94.3	-1.218	0.00356	0.459	0.531	0.595	0.652	0.704	0.753	0.842	0.923	0.997	1.066	1.131	1.192	.
200	4	0.9988	98.5	-1.327	0.00415	0.458	0.541	0.613	0.678	0.736	0.791	0.889	0.978	1.060	1.136	1.206	1.273	.
200	4	0.9985	98.8	-1.374	0.00464	0.385	0.491	0.577	0.653	0.720	0.782	0.893	0.991	1.081	1.163	1.241	1.313	.
200	5	0.9988	90.4	-1.109	0.00314	0.397	0.469	0.532	0.588	0.639	0.687	0.773	0.850	0.921	0.987	1.049	1.107	.
200	5	0.9989	93.7	-1.113	0.00314	0.350	0.431	0.498	0.558	0.611	0.661	0.750	0.830	0.902	0.969	1.032	1.091	.
250	1	0.9990	98.5	-1.511	0.00522	0.576	0.660	0.735	0.803	0.866	0.924	1.031	1.127	1.216	1.299	1.377	1.451	.
250	1	0.9989	94.1	-1.543	0.00580	0.562	0.657	0.740	0.815	0.883	0.946	1.062	1.166	1.261	1.350	1.433	1.512	.
250	2	0.9972	104.4	-1.624	0.00584	0.564	0.659	0.743	0.817	0.886	0.950	1.065	1.170	1.266	1.355	1.438	1.517	1.592
250	2	0.9987	100.8	-1.759	0.00741	0.504	0.634	0.742	0.836	0.921	0.998	1.137	1.260	1.373	1.477	1.574	1.666	1.753
250	3	0.9966	99.5	-1.552	0.00542	0.600	0.684	0.759	0.828	0.891	0.949	1.057	1.155	1.246	1.330	1.409	1.484	1.555
250	3	0.9991	89.8	-1.583	0.00513	0.875	0.932	0.985	1.036	1.084	1.131	1.218	1.300	1.376	1.449	1.518	1.584	.
250	4	0.9991	97.6	-1.812	0.00775	0.643	0.754	0.851	0.937	1.017	1.090	1.224	1.345	1.456	1.558	1.655	1.746	.
250	4	0.9993	97.1	-1.929	0.00882	0.688	0.806	0.909	1.001	1.086	1.164	1.307	1.435	1.553	1.663	1.766	1.863	.
250	5	0.9989	96.7	-1.489	0.00568	0.364	0.496	0.600	0.688	0.766	0.837	0.963	1.075	1.176	1.269	1.355	1.437	.
250	5	0.9970	101.9	-1.501	0.00533	0.432	0.542	0.633	0.712	0.783	0.849	0.966	1.071	1.166	1.254	1.337	1.414	1.488

Appendix P. Coefficient of Determination, Parameter Estimates, and Drying Rates of Tangentially-cut 25x152 mm Sweetgum Flakes.

TEMP						DRYING RATE (%/SEC)												
(C)	REP	R^2	β_0	β_1	β_2	5	10	15	20	25	30	40	50	60	70	80	90	100
150	1	0.9990	97.0	-0.770	0.00143	0.256	0.307	0.350	0.389	0.424	0.457	0.516	0.568	0.617	0.662	0.704	0.743	.
150	1	0.9987	96.9	-0.758	0.00137	0.264	0.312	0.353	0.390	0.424	0.455	0.512	0.563	0.610	0.653	0.694	0.732	.
150	2	0.9985	100.3	-0.842	0.00168	0.258	0.316	0.366	0.409	0.449	0.485	0.550	0.608	0.661	0.710	0.756	0.799	0.840
150	2	0.9989	100.2	-0.856	0.00170	0.289	0.343	0.390	0.431	0.469	0.504	0.568	0.625	0.677	0.726	0.771	0.814	0.855
150	3	0.9982	99.1	-0.933	0.00206	0.307	0.368	0.421	0.467	0.509	0.548	0.619	0.682	0.740	0.794	0.845	0.892	.
150	3	0.9989	95.1	-0.948	0.00222	0.315	0.379	0.433	0.482	0.526	0.566	0.640	0.706	0.766	0.822	0.874	0.923	.
150	4	0.9987	102.6	-0.822	0.00152	0.285	0.334	0.377	0.415	0.450	0.483	0.542	0.596	0.645	0.691	0.734	0.774	0.812
150	4	0.9988	100.8	-0.810	0.00148	0.297	0.343	0.384	0.421	0.455	0.486	0.544	0.596	0.644	0.688	0.730	0.770	0.807
150	5	0.9981	91.6	-0.856	0.00198	0.219	0.296	0.356	0.408	0.454	0.496	0.570	0.636	0.695	0.750	0.801	0.849	.
150	5	0.9983	90.7	-0.812	0.00176	0.234	0.300	0.354	0.401	0.442	0.481	0.549	0.610	0.665	0.716	0.764	0.809	.
200	1	0.9988	102.8	-1.155	0.00295	0.423	0.488	0.545	0.597	0.644	0.688	0.769	0.843	0.910	0.973	1.032	1.087	1.140
200	1	0.9985	104.9	-1.169	0.00302	0.400	0.469	0.530	0.584	0.634	0.680	0.763	0.839	0.908	0.972	1.032	1.089	1.143
200	2	0.9979	101.1	-1.206	0.00341	0.381	0.462	0.530	0.591	0.646	0.697	0.788	0.871	0.946	1.015	1.080	1.141	1.200
200	2	0.9990	98.4	-1.169	0.00311	0.452	0.516	0.574	0.626	0.673	0.718	0.800	0.875	0.943	1.007	1.067	1.124	.
200	3	0.9986	94.4	-1.350	0.00455	0.441	0.534	0.614	0.684	0.747	0.806	0.912	1.007	1.094	1.174	1.249	1.320	.
200	3	0.9984	96.5	-1.377	0.00459	0.464	0.554	0.632	0.701	0.763	0.821	0.926	1.020	1.107	1.187	1.262	1.332	.
200	4	0.9983	104.9	-1.161	0.00294	0.417	0.482	0.540	0.592	0.639	0.684	0.765	0.838	0.906	0.968	1.027	1.083	1.136
200	4	0.9980	101.3	-1.185	0.00323	0.402	0.475	0.539	0.596	0.648	0.696	0.783	0.862	0.933	1.000	1.063	1.122	1.178
200	5	0.9988	90.3	-1.144	0.00342	0.375	0.457	0.527	0.588	0.644	0.695	0.787	0.870	0.945	1.015	1.080	1.142	.
200	5	0.9981	94.3	-1.157	0.00325	0.421	0.492	0.554	0.610	0.661	0.709	0.795	0.873	0.945	1.012	1.074	1.133	.
250	1	0.9993	98.9	-1.554	0.00560	0.556	0.649	0.731	0.804	0.871	0.933	1.046	1.148	1.242	1.329	1.411	1.488	.
250	1	0.9980	100.8	-1.560	0.00576	0.476	0.585	0.676	0.757	0.829	0.896	1.016	1.124	1.222	1.313	1.398	1.478	1.554
250	2	0.9993	96.9	-1.531	0.00533	0.619	0.700	0.772	0.838	0.900	0.957	1.063	1.159	1.248	1.330	1.408	1.482	.
250	2	0.9987	96.3	-1.602	0.00630	0.517	0.627	0.720	0.803	0.878	0.947	1.072	1.183	1.286	1.380	1.468	1.552	.
250	3	0.9978	97.6	-1.835	0.00787	0.671	0.780	0.875	0.961	1.039	1.113	1.246	1.367	1.477	1.580	1.677	1.769	.
250	3	0.9954	99.8	-1.831	0.00778	0.635	0.747	0.845	0.932	1.012	1.086	1.221	1.343	1.454	1.557	1.654	1.745	1.832
250	4	0.9987	95.8	-1.512	0.00553	0.529	0.625	0.708	0.782	0.850	0.912	1.026	1.129	1.223	1.310	1.392	1.469	.
250	4	0.9982	100.7	-1.526	0.00531	0.544	0.634	0.713	0.784	0.849	0.909	1.019	1.119	1.210	1.295	1.374	1.449	1.521
250	5	0.9989	96.2	-1.475	0.00444	0.744	0.802	0.855	0.906	0.954	0.999	1.084	1.163	1.238	1.307	1.374	1.437	.
250	5	0.9986	97.1	-1.574	0.00566	0.628	0.712	0.788	0.857	0.920	0.980	1.089	1.189	1.280	1.366	1.447	1.523	.

Appendix Q. Coefficient of Determinatin, Parameter Estimates, and Drying Rates of Radially-cut 15x117 mm Yellow-poplar Flakes.

TEMP						DRYING RATE (%/SEC)										
(C)	REP	R^2	β_0	β_1	β_2	5	10	15	20	25	30	40	50	60	70	80
150	1	0.9995	82.6	-0.643	0.00127	0.142	0.213	0.266	0.310	0.348	0.383	0.444	0.498	0.547	0.591	0.632
150	1	0.9995	78.7	-0.680	0.00149	0.152	0.230	0.288	0.335	0.377	0.415	0.481	0.540	0.593	0.641	.
150	2	0.9996	78.6	-0.658	0.00141	0.129	0.212	0.270	0.318	0.360	0.397	0.463	0.521	0.572	0.620	.
150	2	0.9997	79.7	-0.695	0.00153	0.159	0.236	0.294	0.342	0.384	0.422	0.489	0.548	0.602	0.650	0.696
150	3	0.9997	81.7	-0.667	0.00140	0.127	0.210	0.268	0.316	0.358	0.395	0.461	0.518	0.569	0.617	0.660
150	3	0.9998	82.4	-0.706	0.00152	0.170	0.243	0.299	0.346	0.387	0.425	0.491	0.549	0.602	0.650	0.695
150	4	0.9995	79.8	-0.759	0.00179	0.202	0.277	0.335	0.385	0.429	0.469	0.540	0.602	0.659	0.711	0.760
150	4	0.9998	82.9	-0.799	0.00189	0.220	0.294	0.353	0.403	0.447	0.488	0.560	0.624	0.682	0.736	0.785
150	5	0.9996	82.1	-0.795	0.00192	0.199	0.279	0.341	0.394	0.440	0.481	0.556	0.621	0.680	0.734	0.785
150	5	0.9996	86.8	-0.815	0.00191	0.201	0.280	0.341	0.393	0.439	0.481	0.554	0.619	0.678	0.732	0.782
200	1	0.9993	81.1	-0.976	0.00285	0.293	0.378	0.447	0.507	0.560	0.609	0.696	0.774	0.844	0.909	0.970
200	1	0.9990	79.6	-0.986	0.00299	0.284	0.375	0.448	0.510	0.566	0.616	0.707	0.787	0.859	0.926	0.989
200	2	0.9995	82.9	-0.969	0.00283	0.238	0.337	0.412	0.476	0.532	0.583	0.673	0.753	0.824	0.890	0.952
200	2	0.9994	79.7	-1.009	0.00322	0.239	0.348	0.431	0.500	0.561	0.615	0.712	0.798	0.875	0.945	1.011
200	3	0.9989	81.8	-1.062	0.00339	0.299	0.396	0.474	0.541	0.600	0.654	0.750	0.836	0.913	0.985	1.051
200	3	0.9988	83.1	-1.073	0.00340	0.299	0.397	0.475	0.542	0.601	0.655	0.752	0.838	0.915	0.987	1.053
200	4	0.9996	88.5	-1.103	0.00339	0.291	0.391	0.470	0.537	0.597	0.651	0.748	0.834	0.911	0.983	1.050
200	4	0.9997	87.3	-1.103	0.00345	0.283	0.386	0.467	0.536	0.597	0.652	0.750	0.837	0.916	0.988	1.056
200	5	0.9995	88.3	-1.146	0.00363	0.325	0.422	0.500	0.568	0.629	0.684	0.783	0.871	0.950	1.024	1.092
200	5	0.9997	86.5	-1.207	0.00422	0.284	0.406	0.500	0.578	0.647	0.709	0.820	0.917	1.005	1.085	1.161
250	1	0.9994	74.8	-1.339	0.00582	0.410	0.533	0.633	0.719	0.796	0.866	0.991	1.102	1.203	1.296	.
250	1	0.9982	78.0	-1.368	0.00587	0.396	0.524	0.626	0.714	0.792	0.863	0.990	1.102	1.204	1.298	.
250	2	0.9989	81.6	-1.411	0.00598	0.396	0.526	0.630	0.719	0.797	0.869	0.998	1.111	1.214	1.309	1.397
250	2	0.9992	82.4	-1.272	0.00484	0.344	0.464	0.559	0.640	0.711	0.776	0.892	0.995	1.088	1.174	1.253
250	3	0.9997	85.1	-1.379	0.00544	0.395	0.515	0.611	0.695	0.769	0.837	0.958	1.066	1.163	1.254	1.338
250	3	0.9995	81.3	-1.402	0.00581	0.440	0.556	0.653	0.736	0.811	0.880	1.003	1.113	1.213	1.305	1.391
250	4	0.9993	89.2	-1.471	0.00578	0.466	0.577	0.670	0.751	0.825	0.892	1.013	1.122	1.220	1.312	1.397
250	4	0.9995	85.0	-1.576	0.00708	0.467	0.600	0.708	0.802	0.886	0.962	1.100	1.222	1.332	1.435	1.530
250	5	0.9996	83.3	-1.561	0.00711	0.454	0.591	0.701	0.796	0.881	0.958	1.097	1.220	1.331	1.434	1.530
250	5	0.9989	86.7	-1.686	0.00801	0.472	0.619	0.737	0.839	0.929	1.012	1.160	1.290	1.409	1.519	1.621

Appendix R. Coefficient of Determination, Parameter Estimates, and Drying Rates of Radially-cut 15x152 mm Yellow-poplar Flakes.

TEMP						DRYING RATE (%/SEC)									
(C)	REP	R^2	β_0	β_1	β_2	5	10	15	20	25	30	40	50	60	70
150	1	0.9998	62.2	-0.743	0.00227	0.182	0.280	0.352	0.411	0.463	0.510	0.592	0.665	0.730	.
150	1	0.9995	68.8	-0.784	0.00220	0.230	0.311	0.375	0.430	0.479	0.523	0.601	0.670	0.733	.
150	2	0.9997	72.1	-0.804	0.00227	0.194	0.288	0.358	0.417	0.468	0.514	0.596	0.668	0.733	0.792
150	2	0.9997	73.2	-0.773	0.00203	0.208	0.290	0.353	0.406	0.453	0.496	0.572	0.639	0.700	0.755
150	3	0.9997	63.0	-0.744	0.00224	0.189	0.283	0.354	0.412	0.463	0.509	0.591	0.662	0.726	.
150	3	0.9993	73.2	-0.783	0.00206	0.227	0.305	0.366	0.419	0.465	0.508	0.583	0.650	0.711	0.766
150	4	0.9998	70.0	-0.794	0.00231	0.177	0.279	0.352	0.412	0.465	0.512	0.595	0.668	0.734	0.795
150	4	0.9995	75.7	-0.747	0.00186	0.183	0.266	0.328	0.381	0.427	0.468	0.542	0.606	0.665	0.718
150	5	0.9994	72.0	-0.801	0.00223	0.207	0.296	0.364	0.421	0.471	0.516	0.596	0.667	0.731	0.790
150	5	0.9995	78.1	-0.792	0.00204	0.174	0.267	0.334	0.391	0.440	0.484	0.562	0.630	0.692	0.749
200	1	0.9997	73.0	-1.094	0.00408	0.294	0.410	0.500	0.576	0.643	0.703	0.811	0.906	0.992	1.071
200	1	0.9982	74.4	-1.174	0.00455	0.339	0.454	0.545	0.623	0.692	0.755	0.867	0.967	1.057	1.140
200	2	0.9980	77.8	-1.090	0.00378	0.298	0.405	0.489	0.561	0.625	0.683	0.786	0.876	0.959	1.034
200	2	0.9980	77.9	-1.110	0.00375	0.372	0.462	0.537	0.603	0.662	0.717	0.815	0.902	0.982	1.056
200	3	0.9995	75.6	-1.206	0.00476	0.331	0.453	0.548	0.629	0.700	0.765	0.881	0.983	1.076	1.161
200	3	0.9997	72.0	-1.099	0.00421	0.281	0.404	0.497	0.576	0.645	0.707	0.818	0.915	1.003	1.084
200	4	0.9995	73.3	-1.112	0.00423	0.285	0.407	0.500	0.579	0.648	0.710	0.821	0.918	1.006	1.087
200	4	0.9996	75.7	-1.066	0.00378	0.256	0.375	0.465	0.541	0.607	0.666	0.771	0.864	0.947	1.024
200	5	0.9996	79.0	-1.157	0.00433	0.240	0.379	0.480	0.563	0.635	0.700	0.815	0.915	1.005	1.088
200	5	0.9993	79.1	-1.132	0.00408	0.267	0.391	0.484	0.562	0.631	0.693	0.802	0.898	0.985	1.064
250	1	0.9974	76.2	-1.582	0.00803	0.465	0.614	0.733	0.836	0.927	1.010	1.158	1.289	1.409	1.518
250	1	0.9980	74.8	-1.529	0.00739	0.525	0.651	0.756	0.848	0.931	1.007	1.145	1.267	1.379	1.482
250	2	0.9994	64.9	-1.507	0.00861	0.453	0.614	0.741	0.850	0.945	1.033	1.188	1.325	1.449	.
250	2	0.9990	73.3	-1.430	0.00691	0.395	0.543	0.658	0.756	0.842	0.921	1.060	1.184	1.295	1.398
250	3	0.9996	78.5	-1.442	0.00668	0.341	0.500	0.619	0.719	0.806	0.885	1.025	1.148	1.259	1.361
250	3	0.9986	77.4	-1.507	0.00721	0.427	0.571	0.686	0.784	0.871	0.950	1.092	1.217	1.330	1.434
250	4	0.9995	75.2	-1.524	0.00779	0.368	0.540	0.669	0.776	0.871	0.956	1.107	1.240	1.360	1.470
250	4	0.9998	69.2	-1.507	0.00816	0.423	0.585	0.711	0.817	0.912	0.997	1.149	1.283	1.405	.
250	5	0.9989	77.8	-1.605	0.00815	0.448	0.603	0.726	0.831	0.924	1.008	1.158	1.292	1.412	1.523
250	5	0.9996	77.1	-1.433	0.00660	0.388	0.532	0.644	0.739	0.824	0.900	1.037	1.157	1.266	1.366

Appendix S. Coefficient of Determinatin, Parameter Estimates, and Drying Rates of Radially-cut 25x117 Yellow-poplar Flakes.

TEMP						DRYING RATE (%/SEC)										
(C)	REP	R^2	β_0	β_1	β_2	5	10	15	20	25	30	40	50	60	70	80
150	1	0.9993	74.1	-0.710	0.00172	0.170	0.251	0.312	0.363	0.408	0.448	0.519	0.582	0.638	0.690	.
150	1	0.9994	75.9	-0.698	0.00157	0.203	0.270	0.323	0.368	0.409	0.446	0.511	0.570	0.622	0.671	.
150	2	0.9996	69.8	-0.785	0.00224	0.184	0.280	0.351	0.410	0.462	0.508	0.590	0.661	0.726	0.786	.
150	2	0.9995	77.6	-0.789	0.00201	0.194	0.279	0.344	0.398	0.446	0.489	0.565	0.633	0.693	0.749	.
150	3	0.9993	70.1	-0.782	0.00217	0.215	0.299	0.365	0.420	0.469	0.513	0.591	0.661	0.723	0.781	.
150	3	0.9996	75.5	-0.767	0.00194	0.201	0.282	0.344	0.396	0.442	0.484	0.559	0.624	0.684	0.738	.
150	4	0.9996	75.6	-0.722	0.00172	0.183	0.261	0.320	0.370	0.414	0.454	0.524	0.586	0.643	0.694	.
150	4	0.9995	75.9	-0.697	0.00159	0.188	0.259	0.314	0.361	0.403	0.440	0.507	0.566	0.620	0.669	.
150	5	0.9997	74.2	-0.737	0.00185	0.177	0.262	0.325	0.377	0.424	0.465	0.539	0.604	0.662	0.716	.
150	5	0.9998	69.0	-0.724	0.00187	0.215	0.289	0.347	0.398	0.442	0.482	0.554	0.618	0.676	.	.
200	1	0.9973	76.8	-1.235	0.00488	0.349	0.468	0.563	0.644	0.716	0.781	0.897	1.000	1.094	1.180	.
200	1	0.9994	76.4	-1.200	0.00453	0.380	0.485	0.571	0.645	0.712	0.773	0.883	0.980	1.069	1.150	.
200	2	0.9990	78.5	-1.109	0.00381	0.334	0.433	0.514	0.583	0.645	0.702	0.803	0.893	0.974	1.050	.
200	2	0.9988	78.3	-1.162	0.00419	0.349	0.454	0.538	0.611	0.676	0.736	0.842	0.936	1.022	1.101	.
200	3	0.9993	76.6	-1.099	0.00390	0.303	0.412	0.498	0.571	0.636	0.694	0.799	0.891	0.975	1.052	.
200	3	0.9993	74.8	-1.091	0.00394	0.298	0.410	0.497	0.571	0.636	0.695	0.801	0.894	0.978	1.056	.
200	4	0.9994	74.4	-0.987	0.00326	0.263	0.366	0.447	0.514	0.574	0.629	0.725	0.810	0.887	0.957	.
200	4	0.9992	74.0	-1.031	0.00362	0.250	0.367	0.455	0.529	0.594	0.652	0.755	0.845	0.927	1.002	.
200	5	0.9992	71.8	-1.067	0.00393	0.296	0.408	0.495	0.569	0.634	0.694	0.799	0.892	0.976	1.054	.
200	5	0.9993	71.8	-1.080	0.00397	0.324	0.430	0.514	0.586	0.650	0.709	0.813	0.905	0.989	1.067	.
250	1	0.9986	77.9	-1.337	0.00548	0.439	0.550	0.642	0.722	0.794	0.860	0.979	1.085	1.182	1.271	.
250	1	0.9972	78.7	-1.369	0.00565	0.456	0.567	0.659	0.740	0.812	0.879	0.999	1.107	1.204	1.295	.
250	2	0.9978	80.2	-1.583	0.00746	0.510	0.640	0.748	0.842	0.926	1.003	1.142	1.266	1.379	1.484	1.581
250	2	0.9993	75.5	-1.581	0.00799	0.496	0.637	0.752	0.852	0.941	1.023	1.169	1.298	1.416	1.525	.
250	3	0.9991	78.2	-1.640	0.00859	0.416	0.588	0.719	0.830	0.928	1.016	1.173	1.311	1.436	1.551	.
250	3	0.9989	69.5	-1.569	0.00859	0.499	0.648	0.769	0.874	0.967	1.052	1.204	1.339	1.462	1.575	.
250	4	0.9988	71.6	-1.470	0.00742	0.428	0.576	0.693	0.793	0.882	0.962	1.106	1.233	1.348	1.454	.
250	4	0.9987	71.9	-1.366	0.00606	0.493	0.604	0.697	0.779	0.853	0.922	1.045	1.155	1.255	1.349	.
250	5	0.9993	72.3	-1.432	0.00704	0.396	0.545	0.662	0.761	0.848	0.928	1.069	1.193	1.306	1.409	.
250	5	0.9993	70.8	-1.443	0.00729	0.407	0.558	0.676	0.776	0.865	0.946	1.089	1.216	1.330	1.436	.

Appendix T. Coefficient of Determination, Parameter Estimates, and Drying Rates of Radially-cut 25x152 mm Yellow-poplar Flakes.

TEMP						DRYING RATE (%/SEC)										
(C)	REP	R^2	β_0	β_1	β_2	5	10	15	20	25	30	40	50	60	70	80
150	1	0.9996	76.6	-0.824	0.00218	0.234	0.313	0.377	0.431	0.479	0.522	0.600	0.669	0.731	0.789	.
150	1	0.9994	80.8	-0.845	0.00221	0.212	0.299	0.365	0.421	0.471	0.515	0.595	0.665	0.728	0.787	0.841
150	2	0.9993	79.2	-0.811	0.00207	0.205	0.289	0.354	0.408	0.456	0.499	0.577	0.644	0.706	0.762	.
150	2	0.9994	73.3	-0.804	0.00220	0.208	0.296	0.363	0.419	0.469	0.514	0.593	0.663	0.727	0.785	.
150	3	0.9991	68.3	-0.800	0.00233	0.227	0.313	0.380	0.437	0.488	0.533	0.614	0.686	0.751	.	.
150	3	0.9992	72.8	-0.817	0.00230	0.209	0.300	0.368	0.426	0.477	0.523	0.605	0.677	0.742	0.801	.
150	4	0.9995	66.5	-0.824	0.00262	0.184	0.294	0.373	0.437	0.494	0.544	0.633	0.711	0.782	.	.
150	4	0.9991	73.5	-0.843	0.00242	0.215	0.307	0.378	0.438	0.490	0.537	0.621	0.694	0.761	0.822	.
150	5	0.9996	67.2	-0.807	0.00247	0.194	0.295	0.369	0.431	0.485	0.533	0.619	0.694	0.762	.	.
150	5	0.9994	69.8	-0.796	0.00226	0.217	0.304	0.371	0.427	0.478	0.523	0.603	0.674	0.738	0.797	.
200	1	0.9991	81.3	-1.226	0.00455	0.340	0.454	0.545	0.623	0.692	0.755	0.867	0.967	1.056	1.139	1.217
200	1	0.9996	78.0	-1.155	0.00422	0.317	0.430	0.519	0.595	0.662	0.723	0.831	0.927	1.014	1.094	.
200	2	0.9993	74.1	-1.121	0.00417	0.325	0.435	0.522	0.596	0.662	0.723	0.830	0.925	1.011	1.090	.
200	2	0.9987	81.9	-1.138	0.00367	0.407	0.489	0.559	0.621	0.678	0.730	0.824	0.909	0.986	1.058	1.125
200	3	0.9990	75.5	-1.154	0.00427	0.356	0.461	0.546	0.619	0.685	0.744	0.851	0.947	1.033	1.112	.
200	3	0.9980	77.2	-1.255	0.00502	0.353	0.474	0.570	0.653	0.725	0.792	0.910	1.014	1.109	1.196	.
200	4	0.9983	73.1	-1.180	0.00462	0.365	0.475	0.564	0.641	0.709	0.772	0.883	0.982	1.072	1.155	.
200	4	0.9996	66.9	-1.157	0.00495	0.340	0.463	0.560	0.642	0.715	0.781	0.899	1.003	1.097	.	.
200	5	0.9996	65.1	-1.155	0.00510	0.328	0.458	0.558	0.643	0.718	0.786	0.906	1.013	1.109	.	.
200	5	0.9991	67.1	-1.141	0.00476	0.346	0.463	0.557	0.637	0.707	0.772	0.887	0.988	1.080	.	.
250	1	0.9977	81.1	-1.664	0.00831	0.489	0.636	0.756	0.859	0.951	1.034	1.184	1.317	1.438	1.549	1.653
250	1	0.9969	83.0	-1.529	0.00641	0.581	0.683	0.771	0.850	0.923	0.990	1.112	1.222	1.323	1.416	1.504
250	2	0.9989	74.7	-1.472	0.00672	0.539	0.652	0.748	0.833	0.910	0.981	1.110	1.225	1.330	1.428	.
250	2	0.9987	73.1	-1.488	0.00713	0.522	0.645	0.747	0.837	0.918	0.993	1.127	1.248	1.357	1.458	.
250	3	0.9987	75.5	-1.541	0.00769	0.453	0.599	0.716	0.816	0.906	0.987	1.132	1.261	1.377	1.485	.
250	3	0.9994	70.4	-1.580	0.00881	0.436	0.605	0.737	0.848	0.946	1.035	1.193	1.333	1.459	1.575	.
250	4	0.9995	68.1	-1.497	0.00814	0.432	0.591	0.716	0.821	0.915	1.000	1.151	1.285	1.406	.	.
250	4	0.9993	67.1	-1.540	0.00887	0.412	0.589	0.724	0.838	0.938	1.028	1.188	1.329	1.456	.	.
250	5	0.9995	58.6	-1.514	0.00983	0.431	0.618	0.761	0.881	0.986	1.081	1.250	1.398	.	.	.
250	5	0.9991	65.1	-1.514	0.00847	0.506	0.652	0.771	0.874	0.966	1.050	1.201	1.334	1.456	.	.

Appendix U. Coefficient of Determination, Parameter Estimates, and Drying Rates of Tangentially-cut 15x117 mm Yellow-poplar Flakes.

TEMP						DRYING RATE (%/SEC)											
(C)	REP	R^2	β_0	β_1	β_2	5	10	15	20	25	30	40	50	60	70	80	90
150	1	0.9995	60.1	-0.848	0.00305	0.218	0.330	0.412	0.480	0.540	0.594	0.689	0.773	0.848	.	.	.
150	1	0.9993	57.1	-0.808	0.00293	0.206	0.318	0.400	0.467	0.526	0.579	0.673	0.755	.	.	.	.
150	2	0.9985	74.2	-0.970	0.00314	0.266	0.365	0.443	0.509	0.567	0.620	0.714	0.798	0.873	0.942	.	.
150	2	0.9991	73.7	-0.912	0.00279	0.259	0.350	0.422	0.484	0.538	0.588	0.676	0.754	0.825	0.890	.	.
150	3	0.9989	78.8	-0.866	0.00236	0.230	0.316	0.384	0.441	0.491	0.537	0.619	0.691	0.756	0.816	.	.
150	3	0.9995	87.0	-0.913	0.00235	0.251	0.332	0.396	0.452	0.501	0.546	0.626	0.697	0.761	0.821	0.876	.
150	4	0.9994	87.5	-0.936	0.00243	0.272	0.350	0.414	0.469	0.518	0.563	0.643	0.715	0.780	0.840	0.896	.
150	4	0.9996	92.5	-0.937	0.00232	0.258	0.336	0.399	0.453	0.502	0.546	0.625	0.696	0.759	0.818	0.873	0.924
150	5	0.9998	81.3	-0.881	0.00240	0.208	0.302	0.373	0.433	0.485	0.533	0.616	0.690	0.756	0.817	0.874	.
150	5	0.9995	80.7	-0.836	0.00220	0.181	0.277	0.348	0.406	0.457	0.503	0.584	0.655	0.719	0.778	0.832	.
200	1	0.9988	54.5	-1.169	0.00640	0.317	0.478	0.597	0.696	0.783	0.860	0.998	1.119	.	.	.	.
200	1	0.9989	52.8	-1.169	0.00637	0.386	0.526	0.635	0.729	0.811	0.886	1.020	1.138	.	.	.	.
200	2	0.9996	70.9	-1.238	0.00539	0.330	0.466	0.570	0.658	0.735	0.805	0.930	1.039	1.138	1.230	.	.
200	2	0.9964	71.2	-1.249	0.00531	0.394	0.511	0.606	0.688	0.761	0.828	0.948	1.054	1.150	1.239	.	.
200	3	0.9987	93.5	-1.387	0.00504	0.370	0.488	0.582	0.663	0.735	0.801	0.918	1.022	1.116	1.203	1.284	1.361
200	3	0.9977	93.4	-1.395	0.00503	0.410	0.518	0.608	0.686	0.755	0.819	0.934	1.036	1.129	1.215	1.295	1.371
200	4	0.9993	95.6	-1.353	0.00475	0.331	0.453	0.548	0.628	0.700	0.765	0.880	0.982	1.075	1.160	1.239	1.314
200	4	0.9996	94.3	-1.338	0.00475	0.304	0.433	0.532	0.615	0.688	0.754	0.871	0.974	1.067	1.153	1.232	1.307
200	5	0.9991	78.6	-1.137	0.00418	0.249	0.382	0.479	0.560	0.630	0.693	0.805	0.903	0.991	1.072	.	.
200	5	0.9991	69.3	-1.162	0.00500	0.253	0.405	0.514	0.604	0.681	0.751	0.874	0.982	1.079	.	.	.
250	1	0.9968	49.8	-1.501	0.01133	0.472	0.670	0.822	0.950	1.062	1.164	1.345	1.504	.	.	.	.
250	1	0.9955	49.3	-1.383	0.00896	0.569	0.709	0.826	0.928	1.020	1.105	1.256	1.392	.	.	.	.
250	2	0.9988	76.1	-1.773	0.01044	0.418	0.619	0.770	0.895	1.005	1.104	1.279	1.433	1.572	1.700	.	.
250	2	0.9985	78.7	-1.697	0.00916	0.420	0.600	0.737	0.852	0.954	1.045	1.208	1.351	1.481	1.600	.	.
250	3	0.9980	98.4	-1.870	0.00874	0.481	0.637	0.762	0.870	0.965	1.052	1.206	1.344	1.468	1.583	1.689	1.790
250	3	0.9992	92.2	-1.777	0.00822	0.540	0.676	0.788	0.886	0.974	1.055	1.201	1.331	1.449	1.558	1.660	1.757
250	4	0.9993	92.0	-1.772	0.00814	0.554	0.685	0.795	0.892	0.979	1.059	1.203	1.331	1.448	1.557	1.658	1.753
250	4	0.9991	83.2	-1.827	0.00980	0.521	0.684	0.815	0.927	1.028	1.119	1.282	1.427	1.558	1.679	1.792	.
250	5	0.9985	56.5	-1.550	0.01088	0.400	0.614	0.771	0.902	1.015	1.117	1.297	1.456	.	.	.	.
250	5	0.9991	49.5	-1.543	0.01227	0.444	0.665	0.829	0.966	1.086	1.193	1.384	1.551	.	.	.	.

Appendix V. Coefficient of Determination, Parameter Estimates, and Drying Rates of Tangentially-cut 15x152 mm Yellow-poplar Flakes.

TEMP						DRYING RATE (%/SEC)												
(C)	REP	R^2	β_0	β_1	β_2	5	10	15	20	25	30	40	50	60	70	80	90	100
150	1	0.9992	75.9	-0.915	0.00268	0.275	0.360	0.428	0.486	0.539	0.587	0.672	0.747	0.816	0.879	.	.	.
150	1	0.9993	80.8	-0.883	0.00239	0.237	0.323	0.390	0.447	0.497	0.543	0.625	0.697	0.762	0.822	0.879	.	.
150	2	0.9994	84.3	-0.897	0.00241	0.204	0.299	0.371	0.431	0.484	0.531	0.615	0.689	0.756	0.817	0.874	.	.
150	2	0.9995	75.4	-0.862	0.00251	0.188	0.293	0.368	0.431	0.486	0.535	0.622	0.698	0.767	0.830	.	.	.
150	3	0.9985	90.6	-0.995	0.00260	0.315	0.389	0.451	0.505	0.554	0.599	0.681	0.753	0.819	0.881	0.938	0.992	.
150	3	0.9977	99.2	-1.065	0.00275	0.316	0.394	0.458	0.515	0.565	0.612	0.696	0.771	0.839	0.902	0.961	1.017	.
150	4	0.9991	62.5	-1.005	0.00402	0.291	0.406	0.496	0.571	0.637	0.698	0.805	0.899	0.984	.	.	.	.
150	4	0.9983	65.8	-1.027	0.00390	0.326	0.429	0.512	0.583	0.647	0.704	0.808	0.899	0.982	.	.	.	.
150	5	0.9985	94.5	-0.966	0.00236	0.296	0.367	0.427	0.479	0.526	0.569	0.647	0.716	0.779	0.838	0.892	0.944	.
150	5	0.9992	95.0	-1.015	0.00256	0.328	0.398	0.458	0.511	0.559	0.603	0.683	0.754	0.819	0.880	0.936	0.989	.
200	1	0.9990	93.9	-1.327	0.00453	0.385	0.489	0.574	0.648	0.715	0.776	0.885	0.982	1.070	1.152	1.228	1.300	.
200	1	0.9992	100.7	-1.403	0.00476	0.382	0.491	0.580	0.657	0.726	0.788	0.901	1.001	1.092	1.176	1.254	1.328	1.398
200	2	0.9987	66.0	-1.242	0.00551	0.445	0.555	0.647	0.727	0.799	0.865	0.984	1.091	1.187	.	.	.	.
200	2	0.9993	57.4	-1.209	0.00626	0.386	0.523	0.632	0.724	0.806	0.880	1.013	1.130	.	.	.	.	.
200	3	0.9986	94.2	-1.464	0.00520	0.535	0.625	0.703	0.774	0.838	0.898	1.007	1.106	1.196	1.280	1.359	1.434	.
200	3	0.9988	98.1	-1.482	0.00554	0.364	0.493	0.595	0.682	0.759	0.829	0.953	1.063	1.163	1.254	1.340	1.420	.
200	4	0.9990	73.7	-1.435	0.00688	0.410	0.553	0.666	0.762	0.848	0.925	1.064	1.186	1.297	1.399	.	.	.
200	4	0.9979	82.5	-1.451	0.00625	0.410	0.541	0.646	0.737	0.817	0.890	1.021	1.137	1.242	1.338	1.429	.	.
200	5	0.9990	93.7	-1.413	0.00506	0.448	0.550	0.635	0.710	0.778	0.841	0.954	1.054	1.146	1.231	1.311	1.386	.
200	5	0.9986	94.1	-1.439	0.00529	0.432	0.541	0.631	0.710	0.781	0.846	0.963	1.067	1.162	1.250	1.332	1.409	.
250	1	0.9989	98.8	-1.778	0.00749	0.591	0.707	0.806	0.894	0.974	1.048	1.183	1.303	1.414	1.516	1.612	1.702	.
250	1	0.9982	80.1	-1.724	0.00897	0.528	0.677	0.798	0.904	0.998	1.084	1.238	1.376	1.500	1.616	1.723	.	.
250	2	0.9990	59.2	-1.653	0.01157	0.477	0.677	0.831	0.960	1.074	1.176	1.359	1.520	1.665	.	.	.	.
250	2	0.9986	50.2	-1.609	0.01289	0.512	0.721	0.882	1.017	1.137	1.245	1.437	1.607	.	.	.	.	.
250	3	0.9994	81.1	-1.899	0.01099	0.511	0.694	0.837	0.959	1.068	1.166	1.341	1.496	1.637	1.766	1.886	.	.
250	3	0.9994	60.6	-1.832	0.01335	0.621	0.808	0.959	1.089	1.206	1.312	1.501	1.670	1.823	.	.	.	.
250	4	0.9992	87.5	-1.970	0.01067	0.599	0.756	0.886	0.999	1.101	1.194	1.361	1.509	1.645	1.770	1.886	.	.
250	4	0.9990	93.5	-1.906	0.00919	0.616	0.750	0.864	0.965	1.056	1.139	1.291	1.426	1.549	1.664	1.771	1.872	.
250	5	0.9982	104.8	-2.007	0.00925	0.578	0.720	0.839	0.943	1.036	1.122	1.276	1.414	1.539	1.655	1.763	1.865	1.962
250	5	0.9988	98.1	-1.933	0.00910	0.589	0.727	0.843	0.945	1.037	1.121	1.273	1.409	1.533	1.647	1.754	1.855	.

Appendix W. Coefficient of Determination, Parameter Estimates, and Drying Rates of Tangentially-cut 25x117 mm Yellow-poplar Flakes.

TEMP						DRYING RATE (%/SEC)												
(C)	REP	R^2	β_0	β_1	β_2	5	10	15	20	25	30	40	50	60	70	80	90	100
150	1	0.9987	85.9	-0.967	0.00268	0.259	0.348	0.418	0.478	0.531	0.579	0.666	0.742	0.811	0.875	0.934	.	.
150	1	0.9991	86.4	-0.925	0.00246	0.230	0.320	0.389	0.448	0.500	0.547	0.631	0.705	0.771	0.833	0.890	.	.
150	2	0.9994	98.4	-0.918	0.00213	0.216	0.299	0.363	0.418	0.466	0.510	0.588	0.656	0.718	0.775	0.829	0.879	.
150	2	0.9992	97.8	-0.893	0.00201	0.227	0.303	0.363	0.415	0.461	0.502	0.577	0.643	0.702	0.757	0.809	0.857	.
150	3	0.9997	68.9	-0.833	0.00254	0.213	0.310	0.383	0.444	0.498	0.547	0.633	0.709	0.777	.	.	.	.
150	3	0.9992	70.3	-0.884	0.00267	0.291	0.372	0.438	0.495	0.546	0.593	0.677	0.752	0.820	0.882	.	.	.
150	4	0.9992	71.2	-0.800	0.00226	0.207	0.297	0.365	0.422	0.473	0.518	0.599	0.670	0.734	0.793	.	.	.
150	4	0.9994	69.9	-0.788	0.00224	0.203	0.293	0.361	0.419	0.469	0.515	0.595	0.666	0.730	0.789	.	.	.
150	5	0.9990	55.3	-0.743	0.00249	0.227	0.318	0.389	0.448	0.501	0.548	0.632	0.707	.	.	.	.	.
150	5	0.9987	54.3	-0.751	0.00261	0.222	0.319	0.392	0.454	0.508	0.557	0.644	0.720	.	.	.	.	.
200	1	0.9987	97.5	-1.253	0.00403	0.285	0.402	0.492	0.568	0.635	0.695	0.803	0.898	0.983	1.062	1.135	1.204	.
200	1	0.9984	90.2	-1.302	0.00466	0.324	0.445	0.540	0.620	0.692	0.756	0.871	0.972	1.064	1.148	1.226	1.300	.
200	2	0.9984	99.6	-1.242	0.00382	0.315	0.419	0.502	0.573	0.636	0.694	0.796	0.887	0.969	1.045	1.116	1.182	1.245
200	2	0.9990	94.7	-1.296	0.00430	0.369	0.471	0.555	0.628	0.693	0.752	0.859	0.954	1.040	1.120	1.194	1.264	.
200	3	0.9992	64.1	-1.266	0.00617	0.382	0.519	0.626	0.718	0.799	0.873	1.004	1.120	1.226	.	.	.	.
200	3	0.9983	63.2	-1.207	0.00565	0.375	0.504	0.606	0.693	0.770	0.840	0.965	1.076	1.176	.	.	.	.
200	4	0.9990	68.3	-1.133	0.00478	0.275	0.413	0.516	0.602	0.676	0.744	0.862	0.967	1.061	.	.	.	.
200	4	0.9975	63.1	-1.077	0.00449	0.339	0.453	0.543	0.620	0.689	0.751	0.863	0.961	1.051	.	.	.	.
200	5	0.9981	53.8	-1.055	0.00508	0.349	0.472	0.570	0.653	0.727	0.794	0.913	1.018	.	.	.	.	.
200	5	0.9988	51.2	-1.034	0.00260	0.768	0.801	0.833	0.864	0.893	0.922	0.977	1.028	.	.	.	.	.
250	1	0.9983	98.3	-1.914	0.00904	0.537	0.685	0.806	0.912	1.006	1.092	1.247	1.384	1.509	1.625	1.732	1.834	.
250	1	0.9986	102.2	-1.851	0.00825	0.468	0.620	0.741	0.845	0.937	1.022	1.172	1.305	1.426	1.537	1.641	1.739	1.831
250	2	0.9993	85.4	-1.662	0.00791	0.463	0.611	0.729	0.830	0.921	1.003	1.150	1.280	1.398	1.507	1.609	.	.
250	2	0.9983	80.8	-1.632	0.00817	0.430	0.590	0.716	0.822	0.916	1.001	1.153	1.287	.	.	.	.	.
250	3	0.9986	55.1	-1.623	0.01219	0.441	0.662	0.826	0.962	1.081	1.189	1.379	1.545	.	.	.	.	.
250	3	0.9981	51.9	-1.582	0.01165	0.564	0.742	0.885	1.008	1.118	1.218	1.396	1.554	.	.	.	.	.
250	4	0.9985	57.7	-1.451	0.00905	0.446	0.617	0.749	0.861	0.961	1.051	1.211	1.352	.	.	.	.	.
250	4	0.9987	53.4	-1.420	0.00929	0.467	0.635	0.768	0.881	0.980	1.071	1.232	1.375	.	.	.	.	.
250	5	0.9992	48.6	-1.443	0.01102	0.399	0.616	0.775	0.906	1.020	1.123	1.304	.	.	.	.	.	.
250	5	0.9937	51.0	-1.339	0.00807	0.555	0.685	0.794	0.890	0.977	1.056	1.199	1.327	.	.	.	.	.

Appendix X. Coefficient of Determination, Parameter Estimates, and Drying Rates of Tangentially-cut 25x152 mm Yellow-poplar Flakes.

TEMP						DRYING RATE (%/SEC)											
(C)	REP	R^2	β_0	β_1	β_2	5	10	15	20	25	30	40	50	60	70	80	90
150	1	0.9986	87.2	-0.921	0.00237	0.266	0.344	0.407	0.462	0.510	0.555	0.634	0.705	0.769	0.828	0.884	.
150	1	0.9988	91.9	-0.933	0.00229	0.276	0.349	0.410	0.462	0.509	0.552	0.630	0.698	0.761	0.819	0.873	0.924
150	2	0.9995	73.7	-0.898	0.00279	0.203	0.312	0.391	0.457	0.514	0.566	0.657	0.737	0.809	0.875	.	.
150	2	0.9992	66.7	-0.819	0.00255	0.205	0.305	0.379	0.441	0.496	0.545	0.631	0.708	0.776	.	.	.
150	3	0.9983	58.4	-0.813	0.00280	0.251	0.345	0.418	0.480	0.535	0.585	0.674	0.753	.	.	.	.
150	3	0.9980	57.5	-0.813	0.00286	0.246	0.343	0.418	0.481	0.538	0.588	0.679	0.758	.	.	.	.
150	4	0.9993	82.0	-0.862	0.00225	0.225	0.309	0.375	0.431	0.480	0.525	0.604	0.675	0.738	0.797	0.851	.
150	4	0.9989	83.4	-0.867	0.00222	0.238	0.318	0.381	0.435	0.484	0.527	0.606	0.675	0.738	0.795	0.849	.
150	5	0.9988	76.6	-0.863	0.00235	0.270	0.346	0.408	0.462	0.511	0.555	0.634	0.704	0.768	0.827	.	.
150	5	0.9989	81.2	-0.938	0.00255	0.322	0.393	0.453	0.506	0.554	0.599	0.678	0.750	0.815	0.875	0.931	.
200	1	0.9976	93.2	-1.313	0.00458	0.329	0.447	0.540	0.619	0.689	0.753	0.866	0.966	1.057	1.140	1.218	1.291
200	1	0.9984	97.1	-1.342	0.00458	0.334	0.451	0.543	0.622	0.692	0.755	0.868	0.968	1.058	1.142	1.219	1.292
200	2	0.9985	68.6	-1.179	0.00511	0.299	0.438	0.542	0.629	0.706	0.775	0.897	1.005	1.102	.	.	.
200	2	0.9982	66.1	-1.201	0.00545	0.331	0.467	0.572	0.661	0.738	0.809	0.934	1.044	1.144	.	.	.
200	3	0.9976	54.1	-1.145	0.00592	0.384	0.516	0.620	0.709	0.788	0.860	0.988	1.102	.	.	.	.
200	3	0.9991	53.3	-1.146	0.00611	0.363	0.504	0.614	0.706	0.788	0.862	0.994	1.110	.	.	.	.
200	4	0.9980	85.7	-1.290	0.00479	0.343	0.462	0.556	0.637	0.708	0.773	0.888	0.990	1.082	1.168	1.247	.
200	4	0.9989	91.2	-1.378	0.00499	0.420	0.526	0.613	0.690	0.759	0.822	0.936	1.037	1.129	1.214	1.294	1.369
200	5	0.9987	84.8	-1.277	0.00458	0.414	0.513	0.595	0.668	0.733	0.793	0.901	0.998	1.085	1.167	1.243	.
200	5	0.9989	94.1	-1.287	0.00432	0.340	0.449	0.537	0.612	0.679	0.740	0.849	0.945	1.033	1.113	1.188	1.259
250	1	0.9965	98.9	-1.746	0.00729	0.557	0.675	0.776	0.865	0.945	1.019	1.154	1.274	1.383	1.485	1.580	1.670
250	1	0.9945	95.2	-1.639	0.00659	0.557	0.665	0.757	0.840	0.915	0.984	1.110	1.223	1.327	1.423	1.512	1.597
250	2	0.9973	64.8	-1.582	0.00968	0.432	0.616	0.757	0.876	0.980	1.074	1.241	1.389	1.522	.	.	.
250	2	0.9991	58.9	-1.651	0.01187	0.405	0.634	0.799	0.936	1.055	1.163	1.351	1.517	.	.	.	.
250	3	0.9992	48.6	-1.532	0.01200	0.506	0.704	0.858	0.988	1.103	1.207	1.391	.	.	.	.	.
250	3	0.9974	52.7	-1.520	0.01035	0.579	0.736	0.866	0.978	1.079	1.171	1.336	1.483	.	.	.	.
250	4	0.9992	85.3	-1.687	0.00823	0.450	0.606	0.729	0.834	0.928	1.013	1.164	1.298	1.419	1.531	1.635	.
250	4	0.9976	83.0	-1.526	0.00695	0.400	0.547	0.662	0.760	0.846	0.925	1.065	1.188	1.300	1.403	1.498	.
250	5	0.9987	92.3	-1.875	0.00919	0.553	0.700	0.821	0.926	1.021	1.107	1.262	1.400	1.526	1.642	1.750	1.852
250	5	0.9986	95.9	-1.862	0.00877	0.525	0.672	0.792	0.896	0.989	1.074	1.227	1.362	1.485	1.599	1.705	1.805

Appendix Y. P-values at Different Moisture Content Levels of Complete Data Set.

SOURCE	DF	MOISTURE CONTENT (%) 5	10	15	20	25	30	40	50
S	2	<0.0001	<0.0001	<0.0001	<0.0001	<0.0001	<0.0001	0.0006	0.0039
C	1	<0.0001	<0.0001	<0.0001	<0.0001	<0.0001	<0.0001	<0.0001	<0.0001
S x C	2	0.0795	0.0322	0.0187	0.0135	0.0014	0.0103	0.0093	0.0108
D	3	<0.0001	<0.0001	<0.0001	<0.0001	<0.0001	<0.0001	<0.0001	<0.0001
S x D	6	0.5129	0.4399	0.2848	0.1849	0.1278	0.0964	0.0651	0.0557
C x D	3	0.3954	0.1426	0.0433	0.0174	0.0091	0.0058	0.0032	0.0020
S x C x D	6	0.0397	0.2179	0.3501	0.3676	0.3291	0.2880	0.2186	0.0166
T	2	<0.0001	<0.0001	<0.0001	<0.0001	<0.0001	<0.0001	<0.0001	<0.0001
S x T	4	0.0001	0.0013	0.0084	0.0191	0.0183	0.0108	0.0027	0.0015
C x T	2	0.8156	0.1857	0.0124	0.0008	<0.0001	<0.0001	<0.0001	<0.0001
S x C x T	4	0.0002	0.0027	0.0263	0.1116	0.2035	0.2359	0.1682	0.1636
D x T	6	0.4324	0.5122	0.5894	0.6140	0.5990	0.5692	0.4915	0.3747
S x D x T	12	0.5083	0.5849	0.5856	0.5468	0.4866	0.4067	0.3026	0.2769
C x D x T	6	0.1591	0.3309	0.5392	0.6552	0.6636	0.6135	0.4770	0.3007
S x C x D x T	12	0.0476	0.0787	0.1422	0.2386	0.3316	0.3899	0.4454	0.4516

Appendix Z. P-values at Different Moisture Content Levels of Southern Yellow Pine and Sweetgum.

SOURCE	DF	MOISTURE CONTENT (%) 60	70	80
S	1	0.0074	0.0135	0.0207
C	1	0.0026	0.0030	0.0033
S x C	1	0.6230	0.5930	0.5727
D	3	<0.0001	<0.0001	<0.0001
S x D	3	0.3795	0.3532	0.3341
C x D	3	0.0592	0.0511	0.0457
S x C x D	3	0.0780	0.0667	0.0588
T	2	<0.0001	<0.0001	<0.0001
S x T	2	0.0050	0.0066	0.0085
C x T	2	0.0042	0.0043	0.0046
S x C x T	2	0.1995	0.1051	0.0625
D x T	6	0.0968	0.0840	0.0793
S x D x T	6	0.0154	0.0115	0.0103
C x D x T	6	0.4088	0.3003	0.2281
S x C x D x T	6	0.0479	0.0455	0.0454

Appendix AA. P-values at Different Moisture Content Levels of Southern Yellow Pine.

SOURCE	DF	MOISTURE CONTENT (%) 5	10	15	20	25	30	40	50	60	70	80	90	100	110	120
C	1	0.0121	0.0118	0.0146	0.0196	0.0252	0.0311	0.0431	0.0540	0.0638	0.0719	0.0784	0.0850	0.0900	0.0947	0.0985
D	3	0.0247	0.0275	0.0330	0.0389	0.0448	0.0495	0.0572	0.0624	0.0662	0.0687	0.0708	0.0724	0.0737	0.0749	0.0759
C x D	3	0.3976	0.4892	0.5468	0.5670	0.5666	0.5581	0.5326	0.5116	0.4927	0.4772	0.4634	0.4536	0.4452	0.4404	0.4334
T	2	<.0001	<.0001	<.0001	<.0001	<.0001	<.0001	<.0001	<.0001	<.0001	<.0001	<.0001	<.0001	<.0001	<.0001	<.0001
C x T	2	0.0113	0.0112	0.0138	0.0202	0.0317	0.0467	0.0939	0.1506	0.1956	0.2323	0.2656	0.2864	0.2939	0.3067	0.3102
D x T	6	0.3505	0.4314	0.4585	0.4447	0.3797	0.2992	0.1743	0.1131	0.0759	0.0560	0.0471	0.0396	0.0344	0.0320	0.0285
C x D x T	6	0.1646	0.1166	0.0995	0.1021	0.1178	0.1413	0.2190	0.3145	0.4051	0.4868	0.5486	0.6003	0.6409	0.6731	0.7047

Appendix BB. P-values at Different Moisture Content Levels of Sweetgum.

SOURCE	DF	MOISTURE CONTENT (%) 5	10	15	20	25	30	40	50	60	70	80
C	1	0.1484	0.0447	0.0262	0.0212	0.0191	0.0183	0.0178	0.0179	0.0179	0.0183	0.0185
D	3	0.0074	0.0058	0.0039	0.0029	0.0023	0.0020	0.0017	0.0015	0.0014	0.0013	0.0013
C x D	3	0.1898	0.4534	0.2930	0.1578	0.0904	0.0590	0.0316	0.0214	0.0161	0.0132	0.0113
T	2	<.0001	<.0001	<.0001	<.0001	<.0001	<.0001	<.0001	<.0001	<.0001	<.0001	<.0001
C x T	2	0.0046	0.0650	0.4184	0.8541	0.6503	0.2944	0.0539	0.0142	0.0059	0.0033	0.0022
D x T	6	0.3083	0.3252	0.2626	0.1681	0.1093	0.0713	0.0414	0.0322	0.0284	0.0263	0.0268
C x D x T	6	0.0337	0.1703	0.5325	0.8219	0.8343	0.6736	0.2867	0.1202	0.0595	0.0343	0.0234

Appendix CC. P-values at Different Moisture Content Levels of Yellow-poplar.

SOURCE	DF	MOISTURE CONTENT (%) 5	10	15	20	25	30	40	50
C	1	<.0001	<.0001	<.0001	<.0001	<.0001	<.0001	<.0001	<.0001
D	3	0.0239	0.0030	0.0020	0.0023	0.0030	0.0039	0.0060	0.0061
C x D	3	0.0125	0.0044	0.0034	0.0036	0.0042	0.0049	0.0062	0.0048
T	2	<.0001	<.0001	<.0001	<.0001	<.0001	<.0001	<.0001	<.0001
C x T	2	0.9314	0.2045	0.0225	0.0045	0.0015	0.0009	0.0005	0.0010
D x T	6	0.9221	0.9430	0.9669	0.9814	0.9873	0.9881	0.9896	0.9897
C x D x T	6	0.4156	0.4815	0.5803	0.6570	0.7037	0.7299	0.7568	0.7108

Appendix DD. Front2D Algorithm (Perre et al., 1999).

Program Front2D
Set external transfer parameters
Set internal transfer parameters
Set geometrical parameters
Set initial conditions
Set thermopysical constants
Set calculation parameters
Open saving files
Loop until final drying time
Compute front position e
If (e=0) **Then** (constant rate period)
Set $T_{surf}=T_{boiling}$
Set $T_{front}=T_{boiling}$
Compute $\langle q_m \rangle = \dfrac{q_{cext}}{L_v}$
Else (falling rate period)
Choose $T_{surf}^{(0)}$ and $<qm>^{(0)}$
Set i=0
Loop until stopping criterion has been satisfied
Compute front position e
Compute q_{cext}
Compute $T_{front} = T_{surf} - \dfrac{\langle q_m \rangle^{(i)} L_v}{\lambda e}$, hence P_{vfront}
Compute $<q_m>calc$
Compute $\Im_1$ and $\Im_2$
Compute Jacobian J
Compute du
Set $T_{surf}^{(i+1)}=T_{surf}^{(i)} + du_1$
Set $<qm>^{(i+1)}=<qm>^{(i)} + du_2$
Set $i=i+di$
End Loop
End If
Compute $d\langle X \rangle = \dfrac{\langle q_m \rangle dt}{\rho_s l}$
Set $\langle X \rangle (t+dt) = \langle X \rangle + d\langle X \rangle$
Set $t = t + dt$
If
End Loop

End Program Front2D

Appendix EE. Bending Properties of Southern Yellow Pine.

DRYER TEMP (°C)	REP	RADIALLY-CUT MOE (N/mm^2)	MOR (N/mm^2)	SPL (N/mm^2)	MC (%)	SG	TANGENTIALLY-CUT MOE (N/mm^2)	MOR (N/mm^2)	SPL (N/mm^2)	MC (%)	SG
150	1	4430.3	52.8	33.3	11.9	0.63	9830.0	172.3	127.2	11.5	0.65
	2	5160.8	69.0	35.1	11.6	0.56	3774.7	54.4	43.3	11.4	0.61
	3	5436.3	79.7	60.0	11.3	0.68	13901.0	213.2	153.7	10.7	0.53
	4	3636.9	46.8	30.3	11.6	0.66	6574.4	78.9	58.8	9.9	0.49
	5	3910.8	39.6	21.8	11.4	0.68	4734.2	83.6	62.7	10.0	0.55
	6	3527.7	57.2	29.5	8.8	0.60	2444.0	37.3	28.8	10.3	0.55
	7	3699.0	70.5	44.4	10.4	0.64	7202.9	150.0	117.8	9.7	0.55
	8	3889.1	60.5	36.4	10.3	0.59	3505.3	42.2	32.7	10.1	0.59
	9	4845.4	57.1	33.5	10.2	0.66	5740.5	98.7	76.6	9.4	0.64
	10	5323.7	87.6	52.8	10.7	0.54	2571.2	34.7	26.5	8.8	0.55
200	1	2989.4	64.2	46.8	11.9	0.57	2397.6	44.8	31.2	11.6	0.47
	2	3278.8	51.4	36.3	10.5	0.67	7137.0	125.8	95.3	11.2	0.64
	3	3005.8	53.9	30.1	11.3	0.60	3639.5	64.0	43.7	10.0	0.43
	4	2675.0	55.3	43.0	10.4	0.64	7062.1	123.8	105.3	10.2	0.56
	5	2877.2	50.2	37.2	10.4	0.63	4445.0	73.5	59.3	9.5	0.51
	6	3446.0	51.8	36.8	9.7	0.63	4635.4	89.5	70.6	10.8	0.55
	7	2314.3	40.0	24.1	10.8	0.52	5088.3	97.6	79.8	10.0	0.54
	8	2657.1	48.3	30.4	9.4	0.63	2986.6	39.2	31.8	9.9	0.46
	9	4095.3	75.1	58.6	9.8	0.60	3918.8	56.3	42.5	8.3	0.60
	10	4176.3	59.2	44.1	9.0	0.55	2627.2	43.2	32.5	7.9	0.43
250	1	3372.4	56.4	43.9	12.9	0.58	5160.0	76.4	61.9	10.5	0.57
	2	3207.3	47.6	36.0	11.2	0.65	5680.9	99.3	87.1	10.4	0.56
	3	2955.8	39.7	23.6	11.7	0.66	3058.4	42.9	36.7	9.6	0.42
	4	2199.9	38.3	28.4	11.5	0.59	5020.5	82.5	62.3	10.5	0.64
	5	2963.6	56.3	37.4	10.2	0.58	2268.3	34.3	24.3	10.9	0.52
	6	2882.7	47.5	25.0	10.2	0.65	2056.5	31.3	24.0	9.2	0.54
	7	2053.8	45.3	34.1	10.2	0.59	4462.6	95.7	79.2	9.1	0.54
	8	3368.8	53.1	36.5	9.6	0.55	2145.8	33.4	25.2	8.1	0.52
	9	2303.6	41.0	31.3	11.5	0.57	2527.0	31.6	24.8	9.5	0.54
	10	3204.7	59.4	38.9	10.0	0.62	4729.1	55.2	40.0	8.4	0.51

Appendix FF. Bending Properties of Sweetgum.

DRYER TEMP (°C)	REP	RADIALLY-CUT MOE (N/mm²)	MOR (N/mm²)	SPL (N/mm²)	MC (%)	SG	TANGENTIALLY-CUT MOE (N/mm²)	MOR (N/mm²)	SPL (N/mm²)	MC (%)	SG
150	1	4670.6	75.2	59.4	11.8	0.64	4339.1	87.4	67.3	10.7	0.51
	2	5558.9	85.6	60.0	11.2	0.67	4658.6	93.6	68.1	11.6	0.58
	3	3601.9	65.9	48.1	11.3	0.60	4973.0	101.8	79.5	11.5	0.63
	4	4293.1	74.6	57.3	10.8	0.62	4659.6	97.8	78.1	11.3	0.56
	5	3329.9	59.1	43.4	11.7	0.62	4948.5	99.4	77.1	11.5	0.63
	6	4016.4	78.5	61.7	11.0	0.61	5797.1	124.4	95.4	12.7	0.53
	7	4311.3	73.8	51.1	10.2	0.64	6137.9	109.2	85.5	12.0	0.59
	8	4657.7	85.1	66.2	11.1	0.65	5644.4	109.7	87.0	12.3	0.61
	9	5347.5	99.7	69.7	11.5	0.59	5862.9	102.3	79.9	11.8	0.63
	10	5811.5	91.9	68.8	10.9	0.64	5623.9	99.9	85.0	11.7	0.62
200	1	2551.7	52.3	26.7	14.5	0.68	4221.5	94.4	66.0	9.1	0.69
	2	4681.1	84.0	47.9	13.7	0.70	4287.9	83.4	63.8	11.1	0.68
	3	5483.3	80.8	48.6	15.0	0.68	4497.5	75.7	56.8	10.6	0.67
	4	3786.8	61.2	36.9	13.0	0.69	3862.1	70.3	55.8	11.4	0.66
	5	3622.1	67.3	52.9	15.2	0.62	4162.8	65.2	42.5	11.4	0.68
	6	4555.1	76.8	54.9	13.4	0.69	4657.7	89.9	64.5	11.4	0.66
	7	3536.8	54.9	35.6	14.3	0.50	5076.8	102.0	70.6	18.3	0.66
	8	2989.1	52.4	38.7	13.2	0.63	4414.0	89.4	60.7	11.4	0.69
	9	3691.7	72.3	52.8	12.9	0.63	4160.7	80.1	55.1	10.8	0.63
	10	4874.9	72.5	46.2	13.1	0.69	4987.1	92.5	67.5	11.4	0.64
250	1	5534.9	84.4	63.4	12.1	0.63	4406.6	88.0	60.7	13.4	0.65
	2	3079.2	51.6	36.2	11.1	0.66	4324.8	85.7	59.9	12.4	0.67
	3	3778.0	57.0	41.2	12.0	0.67	4512.1	77.5	55.7	13.7	0.69
	4	4197.6	62.7	40.9	11.5	0.65	4328.9	89.4	63.3	13.8	0.63
	5	3075.4	55.6	34.4	9.9	0.69	4738.6	79.3	54.4	15.0	0.63
	6	3091.6	55.5	36.3	10.9	0.69	4079.1	67.9	43.0	14.7	0.60
	7	3728.2	48.6	32.0	9.0	0.63	4518.5	77.6	53.1	14.3	0.63
	8	4448.5	59.9	37.6	10.3	0.65	5016.3	87.1	57.6	13.7	0.66
	9	4197.3	55.0	42.2	11.0	0.65	4227.9	78.1	57.2	9.2	0.66
	10	4099.1	44.1	32.3	10.1	0.65	4111.4	78.5	58.1	9.4	0.65

Appendix GG. Bending Properties of Yellow-poplar.

DRYER TEMP (°C)	REP	RADIALLY-CUT MOE (N/mm^2)	MOR (N/mm^2)	SPL (N/mm^2)	MC (%)	SG	TANGENTIALLY-CUT MOE (N/mm^2)	MOR (N/mm^2)	SPL (N/mm^2)	MC (%)	SG
150	1	5132.4	92.6	66.4	11.4	0.54	4418.7	72.5	57.2	9.9	0.60
	2	5506.8	90.1	66.4	10.7	0.66	4585.1	81.1	55.3	9.0	0.54
	3	5723.6	92.2	62.5	11.2	0.55	8367.5	114.9	91.3	10.0	0.63
	4	6143.0	101.4	77.5	10.3	0.62	5817.9	97.0	73.4	9.8	0.56
	5	6602.0	107.9	77.4	10.7	0.65	8744.7	131.5	102.6	9.5	0.52
	6	5455.3	84.5	56.3	10.9	0.57	7389.7	99.3	76.3	10.0	0.51
	7	4950.3	81.8	65.5	9.9	0.62	5510.0	95.7	72.9	9.8	0.51
	8	6156.1	97.8	72.2	9.9	0.57	6314.6	98.1	74.1	9.7	0.57
	9	5482.1	83.1	64.2	9.9	0.61	5349.4	88.0	62.7	9.4	0.53
	10	4805.8	55.3	37.6	9.6	0.61	9256.2	98.7	72.4	9.3	0.55
200	1	4154.8	74.0	53.8	11.0	0.58	3988.6	81.7	51.6	9.8	0.54
	2	6918.4	107.2	83.4	10.4	0.57	4491.7	76.4	54.1	10.4	0.59
	3	6117.4	84.9	66.8	10.5	0.63	6665.9	100.7	72.7	9.5	0.60
	4	5717.0	92.5	72.1	10.2	0.61	6501.7	103.8	82.0	9.0	0.59
	5	4620.1	82.3	54.2	9.3	0.64	6950.2	106.2	81.5	9.5	0.51
	6	4856.9	71.6	50.1	10.2	0.62	7375.8	101.3	76.2	9.3	0.63
	7	4361.7	77.4	57.7	10.0	0.59	5703.0	93.5	75.5	9.4	0.51
	8	6116.5	99.9	71.7	10.0	0.61	6460.0	96.1	75.8	9.5	0.59
	9	7075.0	113.4	82.9	9.7	0.62	7420.1	110.0	87.0	8.8	0.58
	10	5381.1	64.6	42.1	9.3	0.65	9476.2	93.6	74.1	8.3	0.51
250	1	4897.7	82.7	63.4	10.3	0.55	3988.6	70.5	51.6	8.6	0.56
	2	2776.7	53.2	33.5	9.7	0.60	5203.4	75.7	62.7	8.1	0.54
	3	5850.2	94.7	63.8	9.7	0.56	6033.0	84.9	65.8	8.4	0.53
	4	4125.2	76.1	52.1	9.4	0.62	7062.2	106.6	89.1	7.9	0.52
	5	3990.7	66.6	46.8	9.0	0.67	3763.0	71.6	44.1	8.1	0.56
	6	6039.8	79.2	62.4	9.7	0.57	6220.7	91.0	64.2	7.2	0.53
	7	5133.7	89.7	68.0	9.0	0.61	4294.1	72.3	56.8	8.3	0.52
	8	4636.9	79.3	54.4	9.4	0.58	6156.1	98.2	72.2	8.0	0.60
	9	4619.3	79.5	54.1	8.4	0.60	7393.6	108.9	86.6	8.0	0.61
	10	5888.8	67.6	46.1	9.4	0.57	9628.5	100.1	75.3	7.8	0.49

VITA

Edgar Dela Cruz Deomano was born in San Pablo City, Philippines on 31 May 1968, the third of six children of Oscar Perez Deomano (deceased) and Nelia Candelaria Dela Cruz. He is married to Norilyn Reyes Deomano and they have a daughter, Annika.

He obtained his Bachelor of Science in Forest Products Engineering in 1988 and Master of Science in Forestry (Wood Science and Technology) in 1995 from the University of the Philippines Los Baños. For his master's thesis, he was awarded a fellowship by the International Tropical Timber Organization (ITTO) and thesis grant by the Philippine Council for Agriculture, Forestry, and Natural Resource Research and Development (PCARRD).

He was a Science Research Specialist at the Forest Products Research and Development Institute (FPRDI) from 1989 to 1997. From 1993 to 1996, he also worked as a Technical Consultant of Extensive Wood Processing Corporation.

Edgar started his graduate program at Department of Wood Science and Forest Products in January 1998. During his enrollment at Virginia Tech, he was awarded a Graduate Research Assistantship. He completed his Doctor of Philosophy in Wood Science and Forest Products degree in August 2001.